Photochemical Electron Transfer at Fixed Distance: A Synthetic Model of the Photosynthetic Primary Process

Thesis by

Alvin David Joran

In Partial Fulfillment of the Requirements

for the Degree of

Doctor of Philosophy

California Institute of Technology

Pasadena, California

1986

(submitted 24 March 1986)

For My Parents

Acknowledgments

I thank my research advisors, Peter Dervan and John Hopfield, for offering the challenging and intriguing seed ideas which grew into this thesis. Their support and advice suffuse every phase of this work. It has been a real privilege to collaborate with them.

I am grateful to Burton Leland, whose dedication to the electron transfer project never flagged. His knowledge and abilities helped advance this work in ways too numerous to list here. George Geller deserves credit for a key design insight that speeded my progress. I am indebted to my good friend, Mike Lewy, whose concern, perspective, and humor carried me through the dark times when nothing seemed to work (and that which did led nowhere). His intellect and humanity were an inspiration. Joyce Rosenberg, Tony Straceski, Joel Chaiken, Mike Weimar, and R. Michael Perelmuter have been important sources of encouragement. Thanks go to the members of the Dervan Group, especially Brenda Baker, Mike Lewis, Geoff Dreyer, Philippe Kahn, Jim Hanson, and Warren Wade, for innumerable suggestions and kind support. I thank members of the Hopfield Group, Dave Beratan, José Nelson Onuchic, and Noam Agmon, for helpful discussions on theory, for their friendly companionship, and our memorable skiing and camping trips in Mineral King, Mammoth, and Yosemite. I thank Burt Leland, Dave Beratan, José Onuchic, Jim Hanson, and Warren Wade for reading parts of the manuscript and for offering critical improvements. Peter Felker ably

carried out the picosecond fluorescence spectroscopy in the labs of A.H. Zewail. Harry Gray, Gerhard Closs, Rudy Marcus, Sunney Chan, and Janet Osteryoung have all contributed substantially to my understanding of electron transfer.

Finally, I am grateful to my early mentors in research, Ken Samonds and Harbans and Krishna Sachdev, who first excited my interest in chemistry a decade ago.

This research was supported by the National Science Foundation.

Abstract

A series of *meso*-phenyloctamethylporphyrins covalently bonded at the 4′-phenyl position to quinones *via* rigid bicyclo[2.2.2]octane spacers were synthesized for the study of the dependence of electron transfer reaction rate on solvent, distance, temperature, and energy gap. A general and convergent synthesis was developed based on the condensation of ac-biladienes with masked quinone-spacer-benzaldehydes. From picosecond fluorescence spectroscopy emission lifetimes were measured in seven solvents of varying polarity. Rate constants were determined to vary from $5.0\times10^{9}\text{sec}^{-1}$ in N,N-dimethylformamide to 1.15×10^{10} sec^{-1} in benzene, and were observed to rise at most by about a factor of three with decreasing solvent polarity. Experiments at low temperature in 2-MTHF glass (77K) revealed fast, nearly temperature-independent electron transfer characterized by non-exponential fluorescence decays, in contrast to monophasic behavior in fluid solution at 298K. This example evidently represents the first photosynthetic model system not based on proteins to display nearly temperature-independent electron transfer at high temperatures (nuclear tunneling). Low temperatures appear to freeze out the rotational motion of the chromophores, and the observed nonexponential fluorescence decays may be explained as a result of electron transfer from an ensemble of rotational conformations. The non-exponentiality demonstrates the sensitivity of the electron transfer rate to the precise magnitude of the electronic matrix element, which supports the expec-

tation that electron transfer is nonadiabatic in this system. The addition of a second bicyclooctane moiety (15 Å *vs.* 18 Å edge-to-edge between porphyrin and quinone) reduces the transfer rate by at least a factor of 500-1500. Porphyrin-quinones with variously substituted quinones allowed an examination of the dependence of the electron transfer rate constant k_{ET} on reaction driving force. The classical trend of increasing rate *versus* increasing exothermicity occurs from 0.7 eV$\leq |\Delta G^{0'}(R)| \leq$ 1.0 eV until a maximum is reached ($k_{ET} = 3 \times 10^8$ sec^{-1} rising to 1.15×10^{10} sec^{-1} in acetonitrile). The rate remains insensitive to ΔG^0 for $\sim$ 300 mV from 1.0 eV$\leq |\Delta G^{0'}(R)| \leq$ 1.3 eV, and then slightly decreases in the most exothermic case studied (cyanoquinone, $k_{ET} = 5 \times 10^9$ sec^{-1}).

Table of Contents *page*

List of Figures *page*

Chapter 1

Chapter 2

Chapter 6

List of Tables

Chapter 3

Chapter 4

Chapter 6

List of Schemes

Chapter 1

Chapter 2

Chapter 3

Chapter 6

Chapter 1

Introduction

Introduction

The transfer of an electron from one chemical species to another is a fundamental process in nature, essential for cellular mechanisms of energy metabolism.[1] Oxidative phosphorylation occurs in mitochondria, and takes the products of glucose fermentation and oxidizes them further by an electron transport chain to carbon dioxide providing the directly useful energy source adenosine triphosphate (ATP). Photosynthesis transforms photon energy into chemical energy by photoexcitation of highly absorbing pigments and an electron transport pathway capable of separating opposite charges. The electric field generated provides an oxidizing equivalent on the outer side of the membrane and a reducing equivalent on the inner side. Carbon dioxide is reduced to glucose which is then metabolized by fermentation (and the citric acid cycle in certain species) to obtain valuable pyrophosphoryl bonds. Water is the common sacrificial electron donor that reduces the cytochrome preparing the pathway for another cycle. Photosynthesis follows schemes of varying complexity in green plants, algae, and photosynthetic bacteria. Because bacteria are the simplest in structure and the best characterized, the electron transfer processes of bacterial photosynthesis are the object of current modeling efforts.

---

[1] (a) B. Chance, D.C. DeVault, H. Frauenfelder, R.A. Marcus, J.R. Schrieffer, and N. Sutin, *Tunneling in Biological Systems*, Academic, New York, 1979. (b) C. Ho, ed., *Electron Transport and Oxygen Utilization*, Elsevier, New York, 1982. (c) K. Sauer, *Bioenergetics of Photosynthesis*, Academic, New York, 1975.

Analysis of detergent-solubilized preparations of the reaction center of the purple bacterium *Rhodopseudomonas sphaeroides*[2] revealed the presence of four bacteriochlorophylls (*BChl*), two bacteriopheophytins (*BPhe*), an iron-quinone complex, and three polypeptide chains (21 kD, 24 kD, and 27 kD).[3] Two of the *BChls* are associated in the so-called special pair,[4] with λ_{max} 865, 800, and 605 nm. The *BChl* monomers absorb at 800 and 595 nm, and *BPhe* at 757 and 535 nm. Most bacterial species also contain two high-potential and two low-potential *c* type cytochromes.[5]

The x-ray crystal structure of a photochemically active crystal[6] of the reaction center complex of *Rhodospeudomonas viridis* at 3 Å resolution has been reported (Figure 1).[7] The four cytochromes line up and point into a bowed arrange-

---

[2] D.W. Reed and R.K. Clayton, *Biochem. Biophys. Res. Commun.*, **30**, 471 (1968).

[3] G. Feher and M.Y. Okamura, *Brookhaven Symp. Biol.*, **28**, 183 (1977).

[4] For a discussion of its optical and electron paramagnetic resonance properties, see (a) J.J. Katz, J.R. Norris, and L.L. Shipman, *Brookhaven Symp. Biol.*, **28**, 16 (1977). (b) J.J. Katz, in H. Gerischer and J.J. Katz, eds., *Light-Induced Charge Separation in Biology and Chemistry*, Dahlem Konferenzen, Springer-Verlag, Heidelberg, 1979.

[5] P.L. Dutton and R.C. Prince, in R.K. Clayton and W.R. Sistrom, eds., *The Photosynthetic Bacteria*, Plenum Press, New York, 1978, pp. 526ff.

[6] W. Zinth, W. Kaiser, and H. Michel, *Biochim. Biophys. Acta*, **723**, 128 (1983).

[7] (a) J. Deisenhofer, O. Epp, K. Miki, R. Huber, and H. Michel, *Nature (London)*, **318**, 618 (1985). (b) J. Deisenhofer, O. Epp, K. Miki, R. Huber, and H. Michel, *J. Mol. Biol.*, **180**, 385 (1984).

ment of two symmetrically disposed sets of chromophores, starting with $(BChl)_2$, $BChl$, BPh, Q_A, and Fe^{2+}.[7a] The heme-iron of the nearest cytochrome *c* is ~ 21 Å from the $(BChl)_2$ Mg atoms, equivalent to about 11 Å edge-to-edge. Q_A is missing from one set, probably lost during crystal preparation.[7] The monomeric $BChl$ is 13 Å away center-to-center from the nearest Mg atom of $(BChl)_2$, with an angle of 70° between planes. $BPhe$ is 11 Å away center-to-center, at a 64° incline. The hydrophobic surface of the central part of the reaction center complex (subunits L and M) and the amino terminal helix of subunit H suggest this to be the region traversing the membrane.[7]

Years before the crystal structure was known, a considerable amount of structural and mechanistic information had been obtained by other techniques, including epr, nmr, and fluorescence energy transfer. Kinetic data on most of the processes of the reaction center were obtained using transient absorption spectroscopy (Scheme I). A classic experiment in the field was the study of cytochrome *c* oxidation by the special pair dimer $(BChl)_2$ in *Chromatium vinosum* by flash photolysis (Figure 2).[8] The important result of this experiment was the observation of temperature-independent electron transfer at temperatures from about 100K down to 4K, and the proposal that the mechanism must include electron tunneling; only later was it realized that nuclear tunneling is responsible for this temperature independence. Most of the rate constants for the pri-

---

[8] (a) D. DeVault and B. Chance, *Biophys. J.*, **6**, 825 (1966).

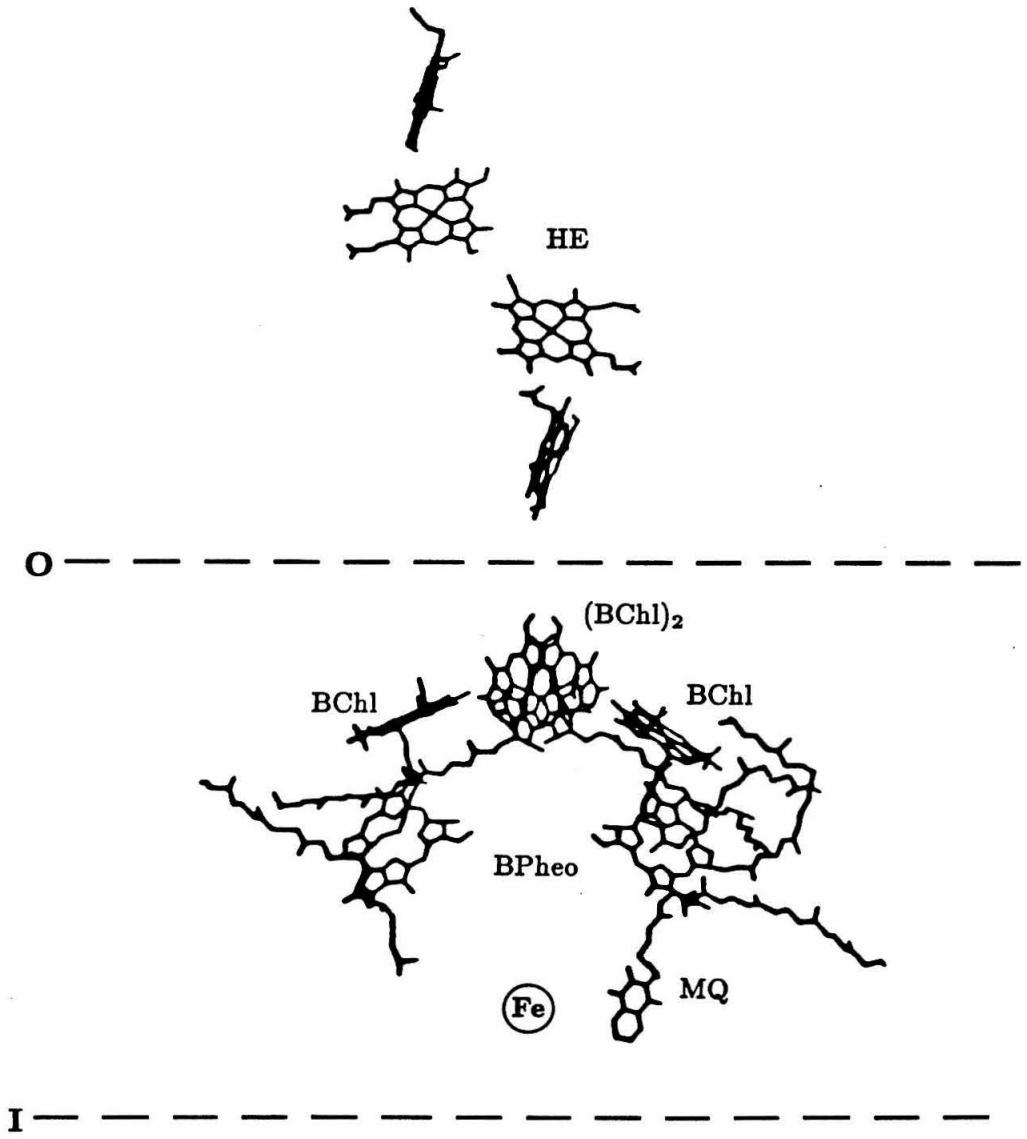

Figure 1. X-ray crystal structure of the reaction center pigment-protein complex from *Rhodopseudomonas viridis.*[7a]

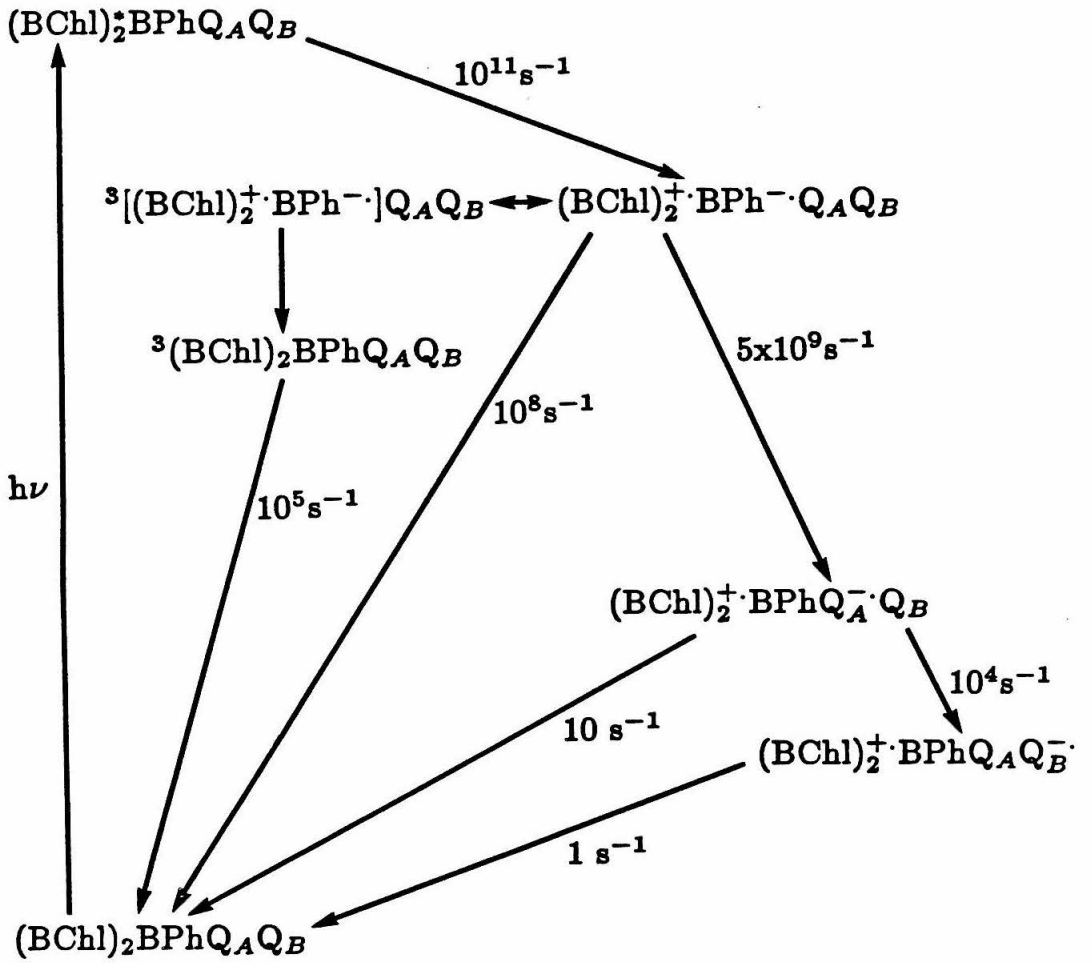

Scheme I. Kinetic scheme of reaction center electron transfer reactions in bacterial photosynthesis.

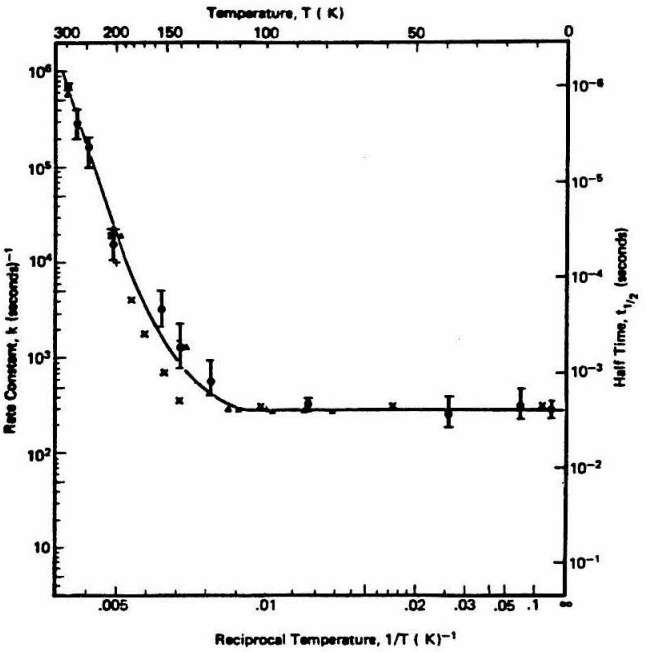

Figure 2. Cytochrome *c* oxidation rate in *Chromatium vinosum* as a function of temperature.[8]

mary processes were determined over the subsequent ten years, and are shown in Scheme I. The forward reactions are outstandingly fast, and the back reactions to the ground-state cation of the special pair dimer $(BChl)_2$ are all orders of magnitude slower. The overall sequence of steps results in rapid separation of opposite charges across the membrane, providing the necessary reducing equivalents for energy transduction. The DeVault-Chance experiment prompted investigations of the temperature dependence of the other reactions of the scheme. For example, the primary photoprocess $^*(BChl)_2BPhe \rightarrow (BChl)_2^{+\cdot}BPhe^{-\cdot}$ is

temperature-independent from room temperature down to 4K.[9] The back reaction $(BChl)_2^{+\cdot}BPheQ^{-\cdot} \rightarrow (BChl)_2BPheQ$ is also independent of temperature.[9] These and other results have inspired a wealth of experimental and theoretical work seeking to understand the unique nature of these reactions, and have been thoroughly reviewed elsewhere.[9]

Theory

The potential energy surfaces of the reactant and product are helpful for understanding several important physical principles governing electron transfer reactions (Figure 3). In the adiabatic limit strong interactions between the donor and acceptor (zero-order) surfaces lead to a separation of magnitude $2\,|T_{ab}|$ between the (first-order) surfaces at the crossing point. In the non-adiabatic limit, the zero-order surfaces are unperturbed.

The transferring electron couples with the vibrational motion of the atoms on the centers donating and receiving the electron. In the Condon approximation the nature of coupling of the nuclei to the electron does not influence the magnitude of $|T_{ab}|$ (electronic interaction between initial and final state), whereas recent work shows that the Born-Oppenheimer/Franck-Condon picture may break

---

[9] (a) D. DeVault, *Q. Rev. Biophys.*, **13**, 387 (1980). (b) D. DeVault, *Quantum-Mechanical Tunneling in Biological Systems*, 2nd ed., Cambridge University Press, New York, 1984.

down at long distances.[10] Hopfield's thermally activated tunneling electron transfer theory is specifically intended to understand the nature of electron transfer in biological systems.[11] Sites are fixed and distant in proteins embedded in or across membranes. Because of the distances involved the rate of electron transfer will depend strongly on the magnitude of the overlap of electronic wavefunctions for the initial and final states. The long distances between donor and acceptor suggest that electron tunneling must be occurring in most cases of biological electron transfer.[11]

The electronic energy of the state identified with the removal of an electron from site a to b is broadened into a distribution by nuclear displacements coupled to the transfer.[11] The electronic energy of state b on insertion of an electron is likewise broadened by nuclear motion. The Franck-Condon approximation states that an electronic transition takes place faster than nuclear readjustment ("vertical"); that is, the transition must occur in less than the time needed to sample a new position along the multidimensional reaction ("horizontal") coordinate. In addition, energy conservation must be enforced during the transfer, which implies that the electron can transfer only because of the broadness of the electron insertion and removal spectral energy distributions. If there were no broadening due to the vibrational motion of nuclei, no matching of energies could occur, and

---

[10] J.N. Onuchic, D.N. Beratan, and J.J. Hopfield, *J. Phys. Chem.*, **90**, 0000 (1986).

[11] J.J. Hopfield, *Proc. Natl. Acad. Sci. U.S.A.*, **71**, 3640 (1974).

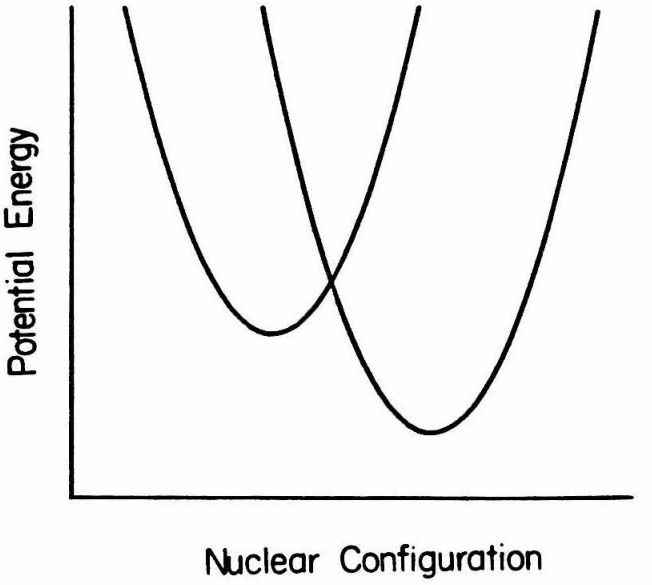

Figure 3(a). Potential energy surface in the non-adiabatic limit.

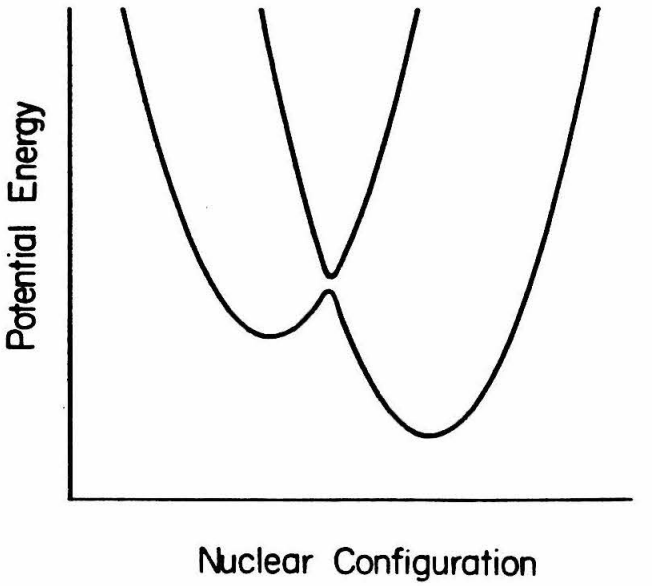

Figure 3(b). Potential energy surface in the adiabatic limit.

energy would not be conserved during the electron transfer. Thus, in the classical regime, only at the crossing point of the double parabola model of electron transfer reactions do both principles apply.

In transition state theory, an electron transfer rate can be calculated by multiplying the frequency of reaching the curve-crossing region by the transition (tunneling) probability for the electron to cross over to the product surface (κ, also known as the transmission coefficient). The first part depends on temperature, while the electronic part is temperature-independent. Thus, for unimolecular reactions,

$$k_{ET} = \kappa\nu \exp(-\Delta G^{\ddagger}/RT), \qquad [1.1]$$

where ν is the nuclear frequency, and $\Delta G^{\ddagger}$ is the activation free energy. Marcus's classical theory relates $\Delta G^{\ddagger}$ to the driving force of the reaction $\Delta G^{0'}$, giving the energy gap law:[12,13]

$$\Delta G^{\ddagger} = w^r + \frac{\lambda}{4}(1 + \Delta G^{0'}/\lambda)^2, \qquad [1.2]$$

where $\Delta G^{0'} = \Delta G^0 + w^p - w^r$, in which w^r and w^p are the work needed to bring the reactants to the encounter complex and to separate the products after

---

[12] (a) R.A. Marcus, *J. Chem. Phys.*, **24**, 966 (1956). (b) R.A. Marcus, *Discuss. Faraday Soc.*, **29**, 21 (1960).

[13] R.A. Marcus and N. Sutin, *Biochim. Biophys. Acta*, **811**, 256 (1985).

reaction, $\lambda = \lambda_i + \lambda_o$ is the total reorganization energy, summing contributions from inner-sphere vibrational reorganization λ_i and outer-sphere solvational reorganization λ_o. The vibrational component is obtained classically[12] by summing vibrational displacement energies for bond displacements (Δq_j) using estimated spring constants $f_j^{r,p}$ suitably averaged:

$$\lambda_i = \sum_j \frac{f_j^r f_j^p}{f_j^r + f_j^p} (\Delta q_j)^2. \qquad [1.3]$$

The outer-sphere contribution to the reorganization (solvent polarization) was calculated from dielectric continuum theory:[12]

$$\lambda_o = (\Delta e)^2 \left[\frac{1}{2a_1} + \frac{1}{2a_2} - \frac{1}{r}\right]\left[\frac{1}{D_{op}} - \frac{1}{D_s}\right] \qquad [1.4]$$

where a_1 and a_2 are the radii of the donor and acceptor, r is the separation distance, Δe is the number of electrons transferred, D_{op} and D_s are, respectively, the high- and low-frequency dielectric constants of the solvent. The energy gap law expressing the activation energy as a function of the thermodynamic driving force and the reorganization parameter λ predicts that for very exothermic processes k_{ET} becomes slower (*i.e.*, when $|\Delta G^{0'}(R)| > \lambda$), and thus displays "inverted" behavior,[11] as opposed to "normal" behavior when $|\Delta G^{0'}(R)| < \lambda$. Graphically, lowering the product surface reduces the activation barrier until the curves intersect at the minimum potential, at which point any further lowering results in a barrier again (Figure 4). This prediction may account for the slowness of the back transfer reactions of photosynthetic charge separation, and also for

the high conversion efficiency (*i.e.*, only a little energy is wasted to obtain high forward electron transfer rates). The classical theory, however, does not account for low-temperature tunneling effects in photosynthesis.

Hopfield's expression for the electron transfer rate (Eq. [1.5]) opened up a way of dealing with low-temperature effects by the use of an effective temperature in the calculation of the Franck-Condon factor.[10]

$$W_{ab} = \frac{2\pi}{\hbar}|T_{ab}|^2 \int D_a(E) D'_b(E) dE \qquad [1.5]$$

Assuming the electron removal and insertion spectra D_a and D'_b to be Gaussian probability distributions, Hopfield derived the semiclassical expression for k_{ET}:

$$k_{ET} = \frac{2\pi}{\hbar}|T_{ab}|^2 \frac{1}{\sqrt{2\pi\hbar\omega\lambda T_{eff}}} \exp\left[-(\Delta G^{0'} + \lambda)^2 / 2\lambda T_{eff}\right], \qquad [1.6]$$

where $T_{eff} = \hbar\omega\lambda \coth(\hbar\omega/2k_BT)$ and approaches k_BT at high temperatures and $\hbar\omega/2$ at low temperatures and takes into account the zero-point motion of the pertinent vibrational modes. Eq. [1.6] was the earliest to give reasonably good quantitative agreement with the data of DeVault and Chance on cytochrome *c* oxidation in *Chromatium vinosum*.[10] The maximum overlap of the electron insertion and electron removal spectral energy distributions occurs at the average of the individual electronic energies of the donor and acceptor weighted by the reorganization energies of each:[14]

$$E^{\ddagger} = \frac{\lambda_a E_d + \lambda_d E_a}{\lambda_a + \lambda_d} \qquad [1.7]$$

---

[14] D.N. Beratan, *Dissertation*, California Institute of Technology, 1986.

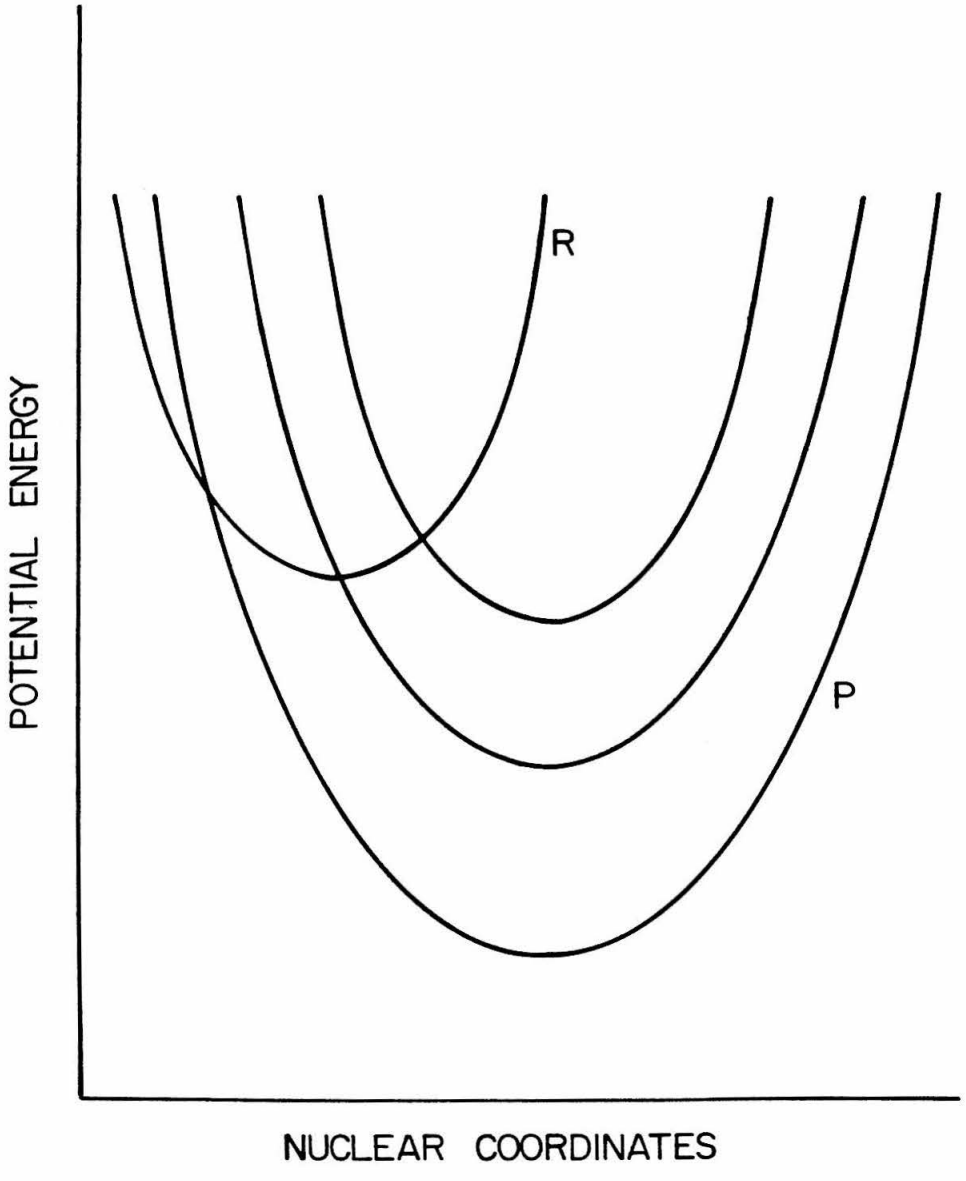

Figure 4. Dependence of barrier height on energy gap.

The magnitude of the inner-sphere reorganization energy is roughly inversely proportional to the number of bonds over which the transferred electron can delocalize. Inner-sphere reorganization is expected to involve nuclear tunneling (even at room temperature) if the spacing of the vibrational energy levels $\hbar\omega$ is much larger than k_BT (Figure 5).[14,15] Because wavefunctions decay exponentially in classically forbidden regions according to elementary theory, the matrix element $|T_{ab}|$ is also expected in simple theory to decay exponentially with distance:

$$|T_{ab}| = V_0 \exp(-\alpha R), \qquad [1.8]$$

where V_0 is the electron exchange energy in the adiabatic limit.[10] Somewhat non-exponential decay is now considered possible when both the donor and acceptor are strongly coupled to vibrational modes.[9]

Sources of Confusion in the Inverted Region

Convincing observations of inverted reactivity (*i.e.*, the quadratic dependence of the activation energy on driving force, as in Eq. [1.2]) have been elusive for a variety of reasons. Literature statements of its discovery have often been based on the study of one or two molecules. Transcending the insufficiency of the number of experimental substrates, some of the theoretical requirements to be convincing include the following: (a) The tunneling matrix element T_{ab} must be

---

[15] R.A. Marcus, in H. Gerischer and J.J. Katz, eds., *Light-Induced Charge Separation in Biology and Chemistry*, Dahlem Konferenzen, Springer-Verlag, Heidelberg, 1979.

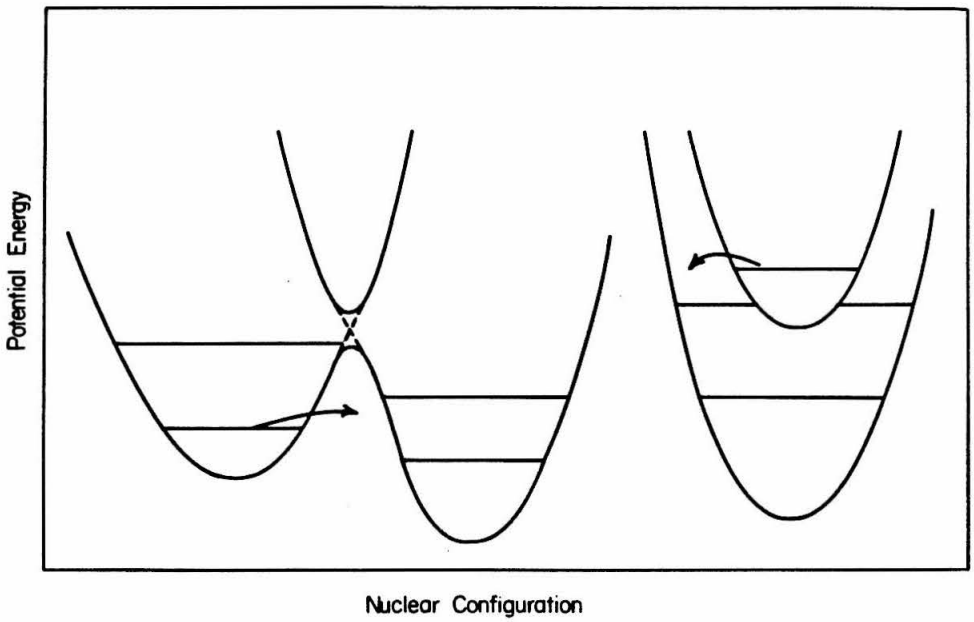

Figure 5. Nuclear tunneling at low temperature ($k_BT \ll \hbar\omega$) (a) in the normal region and (b) in the inverted region.

as constant as possible; there should be no change in electronic interaction between donor and acceptor in the series. (b) Inner-sphere reorganization must be similar as well throughout the series; there should be no major changes in donor or acceptor structure. (c) Solvent polarity should not be altered to obtain different driving forces (see the discussion on electrochemistry in Chapter 4). Beratan and Hopfield[16] pointed out that, if either donor or acceptor energy levels approach

---

[16] (a) D.N. Beratan and J.J. Hopfield, *J. Amer. Chem. Soc.*, **106**, 1584 (1984).

the levels of the bridge states, appreciable mixing occurs and significant enhancements in electron transfer rate may result. In a series of test compounds, it is important to keep the extent of mixing as constant as possible. Calculations by Beratan and Hopfield showed that states close to the middle of the gap between highest occupied and lowest unoccupied molecular orbitals (HOMO/LUMO) of the bridge, the tunneling matrix element is nearly independent of the precise positions of the localized states.[16] Synthetic efforts to test energy gap laws (including the present investigation) must respond to these constraints imposed by theory in order to obtain meaningful results. The bridge should have a large band gap. The energy differences between the unoccupied bridge orbital and the donor excited state, and between the highest occupied bridge state and the acceptor ground state, must also be reasonably large to avoid sizeable changes in rate enhancements due to differential mixing of these states from compound to compound in a reaction series. The uncertainty in the extent of this interaction between bridge and localized states leads to the necessity of studying many different bridges to develop a sense for trends. Given a constant pair of donor and acceptor, molecules containing spacers with differing relative energies will allow a test of the above predictions. The study of the dependence of rate on distance is also expected to depend sensitively on the nature of the interaction with bridge states.[16]

(b) D.N. Beratan and J.J Hopfield, *J. Chem. Phys.*, **81**, 5753 (1984).

Previous Experiments

The classical theory has had remarkable success in predicting correlations in the rates of outer-sphere electron transfer reactions, especially in applications of the cross-relation to self-exchange reactions.[17] The case of highly exothermic reactions ($|\Delta G^{0'}(R)| > \lambda$) has not been as successful. Rehm and Weller examined the quenching of fluorescence of aromatic compounds by electron transfer,[18] and discovered that the second-order quenching rate constant increased with energy gap until the diffusion-control limit, and did not slow as predicted. These and similar results by others[19] have been rationalized as due to complex or exciplex formation or transfer to an excited state.

During the 1970's and early 80's a large synthetic drive was focused towards the development of covalently linked systems as a way to avoid diffusion-control limits to the observed rate constant. These ranged in make-up from dimers of porphyrins and chlorophyll derivatives[20] to fused aromatics linked to amines[21]

---

[17] N. Sutin, *Progr. Inorg. Chem.*, **30**, 441 (1983). (b) R.D. Cannon, *Electron Transfer Reactions*, Butterworths, London, 1980.

[18] D. Rehm and A. Weller, *Isr. J. Chem.*, **8**, 259 (1970).

[19] For example, see (a) R. Scheerer and M. Graetzel, *J. Amer. Chem. Soc.*, **99**, 865 (1977) and (b) C.R. Bock, T.J. Meyer, and D.G. Whitten, *J. Amer. Chem. Soc.*, **97**, 2909 (1975).

[20] (a) F.P. Schwartz, M. Gouterman, Z. Muljiani, and D. Dolphin, *Bioinorg. Chem.*, **2**, 1 (1972). (b) D. Dolphin, J. Hiom, and J.B. Paine III, *Heterocycles*, **16**, 417 (1981). (c) J.B. Paine III, and D. Dolphin, *Can. J. Chem.*, **56**, 1710 (1978). (d)

to porphyrins linked to quinones.[22] The most thoroughly studied of these flexibly linked systems was a trimethyleneamide-linked tetraphenylporphyrin-quinone (I, $n = 3$).[22c,23] Because the flexible nature of the linker allows a distribution of distances between donor and acceptor, the fluorescence decays were multiexponential,[23a] and no conclusions regarding distance or energy gap effects could be drawn.

Recently, photoexcited electron transfer has been examined in structurally better constrolled systems, incorporating rigidly coupled donor/acceptor pairs. *meso*-Triphenyl(*p*-benzoquinone)porphyrin (II), which uses a CC single bond as a "rigid linker," showed subpicosecond excited-state deactivation, implying a for-

---

S.G. Boxer and G.L. Closs, *J. Amer. Chem. Soc.*, **98**, 5406 (1976).

[21] (a) K. Gnadig and K.B. Eisenthal, *Chem. Phys. Lett.*, **46**, 339 (1977). (b) M. Migita, M. Kawai, N. Mataga, Y. Sakata, and S. Misumi, *Chem. Phys. Lett.*, **53**, 67 (1978).

[22] (a) I. Tabushi, N. Koga, and M. Yanagita, *Tetrahedron Lett.*, 257 (1979). (b) J. Dalton and L.R. Milgrom, *J. Chem. Soc., Chem. Commun.*, 609 (1979). (c) J.L.Y. Kong and P.A. Loach, *J. Heterocyclic Chem.*, **17**, 737 (1980). (d) K.N. Ganesh and J.K.M. Sanders, *J. Chem. Soc., Chem. Commun.*, 1129 (1980). (e) A. Harriman and R.J. Hosie, *J. Photochem.*, **15**, 163 (1981). (f) M. Migita, T. Okada, N. Mataga, S. Nishitani, N. Kurata, Y. Sakata, and S. Misumi, *Chem. Phys. Lett.*, **84**, 263 (1981). (g) K.N. Ganesh and J.K.M. Sanders, *J. Chem. Soc.* , *Perkin Trans.*, 1 , 1611 (1982).

[23] (a) A.R. McIntosh, A. Siemiarczuk, J.R. Bolton, M.J. Stillman, T.-F. Ho, and A.C. Weedon, *J. Amer. Chem. Soc.*, **105**, 7215 (1983). (b) A. Siemiarczuk, A.R. McIntosh, T.-F. Ho, M.J. Stillman, K.J. Roach, A.C. Weedon, J.R. Bolton, and J.S. Connolly, *J. Amer. Chem. Soc.*, **105**, 7224 (1983) and refs. cited therein.

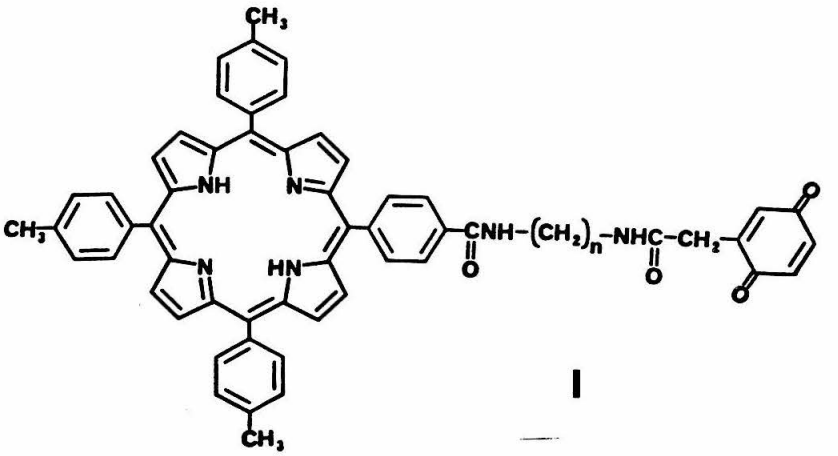

I

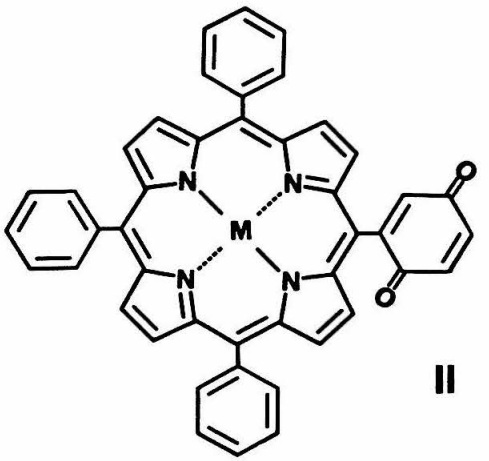

II

ward electron transfer rate of $> 10^{12}$ sec^{-1}.[24] The rates are high possibly due to adiabaticity, and sensitivity to energy gap, solvent, and distance may not be readily measureable. A cofacial tetraphenylporphyrin-quinone (III) separated by 10 Å using tetraamidophenoxy spacers exhibited a biexponential fluorescence decay, perhaps indicative of two stable conformations.[25]

---

[24] M.A. Bergkamp, J. Dalton, and T.L. Netzel, *J. Amer. Chem. Soc.*, **104**, 253 (1982).

[25] (a) J.S. Lindsey and D. Mauzerall, *J. Amer. Chem. Soc.*, **104**, 4498 (1982). (b)

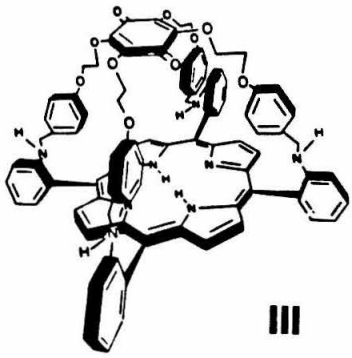

III

After the present research was published, a tetraphenylporphyrin-quinone linked by a bicyclo[2.2.2]octane spacer appeared, but was able to undergo observable electron transfer only in polar solvents probably because of the low $|\Delta G^{0'}(R)| \sim -0.3$ eV.[26] Charge-transfer bands resulting from complexes substituted with $Ru(NH_2)_5^{II/III}$ moieties linked by a bisthiaspirobutane oligomer lends support to the exponential dependence of $|T_{ab}|$ on distance.[27]

In the context of the present study, the porphyrin-quinones prepared by Wasielewski and his collaborators deserve detailed comment. These compounds consist of *meso*-tetraarylporphyrins coupled by a rigid triptycene bridge to a

---

J.S. Lindsey, D. Mauzerall, and H.S. Linschitz, *J. Amer. Chem. Soc.*, **105**, 6528 (1983).

[26] J.R. Bolton, T.-F. Ho, A. Siemiarczuk, C.S.K. Wan, and A.C. Weedon, *J. Chem. Soc., Chem. Commun.*, 559 (1985).

[27] C.A. Stein, N.A. Lewis, and G. Seitz, *J. Amer. Chem. Soc.*, **104**, 2596 (1982).

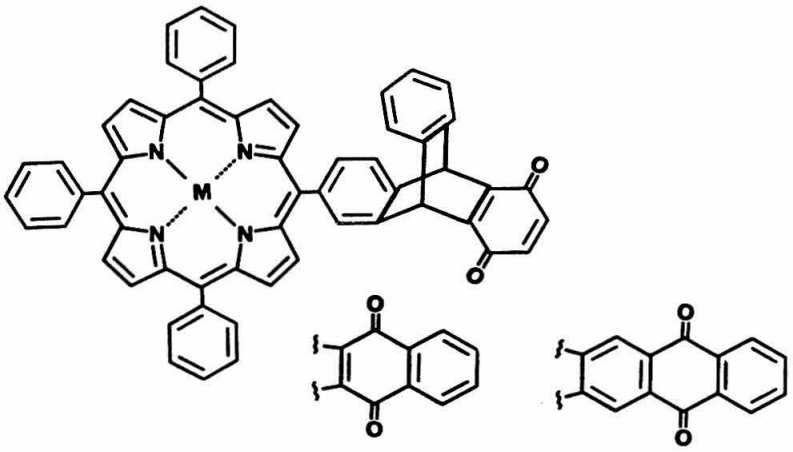

benzoquinone.[28] This system was one of the earliest to exhibit monoexponential fluorescence decay in a porphyrin-quinone, indicating electron transfer kinetics uncomplicated by the presence of multiple conformational states. In subsequent work two more compounds were reported, one with a naphthoquinone and one with an anthroquinone in place of the benzoquinone.[29] The three compounds allowed the measurement of six electron transfer rate constants, three for forward intramolecular transfers from the porphyrin excited singlet state to each respective quinone, and three for the corresponding "back" transfers from the ground state semiquinone to the porphyrin radical cation. The data when plotted as $\log k_{ET}$ *vs.* $\Delta G^{0'}$ (corrected by a method to be discussed below for changes in

---

[28] M.R. Wasielewski and M.P. Niemczyk, *J. Amer. Chem. Soc.*, **106**, 5043 (1984).

[29] M.R. Wasielewski, M.P. Niemczyk, and E.B. Pewitt, *J. Amer. Chem. Soc.*, **107**, 1080 (1985).

solvent), suggest that the "back" transfers fall in the inverted region (Figure 6). The fundamental issue arises of whether the quinone series used really comprises a homologous reaction series. Calculations of Beratan and Hopfield[16] show that the tunneling matrix elements for electron transfer from excited states decay much more rapidly with distance than for ground states in porphyrin-quinone systems. As a consequence, the forward and reverse transfers may not be part of the same Marcus plot. (Regarding the electron transfers in photosynthesis, which involve large delocalized chromophores, it is not entirely clear whether their wave functions are similar enough in ground and excited states even to put them in the same reaction series.) It is also uncertain how $|T_{ab}|$ will be affected by a change from benzoquinone to anthraquinone, considering the change in ring size and aromaticity. Are the slower kinetics in the latter a result of a smaller value of $|T_{ab}|$ or a less favorable Franck-Condon barrier?

The literature value of $E_{1/2}$ for $NQ/NQ^{-\cdot}$ is -0.71 V (*vs.* SCE, acetonitrile, 25°), and for $BQ/BQ^{-\cdot}$ it is -0.51 V (SCE, AN, 25°). The rate constants for ZnTPPBQ and ZnTPPNQ are the same within a factor of two for both directions, despite the 200 mV difference in $E_{1/2}$, whereas, the back transfer rate for ZnTPPAQ is 500-fold slower than for ZnTPPNQ, which is only 40 mV less exothermic than the former. The semiquinones of these systems have different extents of delocalization, and thus it seems likely that reorganization energies are shifting somewhat from quinone to quinone.

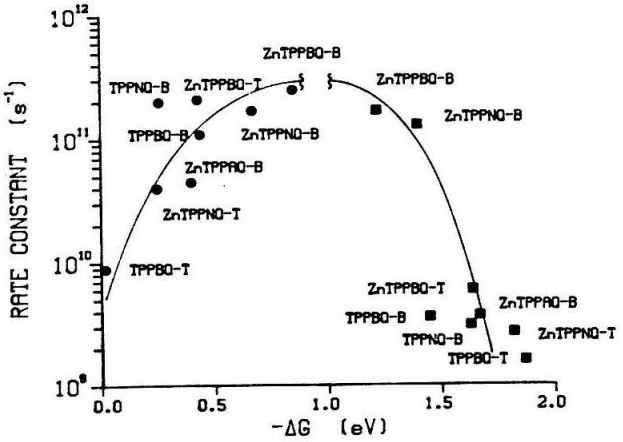

Figure 6. Dependence of electron transfer rate constant on energy gap in triptycene-linked porphyrin-quinone.[29]

Another major avenue of approach to the study of electron transfer reactions involves the method of pulse radiolysis. In this technique high-energy electrons (15-20 MeV) are pulsed at a sample, ionizing solvent and substrate molecules. Substrates capture electrons and undergo electron transfer processes which may be followed by time-resolved spectroscopy. The extensive pulse radiolysis studies of Miller, Closs, and their collaborators[30] on covalently linked and isolated

---

[30] (a) J.R. Miller, L.T. Calcaterra, G.L. Closs, *J. Amer. Chem. Soc.*, **106**, 3047 (1984). (b) L.T. Calcaterra, G.L. Closs, and J.R. Miller, *J. Amer. Chem. Soc.*, **105**, 670 (1983). (c) J.R. Miller, J.V. Beitz, and R.K. Huddleston, *J. Amer. Chem. Soc.*, **106**, 5057 (1984). (d) J.R. Miller and J.V. Beitz, *J. Chem. Phys.*, **74**, 6746 (1981), and references cited therein.

donors and acceptors suggested the existence of inverted reactivity, and further indicated that a large range of exothermicities may be necessary to observe this behavior. In early work the Miller group studied the rate of electron attachment to a large variety of organic acceptors distributed in rigid matrix, and observed the classical rise in rates as the electron affinity of the acceptor rises and a scatter of rates ranging from the rate predicted by the energy gap laws to a maximal rate. Using data from different distances, decay constants (α) for $|T_{ab}|^2$ were calculated to be about 1.2 Å^{-1}. It is of some concern that there is a considerable range of exothermicities where the rate does not change much (about one order of magnitude for a 0.5 eV change in ΔG^0).[30c,d] This result contrasts with the kinetics of photosynthetic charge separation in bacterial reaction centers, where the back electron transfers are over three orders of magnitude slower than the forward reactions.

Also, in a closer look at the experimental data, the flatness of the survival probability curves (the optically detected concentration of anion that has not transferred yet as a function of time) has not been fully explained in case of small ΔG. Even using a large range of constant Franck-Condon factors, the experimental data could not be fit well, leading to the supposition that the Franck-Condon factors might be time-dependent due to slow matrix relaxation. Another possibility is breakdown of the Born-Oppenheimer approximation at the longest distances, leading to non-exponential distance decays.[14,16]

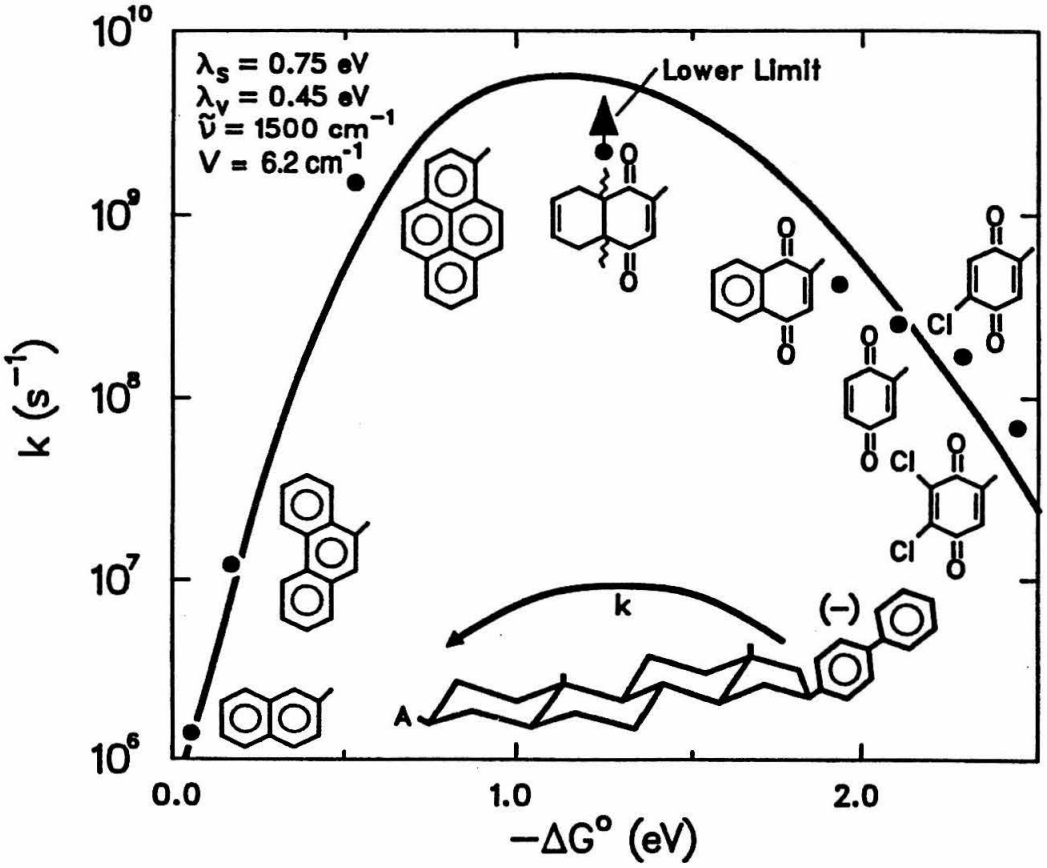

Figure 7. Steroid-linked donor-acceptor molecules: Rate *vs.* energy gap.[30a]

In order to avoid the need to deconvolute survival probability curves to obtain the transfer rate at particular distances, a synthetic system consisting of a biphenyl anion, a rigid steroid spacer, and an aromatic or quinone acceptor was prepared in a collaboration of Closs, Calcaterra, and Miller.[30a] This series showed the classical rise in rate in the less exothermic cases, and a decline in rate in the more exothermic cases (Figure 7). This classic result may be the first example of inverted reactivity predicted by electron transfer theory.[11,12] The issue remains of whether this series is actually two distinct structural series, one being a set of four fused aromatic acceptors and the other being a set of four quinone acceptors (the α,β-unsaturated 1,4-diketone acceptor, which is not a true quinone, may constitute a third series). Considering the structurally dissimilar radical anion resulting from electron transfer, these varying structures might be expected to possess sufficiently different vibrational reorganization energies as to complicate analysis of rate-energy gap dependences. In addition, solvational reorganization should differ in aromatic and semiquinone anions, and the work terms may have different magnitudes in these different systems, contributing to uncertainty about the overall driving force.

Pulse radiolysis experiments on the isolated (unlinked) donors and acceptors were also performed.[30a] It turns out that these donors and acceptors also show inverted behavior when reacting bimolecularly. While it is indeed a small effect relative to the intramolecular effect (a factor of 10), the question remains as to

why it is observed at all. No precedent exists for this effect in fluid solution. Perhaps there is a special characteristic of the pulse radiolysis technique that can explain it. In any case, the effect should not be ignored.

Although the dependence of electron transfer rate on exothermicity has been investigated in anion/neutral reactions,[30] no systematic study has been performed on rigidly defined, structurally homologous systems exhibiting true charge-separating electron transfers beginning with neutral donors and acceptors.[31] It is well established that the photosynthetic reaction center involves electron transfers of the latter type, and therefore models which separate opposite charges are more relevant to the mechanistic problems of biological electron transfer.

Triad Models of the Primary Process of Bacterial Photosynthesis

Two synthetic models of the reaction center of bacterial photosynthesis have appeared in the literature in recent years. One system involves a tetraarylporphyrin coupled to a benzoquinone acceptor by a flexible methylene amide on one side of the porphyrin and to a carotenoid donor chromophore on the other

---

[31] A study of two rigid bichromophoric molecules containing an anisole group and an acrylonitrile or acrylate ester linked by a steroid showed different extents of fluorescence quenching, but no attempt was made to deduce a general relationship between electron transfer rate and driving force. P. Pasman, N.W. Koper, and J.W. Verhoeven, *Recl. Trav. Chim. Pays-Bas*, **101**, 363 (1982). Related systems are treated later in this chapter.

(Figure 8).[32] The second model system consists of a tetraarylporphyrin linked to a benzoquinone acceptor by a rigid triptycene spacer and to a dimethylaniline donor on the opposite side of the porphyrin (Figure 9).[33] In both systems a charge separated state ($C^{+\cdot}PQ^{-\cdot}$ or $A^{+\cdot}PQ^{-\cdot}$, respectively) was observed by flash photolysis techniques to survive for about 1 μsec as a distinct, stable species before recombination, with a quantum yield of 0.04 for the carotenoid system in dichloromethane. (The quantum yield of the primary charge separation in bacterial photosynthesis is 1.02±0.04.[34]) These models were proposed to model the primary charge-stabilization of photosynthesis, and were the first to obtain stable charge separation.

A small build-up of charge-separated species probably results in the triad models from a very fast (probably adiabatic) electron donation to the porphyrin radical cation. Consequently, the opposite charges being at considerable distance, no direct means of recombination exists; *i.e.*, there is no similarly fast, short distance electron transfer from quinone radical anion to the secondary donor. Notably, studies on the dimers corresponding to the triads consisting of porphyrins

---

[32] T.A. Moore, D. Gust, P. Mathis, J.-C. Mialocq, C. Chachaty, R.V. Bensasson, E.J. Land, D. Doizi, P.A. Liddell, W.R. Lehman, G.A. Nemeth, A.L. Moore, *Nature* (*London*), **307**, 630 (1984).

[33] M.R. Wasielewski, M.P. Niemczyk, W.A. Svec, and E.B. Pewitt, *J. Amer. Chem. Soc.*, **107**, 5562 (1985).

[34] C.A. Wraight and R.K. Clayton, *Biochim. Biophys. Acta*, **333**, 246 (1973).

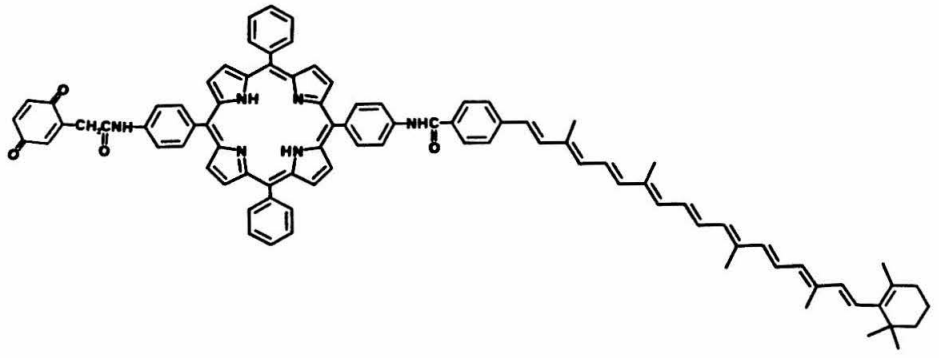

Figure 8. Carotenoid-porphyrin-quinone.[32]

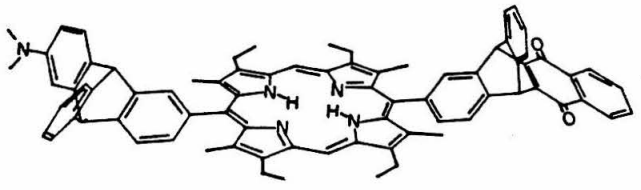

Figure 9. Dimethylaniline-porphyrin-quinone.[33]

linked to quinones (in fact, on all known *PLQ* systems where exciplexes and close-encounter charge transfers are impossible) show fast back transfer. Thus, if the same experiment were carried out in the triad models as was done in the reaction center preparation to determine the back transfer rate constant (that is, the chemical reduction of the quinone, followed by monitoring the electron

transfer by transient absorption):

$$(BChl)_2^{+\cdot} BPhe^{-\cdot} Q^{-\cdot} \longrightarrow (BChl)_2 BPheQ^{-\cdot}$$

no charge stabilization between two adjacent components can be expected. While the triads were probably not intended to model the mechanism of charge separation, it is worthwhile to note that a speculative interpretation of the triad model data is that, if these systems were accurate models of photosynthesis, then there would have to be an intermediary state ($(BChl)_2^{+\cdot} BChl^{-\cdot}$) prior to the transfer to bacteriopheophytin. There is little evidence for the reactivity modelled by the triads for the intermediary role of the monomeric $BChl$ in recent subpicosecond resolution transient absorption experiments,[35] which attempted to confirm the metastable state ($(BChl)_2^{+\cdot} BChl^{-\cdot}$) first reported by Russian workers.[36]

The presence of an additional electron carrier would, if true, controvert the regnant hypothesis that the inverted region is responsible for the slow recombination electron transfers in the primary light process, because the back transfers

---

[35] D. Holten, Proceedings of the International Conference on the Excited States and Dynamics of Porphyrins, Little Rock, Arkansas, 16-19 Nov. 1985.

[36] (a) V.A. Shuvalov, A.V. Klevanik, A.V. Sherkov, J.A. Matveetz, and P.G. Krukov, *FEBS Lett.*, **91**, 135 (1978). (b) V.A Shuvalov and A.V. Klevanik, *FEBS Lett.*, 51 (1983). (c) A formation time of 1 psec was determined by W. Zinth, M.A. Franz, M.C. Nuss, W. Kaiser, and H. Michel, in *Workshop on Antennas and Reaction Centers of Photosynthetic Bacteria–Structure and Dynamics*, ed. by M.E. Michel-Beyerle, Springer-Verlag, Heidelberg, 1985. (d) V.Z. Paschenko, B.N. Kovatovskii, A.A. Kononenko, S.K. Chamorovsky, and A.B. Rubin, *FEBS Lett.*, **191**, 245 (1985).

need not be orders of magnitude slower than, rather only comparable to, the forward transfers. It remains as a major challenge to construct a simple synthetic system which models the mechanistic details of photosynthetic charge separation.

Rigid Bichromophoric Charge-Transfer Models

Several points need to be made about a set of interesting compounds which exhibit charge-transfer fluorescence.[37] These molecules consist of an (alkoxycarbonyl)methylene or dicyanomethylene coupled to two different polycyclic hydrocarbons fused to methoxybenzene. From steady-state fluorescence data, charge transfer rate constants for 1a and 2a were calculated; all the dicyano derivatives were too fast to measure ($>10^{11}$ sec^{-1}). Unfortunately, no two different compounds could be compared because they were either too fast or too slow.

Also, no direct electrochemical measurements of the driving force of the reaction were reported. Instead, differences in driving force were approximated by using the Onsager reaction field model[38] to get estimates of the solvation energy.[39] In this approach, solvatochromic shifts of charge-transfer fluorescence bands ($\tilde{\nu}_{ct}$) were correlated with the solvent parameter Δf, according to

---

[37] P. Pasman, G.F. Mes, N.W. Koper, and J.W. Verhoeven, *J. Amer. Chem. Soc.*, **107**, 5839 (1985).

[38] L. Onsager, *J. Amer. Chem. Soc.*, **58**, 1486 (1936).

[39] (a) E. Lippert, *Z. Elektrochem.*, **61**, 962 (1957). (b) H. Beens, H. Knibbe, and A. Weller, *J. Chem. Phys.*, **47**, 1183 (1967).

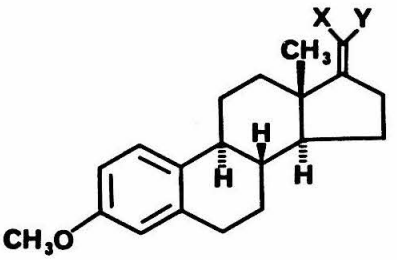

1a X=H ; Y=$COOC_2H_5$
1b X=Y=CN

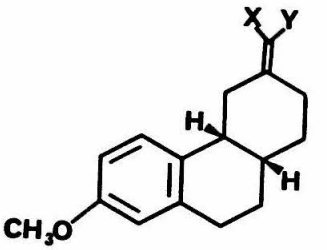

2a X=$COOCH_3$; Y=H
2b X=Y=CN

$\tilde{\nu}_{ct} = \tilde{\nu}_{ct}(0) - 2\mu_{ct}^2 \Delta f/\rho^3 hc$, where

$$\Delta f = f - \frac{1}{2}f' = \left(\frac{\epsilon - 1}{2\epsilon + 1}\right) - \frac{1}{2}\left(\frac{n^2 - 1}{2n^2 + 1}\right). \qquad [1.11]$$

From the slope were obtained estimates of the dipole moment of the charge-separated state D^+A^-, which allowed calculation of the solvation energy E_{solv}:

$$E_{solv} = -\frac{\mu_{ct}^2}{\rho^3}\left(\frac{\epsilon - 1}{2\epsilon + 1}\right) = -\mu_{ct}^2 f/\rho^3. \qquad [1.12]$$

The solvation energy is composed of the electronic polarization of solvent by the solute dipole E_p:

$$E_p = -\frac{\mu_{ct}^2}{\rho^3}\left(\frac{n^2 - 1}{2n^2 + 1}\right) = -\mu_{ct}^2 f'/\rho^3 \qquad [1.13]$$

and the solvent dipole reorganization $E_{op} = -\mu_{ct}^2(f - f')/\rho^3$, due to orientation polarization of the solute. The chromophores in all but 1a interact strongly

enough that an emissive exciplex forms, which contributes to the deactivation of the excited state of the methoxybenzene, in addition to direct quenching by the ground state acceptor. It should be noted that these compounds are rigid on the time scale of the charge-transfer event, but they are able to undergo at least partial chair-boat conformational motion, suggesting the presence of a thermal distribution of conformations and, hence, transfer distances.

In this study, a change in solvent was used in an attempt to alter the driving force of the reaction. Using the semiempirical method described,[39] an estimate of 0.5 eV of difference in solvation energy was calculated.[37] Electrochemical studies on the present porphyrin-quinone system discussed in Chapter 4 (and for reasons given below) indicate that this may not be an adequate approach. Lacking even solvatochromic shift data to obtain empirically based estimates of the dipole moment as above, other workers have resorted to use of the reaction field model to get the solvation energy in different solvents instead of measuring them electrochemically in a flexibly linked methylene amide porphyrin-quinone in which the rates appeared to correlate with the index of refraction of the solvent.[40] The same error was committed in the energy gap study of the triptycene-linked porphyrin-quinone of Wasielewski,[29] in which ΔG was altered by using different solvents, and estimating the change using the inaccurate correction factor in conjunction

---

[40] J.A. Schmidt, A. Siemiarczuk, A.C. Weedon, and J.R. Bolton, *J. Amer. Chem. Soc.*, **107**, 6112 (1985).

with measured redox values in *N*,*N*-dimethylformamide.

Possible reasons for the inadequacy of previous approaches to determining the exothermicity in different solvents are related to the limitations of Onsager theory. (An excellent treatment of the theory and its application is presented in the monograph of Böttcher.[41]) The Onsager reaction field model depends on several assumptions. The simple equation used in the above cases applies only for spherical particles between which there are no specific interactions, such as hydrogen bonding or complexation. The charge transfer dipoles generated in the molecules discussed above probably do not resemble spheres. Most instances of successful application of the theory appear to be in molecules of small dipole moment (μ=0-4D), whereas the cases cited report calculated dipole moments of 72D for the porphyrin-methylene amide-quinone[40] and 23D for the aromatic-dicyano compound.[37] Even though the former used a non-rigid spacer, a linear extended center-to-center separation of R=15 Å was assumed, much longer than the latter with R=5.8 Å. Nonlinear saturation effects may also cause a breakdown of the model at high or rapidly changing fields.[41] The dielectric is nonhomogeneous around the dipole cavity formed by the rather large molecules examined, and so a continuum approximation may not succeed.

Objectives of Current Research

---

[41] C.J.F. Böttcher, *Theory of Electric Polarization*, 2nd ed., volume I, Elsevier, Amsterdam, 1973.

The main objectives of the present research are to (a) design chemical models relevant to the primary process of bacterial photosynthesis that allow for theoretical interpretation; (b) synthesize the model compounds; (c) extract electron transfer rate constants under various conditions of solvent, driving force, and temperature; and, (d) compare experimental observations with the predictions and expectations of theory.

Chapter 2

Synthesis

Design of Rigid Porphyrin-Quinone Molecules.

In light of the previous systems of linked electron donor-acceptor systems, the need for a structurally well-defined case that is amenable to systematic investigation became manifest. The molecule selected for the present series of studies on photoexcited electron transfer reactions appears in Figure 1. It consists of a *meso*-phenyloctamethylporphyrin substituted at the *para* position of the benzene ring with a bicyclo[2.2.2]octane linker which then joins a *p*-benzoquinone moiety.

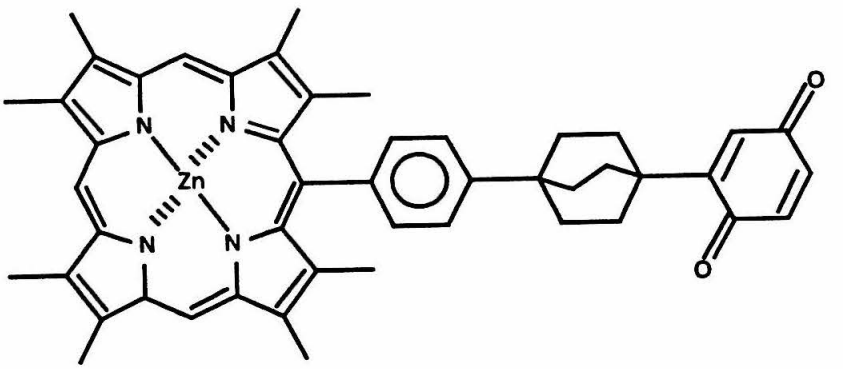

1

Figure 1. [{*meso* (*p*-Benzoquinone)bicyclo[2.2.2]octylphenyl}octamethylporphyrinato]zinc(II) (*ZnPLQ*).

The porphyrin mentioned was chosen as the electron donor for several rea-

sons. (a) It allows for visible light photoexcitation as the means of initiating the electron transfer reaction. (b) The large size and highly delocalized nature of the aromatic porphyrin chromophore preordains a small vibrational reorganization energy. Its small contribution to λ in conjunction with a large reaction exothermicity would enhance the possibility of observing inverted reactivity patterns discussed in the previous chapter. (c) Octaalkyl substitution on the porphyrin results in a 300 mV decrease in the oxidation potential of the porphyrin, when compared with the analogous reaction from the lowest excited singlet state of tetraarylporphyrins,[1] and consequently affords an increase of similar magnitude in the overall driving force of the forward reaction $^{1*}PLQ \longrightarrow P^{+\cdot}LQ^{-\cdot}$.

The bicyclo[2.2.2]octane linker has been used prior to the current work in studies of energy transfer between aromatics and carbonyls and electron exchange in aromatic anions[2,3] as well as intramolecular charge transfer reactions involving amine groups.[4] The principal advantage of using a fully hydrocarbon linker rather than amides or esters as done previously lies in its chemical inertness,

---

[1] J.-W. Führhop, in K.M. Smith, ed., *Porphyrins and Metalloporphyrins*, Elsevier, Amsterdam, 1975.

[2] H.E. Zimmerman and R.D. McKelvey, *J. Amer. Chem. Soc.*, **93**, 3638 (1971).

[3] H.E. Zimmerman, T.D. Goldman, T.K. Hirzel, and S.P. Schmidt, *J. Org. Chem.*, **45**, 3933 (1980).

[4] R.A. Beecroft, R.S. Davidson, D. Goodwin, and J.E. Pratt, *Pure App. Chem.*, **54**, 1605 (1982).

which permits its application in basic, neutral, mildly acidic, or nucleophilic conditions.

Another advantage is its structural rigidity, which enforces a fixed separation distance with an angle of 180° between the donor and acceptor (with the center of the linker as vertex). In addition, the bicyclo[2.2.2]octane is highly symmetric, thereby simplifying considerations of the presumed through-bond pathway for electron transfer. The straight angle relationship between donor and acceptor imposed by the bicyclo[2.2.2]octane linker is unique (even among rigid linked systems) in that the shortest path from donor edge to acceptor edge is through the bonding network, not through-space. Although a rotational distribution of porphyrin-quinone dihedral angles is allowed by the skeletal framework, the distance between the edge atoms of the porphyrin and quinone joining the linker 1,4-positions is held constant by the rigid linker. Furthermore, the use of the highly symmetrical hydrocarbon linker makes possible an investigation of the distance dependence of electron transfer. The construction of porphyrin-quinone systems with additional bicyclo[2.2.2]octane units has recently been achieved.[5,6] As treated by Beratan and Hopfield,[7] a linear series of bicyclo[2.2.2]octane moi-

---

[5] B.A. Leland, *Dissertation*, California Institute of Technology, 1986.

[6] A.D. Joran, B.A. Leland, G.G. Geller, J.J. Hopfield, and P.B. Dervan, *J. Amer. Chem. Soc.*, , **106**, 6090 (1984).

[7] D.N. Beratan and J.J. Hopfield, *J. Amer. Chem. Soc.*, **106**, 1584 (1984).

eties is thought to create a periodic potential, and by application of Bloch's Theorem provides a method for determining the distance dependence of the decay of wavefunctions and the tunneling matrix element in cases of long-distance electron transfer. For several different linkers decay constants ϵ, as a function of redox energy, were determined characterizing the change in the tunneling matrix element T_{ab} with distance. Experimental work relating to the distance dependence in rigid porphyrin-quinone systems will be examined at length in due course.[5]

The decision to use the *p*-benzoquinone moiety as the electron acceptor was based primarily on its having the appropriate redox properties and on its synthetic versatility. In particular, its ability to be inserted in a robust, masked form and then deprotected selectively is valuable. The quinone group also allows for the fairly convenient variation of reaction driving force by altering the substituents on the ring. It should be noted that a possible limitation of using quinones in this kind of study is its large solvational and vibrational reorganization energy, compared with larger, more delocalized chromophores. This family of porphyrin-quinones would permit the investigation of the energy gap laws proposed by Marcus,[8] Hopfield,[9] and Jortner,[10] which are thought to govern the

---

[8] (a) R.A. Marcus, *J. Chem. Phys.*, **24**, 966 (1956). (b) R.A. Marcus, *Ann. Rev. Phys. Chem.*, **15**, 155 (1964).

[9] J.J. Hopfield, *Proc. Natl. Acad. Sci. U.S.A.*, **71**, 3640 (1974).

[10] J. Jortner, *J. Chem. Phys.*, **64**, 4860 (1976).

electron tranfer kinetics of the charge separation processes of photosynthesis and oxidative phosphorylation.[11]

With structural requirements set forth, need remained for an adequate synthetic route. Because of its expected length and complexity, a convergent synthetic scheme is necessary in order to obtain efficiently sufficient quantities of the porphyrin-quinones for characterization and physical studies. The remainder of this chapter will review our efforts at the synthesis of these molecules, including the *cul de sacs* found early on.

Synthesis of Porphyrin-Quinones: Direct Coupling Without a Phenyl Spacer

Several strategies to a directly coupled system lacking a phenyl spacer (Figure 2) were pursued. Despite synthetic efforts over a period of two years, various chemical factors thwarted these attempts. A brief recapitulation of these unfruitful routes is of interest for future workers in the field.

A convergent synthesis of a porphyrin-quinone linked only by a bicyclo[2.2.2]octane (and no phenyl group in between) can be imagined by dividing the molecule into roughly three equal subdivisions: the porphyrin, the linker, and the quinone. A large body of synthetic technology exists for each part, but the question at the outset was unclear whether all three would be mutually com-

---

[11] (a) D. DeVault, *Quart. Rev. Biophys.*, **13**, 387 (1980). (b) D. DeVault, *Quantum-Mechanical Tunneling in Biological Systems*, 2nd ed., Cambridge University Press, New York, 1984.

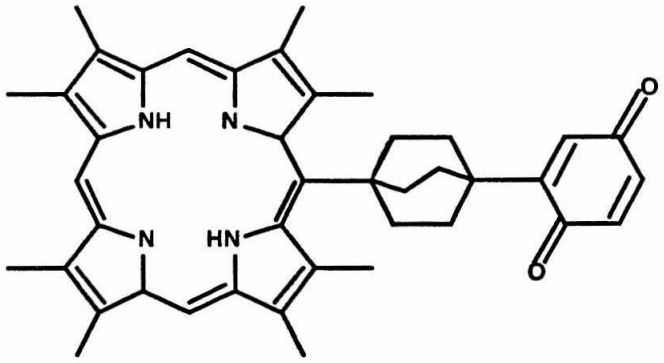

Figure 2. Directly Coupled Porphyrin-Quinone.

patible with the formation of each other. The key issue concerned the chemistry of forming covalent bonds between each part. An early strategy was to establish the linker-porphyrin bond before macrocyclization. Thus, while reducing convergency, the difficult linkage between the tertiary center and the porphyrin might take place. Badger and his collaborators had modified the classic MacDonald-Woodward porphyrin synthesis[12] to obtain *meso*-methylated compounds.[13]

To adapt the MacDonald-Woodward methodology for our purposes, we

---

[12] G.P. Arsenault, E. Bullock, and S.F. MacDonald, *J. Amer. Chem. Soc.*, **82**, 4384 (1960).

[13] G.M. Badger, R.A. Jones, and R.L. Laslett, *Aust. J. Chem.*,**17**, 1157 (1964).

needed to be able to make a dipyrrolic unit with the linker-quinone attached to the methylene bridge. The route illustrated in Scheme I depends on the *in situ* decarboxylation of the *meso*-substituted 5,5′-dicarboxy-2,2′-dipyrrylmethane, and electrophilic reaction with 5,5′-diformyl-2,2′-dipyrrylmethane. In the scheme we show a t-butyl group where the bicyclo[2.2.2]octyl moiety would be. Model studies used trimethylacetaldehyde instead of the precious elaborated aldehyde. The dipyrrolic reactant 3,3′,4,4′-tetramethyl-2,2′-dipyrrylmethane-5,5′-dicarboxylic acid was prepared by the standard procedure of condensing 5-unsubstituted ethyl 3,4-dimethyl-2-carboxylate with paraformaldehyde (EtOH, catalytic HCl, reflux, 4 hrs.)[13] and subsequent saponification with sodium hydroxide (10%, EtOH, H_2O, reflux, 8 hrs.). In the preparation of the *meso*-t-butyldipyrrlymethane, *p*-toluenesulfonic acid was found to be a preferable catalyst to HCl, and the higher boiling solvent toluene replace ethanol. The precursor dimethylpyrrole ester was made by a modification of Kleinspehn's route.[14]

Using the conditions which gave the highest yield of decamethylporphyrin in Badger's work,[13] we attempted to couple the *meso*-t-butyldipyrrylmethane diacid with diformyldipyrrylmethane. After ~18 hrs. of reflux (CH_3OH, catalytic $HClO_4$, O_2, darkness), the reaction was worked up. UV-visible spectra showed that no porphyrin was present. Dipyrryl units were indeed condensing, but were failing to cyclize to form porphyrin. This resistance to

---

[14] G.G. Kleinspehn, *J. Amer. Chem. Soc.*, **77**, 1546 (1955).

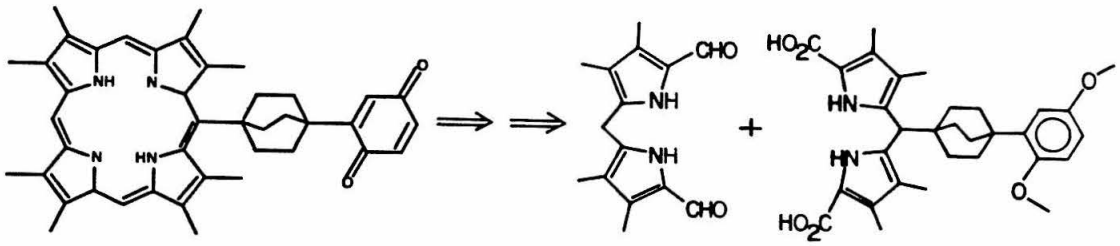

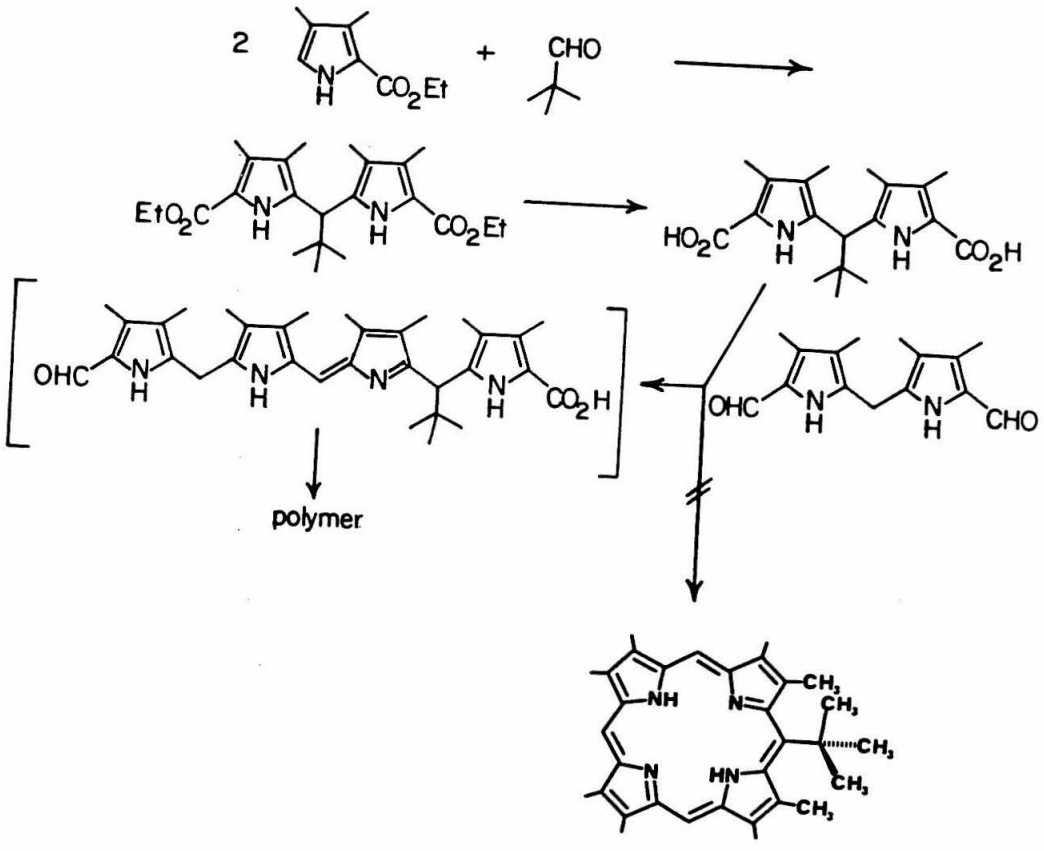

Scheme I. MacDonald-Woodward Strategy.

closure is consistent with the lack of known porphyrins with bulky teritiary alkyl *meso* groups. The closest known structure is a [5,15-bis(t-butyl)-5,15-dihydroporphyrinato]hydroxoiron(III) (porphodimethene), for which a crystal structure has been published.[15]

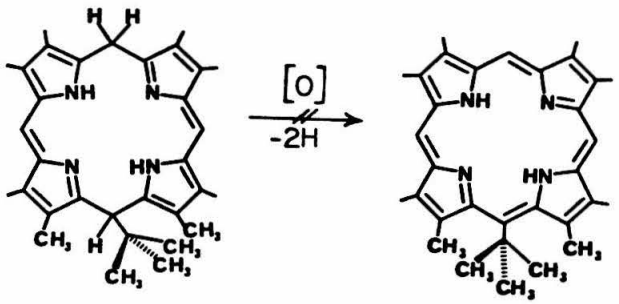

The restriction imposed by steric hindrance compelled us to modify the route. A reasonable modification, we thought, involved removing the two methyl groups flanking the *meso*-substituent, leaving protons. The necessary dimethyldipyrrylmethane diacid or dialdehyde might be prepared *via* the diester from benzyl 3-methylpyrrole-2-carboxylate[16a] under acid catalysis as described

---

[15] J.W. Buchler, K.L.Lay, Y.J. Lee, and W.R. Scheidt, *Angew. Chem. Int. Ed. Engl.*, **21**, 432 (1982).

[16] (a) W.G. Terry, A.H. Jackson, G.W. Kenner, and G. Kornis, *J. Chem. Soc.* , 4389 (1965). (b) R.A. Jones and G.P. Bean, *The Chemistry of Pyrroles*, Academic Press, London, 1977.

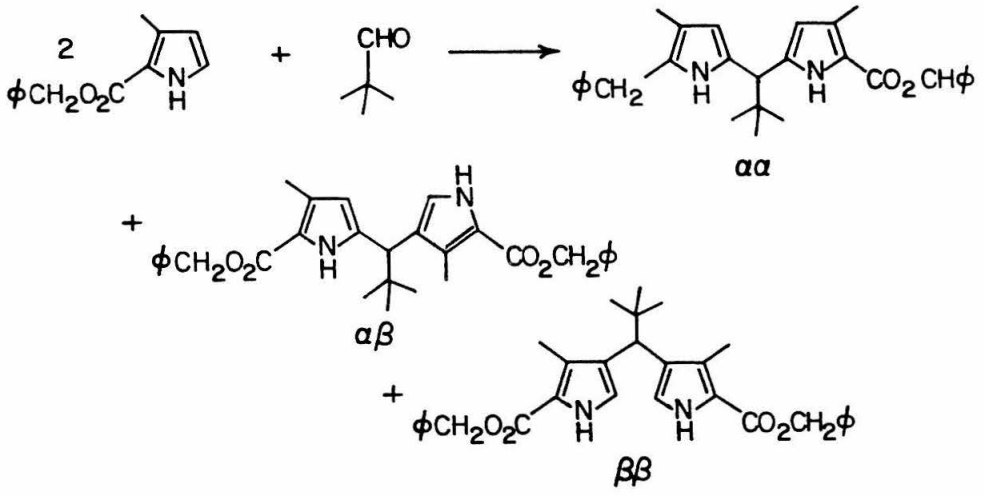

Scheme II. Benzyl pyrrole ester condensation.

before, however, in much lower yield and as a bad mixture of isomers.

The ester in the pyrrole benzyl ester is strongly electron-withdrawing, and as such is a *"meta"* orientation director in pyrrole electrophilic substitution chemistry.[16b] Electron-donating groups such as alkyls are *"ortho/para"* directors. Consequently, there is insufficient preference of *αα versus αβ* or *ββ* regioisomers.

Another series of trials intended to produce a *meso*-substituted dialdehyde for condensation into a porphyrin by the MacDonald-Woodward method focused on protected aldehyde precursors. Dithioacetals of pyrrole aldehydes were known

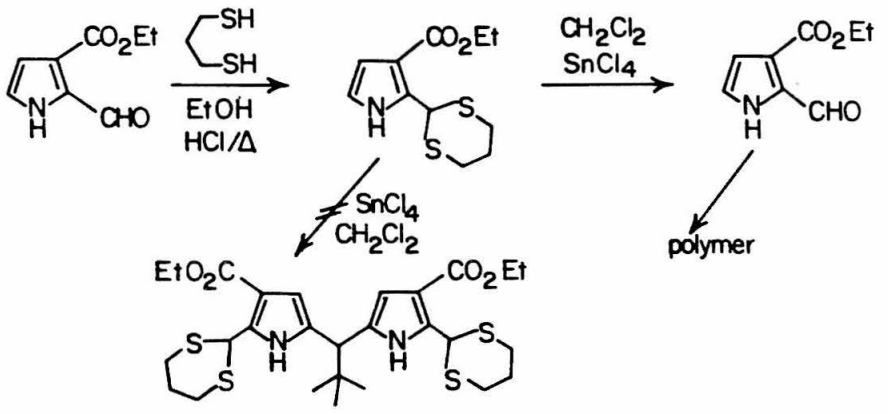

Scheme III. Dithiane pyrrole condensation.

to be fairly stable,[17] but should have the right electronic properties to activate the pyrrole for electrophilic substitution at the 5-position exclusively. The aldehyde, prepared by a Hantzsch synthesis[18] from α,β-dibromoethyl acetate, ethyl 4,4-diethoxy-3-oxobutanoate, and ammonia in low yield (23%), was converted to a thioacetal using propane-1,3-dithiol (EtOH, HCl, 100°C, 25 mins), to give the pyrrole dithiane in 70% yield. Treatment of the dithiane and neopentylaldehyde with an acid catalyst gave no dipyrrylmethane, but rather a good return of

---

[17] P.S. Clezy, C.J.R. Fookes, D.Y.K. Lau, A.W. Nichol, and G.A. Smythe, *Aust. J. Chem.*, **27**, 357 (1974).

[18] (a) E. Bisagni, J.-P. Marquet, and J. André-Louisfert, *Bull. Soc. Chim. France*, (2), 637 (1968). (b) M.W. Roomi and S.F. MacDonald, *Can. J. Chem.*, **48**, 1689 (1970).

the transthioacetal of the neopentylaldehyde and the deprotected pyrrole aldehyde, which polymerized after prolonged heating. By contrast, reaction of 3-(carboethoxy)-2-methylpyrrole with the same alkyl aldehyde gave a good yield of the expected dipyrrylmethane.[19]

In further experiments, statistical tetrapyrrole cyclization with one or more equivalents of the neopentyl aldehyde used as a model substrate provided no product identified as a neopentyl porphyrin. Alkyl aldehydes are much less reactive than aryl aldehydes on the basis of resonance stabilization of the benzylic cation intermediate. Hindered neopentylaldehydes react even more lethargically, enough so as to allow a multitude of destructive processes, *e.g.*, polymerizations, to occur.

Synthesis of Porphyrin-Quinones: Phenylbicyclo[2.2.2]octane Spacer

In view of the ring closure difficulty, a phenyl ring was inserted between the hydrocarbon moiety and the porphyrin to alleviate the steric bulk of the bicyclo[2.2.2]octane moiety. Furthermore, an aromatic aldehyde was expected to be sufficiently reactive to condense efficiently with pyrrole derivatives under aromatic electrophilic substitution conditions in the formation of the linker-porphyrin bond.

---

[19] *Cf.* H. Fischer and F. Schubert, *Hoppe-Seyler's Z. fur Phys. Chem.*, **155**, 88 (1926).

The preparation of the key aldehyde intermediate **16** is shown in Scheme IV . The first six steps were known.[20] From the bromination of **11** on, all reactions represent new chemistry. The bromination of 4-phenyl-1-methoxybicyclo[2.2.2]octane **11** uses a modification of Kochi's method (bromine/benzoyl peroxide/lithium bromide/acetonitrile),[21] and proceeds to completion only in the presence of excess bromine. The bridgehead benzoate is the initial product formed (identified by ^{1}H NMR and ^{13}C NMR), but is readily hydrolyzed on treatment with potassium hydroxide in water/acetonitrile, giving the required 4′-bromophenylbicyclo[2.2.2]octan-1-ol **12** in good yield (80-90%). Friedel-Crafts reaction in trichloroethylene with 1,4-dimethoxybenzene in the presence of *p*-toluenesulfonic acid/boron trifluoride gas gave the expected substitution product **13** after 24 hours of heating at reflux (in about 55% yield). Metal-halogen exchange using n-butyllithium in tetrahydrofuran at -78°C, followed by formylation with excess *N,N*-dimethylformamide, afforded the key intermediate 2″,5″-dimethoxyphenyl-4′-bicyclo[2.2.2]octyl-4-benzaldehyde **16** (yield, 80-90%).

The aldehyde **16** was condensed with an equivalent of ac-biladiene **30**

---

[20] (a) E.C. Horning, M.G. Horning, M.S. Fish, and M.W. Rutenberg, *J. Amer. Chem. Soc.*, **74**, 773 (1952). (b) J.S. Swenton, R.M. Blankenship, and R. Sanitra, *J. Amer. Chem. Soc.*, **97**, 4941 (1975). (c) K.-I. Morita and T. Kobayashi, *J. Org. Chem.*, **31**, 229 (1966). (d) J. Colonge and R. Vuillemet, *Bull. Soc. Chim. France*, 2235 (1961). (e) Z. Suzuki and K. Morita, *J. Org. Chem.*, **32**, 31 (1967).

[21] J.K. Kochi, B.M. Graybill, and M. Kurz, *J. Amer. Chem. Soc.*, **86**, 5257 (1964).

(see below) in boiling methanol in the presence of hydrobromic acid in glacial acetic acid (Scheme VI).[22] The porphyrin-linker-dimethoxybenzene **31** was converted in excellent yield to the porphyrin-hydroquinone using boron triiodide in dichloromethane.[23]

This reagent was found far superior to the usual reagent boron tribromide. Boron triiodide gave fewer side reactions, shorter reaction times, and cleaner product. The oxidation to porphyrin-quinone **1** could either be carried out at this point or delayed till after metallation. It was found that the oxidation occurs *in situ* during work-up of the ether cleavage if basic conditions (ammonia or sodium carbonate) were used. If the alternate order were used, lead dioxide was an efficient oxidant for the process.

Preparation of ac-Biladiene **30**

While octamethylporphyrins are much less soluble than the octaethyl compound, we decided in favor of the methyl. Not only would the ^{1}H NMR be simpler to interpret, it would be more straightforward to make the octamethylporphyrin rather than the octaethyl compound because the starting crotonic ester used in the synthesis of the former is needed in quantities of hundreds of grams and is commercially available, whereas the 2-pentenoic ester needed for the ethyl deriva-

---

[22] D. Harris, A.W. Johnson, and R. Gaete-Holmes, *Bioorganic Chem.*, **9**, 63 (1980).

[23] J.M. Lansinger and R.C. Ronald, *Synth. Commun.*, **9**, 341 (1979).

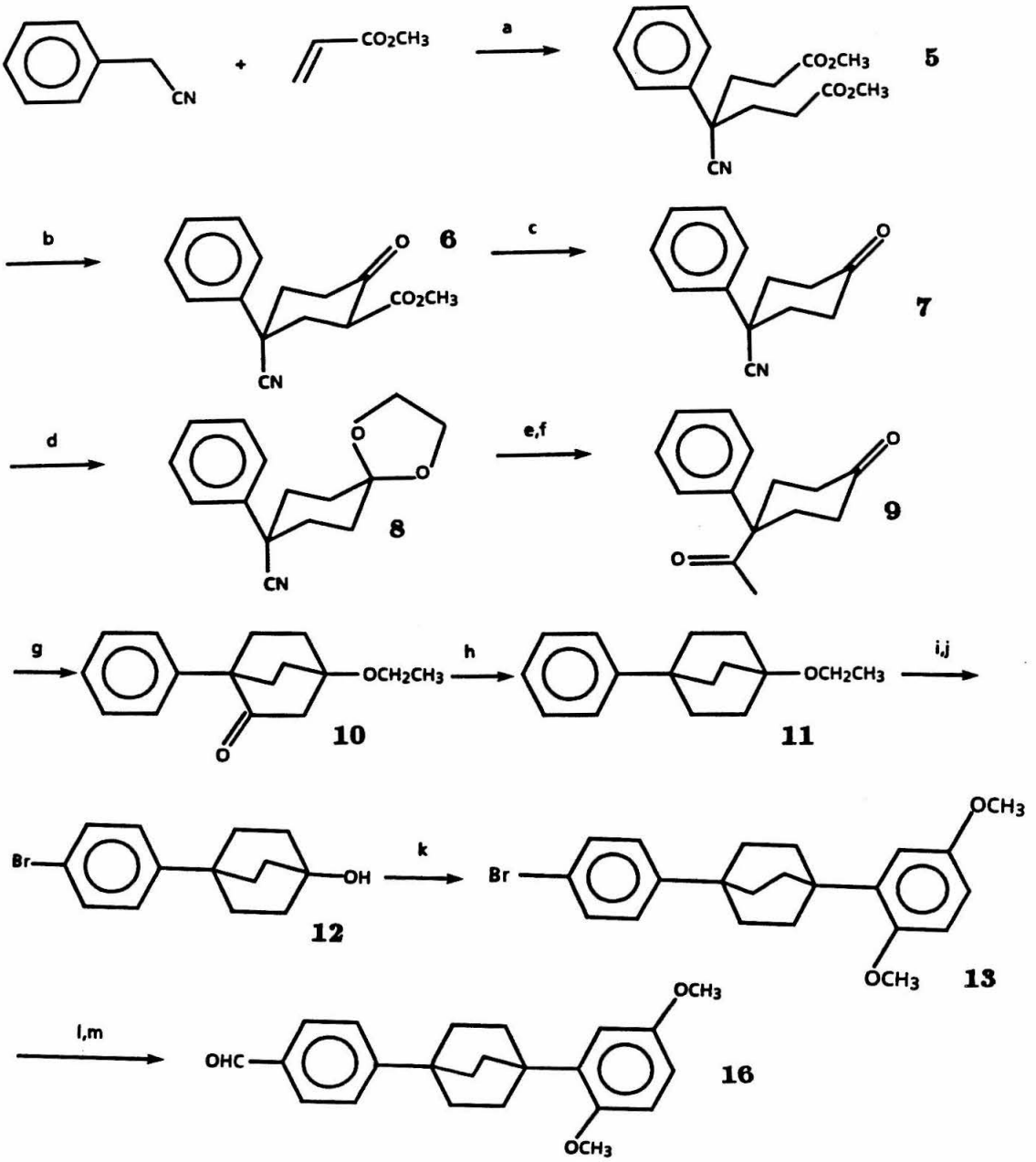

Scheme IV. Synthesis of Key Intermediate Aldehyde **16.**

Notes to Scheme IV: a, Triton B, dioxane, Δ. b, NaH, toluene, MeOH, Δ. c, DMSO, NaCl, H_2O, Δ. d, ethylene glycol, *p*-TsOH, toluene, azeotrope. e, MeMgBr, benzene, ether, Δ. f, HCl, H_2O, Δ. g, $CH(OEt)_3$, EtOH, HCl. h, NH_2NH_2, diethylene glycol, KOH, 240°. i, Br_2, LiBr, Bz_2O_2, CH_3CN. j, KOH, H_2O. k, dimethoxybenzene, trichloroethylene, BF_3, *p*-TsOH, Δ. l, n-BuLi, -78°, THF. m, DMF, -78°.

---

tive is not. We chose the *ac*-biladiene **30** (Scheme V) as a porphyrin precursor because of its adaptability to incorporate nearly any substituted benzaldehyde desired (*e.g.*, **16-18, 52**).[22]

As almost the same number of steps go into the ac-biladiene pathway as the aldehyde intermediate, this route is also efficiently convergent. While the *ac*-biladiene **30** itself is sensitive to light and air, and so must be freshly made before use, its precursors 5,5′-diformyl-3,3′,4,4′-tetramethyl-2,2′-dipyrrylmethane **29** and 3,4-dimethylpyrrole **20** are stable when stored at -20°C. The preparation of these intermediates is essentially the work of Paine, Woodward, and Dolphin,[24] but a few improvements were made to obtain larger quantities. In particular, the 2-cyano-(2-carboethoxy)vinyldimethylpyrrole **22** could be more readily obtained by Vilsmeier-Haak formylation[25] on 3,4-dimethylpyrrole **20** using benzoyl chloride/DMF rather than by proceeding through a somewhat less efficient multistep process ending in iodinative decarboxylation and hydrogenative dehalogenation, as originally designed.[24] The dimethylpyrrole **20** was readily made by

---

[24] J.B. Paine, III, R.B. Woodward, and D. Dolphin, *J. Org. Chem.*, **41**, 2826 (1976).

[25] R. Chong, P.S. Clezy, A.J. Liepa, and A.W. Nichols, *Aust. J. Chem.*,**22**, 229 (1969).

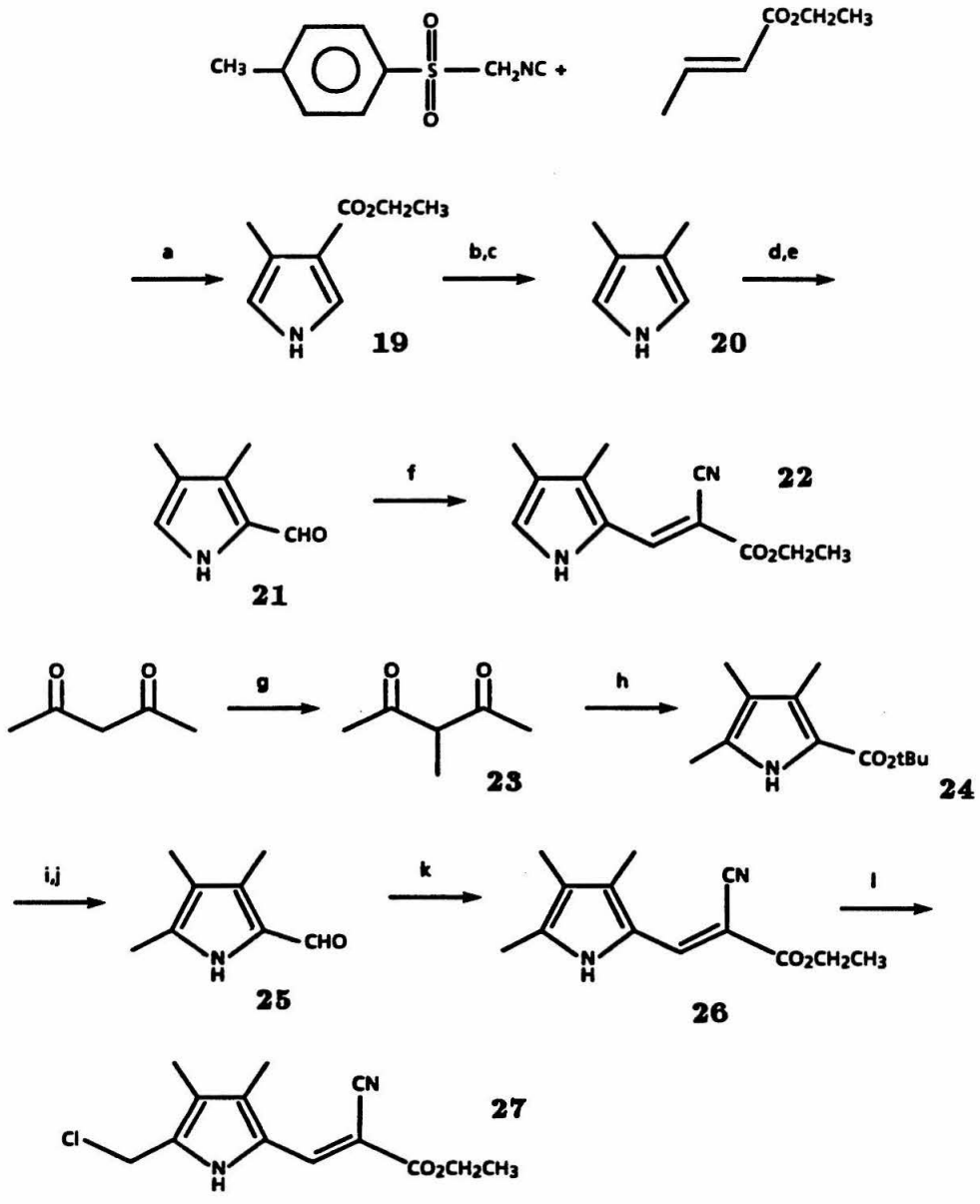

Scheme V. ac-Biladiene Synthesis.

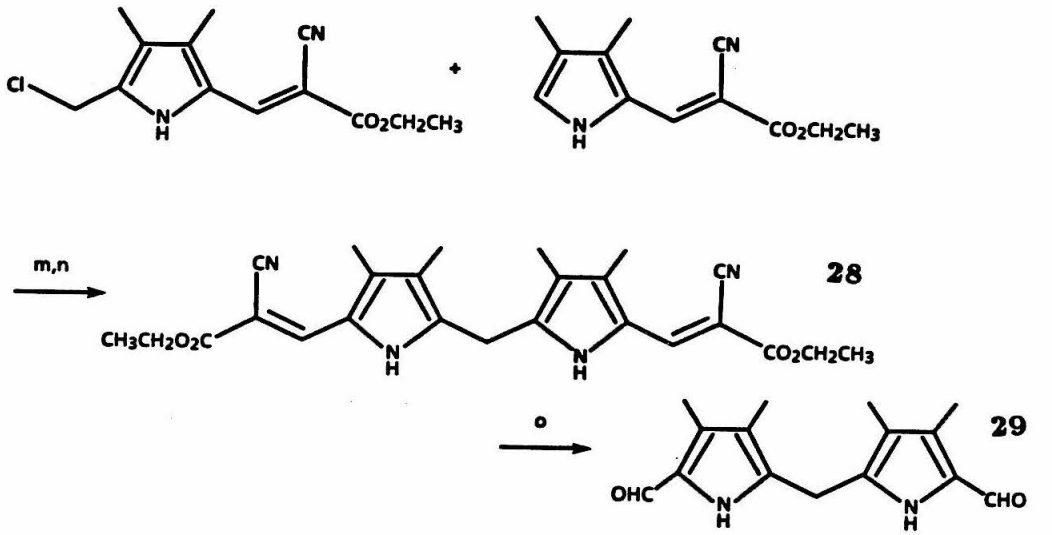

Notes to Scheme V: a, NaH, DMSO, Et_2O. b, Sodium bis(methoxyethoxy)aluminumhydride, toluene, 25°. c, HCl, H_2O. d, DMF, benzoyl chloride. e, sodium carbonate, water. f, ethyl cyanoacetate, diethylamine, benzene azeotrope. g, MeI, K_2CO_3, Δ. h, t-butyl acetate, sodium nitrite, acetic acid $\rightarrow$ Zn, Δ. i, DMF, benzoyl chloride. j, ammonium hydroxide. k, ethyl cyanoacetoacetate, diethylamine, benzene. l, SO_2Cl_2, CH_2Cl_2. m, $SnCl_4$. n, HCl, H_2O. o, NaOH, MeOH, Δ.

a heterocyclic ring closure using *p*-tosylmethylisocyanide,[26] followed by reduction with sodium bis(methoxyethoxy)aluminumhydride.[27] The dimethylpyrrole **20** condensed with the dipyrrylmethanedialdehyde **29** to produce high yields of the ac-biladiene dihydrobromide **30**.[28]

[26] A.M. van Leusen, H. Siderius, B.E. Hoogenboom, and D. van Leusen, *Tetrahedron Lett.*, 5337 (1972).

[27] D.O. Chang, T.L. Bowman, and E. LeGoff, *J. Heterocyclic Chem.*, **13**, 1145 (1976).

[28] A.W. Johnson and I.T. Kay, *J. Chem. Soc.* 1620 (1965).

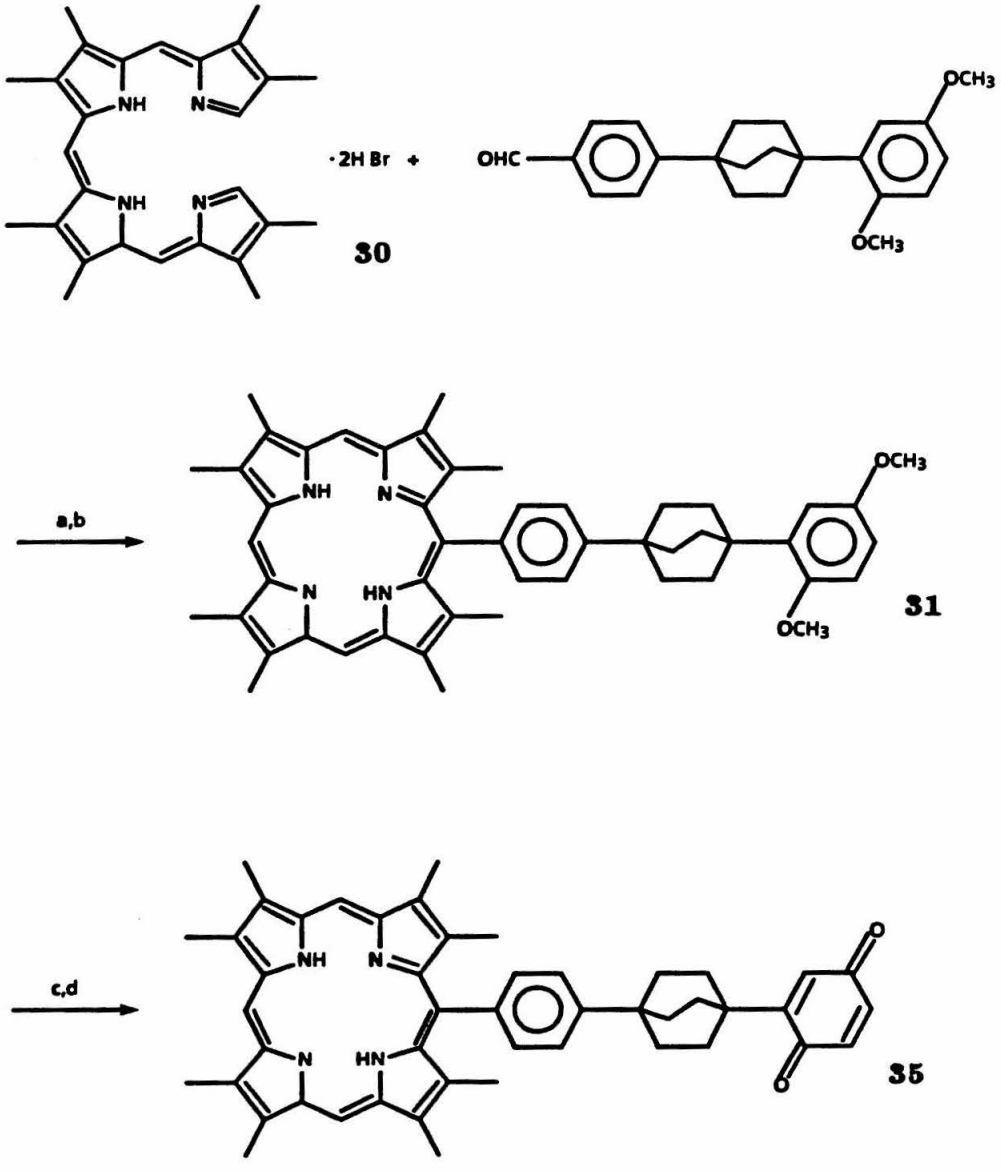

Scheme VI. Preparation of *ZnPLQ*.

Scheme VI (continued)

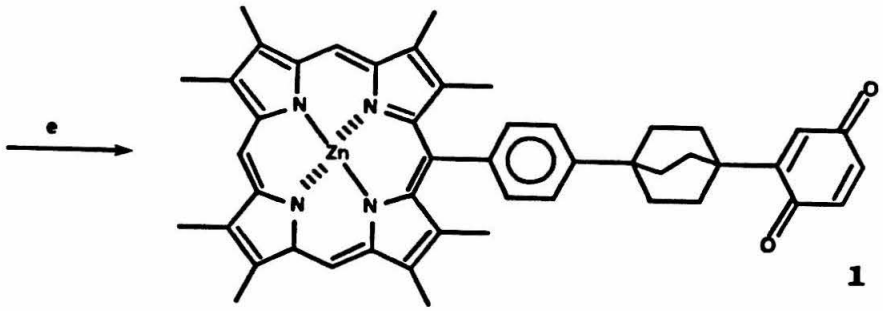

1

Notes for Scheme VI: a, HBr, HOAc, MeOH, Δ, air. b, $NaHCO_3$. c, BI_3, CH_2Cl_2, 25°. d, ammonium hydroxide, air. e, $Zn(OAc)_2 \cdot 2H_2O$, $CHCl_3$, MeOH.

Synthesis of Porphyrin-Quinones with Modified Quinones

In order to probe the validity of the energy gap laws discussed briefly in Chapter 1, a series of porphyrins rigidly coupled to several differently substituted quinones **2-4** was prepared. Unlike previous efforts in this area, the series chosen actually represents a ***structurally*** homologous series of reactions; that is, the porphyrin electron donor is constant in the entire series, and the quinone electron acceptors are all derivatives of *p*-benzoquinone, either mono-, di-, or trisubstituted with alkyl, halogen, or cyano groups. In this way the free energy of reaction may be altered systematically over a reasonable range, while avoiding structurally very different compounds. The question remains open of whether a

structurally homologous series is a sufficient condition for a *functionally* homologous series.

The synthetic preparation of the derivatives of the parent porphyrin-quinone is based on several key intermediates. The 4-methyl- and 3,4-dimethyl-4-quinone systems were produced from 4-bromophenylbicyclo[2.2.2]octyl alcohol **12** by a Friedel-Crafts aromatic substitution reaction with 2-methyl-1,4-dimethoxybenzene and 2,3-dimethyl-1,4-dimethoxybenzene **40**, respectively. Subsequent steps, as shown in Scheme VI, parallel those followed for construction of the parent porphyrin-quinone. Transmetallation with n-butyllithium in tetrahydrofuran at -78°C and formylation with *N,N*-dimethylformamide afforded the important arylbicyclooctylbenzaldehyde intermediates **17, 18**. Condensation of the aldehydes with ac-biladiene dihydrobromide **30** yielded the free-base porphyrin-dimethoxyarenes **32, 33**.

The porphyrin-diethers **32, 33** can be deprotected with boron triiodide as above and oxidized *in situ* during work-up. In contrast to the parent unsubstituted and the cyano hydroquinone, the methyl and dimethyl derivatives have very strong tendencies to oxidize merely in the presence of oxygen and aqueous base (e.g., ammonia or sodium carbonate); the parent unsubstituted hydroquinone also oxidizes, but with a less favorable equilibrium constant, and so requires more vigorous conditions. The preparative ease of forming the porphyrin-quinone is inversely related to the oxidation potential of the hydroquinone. The cyanoquinone

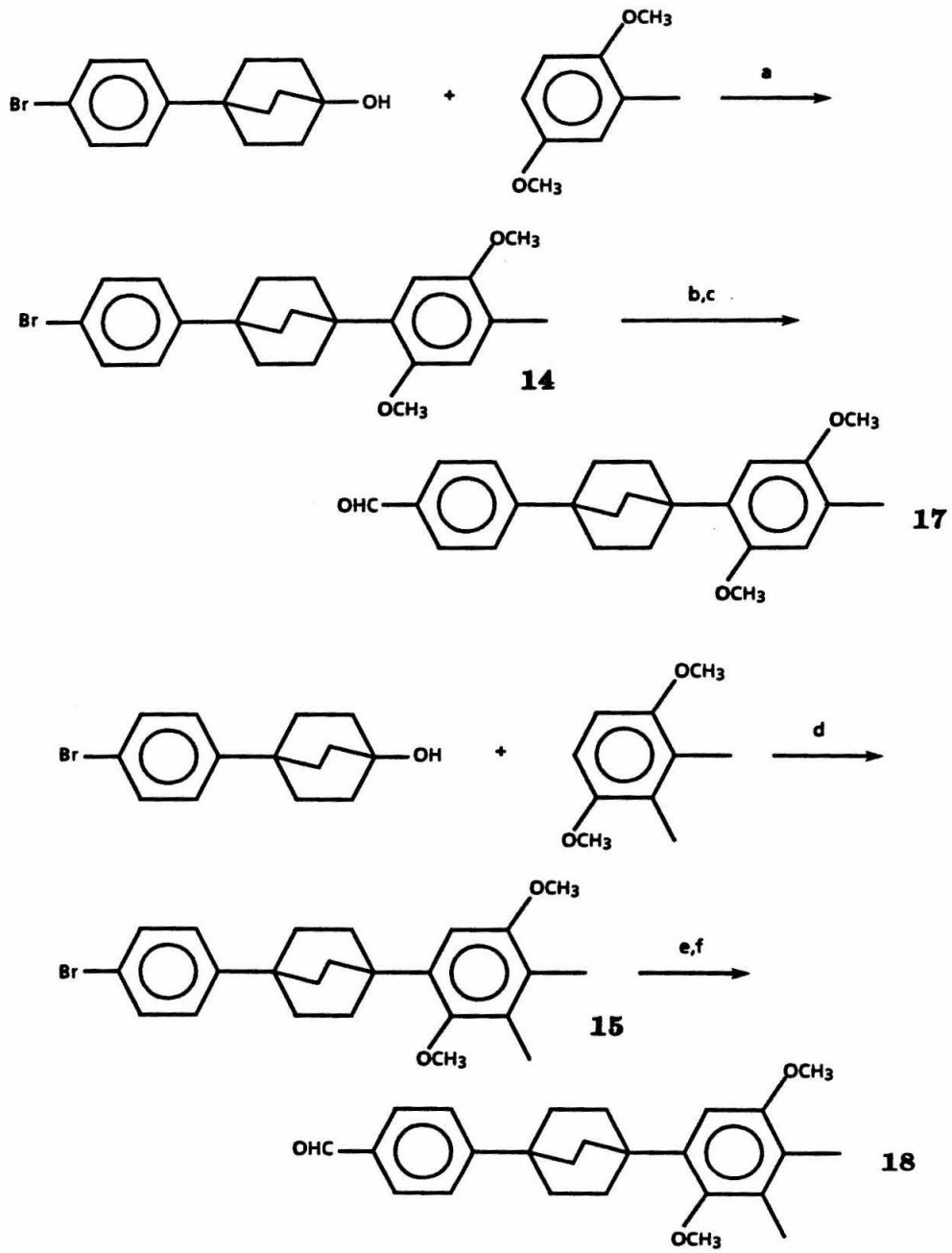

Scheme VII. Aldehyde intermediates **17, 18** for modified porphyrin-quinone synthesis.

Notes for Scheme VII: a, BF_3, *p*-TsOH, trichloroethylene, Δ. b, n-BuLi, THF, -78°. c, DMF, -78°. d, BF_3, *p*-TsOH, trichloroethylene, Δ. e, n-BuLi, THF, -78°. f, DMF, -78°.

4 formed in low yield even in the presence of strong oxidants (e.g., silver oxide or 2,3-dichloro-5,6-dicyanoquinone), but because of its extreme sensitivity could not be purified by chromatography and thus could not be characterized rigorously.

The synthetic steps leading to the haloquinones (4-bromo, 4-chloro, and 3,4-dichloro) were carried out by Burton Leland, starting with dimethoxyphenylbicyclo[2.2.2]octylbenzaldehyde **10**.[29] Attempts were made to synthesize the key intermediate cyanodimethoxyphenylbicyclo[2.2.2]octylbenzaldehyde **48** by a route analogous to that used to make dimethoxyphenylbicyclo[2.2.2]octylbenzaldehydes **10-12** (Scheme IV), that is, by transmetallation of the bromobenzene and formylation with *N,N*-dimethylformamide. Using a variety of conditions, including n-butyllithium, t-butyllithium, and lithium metal, to carry out the transmetallation, this method did not succeed. The cyano group evidently reacts with the organolithium or lithium metal preferentially, thereby making the scheme unsuitable for the preparation of the cyano quinone precursor **52**.

An alternate sequence (Scheme IX) was developed utilizing a methyl group as a protected aldehyde function. The pathway is similar to the route described above for synthesizing the other substituted and also the unsubstituted

[29] B. A. Leland, *Dissertation*, California Institute of Technology, 1986.

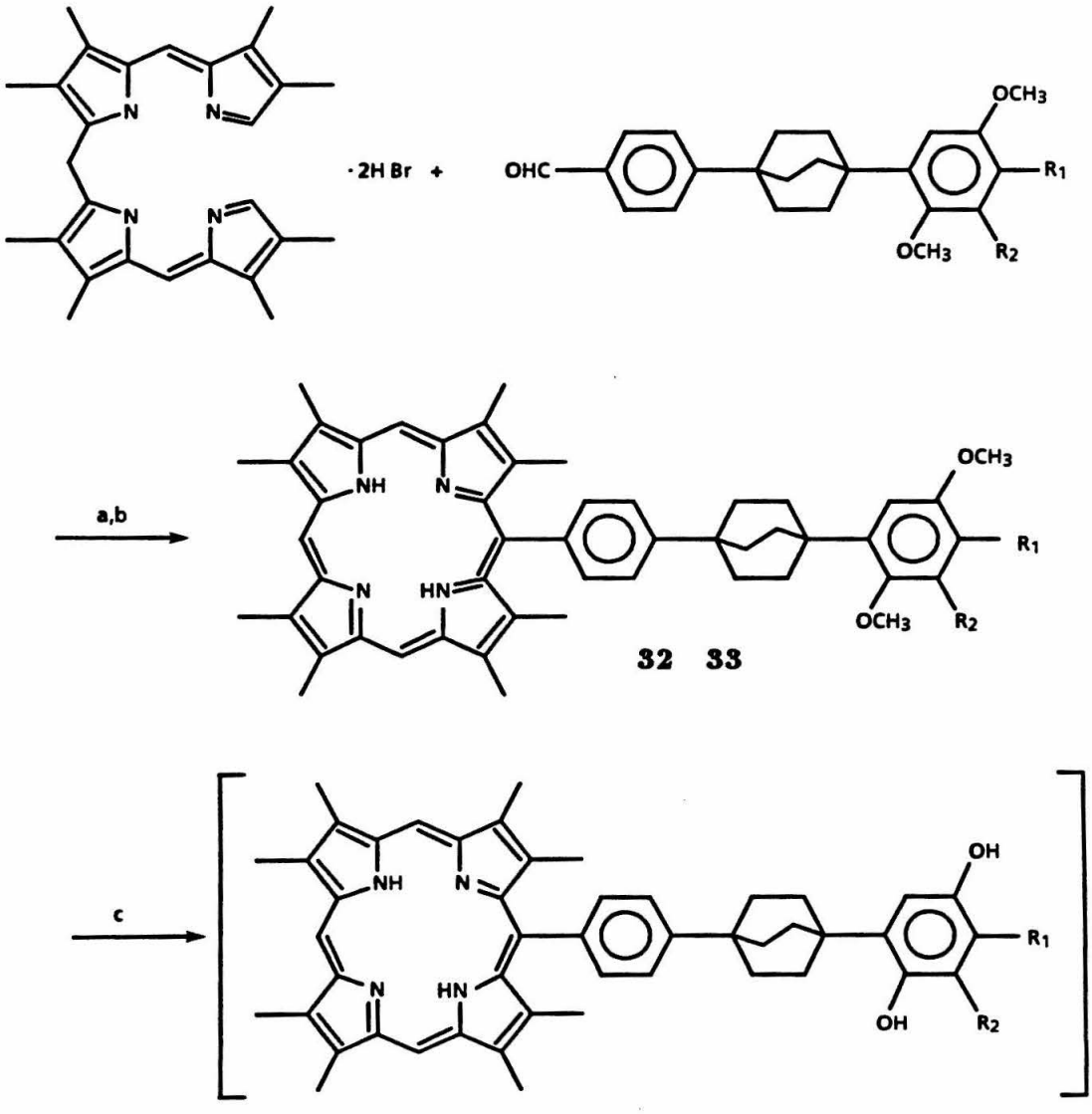

Scheme VIII. Modified porphyrin-quinones.

Scheme VIII (continued).

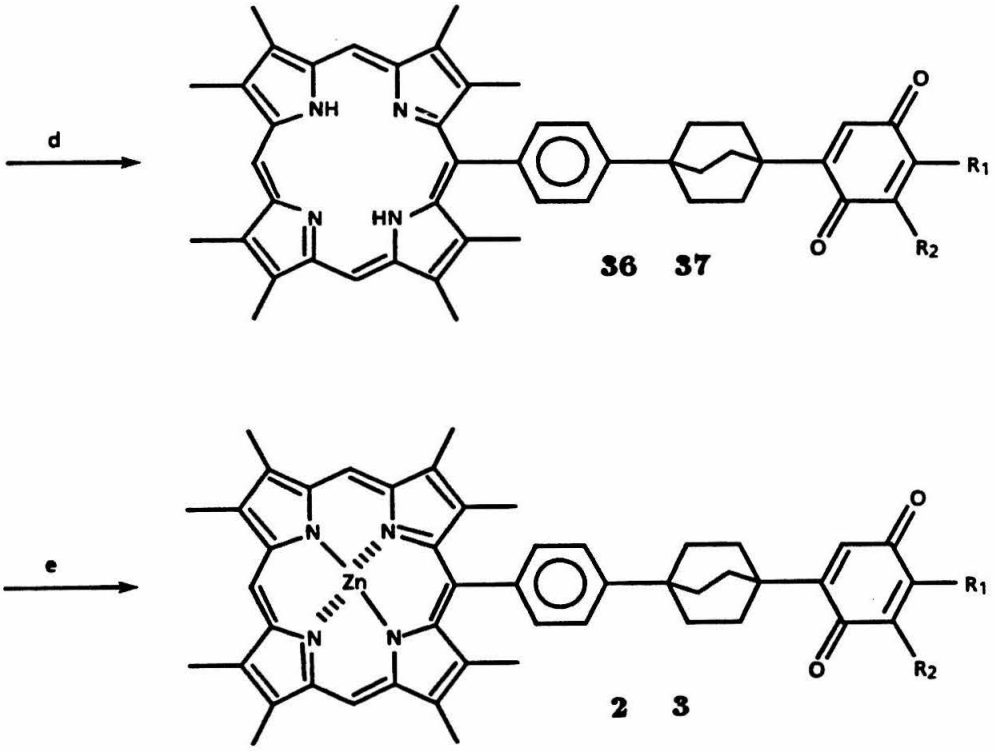

Notes for Scheme VIII: a, HBr, HOAc, MeOH, Δ, air. b, $NaHCO_3$. c, BI_3, CH_2Cl_2. d, ammonium hydroxide, air. e, $Zn(OAc)_2 \cdot 2H_2O$, MeOH, $CHCl_3$.

dimethoxybenzene aldehydes, starting with *p*-tolylacetonitrile instead of phenylacetonitrile, until the Friedel-Crafts step in which dimethoxybenzene is substituted by the bicyclo[2.2.2]octane moiety. The next steps establish the cyano substituent by Lewis acid-catalyzed formylation[30] with α,α-dichloromethyl methyl ether and stannic chloride followed by oximine formation using hydroxylamine

[30] A. Rieche, H. Gross, and E. Höft, *Org. Syn.*, **47**, 1 (1967).

hydrochloride and sodium formate in formic acid. The subsequent chemistry unmasks the methyl group. Free-radical bromination with *N*-bromosuccinimide and benzoyl peroxide provided a good yield of the benzylic bromide **51** (and no evidence according to high field ^{1}H NMR for aromatic ring substitution on either aromatic nucleus).

Oxidation with dimethyl sulfoxide in the presence of a weak base (sodium bicarbonate) to scavenge hydrobromic acid produced by the reaction afforded the desired cyanoarylbicyclooctylbenzaldehyde **52** in satisfactory quantities for porphyrin synthesis. Another method used to carry out this benzylic oxidation involved the sodium salt of 2-nitropropane and sodium ethoxide in absolute ethanol at room temperature,[31] and yielded a cleaner product although it was more tedious to execute on a small scale.

The substituted cyanoaryl aldehyde was condensed with the ac-biladiene dihydrobromide **30** to provide the expected free-base porphyrin hydroquinone dimethyl ether as the major product. Varying amounts of a corrole side-product were also obtained depending on the age of the ac-biladiene, the freshness of the acid catalyst (glacial acetic acid saturated with hydrogen bromide gas), and possibly concentration. If the catalyst appears yellow (perhaps due to polymerization or oxidation), the condensation reaction yields little or no porphyrin, and only

---

[31] H.B. Hass and M.L. Bender, *Org. Syn.*, **30**, 71 (1950).

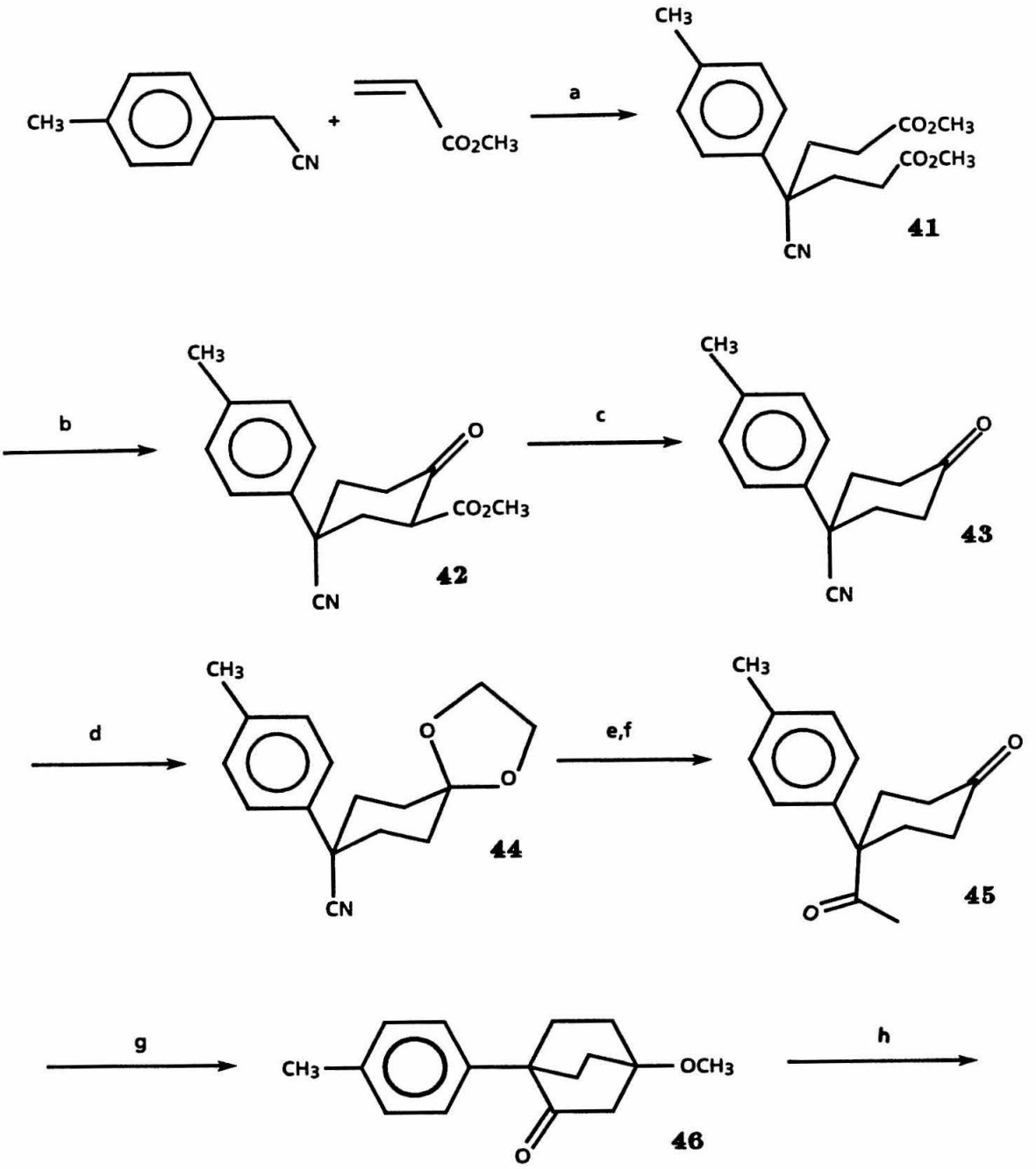

Scheme IX. Route to the Cyano Aldehyde Intermediate **52**.

Scheme IX (continued).

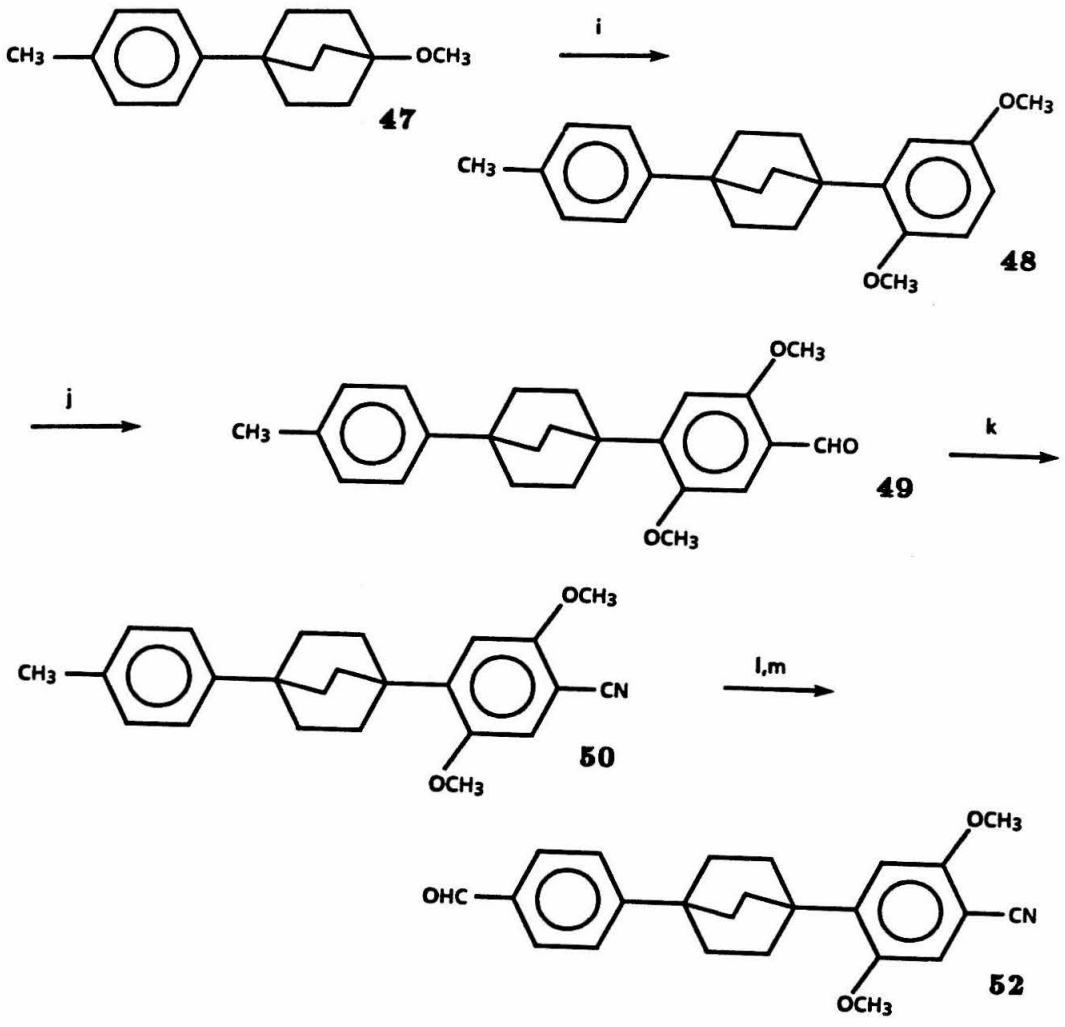

Notes to Scheme IX: a, Triton B, dioxane, Δ. b, NaH, toluene, MeOH, Δ. c, DMSO, NaCl, H_20, Δ. d, ethylene glycol, *p*-TsOH, toluene azeotrope. e, MeMgBr, benzene, Et_2O, Δ. f, HCl, H_2O, Δ. g, $CH(OMe)_3$, MeOH, HCl. h, NH_2NH_2, KOH, diethylene glycol, 240-260°. i, dimethoxybenzene, BF_3, *p*-TsOH, trichloroethylene. j, $SnCl_4$, $Cl_2CHOCH_2OCH_3$. k, $H_2NOH{\cdot}HCl$, formic acid, HCOONa, Δ. l, NBS, Bz_2O_2, Δ. m, DMSO, $NaHCO_3$, 150°.

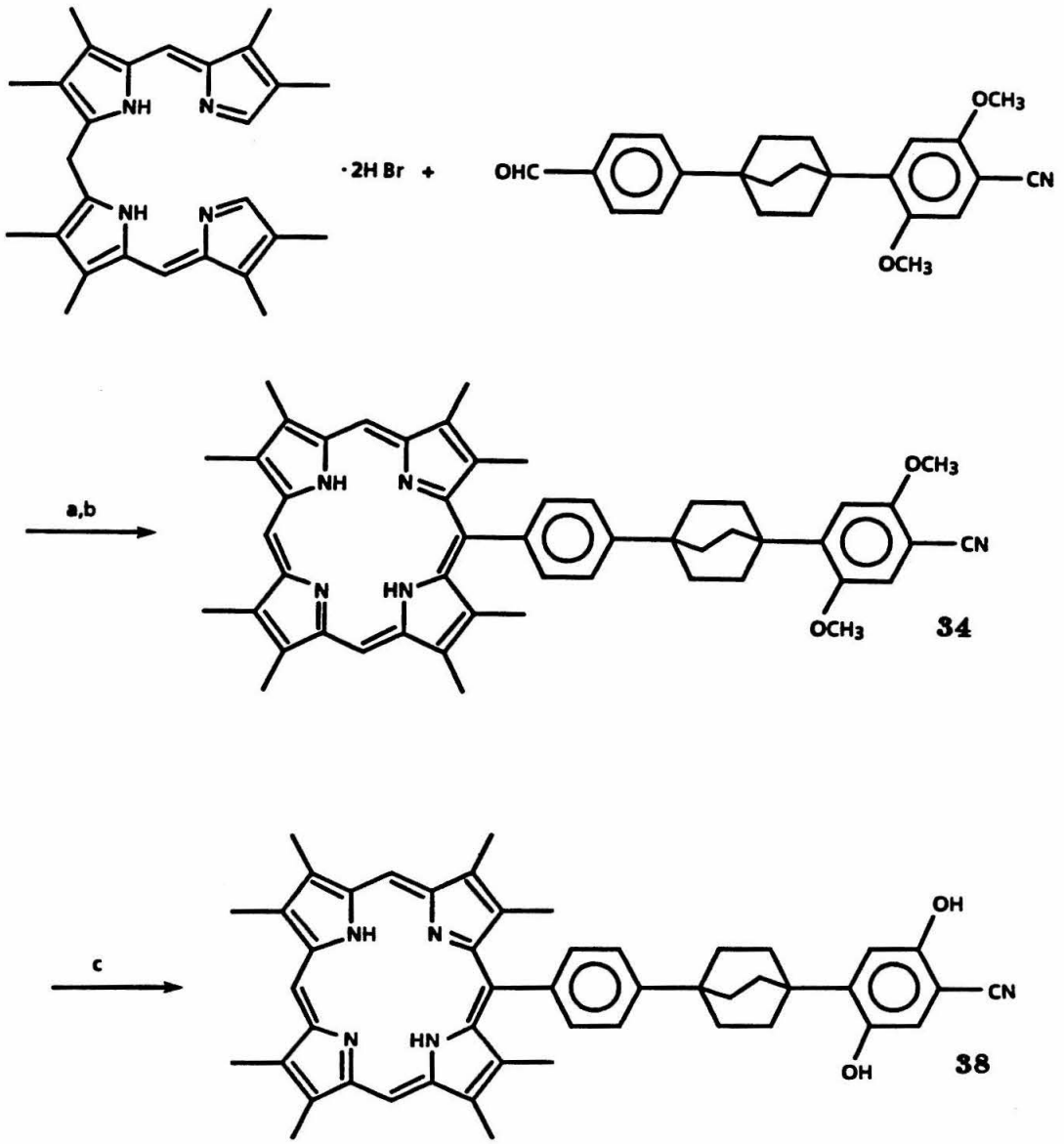

Scheme X. Preparation of Porphyrin-Cyano Quinone.

Scheme X (continued).

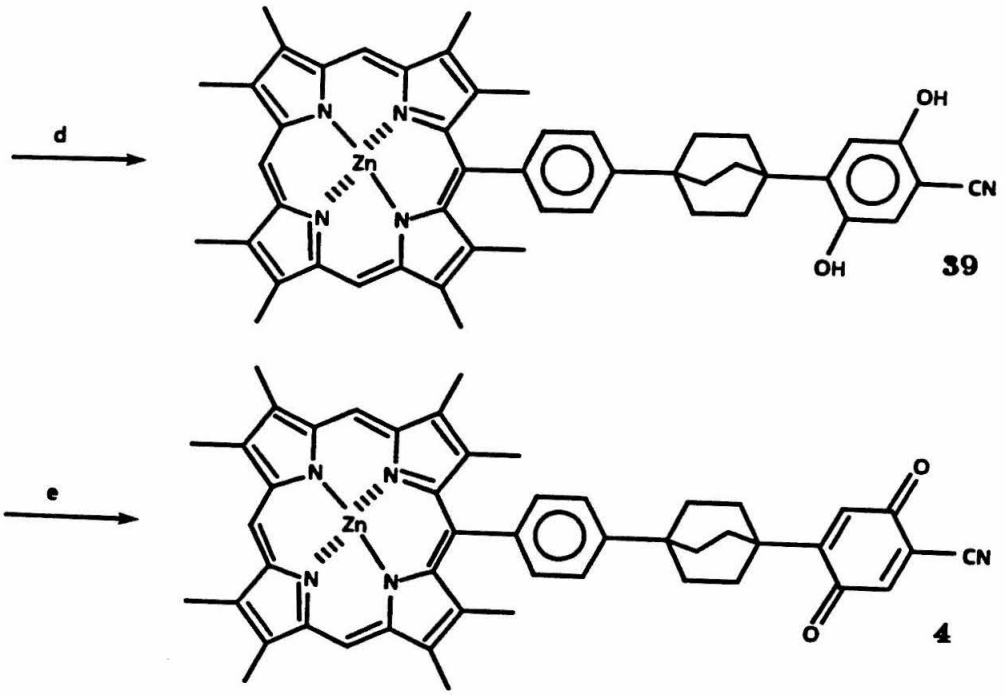

Notes for Scheme X: a, HBr, HOAc, MeOH, Δ b, $NaHCO_3$. c, BI_3, CH_2Cl_2. d, Ag_2O, $NaSO_4$, benzene, CH_2Cl_2.

corrole and deeply colored pyrrolic polymers are formed. These impurities can be removed by flash column chromatography. Deprotection of the methyl ethers required a large excess (>25 equivalents) of boron triiodide. Model studies on 2-cyano-5-methyl-1,4-dimethoxybenzene demonstrated that ten or fewer equivalents of boron triiodide generated the partially deprotected monomethyl ether as the predominant product. The highly insoluble free-base porphyrin cyanohydroquinone was metallated with zinc(II) diacetate dihydrate and then oxidized with

either silver(I) oxide or 2,3-dichloro-5,6-dicyanoquinone (1 equivalent).

Characterization: Electronic Spectra

The electronic spectrum of H_2PLQ **35** and H_2P^tBu **53** in CH_2Cl_2 are presented in Figure 4a,b. The four band pattern $IV > III \sim II > I$ between 500 and 630 nm and the strong Soret band at ~400 nm are typical of unperturbed free-base porphyrins of D_{2d} symmetry. The strongest quinone transition occurs at 248 nm. In polar solvent the wavelength maxima of the porphyrin shift to longer wavelength, indicative of the π, π^* nature of the transition. The spectrum of *p*-methylbenzoquinone is superimposed on that of H_2P^tBu, demonstrating that the electronic transitions of H_2PLQ are essentially a superposition of the spectral bands of the individual constituent chromophores, in terms of λ_{max} and oscillator strength. The only difference is the band attributable to the *meso*-phenyl group, which is slightly shifted in the two compounds due to structural differences between the two compounds, *i.e.*, the presence of a *t*-butyl group *versus* a bicyclo[2.2.2]octane moiety.

A similar comparison can be made of the metallated congeners $ZnPLQ$ **1** and ZnP^tBu **54** shown in Figure 5a,b. A two-band pattern in the visible results on metallation due to an increase in symmetry (D_{4d}). It is evident that the chromophores do not interact appreciably with each other. For contrast with these weakly interacting cases, an electronic spectrum of the directly linked porphyrin-quinone (*meso*-*p*-benzoquinone)octamethylporphyrin (H_2PQ) **56** ap-

pears in Figure 6. The broadness of the visible bands is pronounced, compared with H_2PLQ and H_2P^tBu, and is similar to that observed for the related known compound (*meso*-*p*-benzoquinone)triphenylporphyrin.[32] Figure 6 demonstrates clearly how a strong electronic interaction manifests itself. The absence of chromophore interaction is an essential criterion for a small electronic matrix element, and therefore $ZnPLQ$ is a suitable system for the study of non-adiabatic electron transfer reactions.

Spectra of the modified porphyrin-quinones $ZnPLQMe$ **2** and $ZnPLQMe_2$ **3** and of $ZnPLQH_2CN$ are given in Figures 7, 8, and 9, respectively. These systems also exhibit no interactions between porphyrin and quinone moieties in their electronic transitions.

Nuclear Magnetic Resonance Spectra

An ^{1}H NMR spectrum of $ZnPLQ$ in CD_2Cl_2 is presented in Figure 10, and one of ZnP^tBu is given in Figure 11. Because of the large anisotropic ring current due to the porphyrin and the smaller current due to the *meso*-phenyl group, every equivalent set of protons is clearly resolved. The mirror plane symmetry of the molecules makes the spectra quite straightforward to interpret. The effective magnetic field differences at each proton are accentuated enough to cause the chemical shifts of all four sets of methyl groups to separate over a range of

---

[32] L.R. Milgrom and J. Dalton, *J. Chem. Soc., Perkin*, 2, 707 (1982).

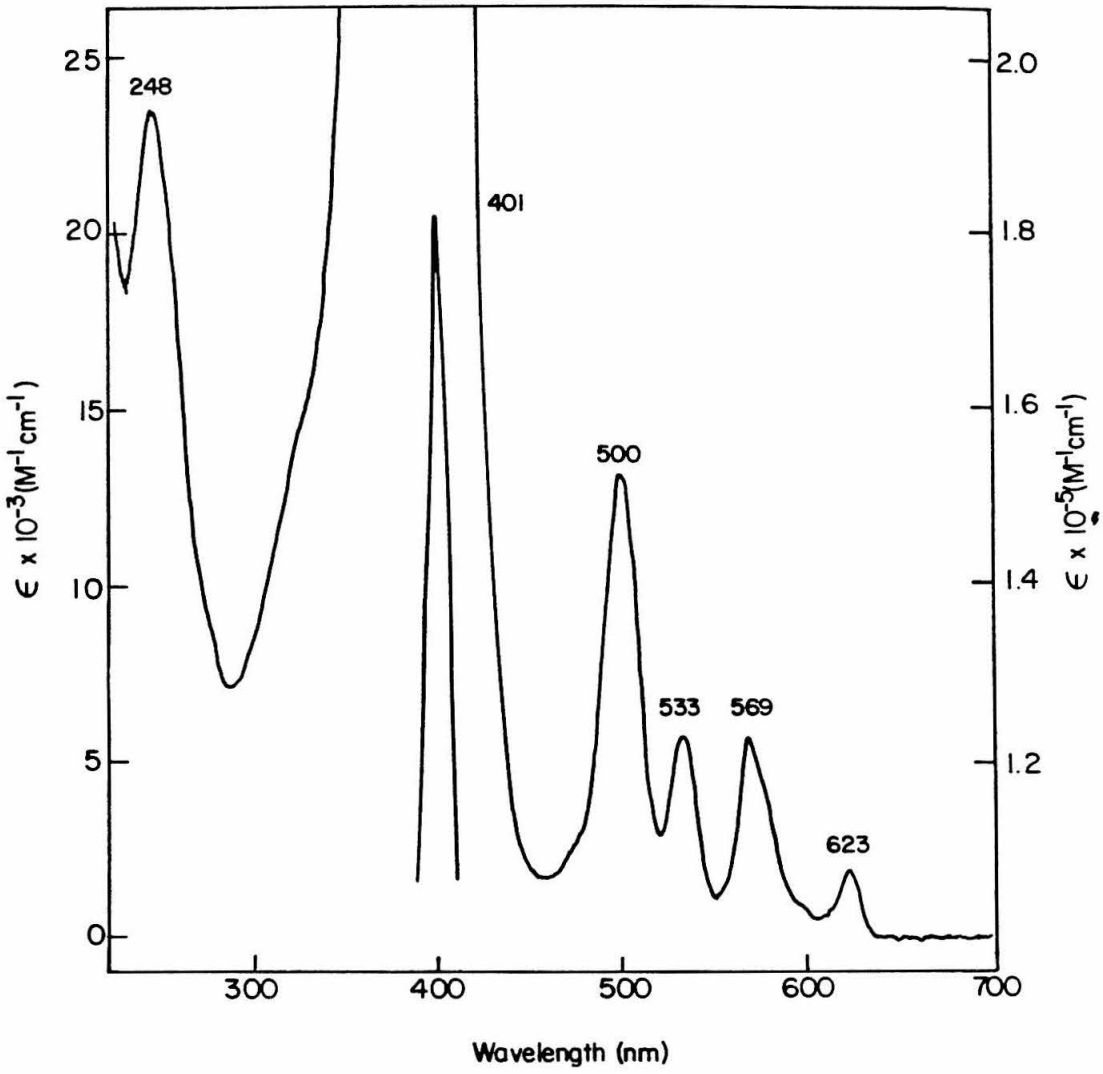

Figure 4a. Electronic spectrum of H_2PLQ in CH_2Cl_2.

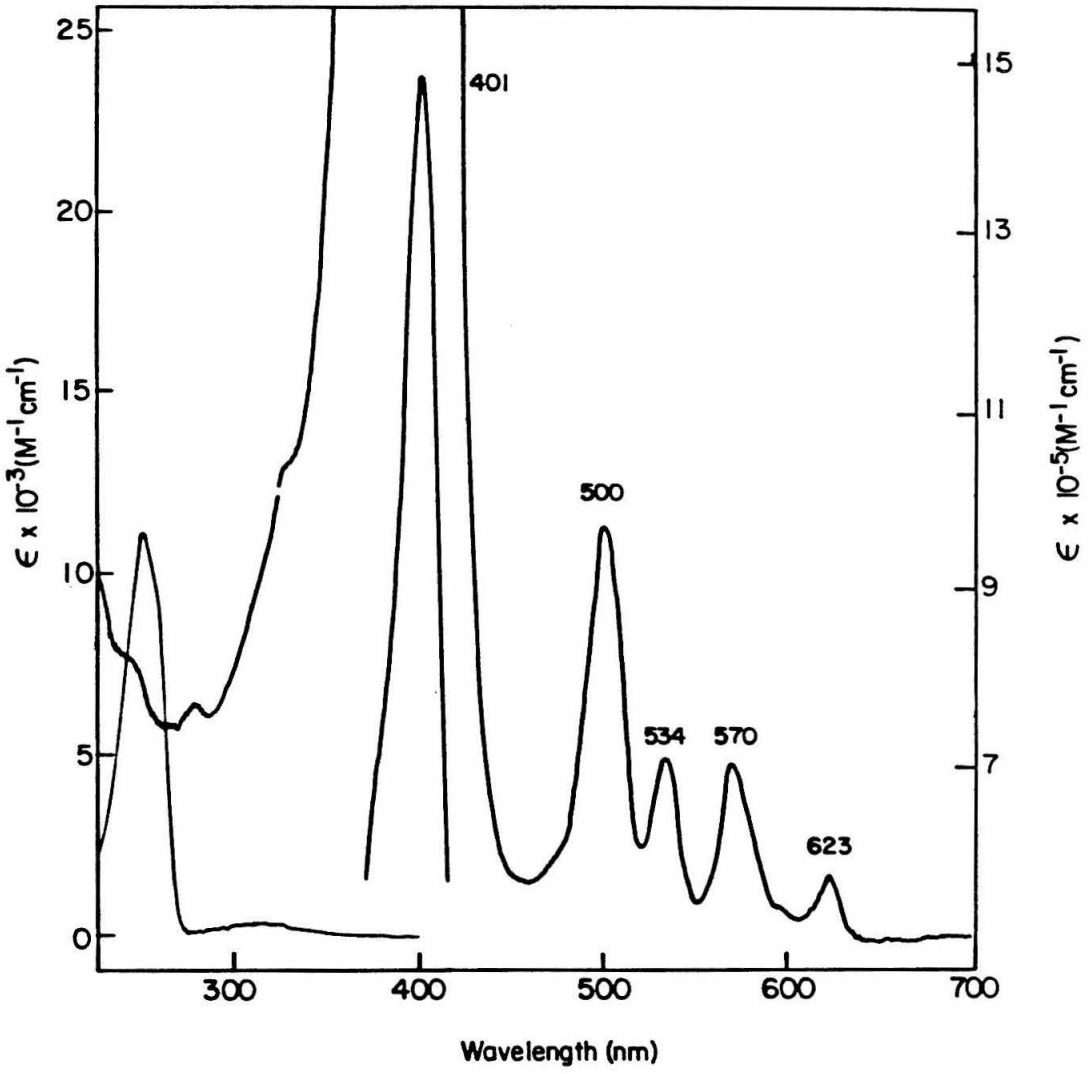

Figure 4b. Electronic spectrum of H_2P^tBu and methyl-*p*-benzoquinone in CH_2Cl_2.

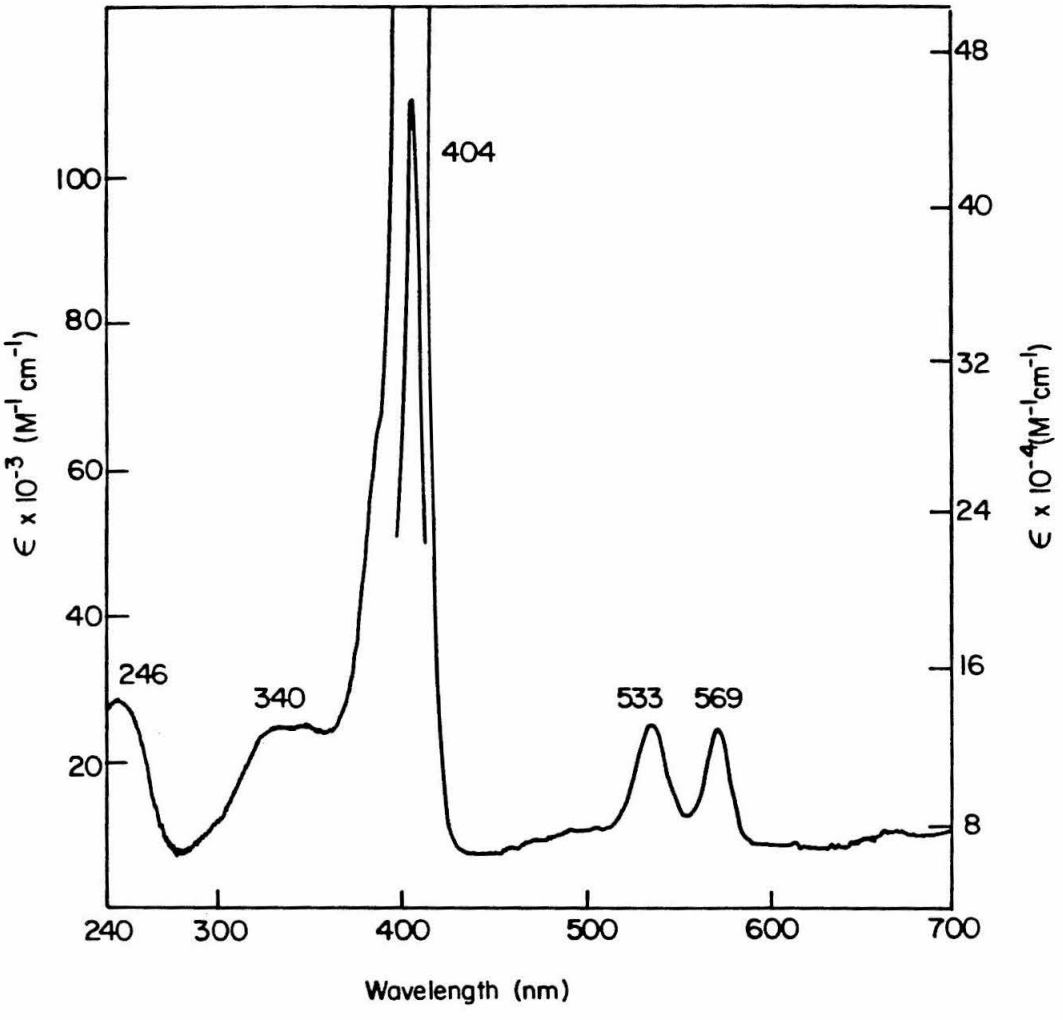

Figure 5a. Electronic spectrum of *ZnPLQ* in CH_2Cl_2.

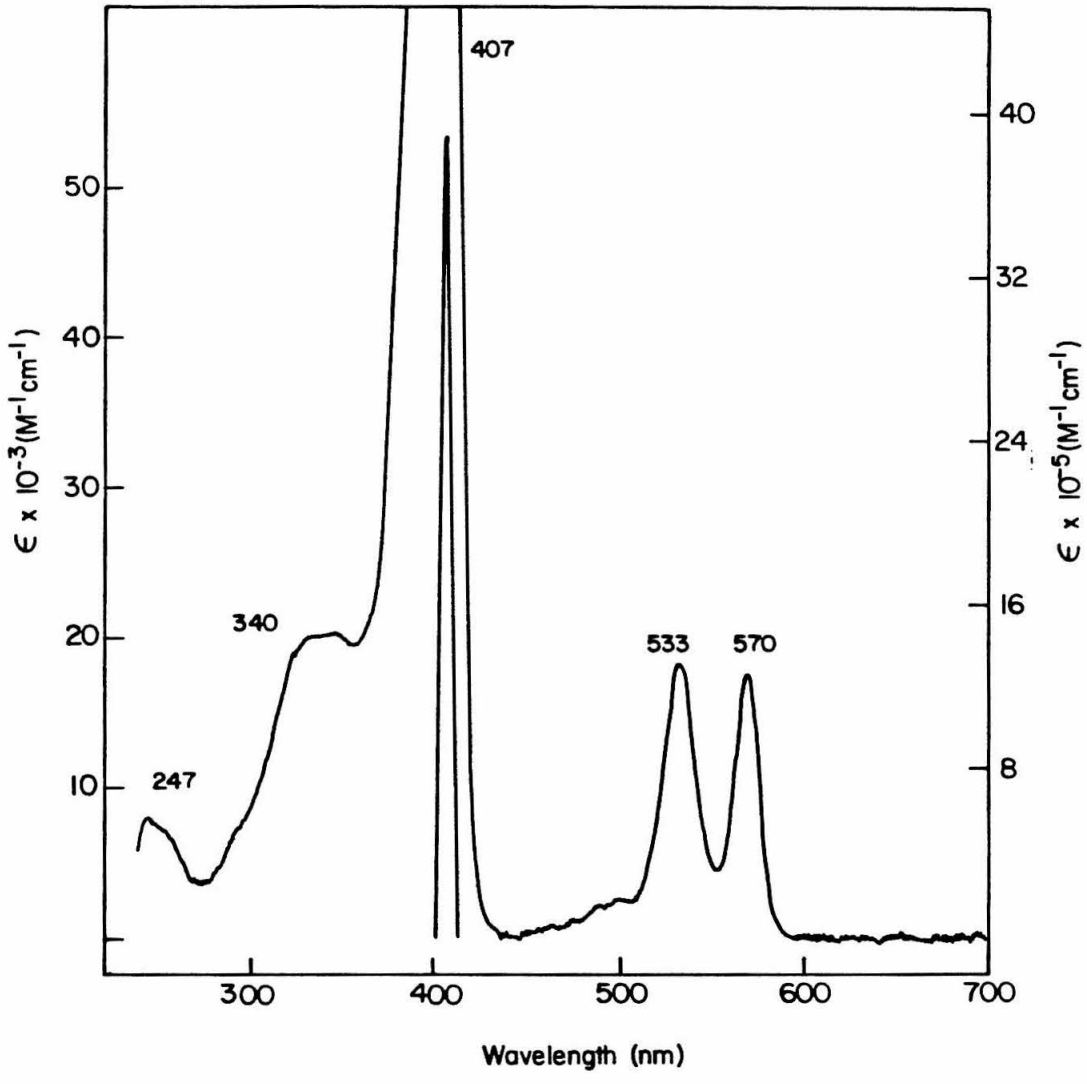

Figure 5b. Electronic spectrum of ZnP^tBu in CH_2Cl_2.

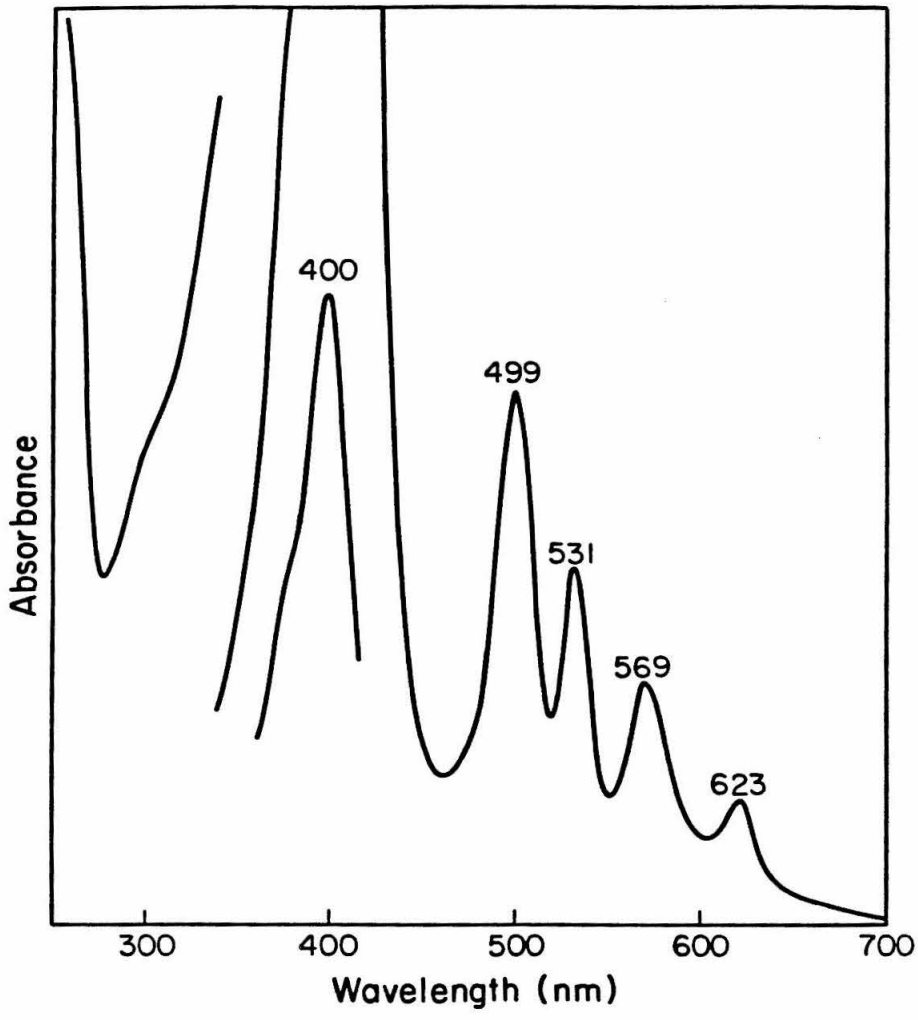

Figure 6. Electronic spectrum of H_2PQ in CH_2Cl_2.

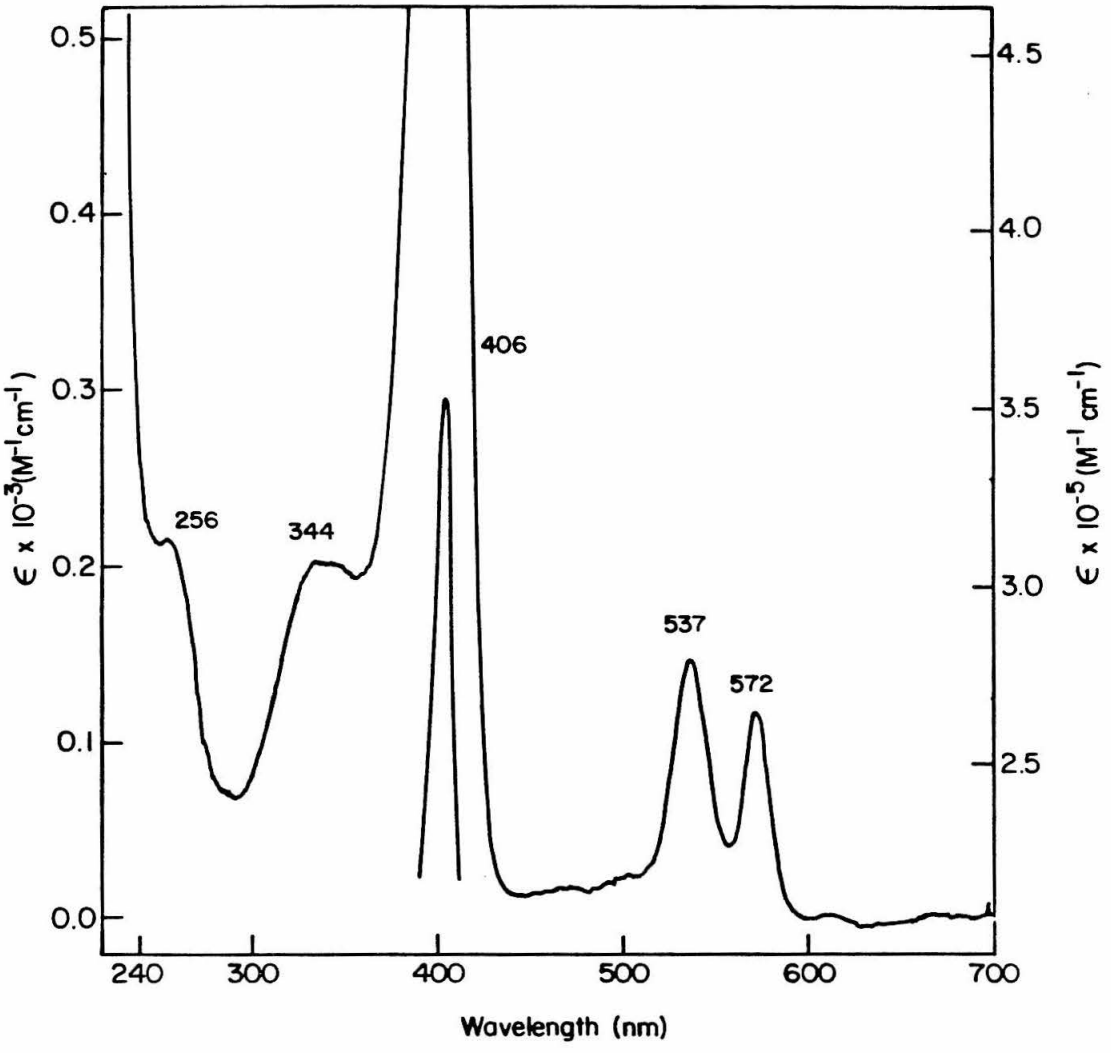

Figure 7. Electronic spectrum of *ZnPLQMe* in CH_2Cl_2.

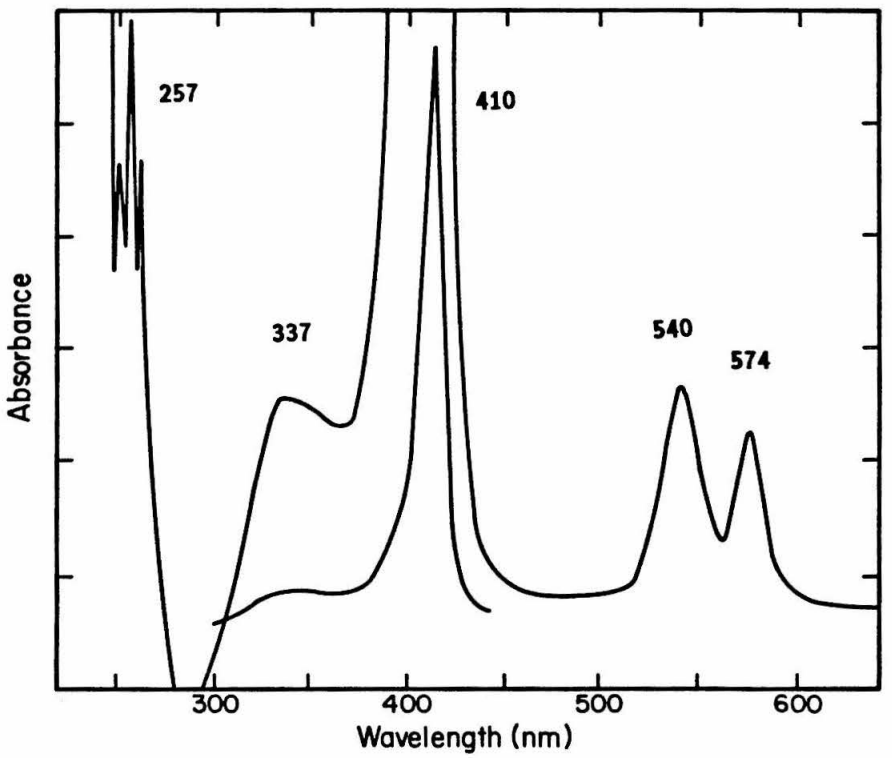

Figure 8. Electronic spectrum of $ZnPLQMe_2$ in 2MTHF.

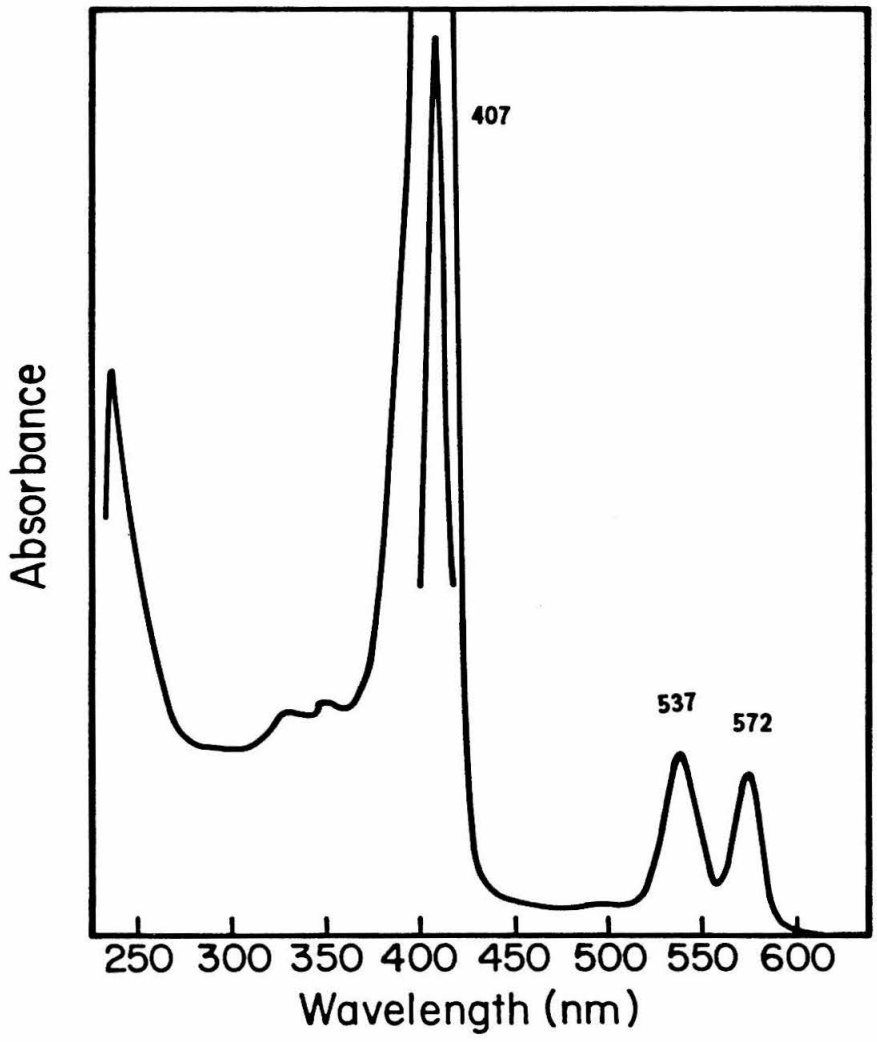

Figure 9. Electronic spectrum of $ZnPLQH_2CN$ in CH_2Cl_2.

1.2 ppm (from 2.4 to 3.6 ppm); the most upfield pair of methyls face the phenyl ring most directly. The *meso*-protons are strongly deshielded by the ring current and are located at about 10 ppm in a 2:1 ratio. For the dimethylquinone analogue H_2PLQMe_2 in $CDCl_3$ (Figure 12) the NH peak appears at about -3.2 ppm, as a consequence of being in the upfield shifted region of region of magnetic anisotropy. The linker methylene protons are situated at 2.0 to 2.2 ppm and are coupled as an $AA'BB'$ doublet of multiplets. The quinone is so distant from the porphyrin (~14.8 Å center-to-center) that the quinone ring protons occur where they do in isolated quinones, *i.e.*, at about 6.5-6.7 ppm. The cyanohydroquinone zinc porphyrin is shown in Figure 13.

The upfield shift of the *meso*-proton opposite the *meso*-phenyl substituent has been attributed to folding of the porphyrin macrocycle induced by the phenyl group across the porphyrin; a reduction in the anisotropic deshielding effect affects the opposite *meso*-proton more than the two equivalent *meso*-protons.[33] In sum, the proton NMR data are consistent with the expected molecular structure. Further characterization on synthetic materials (including mass spectra, ^{13}C NMR, infrared, and elemental analysis on new intermediates) is given in Chapter 6.

---

[33] R.J. Abraham, A.H. Jackson, G.W. Kenner, and D. Warburton, *J. Chem. Soc.* 853 (1963).

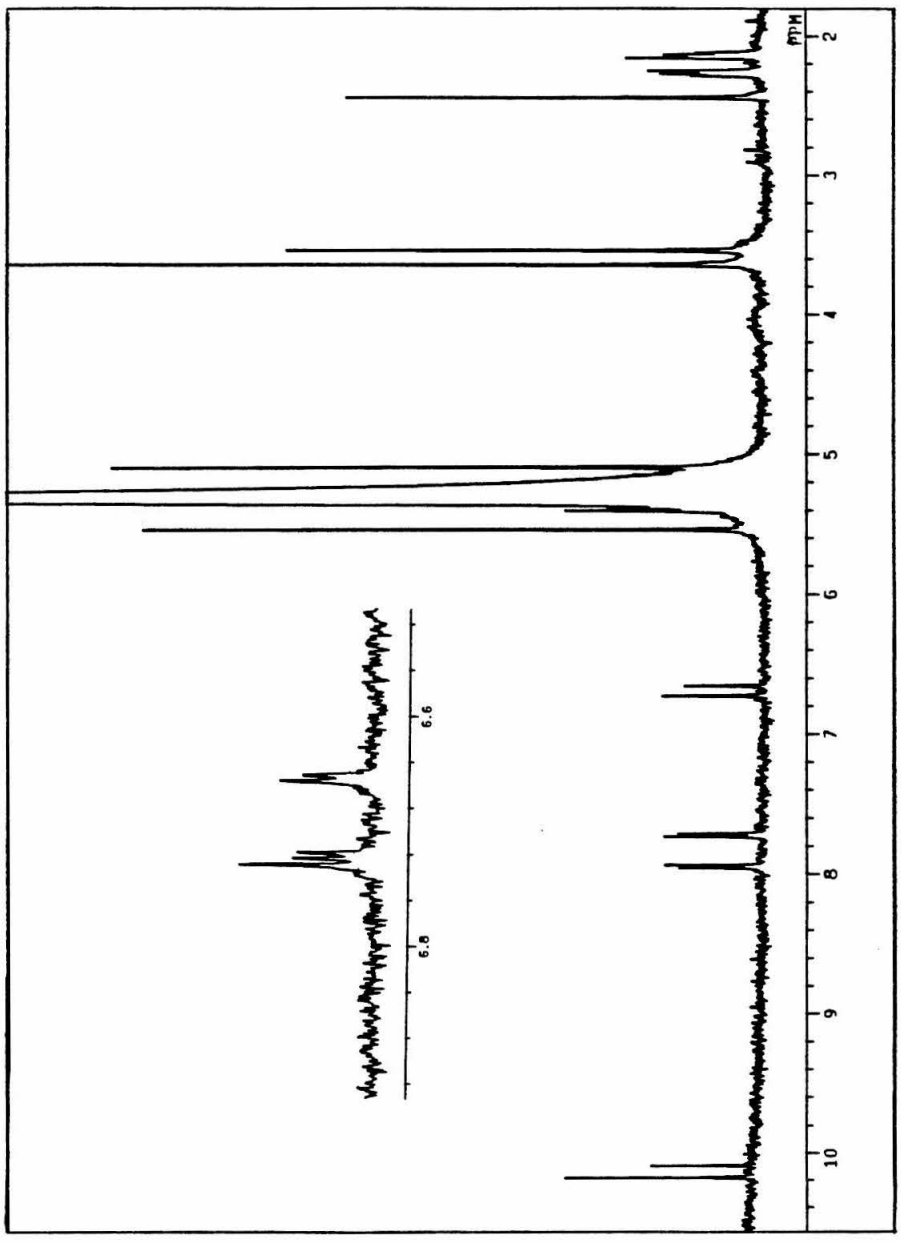

Figure 10. 400MHz ^{1}H NMR spectrum of *ZnPLQ* in CD_2Cl_2.

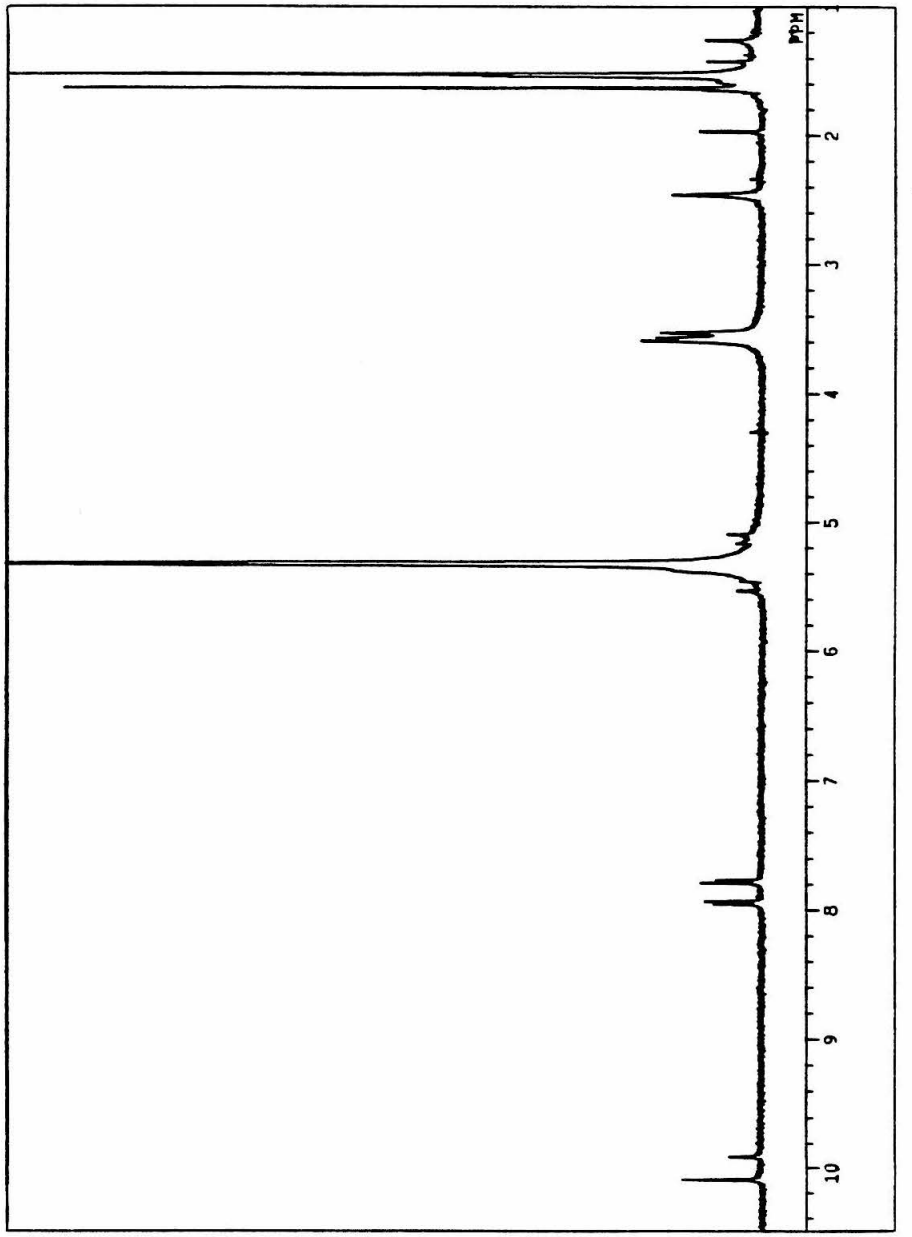

Figure 11. 400MHz ^{1}H NMR spectrum of ZnP^tBu in CD_2Cl_2.

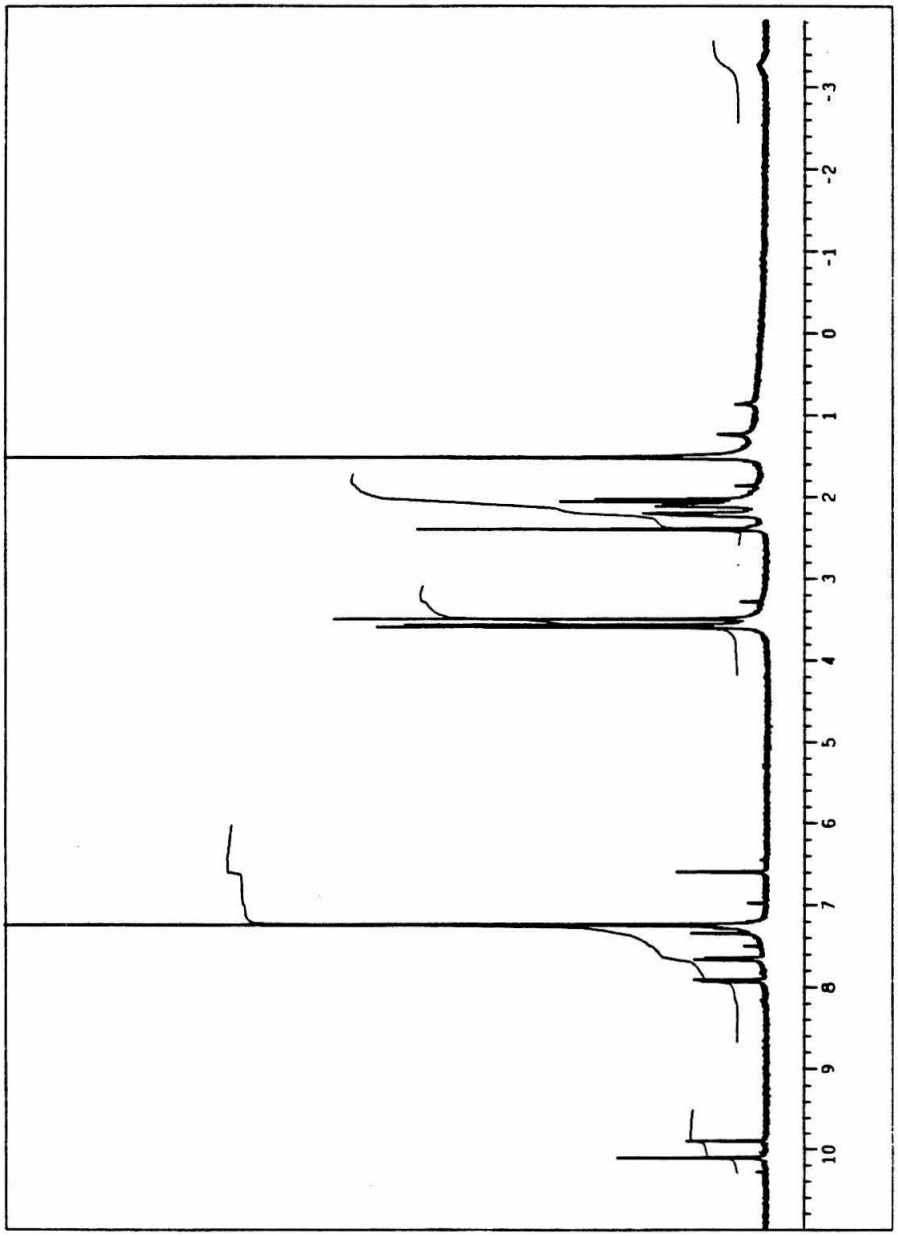

Figure 12. 400MHz ^{1}H NMR spectrum of H_2PLQMe_2 in $CDCl_3$.

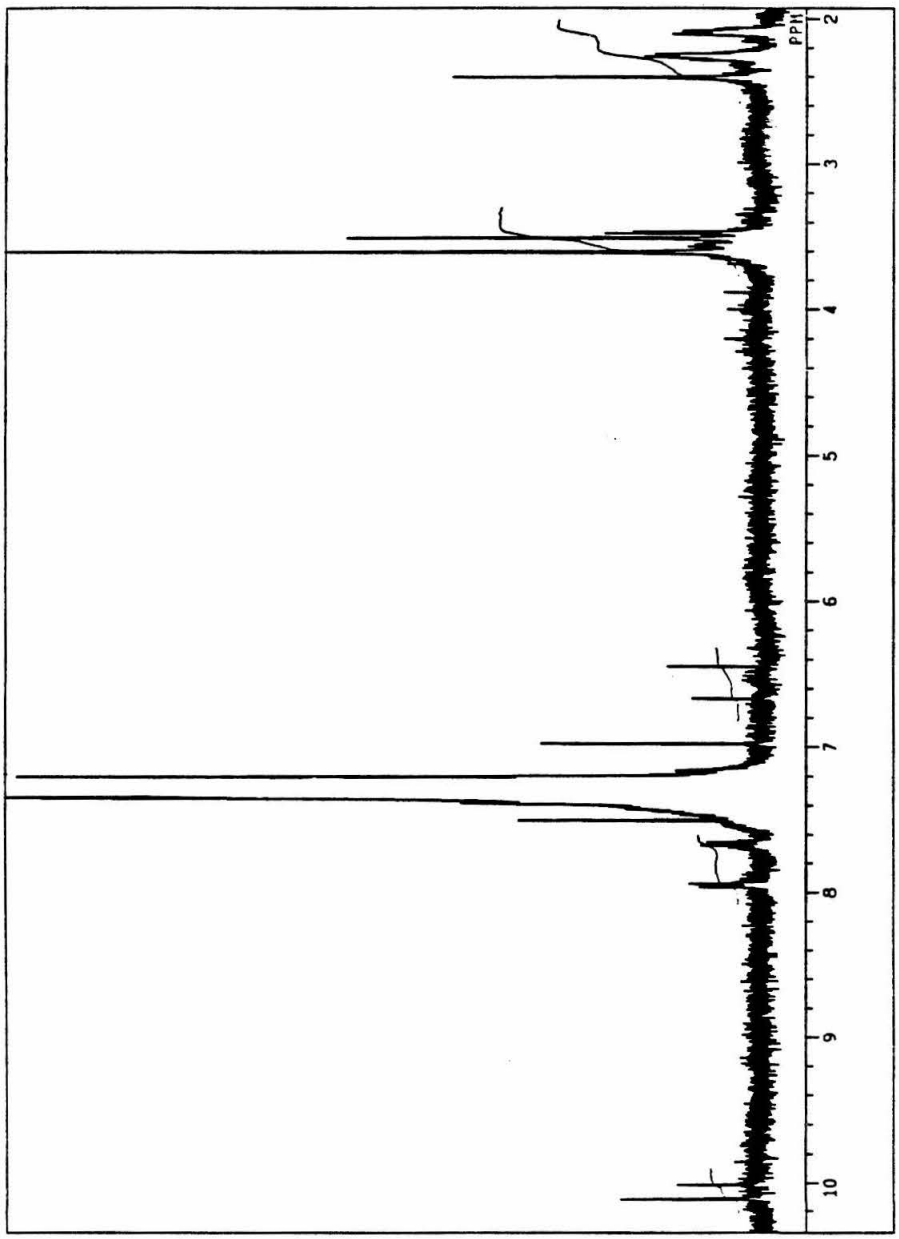

Figure 13. 400MHz ^{1}H NMR spectrum of $ZnPLQH_2CN$ in $CDCl_3$.

Chapter 3

Steady-State Methods

Steady-State Fluorescence Spectroscopy

The fluorescence emission spectra for the free-base and zinc porphyrins H_2P^tBu* and ZnP^tBu† are shown (as the solid lines) in Figures 1 and 2. The two smooth, unstructured bands observed in the visible (570 to 700 nm) are characteristic of D_{4h} and D_{2h} symmetry porphyrins, and have been attributed to the *S(0,0)* and *S(0,1)* vibronic states.[1] The spectra of the quinone-substituted porphyrins (H_2PLQ and $ZnPLQ$) are shown (as the dashed lines) in Figures 1 and 2, and agree in their overall shape and in the wavelengths of their emission maxima with the corresponding unsubstituted porphryins. The only apparent difference lies in the relative intensities of the emission bands, strongly suggestive of an electron transfer quenching mechanism (see below).

Consideration of the kinetic scheme (Scheme I) allows the determination of the electron transfer rate by assuming the validity of the steady-state approximation. Of course, the rate constants obtained in this manner are subject to all the provisos implicit in the method, including the unavoidable problems of exactly matching solution concentrations and, most critically, the nonspecific nature of the method. The origin of the detected emission is not certain; for example, a

---

* *meso*-(4′-t-Butyl)phenyloctamethylporphyrin.

† [*meso*-(4′-t-Butyl)phenyloctamethylporphyrinato]zinc(II).

[1] M. Gouterman in D. Dolphin, ed., *The Porphyrins*, Academic Press, New York, 1978.

trace of porphyrin-hydroquinone with its large emission quantum yield will give an untrue high reading of the relative fluorescence yield and a low estimate of the electron transfer rate.

The emission spectra were found to be independent of excitation wavelength and concentration of the porphyrin in the range $10^{-5} - 10^{-7}$M. Electronic absorption spectra taken after the fluorescence measurements showed no photochemical damage, except in instances of long periods of irradiation, where some singlet oxygen damage is evident, and also when dichloromethane is the solvent, where considerable degradation of the porphyrin chromophore was evident. The electrochemical reduction potential of dichloromethane (approximately -1.4V *vs.* SCE)[2] suggests that photoexcited electron transfer to this solvent is feasible. Independent studies of the photochemical behavior of porphyrins in halogenated organic solvents have demonstrated the formation of free radical species under irradiation.[3]

The similarity of spectral shape and emission wavelengths in both the quinone-substituted porphyrins and the respective reference porphyrins substantiates the electronic and NMR spectral results of Chapter 2 in confirming the lack of direct electronic interaction between chromophores. This observation contrasts

---

[2] A.J. Bard and H. Lund, eds., *Encyclopedia of Electrochemistry of the Elements, Organic Section*, Marcel Dekker, New York, 1980.

[3] Z. Gasyna, W.R. Browett, and M.J. Stillman, *Inorg. Chim. Acta*, **92**, 37 (1984).

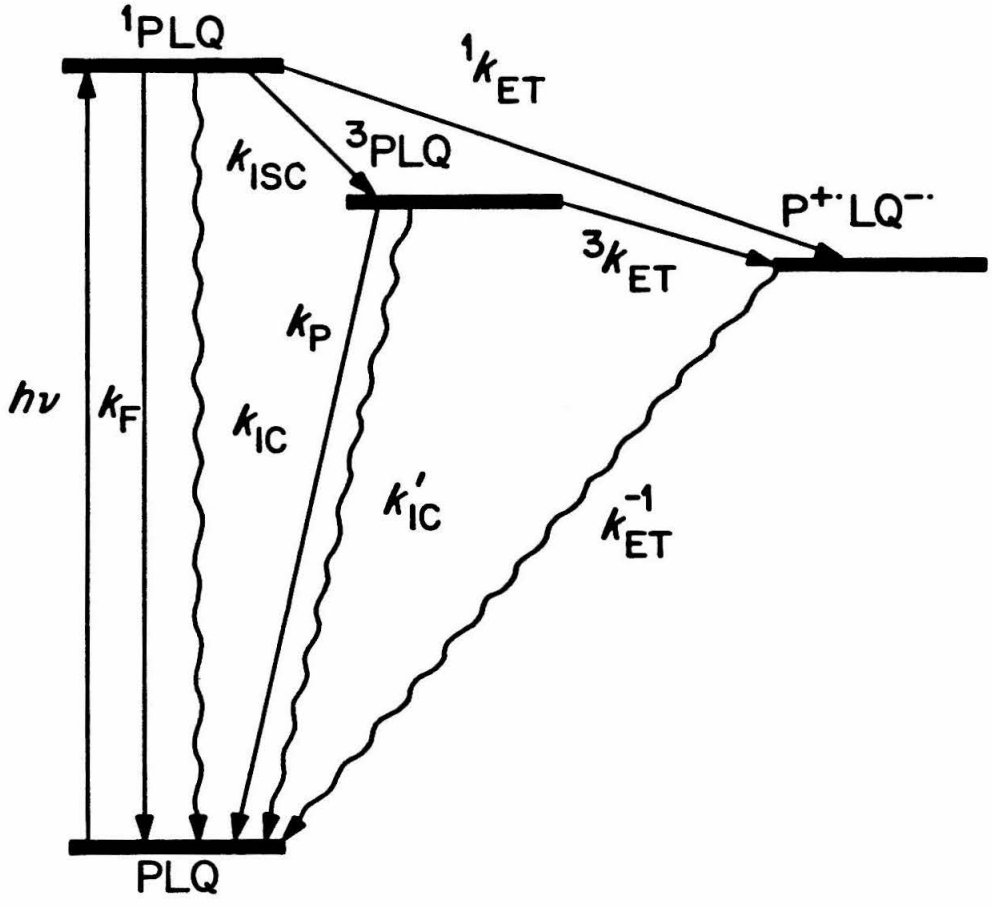

Scheme I. Kinetic Scheme for Excited State Deactivation of Porphyrin-Quinones.

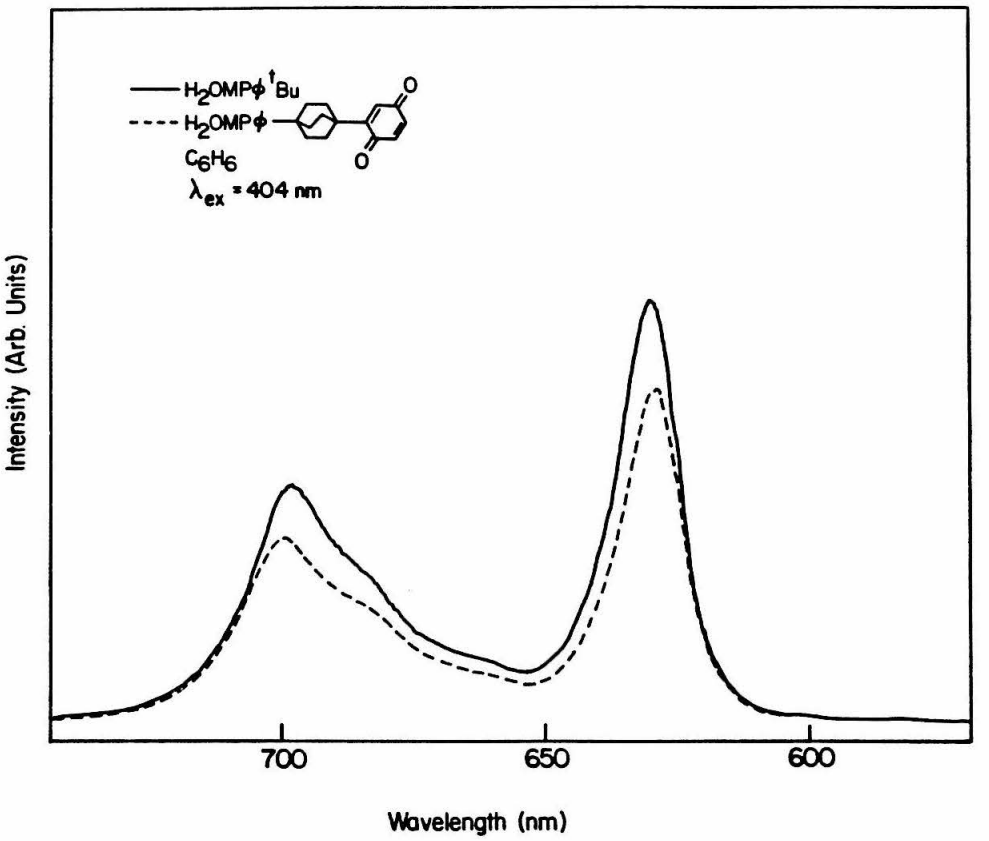

Figure 1. Steady-State Fluorescence Emission Spectrum of H_2PLQ and H_2P^tBu in Benzene.

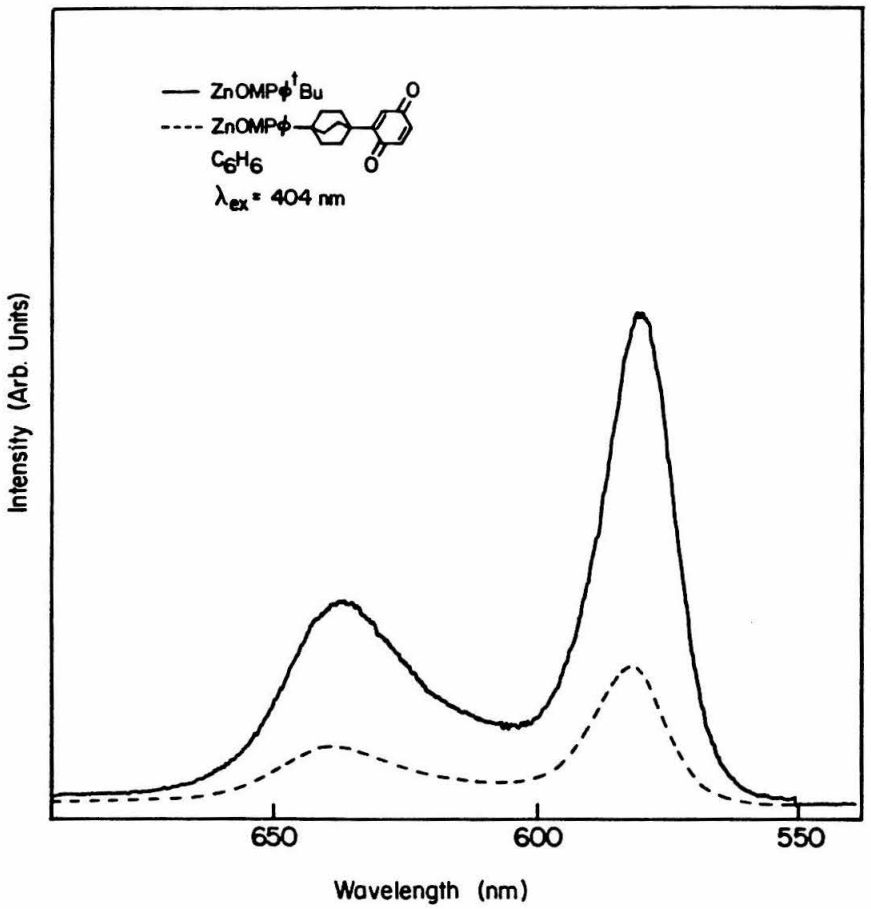

Figure 2. Steady-State Fluorescence Emission Spectrum of *ZnPLQ* and *ZnP^{t}Bu* in Benzene.

Table I. Solvent Dependence of Emission Wavelength Maxima of Free-Base and Zinc Porphyrins.

Compound	Solvent	$\lambda_{max}(S(0,1), S(0,0))^a$ (nm)
H_2PLQ	C_6H_6	697, 630
H_2P^tBu	C_6H_6	697, 630
H_2PLQ	CH_3CN	693, 627
H_2P^tBu	CH_3CN	693, 628
H_2PLQ	DMF	694, 627
H_2P^tBu	DMF	695, 628
H_2PLQ	CH_2Cl_2	694, 628
H_2P^tBu	CH_2Cl_2	694, 628
H_2PLQ	nPrCN	695, 628
H_2P^tBu	nPrCN	695, 628
$ZnPLQ$	C_6H_6	631, 578
ZnP^tBu	C_6H_6	631, 578
$ZnPLQ$	CH_3CN	634, 582
ZnP^tBu	CH_3CN	634, 582
$ZnPLQ$	DMF	637, 584
ZnP^tBu	DMF	639, 584
$ZnPLQ$	CH_2Cl_2	630, 578
ZnP^tBu	CH_2Cl_2	629, 578
$ZnPLQ$	nPrCN	634, 581
ZnP^tBu	nPrCN	635, 582
$ZnPLQ$	Diglyme	635, 580
ZnP^tBu	Diglyme	634, 581

[a] Uncertainty, ± 1 nm.

sharply with the fluorescence spectra determined for porphyrin-quinones coupled by flexible polymethylene ester or amide spacers.[4,5] Steady-state fluorescence spectra of these compounds were strongly excitation wavelength-dependent,[4] and exhibited extensive peak broadening and red-shifting,[5] all of which were attributed to intramolecular interactions.

As a check of the hypothesis that electron transfer to the quinone was responsible for the observed quenching of the porphyrin fluorescence, the porphryin-quinone was chemically reduced with potassium borohydride in methanol (as the proton source) and dichloromethane (in which the porphyrins have appreciable solubility), thus generating the porphyrin-hydroquinone.[6] The resulting solution showed restored fluorescence with an intensity equalling that of the reference porphyrin of similar concentration. The presence of the hydroquinone species was supported by the ^{1}H NMR spectrum taken of the evaporated fluorescence sample reconstituted with deuterated dichloromethane. The two $AA'BB'$ multiplets for the six methylene groups of the bicyclo[2.2.2]octane moiety coalesced into a

---

[4] T.-F. Ho, A.R. McIntosh, and A.C. Weedon, *Can. J. Chem.*, **62**, 967 (1984).

[5] (a) A. Siemiarczuk, A.R. McIntosh, T.-F. Ho, M.J. Stillman, K.J. Roach, A.C. Weedon, J.R. Bolton, and J.S. Connolly, *J. Amer. Chem. Soc.*, **105**, 7224 (1983). (b) T.-F. Ho, A.R. McIntosh, and J.R. Bolton, *Nature* (*London*), **286**, 254 (1980).

[6] *Cf.* (a) P.A. Loach, J.A. Runquist, J.L.Y. Kong, T.J. Dannhauser, and K.G. Spears, *Adv. Chem. Ser.*, **201**, 515 (1982). (b) J.L.Y. Kong and P.A. Loach, *J. Heterocyclic Chem.*, **17**, 737 (1980).

broad singlet characteristic of the hydroquinone, as shown in an authentic sample prepared by cleavage of the methyl ethers of the porphyrin-hydroquinone diether. New but not well resolved (at 90MHz) peaks appear for the hydroquinone in the aromatic shift region. These experiments suggest that the presence of the quinone is most likely responsible for the quenching of porphyrin fluorescence.

The fluorescence spectra of the porphyrins provide a simple technique for determining whether any new deactivation pathways have become available in the photophysics of the quinone-substituted porphyrins described. If an electron transfer process takes place on a time scale roughly comparable to the lifetime of the singlet excited state of the porphyrin, the fluorescence and phosphorescence quantum yields are expected to be diminished in magnitude, and the intensity of the bands of the emission spectra should appear quenched. Energy transfer is not energetically favorable.

The kinetic equations for the singlet manifold of the zinc porphyrin-quinone ($ZnPLQ$) and the reference porphyrin (ZnP^tBu) under the steady-state approximation are as follows.

$$\frac{d[^1{*}ZnPLQ]}{dt} = I[ZnPLQ] - [^1{*}ZnPLQ](k_{ET} + k_f + k_{IC} + k_{ISC}) = 0 \quad [3.1]$$

$$\frac{d[^1{*}ZnP^tBu]}{dt} = I[Zn^tBu] - [^1{*}ZnP^tBu](k_f + k_{IC} + k_{ISC}) = 0 \quad [3.2]$$

If the solutions have identical concentrations and the intensity and wavelength of the light source are the same, then the number of photons absorbed is also

Table II. Relative Fluorescence Yields for H_2PLQ and $ZnPLQ$.

Compound	Solvent	$\phi_{rel} = I/I_0$[a]
H_2PLQ	CH_3CN	0.83
"	DMF	0.76
"	nPrCN	0.63
"	CH_2Cl_2	0.50
"	C_6H_6	0.80
$ZnPLQ$	CH_3CN	0.42
"	DMF	0.37
"	Diglyme	0.31
"	nPrCN	0.26
"	CH_2Cl_2	0.31
"	C_6H_6	0.27

[a] Experimental uncertainty is estimated at ±10%.

similar. $I[ZnPLQ] = I[ZnP^tBu]$, and so

$$\frac{[^{1*}ZnP^tBu]}{[^{1*}ZnPLQ]} = \frac{k_{ET} + k_f + k_{IC} + k_{ISC}}{k_f + k_{IC} + k_{ISC}} = k_{ET}\tau_0 + 1, \qquad [3.3]$$

where I is the intensity of illumination, k_{ET} is the electron transfer rate constant, k_f is the fluorescence rate constant, k_{IC} is the rate constant for internal conversion, and k_{ISC} is the rate constant for intersystem crossing to the triplet state. The concentrations of the steady-state, excited-state intermediate are proportional to the fluorescence quantum yields for the quenched and reference molecules, respectively, ϕ and ϕ_0, which vary directly with the experimentally observed fluorescence emission intensities. Thus,

$$\frac{I_0}{I} = \frac{\phi_0}{\phi} = k_{ET}\tau_0 + 1, \qquad [3.4]$$

where $\tau_0 = 1/(k_{IC} + k_f + k_{ISC})$ represents the natural fluorescence lifetime of the porphyrin chromophore, and is measured in an independent time-resolved picosecond fluorescence spectroscopy experiment.[7]

An important result of the emission studies was the observation of a large effect of distance on the electron transfer rate.[8,13] Relative fluorescence and time-resolved fluorescence and phosphorescence lifetime data for porphyrin-quinone systems coupled by two bicyclo[2.2.2]octane spacers were obtained by Burton A.

---

[7] P.M. Felker, A.D. Joran, B.A. Leland, J.J. Hopfield, P.B. Dervan, and A.H. Zewail, unpublished results.

Leland, and the issue of the distance dependence of electron transfer reactions will be examined in detail by him.[8]

From the steady-state data, $ZnPLQ$ shows greater fluorescence quenching than the free-base analogue H_2PLQ ($\sim 0.2 - 0.4$ compared with $\sim 0.5 - 0.8$, respectively). A likely qualitative explanation for this difference is the larger energy gap in the metalloporphyrin (0.97eV in dichloromethane/0.1M tetra-n-butylammonium perchlorate; TBAP) over the free-base compound (0.55eV).[13b] (Electrochemical measurements are presented in Chapter 4.) Assuming intramolecular electron transfer is the mechanism of quenching, application of the above steady-state formalism provides an estimate of the rate constant. In separate time-resolved fluorescence experiments, the lifetimes of H_2P^tBu in benzene and butyronitrile were determined: $\tau_0 = 17.5(\pm 0.2)$ nsec in benzene and $\tau_0 = 18.1(\pm 0.2)$ nsec in butyronitrile (298K). Thus, from Eq. [3.4] the rate constants for electron transfer k_{ET} are estimated to be $1.4(\pm 0.2) \times 10^7$ sec^{-1} in benzene and $3.2(\pm 0.3) \times 10^7$ sec^{-1} in butyronitrile. For the zinc analogue, lifetimes of the reference porphyrin ZnP^tBu are $\tau_0 = 1.47(\pm 0.05)$ nsec in benzene and $\tau_0 = 1.59(\pm 0.05)$ nsec in butyronitrile (298K). For $ZnPLQ$ estimated values of k_{ET} are $2.2(\pm 0.02) \times 10^9$ sec^{-1} in benzene and $2.4(\pm 0.2) \times 10^9$ sec^{-1} in butyronitrile.

---

[8] B.A. Leland, *Dissertation*, California Institute of Technology, 1986.

An ~0.5 eV increase in driving force produces a rate enhancement of 100-fold in the case of the zinc porphyrin-quinone *versus* the metal-free compound. This rate comparison is consistent with the findings of previous intramolecular and bimolecular[9] experiments examining the classical Marcus relationship of electron transfer rate constant and reaction exothermicity. These studies and the present work thus support electron transfer theories invoking quadratic energy gap laws as they relate to the so-called normal region of reactivity.[10] More quantitative discussion of rate comparisons and exploration of the inverted region will be given following the presentation of results of the picosecond fluorescence studies.

The data obtained from the fluorescence spectra allow two statements to be made. (a) The electronic states of the porphyrin and quinone chromophores do not interact strongly considering the lack of pertubation of the emission spectra—principally as a result of their enforced spatial separation by the intervening bicyclo[2.2.2]octane unit. (b) The relative fluorescence quantum yields are significantly diminished in the quinone-substituted porphyrins, indicating the intervention of a new mechanism for deactivation of the porphyrin singlet excited state not present in the reference porphyrin. In light of the thermodynamic inaccessibility of energy transfer deactivation pathways, the most likely candidate for this process is intramolecular electron transfer. Furthermore, the low

---

[9] D. Rehm and A. Weller, *Isr. J. Chem.*, **8**, 259 (1970).

[10] See References 8-11 in Chapter 2.

concentrations employed ($10^{-5} - 10^{-7}$M) make bimolecular collisional deactivation processes improbable. The main conclusions of the steady-state fluorescence measurements support a basic assumption for the design of the porphyrin-quinone compounds: electron transfer can be observed where strong electronic coupling of chromophores is prevented by a rigid linker in pairs of donors and acceptors.[4-6,11,12] These molecules should prove highly useful in elucidating the role of such critical parameters as distance, conformation, and driving force in electron transfer reactions.[13]

Electron Paramagnetic Resonance Studies

Reports have appeared of the direct observation by the EPR method of pairs of the porphyrin radical cation and the quinone radical anion induced by the steady-state illumination of a flexibly linked porphyrin-quinone.[14] This appar-

---

[11] For examples of flexible porphyrin-quinones, see (a) J.L.Y. Kong, K.G. Spears, and P.A. Loach, *Photochem. Photobiol.*, **35**, 545 (1982). (b) M. Migita, T. Okada, N. Mataga, S. Nishitani, N. Kurata, Y. Sakata, and S. Misumi, *Chem. Phys. Lett.*, **84**, 263 (1981). (c) N. Mataga, A. Karen, T. Okada, S. Nishitani, N. Kurata, Y. Sakata, and S. Misumi, *J. Phys. Chem.*, **88**, 5138 (1984).

[12] For systems with various flexibly linked donors and acceptors, see, for example, (a) A. Harriman and R.J. Hosie, *J. Photochem.*, **15**, 163 (1981). (b) A. Harriman, *Inorg. Chim. Acta*, **88**, 213 (1984). (c) H. Heitele and M.E. Michel-Beyerle, *J. Amer. Chem. Soc.*, **107**, 8286 (1985).

[13] (a) B.A. Leland, A.D. Joran, P.M. Felker, J.J. Hopfield, A.H. Zewail, and P.B. Dervan, *J. Phys. Chem.*, **89**, 5571 (1985). (b) A.D. Joran, B.A. Leland, G.G. Geller, J.J. Hopfield, and P.B. Dervan, *J. Amer. Chem. Soc.*, **106**, 6090 (1984).

[14] (a) T.-F. Ho, A.R. McIntosh, and J.R. Bolton, *Nature* (*London*), **220** (1980).

ent success prompted us to investigate the possibility of observing similar radical cation/anion pairs in $ZnPLQ$ and H_2PLQ directly by EPR.

Experiments on $ZnPLQ$ were initially performed in dichloromethane because of high solubility of the porphyrin-quinones in that solvent. On irradiation with a 200W mercury-xenon arc lamp, with cut-off filters passing light with $\lambda_{max} > 350$ nm, $ZnPLQ$ in dichloromethane solution at 298K, and also in microcrystalline frozen dichloromethane at 77K, gave a strong EPR doublet with some broadened hyperfine structure. The concentration was low enough that it should not have resulted from bimolecular reaction of different porphyrin-quinone molecules. The signal did not decrease at an appreciable rate with time (just as in the previous report[14]) when the arc lamp was turned off at 77K or 298K. A control experiment in which ZnP^tBu alone in dichloromethane (at 298K and 77K) was irradiated showed the formation of a similarly strong signal as well, indicating that intramolecular electron transfer was not the source of the unpaired electrons causing the signal. It was concluded that the observed EPR spectrum resulted from diffusion-controlled photoexcited electron transfer to the solvent.

Experiments on H_2PLQ in more inert solvents like diglyme showed weak EPR signals, probably attributable to residual intermolecular reaction. Higher intensity light sources including a 1 mW helium-neon laser (632nm) did not im-

---

(b) A.R. McIntosh, A. Siemiarczuk, J.R. Bolton, M.J. Stillman, T.-F. Ho, and A.C. Weedon, *J. Amer. Chem. Soc.*, **105**, 7215 (1983).

prove signal strength. A simple calculation indicates that if the back electron transfer were faster than $\sim 10^9$ sec^{-1}, given the dimensions of the illuminated sample, its concentration, a conservative assumption of the quantum yield for charge separation, and the photon flux of the laser, the steady-state concentration of unpaired spins would be less than 10^{11}, which is below the sensitivity range of the standard EPR method. The back transfer rate is probably fast compared to the forward rate, leading to a negligible accumulation of charge-separated species, and thus the inability to observe it. The species observed by previous workers[14] probably resulted from intramolecular exciplex or ground-state complex formation.

Chapter 4

Dynamic Methods

Picosecond Fluorescence Spectroscopy

Picosecond fluorescence spectroscopy allows the direct observation of the singlet excited state of the porphyrin component of *ZnPLQ*, free of many of the complications imposed by steady-state methods. In this way reliable kinetic information about the forward electron transfer may be extracted.

Dilute solutions ($10^{-5} - 10^{-7}$M) of *ZnPLQ* and *ZnP^{t}Bu* were irradiated in quartz cuvettes with a pulsed dye laser λ_{exc} = 570 nm (35 psec FWHM), and emission was analyzed by time-correlated single-photon counting techniques. Fluorescence decays (full rise and decay) were fit to either monoexponential or biexponential decay functions. Lifetimes of the fluorescing state of *ZnP^{t}Bu* are monoexponential in all solvents examined (Figure 1). *ZnPLQ* is biexponential with one major fast component (90-99% in most cases) and a minor component with $\tau \approx 1.5$ nsec, which is most likely porphyrin-hydroquinone (Figure 2). This second component evidently is generated *in situ* by porphyrin-sensitized photoreduction, and accumulates with time. In support of this assignment, a sample obtained by the chemical reduction of *ZnPLQ* with potassium borohydride in CH_2Cl_2/MeOH resulted in a biexponential decay highly enriched in the long-decay component.

Comment on the Free-Base System

Detailed picosecond fluorescence measurements were restricted to the metal-

loporphyrin-quinones. The free-base porphyrin-quinone samples exhibited shortened lifetimes compared with the reference porphyrin, but they also suffered from irreproduceable and multiexponential decay behavior, while the metallo derivatives provided simple and clean biexponential and monoexponential decays. A possible reason for the difficulty in analyzing the free-base porphyrins revolves around the property that H_2PLQ and H_2P^tBu are excellent metal chelators, and are thus expected to scavenge adventitious metal ions (for example, present on surfaces which the sample touches such as silica gel and borosilicate glass[1]). The high stability of the metalloporphyrins is well known, and is exemplified by the association equilibrium constant $K_{assoc} \approx 10^{29}$ for zinc mesoporphyrin IX.[2] At high sensitivity a small amount of metallo-type emission can be detected in steady-state experiments. Because metalloporphyrins have higher molar absorption coefficents and emission efficiencies than the free-base porphyrins, a small amount of the former has a large effect on emission. Metallation of the porphyrin-hydroquinone would add still another component with a distinct lifetime. The presence of the four compounds H_2PLQH_2, H_2PLQ, $MPLQH_2$, and $MPLQ$ would make curve fitting for the free-base system treacherous to interpret, and thus the work described focuses on deliberately metallated systems.

---

[1] Borosilicate glass contains 280,000 ppb Fe: D.T. Sawyer and J.L. Roberts, Jr., *Experimental Electrochemistry for Chemists*, John Wiley & Sons, New York, 1974, p. 135.

[2] J.N. Phillips, *Rev. Pure Appl. Chem.*, **10**, 35 (1960).

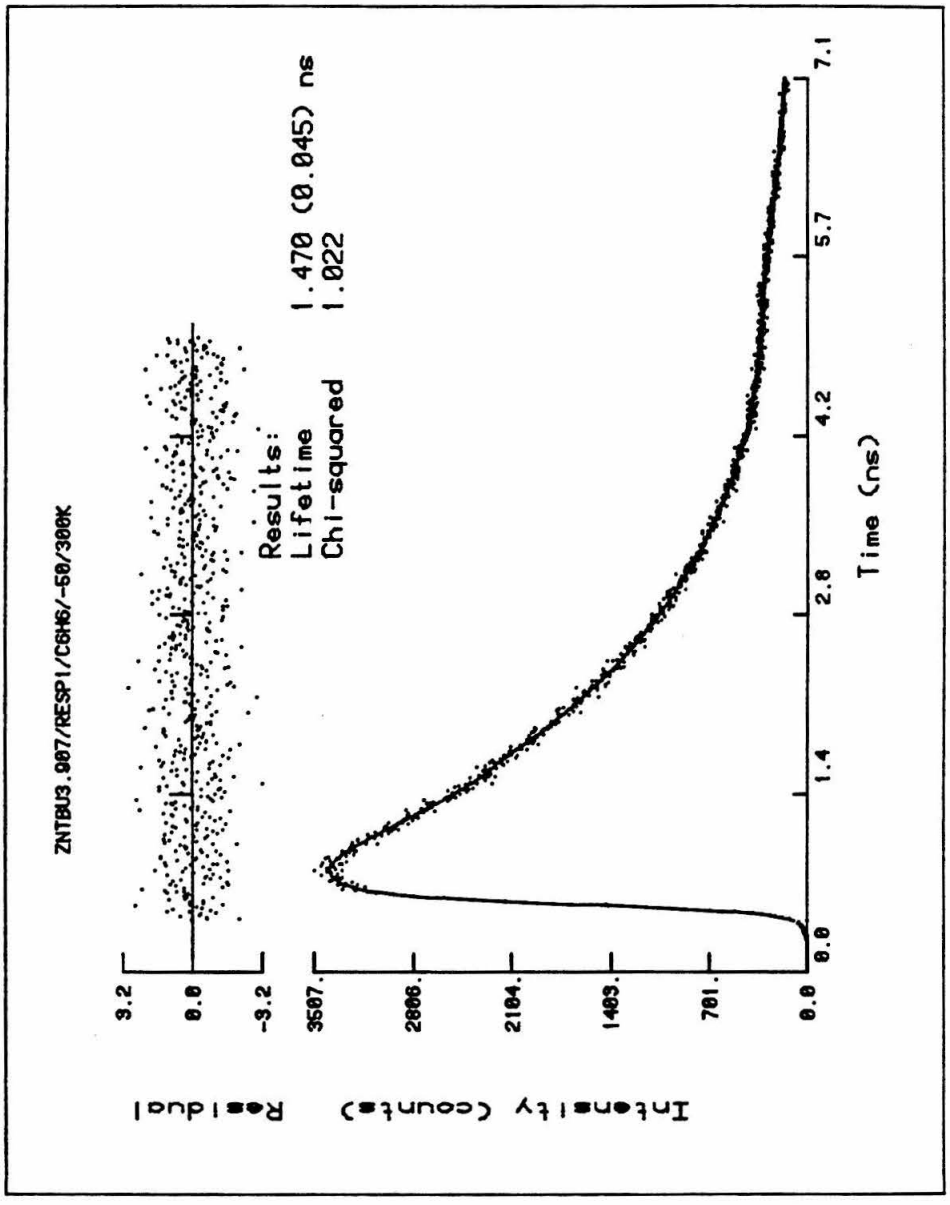

Figure 1. Fluorescence decay of ZnP^tBu in benzene at 298K with monoexponential decay analysis.

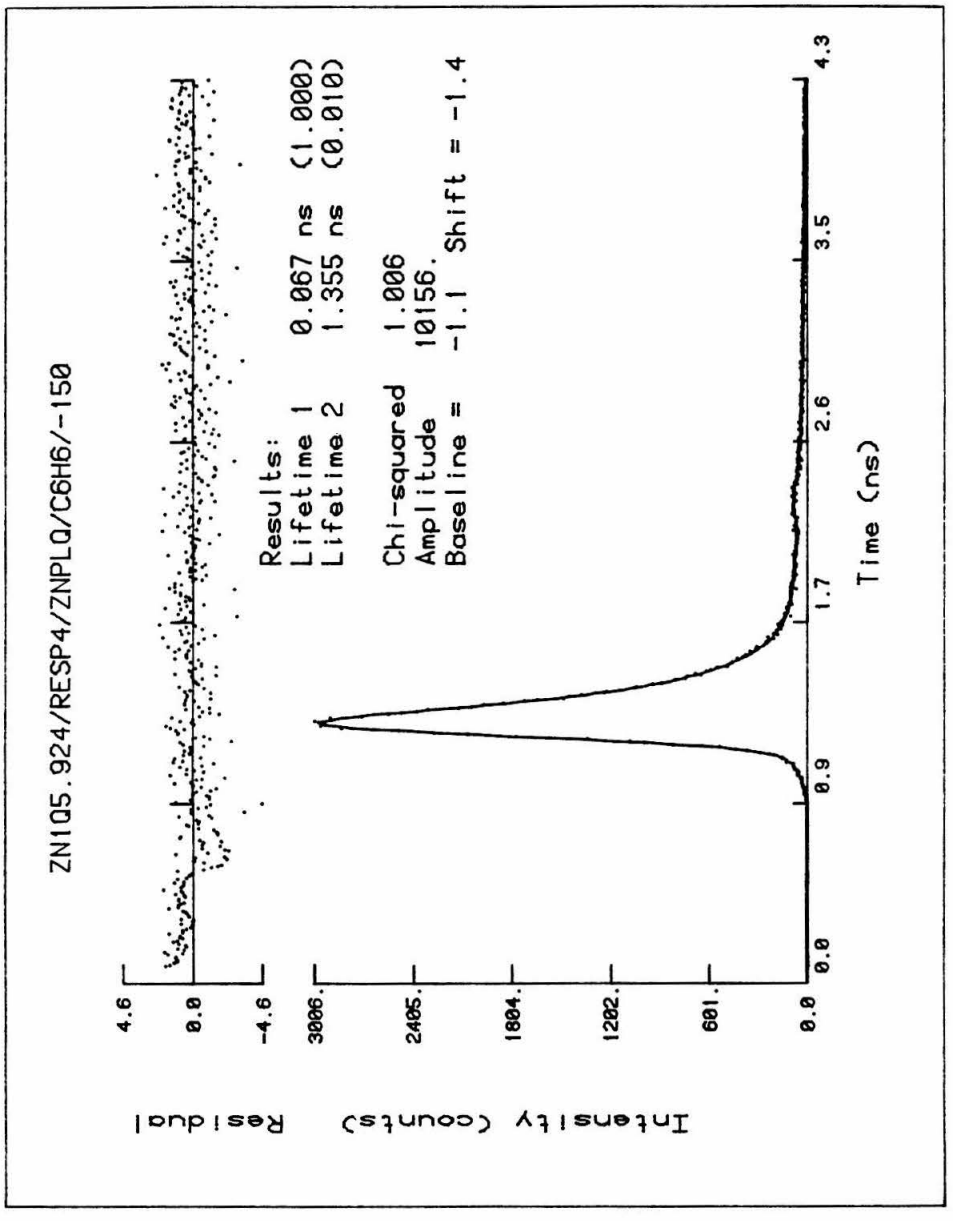

Figure 2. Fluorescence decay of *ZnPLQ* in benzene at 298K with biexponential decay analysis.

Table I. Fluorescence Lifetimes of *ZnPLQ* and *ZnP^{t}Bu* as a Function of Solvent.

Solvent	Compound	τ (nsec)	χ^2_R	ϵ^a
CH_3CN	*ZnPLQ*	0.178	0.976	37.5
"	*ZnP^{t}Bu*	1.64	1.036	
DMF[c]	*ZnPLQ*	0.234	1.011	36.71
"	*ZnP^{t}Bu*	1.71	1.068	
nPrCN[c]	*ZnPLQ*	0.118	1.005	20.3_{21}
"	*ZnP^{t}Bu*	1.59	0.981	
2MTHF	*ZnPLQ*	0.092	1.017	6.24
"	*ZnP^{t}Bu*	1.66	1.059	
o-Xyl[c]	*ZnPLQ*	0.082	1.009	2.568
"	*ZnP^{t}Bu*	1.53	0.995	
C_6H_6 + 2%pyr[c]	*ZnPLQ*	0.051	1.078	NA[b]
"	*ZnP^{t}Bu*	1.60	0.998	
C_6H_6 + 0.1M THAP[c]	*ZnPLQ*	0.091	1.103	NA
"	*ZnP^{t}Bu*	1.48	1.018	
C_6H_6	*ZnPLQ*	0.076	1.081	2.273
"	*ZnP^{t}Bu*	1.47	1.022	
p-dioxane	*ZnPLQ*	0.121	1.021	2.21
"	*ZnP^{t}Bu*	1.68	0.882	

[a] G.J. Janz and R.P.T. Tomkins, *Nonaqueous Electrolytes Handbook*, I, Academic Press, New York, 1972.

[b] Not available.

[c] DMF, *N,N*-Dimethyl formamide; nPrCN, butyronitrile; *o*-xyl, *o*-xylene; pyr, pyridine; THAP, tetra-n-hexylammonium perchlorate.

Solvent Dependence of Electron Transfer Rates

Fluorescence lifetimes for $ZnPLQ$ and the reference porphyrin ZnP^tBu in various solvents are presented in Table I. Rate constants for electron transfer can be calculated from the equation $k_{ET} = 1/\tau - 1/\tau_0$, and are shown in Table II. The data suggest that solvent modulates the electron transfer rate only slightly (within a factor of three).

The observed weak dependence of k_{ET} on solvent polarity is consistent with the view that the solvent undergoes dielectric relaxation after the electron transfer in the nonadiabatic case, when starting from an uncharged state.[3] Only in the back electron transfer which starts from a charged state and polarized solvent distribution will there be a strong solvent effect on rate.[4] It is interesting that the trend towards higher k_{ET} in the porphyrin-methylquinone and porphyrin-dimethylquinone is reversed in benzene, the most nonpolar solvent studied (see below). This may be understood to be a consequence of the fact that the direction of the polarity trend depends on the sign of the quantity $\Delta G^{0'} - \Delta$, where Δ is the vibronic coupling (*i.e.*, the vibrational reorganization energy coupled to the electron transfer). The rate should slow as driving force becomes small

---

[3] J.J. Hopfield, "Low-Temperature Biophysics and Room Temperature Biology," Proceedings of the Conference on Protein Structure: Molecular and Electronic Reactivity, 15-17 April 1985, Philadelphia, Pennsylvania.

[4] T. Kakitani and N. Mataga, *J. Phys. Chem.*, **89**, 8 (1985).

Table II. Electron Transfer Rate Constants in Various Solvents Compared with Solvent Parameters[a,b] ϵ, η, and n^2.

Solvent	k_{ET} (sec^{-1})	ϵ	η(mP)	n^2
CH_3CN	5.00×10^9	37.5_{25}	3.449	1.800
DMF	3.69×10^9	36.71	8.0	2.046
n-PrCN	7.84×10^9	20.3_{21}	5.2_{30}	1.910
2MTHF	1.03×10^{10}	6.24_{25}	4.57	1.977
o-Xyl	1.15×10^{10}	2.568_{25}	8.10	2.267
C_6H_6 + 2% pyr	1.90×10^{10}	NA[c]	NA	NA
C_6H_6 + 0.1M THAP	1.03×10^{10}	NA	NA	NA
C_6H_6	1.25×10^{10}	2.273_{25}	5.961	2.244
p-Dioxane	7.67×10^9	2.21	14.4	2.023

[a] G.J. Janz and R.P.T. Tomkins, *Nonaqueous Electrolytes Handbook*, I, Academic Press, New York, 1972.

[b] CRC, *Handbook of Chemistry and Physics*, 65th ed.

[c] Not available.

compared with vibronic coupling.

Attempts to fit the seven solvent data points by linear regression analysis as $\log k_{ET}$ *vs.* index of refraction $n, n^2, 1/n^2$, or the Marcus solvent parameter

$(1/n^2 - 1/\epsilon)$ gave correlation coefficients of 0.60 or worse. No correlation at all was found for log k_{ET} against viscosity ($r \approx -0.1$). The best fit was with dielectric constant ($r = -0.904$), confirming the weak observed qualitative trend with solvent polarity. The results found contrast with those obtained for adiabatic electron transfer by Kosower and his collaborators.[5] In directly bound aminonaphthalenesulfonamide derivatives, where a phenylamine is the donor and an excited state of naphthalene sulfonamide is the electron acceptor, the electron transfer rate was observed to correlate directly with the dielectric relaxation rate of the solvent, and even better with the "constant-charge corrected" dielectric relaxation rate.[6] Solvents examined were linear alkyl alcohols, and the relaxation times associated with the motion of the OH dipoles gave the best correspondence. According to Eq. [4.1] (Eq 3.21 in Ref. 7a), the electron transfer rate for a nonadiabatic reaction with a diffusive mode is given by:[7a]

$$k_{ET} = \frac{2\pi}{\hbar} \frac{|\, T_{ab} \,|^2}{\sqrt{4\pi\lambda kT}} \left[\frac{1}{1 + (2\pi \,|\, T_{ab} \,|^2 / \hbar\omega_c \lambda)} \right] \exp\left(-\Delta G^{\ddagger}/k_B T\right), \qquad [4.1]$$

which, if $kT \gg \hbar\omega_c$, and if taken to the adiabatic limit, predicts that the rate

---

[5] (a) E.M. Kosower, *J. Amer. Chem. Soc.*, **107**, 1114 (1985). (b) E.M. Kosower and D. Huppert, *Chem. Phys. Lett.*, **96**, 433 (1983). (c) E.M. Kosower, *Acc. Chem. Res.*, **15**, 259 (1982).

[6] (a) H.L. Friedman, *J. Chem. Soc. Faraday Trans.*, **79**, 1465 (1983). (b) H.L. Friedman, *Faraday Discuss. Chem. Soc.*, **74**, 198 (1982).

[7] (a) J.N. Onuchic, D.N. Beratan, and J.J. Hopfield, *J. Phys. Chem.*, **90**, 0000 (1986). (b) W. Bialek, *Dissertation*, University of California, Berkeley, 1983.

becomes proportional to ω_c, the frequency of the solvent mode. This result is in agreement with the classical expression

$$k_{ET} = \kappa\nu \exp\left(-\Delta G^{\ddagger}/k_B T\right) = \nu \exp\left(-\Delta G^{\ddagger}/k_B T\right), \qquad [4.2]$$

which indicates that a nuclear frequency factor should dominate the rate as $\kappa \rightarrow 1$.

The small effect of solvent on electron transfer rate in *ZnPLQ* sharply differs from the sizeable dependence found in a flexible methyleneamide-linked porphyrin-quinone.[8] A range of electron transfer rates varying from 1.4×10^7 sec^{-1} in diethyl ether to 2.3×10^9 sec^{-1} in chloroform was observed. The nearly 200-fold factor may result from a strong dependence of conformation on solvent. Solvent can help increase the rate if there is a *mismatch* of the driving force with the value of an integral number of vibrational spacings; *i.e.*, $\Delta G^{0'} \neq n\hbar\omega$.[7] If there is good match, solvent can only diminish the overall rate by causing broadening and reducing overlap of the spectral energy distributions, and the prefactor $1/\sqrt{4\pi k_B T\lambda}$ starts to have a significant effect. In benzene in normal region cases, little broadening occurs, so the sharp, mismatched states transfer less fast than in more polar solvent (*e.g.*, 2MTHF).

---

[8] J.A. Schmidt, A. Siemiarczuk, A.C. Weedon, and J.R. Bolton, *J. Amer. Chem. Soc.*, **107**, 6112 (1985).

Low-Temperature Fluorescence Studies

The low-temperature fluorescence decay data obtained for the porphyrin-quinone *ZnPLQ* in 2-methyltetrahydrofuran (2MTHF) glass could be fit well using an angle-modulated biexponential function with a statistical goodness-of-fit of $\chi^2_R = 1.11$, according to Equation [4.3] (Figure 3).[3]

$$I(t) = a_0 \sum_{i=1}^{N} \frac{1}{N} e^{-t[(\cos^2\theta_i)/\tau_1 + 1/\tau_2]} + b_0 e^{-t/\tau_2}, \qquad [4.3]$$

where $I(t)$ is the fluorescence intensity at time t, b_0/a_0 is the ratio of initial fluorescence amplitudes, N is the number of dihedral angles $0° \leq \theta_i \leq 90°$ between the planes of porphyrin and quinone. The factor $\cos^2\theta$ occurs because at low temperature in the frozen sample the matrix element T_{ab} varies approximately as $\cos\theta$ as a function of the dihedral angle θ. The rate is proportional to $|T_{ab}|^2$, and so $\cos^2$ correctly modulates $1/\tau_1$.

In the present examples the expected uniform distribution in θ was approximated by N=10 angles, to obtain rapid convergence of the least-squares fitting routine used. The first term represents the contribution to emission deriving from electron transferring states with a distribution of rotational angles about the long axis of the molecule. When $\theta_i = 90°$, the π orbitals of the porphyrin and quinone are orthogonal, and no electron transfer detectable by the fluorescence method should occur in this approximation. The high symmetry of the mediating bicyclo[2.2.2]octyl bridge prevents additional conformational possibili-

ties from confounding the analysis. In this case the porphyrin-quinone molecules should exhibit emission characteristics similar to those for the reference porphyrin *meso-p*-t-butylphenyloctamethylporphyrin or the porphyrin-hydroquinone (reduced quinone). The second term in Equation [4.3] represents emission from the small fraction of porphyrin-hydroquinone most likely resulting from photosensitized reduction of the quinone.

The observed lifetime determined for the long lifetime component in 2MTHF glass by fitting Equation [4.3] is $\tau_2 = 1.67$ nsec, which compares well with the lifetime of the reference porphyrin ZnP^tBu at 77K, which remains cleanly monoexponential (Figure 3(c); $\tau_0 = 1.78$ nsec; $\chi^2_R = 1.01$) so the observed reactivity is not due to a peculiar "site effect" of the glass. The lifetime obtained using the same equation for the quinone $ZnPLQ$ is $\tau_1 = 110$ psec, and may be interpreted as a shortened lifetime due to electron transfer in the optimized conformation with respect to chromophore orientation. This decay lifetime corresponds to a rate constant for electron transfer $k_{ET} = 1/\tau_1 - 1/\tau_0 \approx 8.5 \times 10^9$ sec^{-1}; it is a "minimum" lifetime because it represents the maximum electron transfer rate for any rotational conformation, which means that $\cos\theta$ is a maximum at ($\theta = 0°$). One can calculate a mean lifetime as twice the "minimum" lifetime, since the mean is defined as the average of all the lifetimes modulated by rotation about

the dihedral angle θ:

$$\frac{1}{\langle\tau\rangle} = \lim_{N\to\infty}\frac{1}{\tau_1}\cdot\frac{1}{N}\sum_{i=1}^{N}\cos^2\theta_i = \frac{1}{\tau_1}\cdot\frac{2}{\pi}\int_0^{\pi/2}\cos^2\theta d\theta = \frac{1}{2\tau_1} \qquad [4.4]$$

$$\langle\tau\rangle = 2\tau_1 \qquad [4.5]$$

and thus the average rate constant is $k_{ET} = 4\times10^9$ sec^{-1}. These rates compare with 1.0×10^{10} sec^{-1} for the same molecule at 298K in 2MTHF. The fact that fluorescence decay is nonexponential implies that the electron transfer quenching reaction is sensitive to the precise geometry of the molecule. According to theory, this can result only in the case that the electronic tunneling matrix element is small and "rate-limiting." The probability of passing from the reactant surface to the product surface is low. The observation that a different rate constant can be assigned to each change in dihedral angle indicates that the electron transfer must be nonadiabatic. If the reaction were adiabatic, changes in geometry could not affect the rate drastically through $|T_{ab}|$. Nuclear rearrangements become important; *e.g.*, solvent motions and ligand motions may dominate.

To examine the uniqueness of the angle-modulated biexponential analysis, attempts were made to fit the low-temperature fluorescence decay to a triple exponential function with three additional (and a total of nine adjustable) parameters, and failed to provide good agreement with the data.

ZnPLQMe was also examined at 77K, and found to be reactive. Using eq. [4.3] ($N = 10$), values of $\tau_1 = 0.263$ nsec and $\tau_2 = 1.832$ nsec were obtained

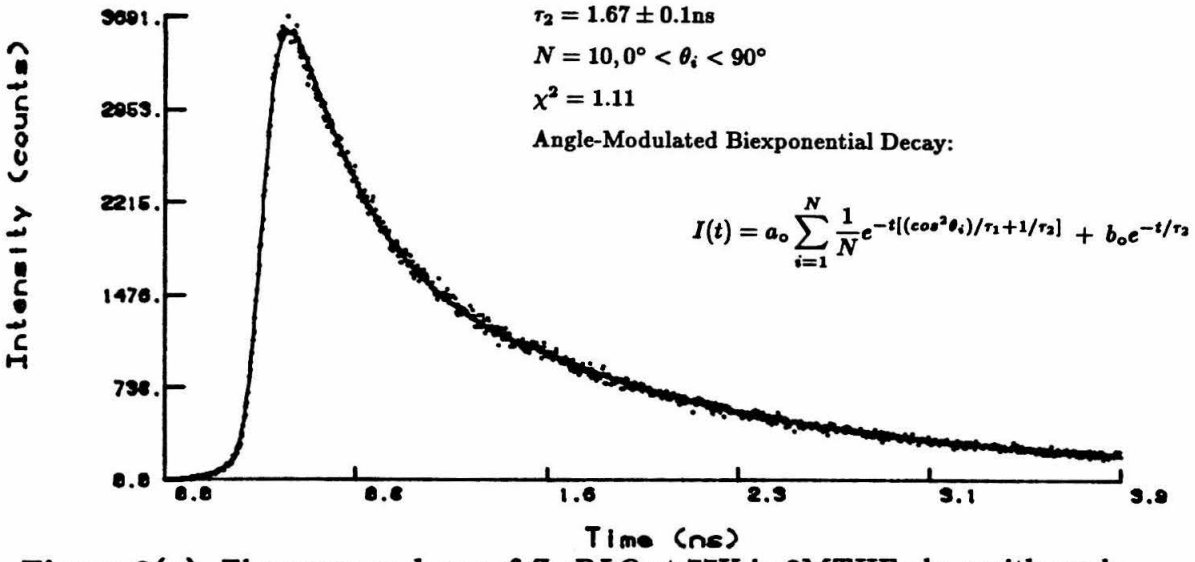

Figure 3(a). Fluorescence decay of *ZnPLQ* at 77K in 2MTHF glass with angle-modulated biexponential analysis.

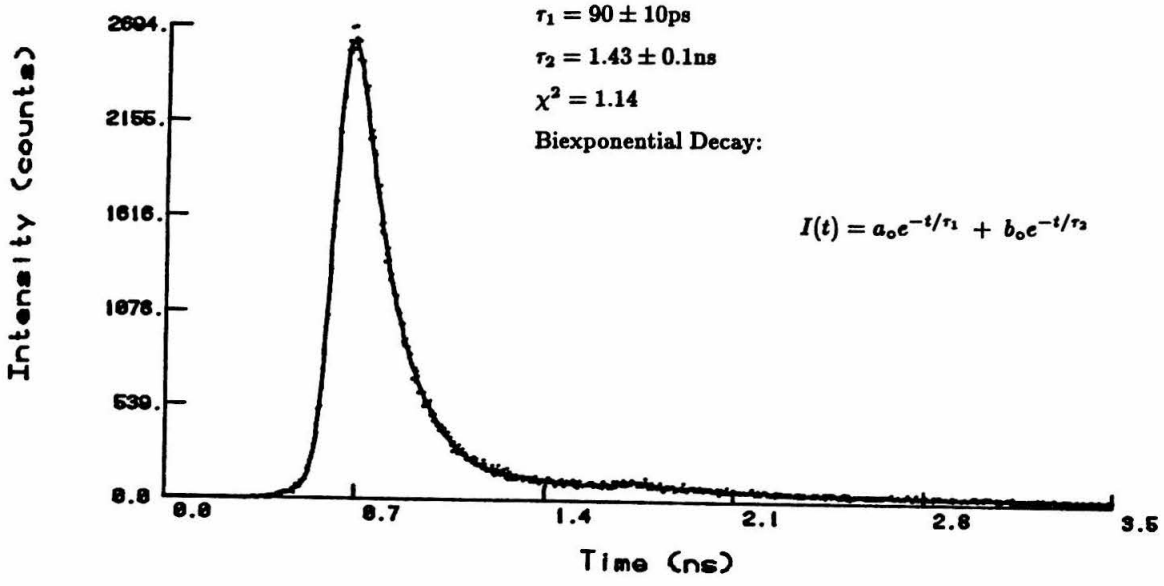

Figure 3(b). Fluorescence decay of *ZnPLQ* at 298K in 2MTHF with biexponential analysis.

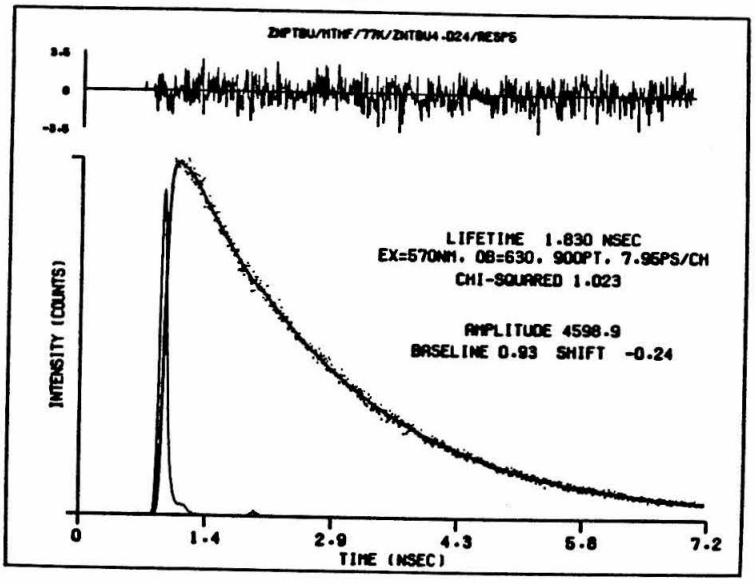

Figure 3(c). Fluorescence decay of ZnP^tBu at 77K in 2MTHF glass with monoexponential decay analysis.

($\chi^2 = 1.024$). The average electron transfer rate constant is 1.35×10^9 sec^{-1}, compared with 2.00×10^9 sec^{-1} (less than a factor of two change) at room temperature. $ZnPLQMe_2$ also showed qualitatively similar behavior at 77K. In constrast to $ZnPLQ$, data for $ZnPLQMe$ (and $ZnPLQMe_2$) at 77K in 2MTHF can actually be fit to a biexponential decay function with excellent statistics. However, the fit for $ZnPLQMe$ is characterized by a large (*ca.* five-fold) increase in the long lifetime component *versus* the decay taken for the *same sample* at room temperature immediately before the low-temperature experiment. A significant amount of short lifetime component is present. A simple interpretation is that because of the lower exothermicity in this case, the maximum rate is lower (as it is, by a factor of 10 at 298K) than for $ZnPLQ$. The distribution of rota-

tional conformations is probably similar to that of $ZnPLQ$, but there are more conformations that are undetectable by the fluorescence technique because they are unfavorable for electron transfer. Thus, the slower rates are being bunched together with similar lifetimes, all close to that of the porphyrin-hydroquinone. The fitting algorithm cannot distinguish among several similar lifetimes; instead, it averages and gives the best line through the points. Likewise, on the fast side the value of $T_{ab}\cos\theta_i$ changes slowly near angles of $\theta \approx 0°$, and so the fast lifetimes are also bunched together around one average number.

The main point remains that $ZnPLQMe$ and $ZnPLQMe_2$, like the more exothermic case $ZnPLQ$, also are appreciably quenched at low temperature. Thus, low-temperature reactivity is not necessarily due to the fact that electron transfer is activationless in either molecule, but rather it is a likely result of nuclear tunneling through the barrier, even at room temperature. When the reaction rate is optimized ($|\Delta G^{0'}(R)| = \lambda$), and the reaction appears formally activationless, the electron must always tunnel its barrier if the reaction is nonadiabatic. If the reaction coordinate is strongly coupled to a high-frequency mode, the nuclear rearrangement is not accessible ($kT \ll \hbar\omega$), and so the nuclei must tunnel so as to bring the electronic energies into a quasi-degenerate condition, thereby fulfilling the requirements of energy conservation. All compounds examined for low-temperature electron transfer (ranging from the methylquinone

to the dichloroquinone[9] derivatives) show reactivity. This pattern of reactivity suggests that quantum effects are dominating electron transfer through the bicyclo[2.2.2]octane bridge. Classical effects appear in the weak solvent interactions, causing broadening of thermal probability distributions.

Precedent exists for nonexponential ligand binding kinetics resulting from distributions of frozen configurations in large heme-proteins. For example, a distribution of different structures has been invoked to explain the nonexponential decay in CO recombination kinetics, wherein each structure or conformation exhibits its own reaction rate.[10] The kinetics has been analyzed in terms of a distribution of activation energies. In this case, as in photosynthetic electron transfer, tunneling is involved, and in both it seems that the reaction is strongly coupled to fast, intramolecular vibrational modes. In *ZnPLQ* the analogous nonexponential kinetics observed result from a distribution of rotational conformations, giving rise to a distribution of different electronic prefactors.

The observation of low-temperature electron transfer activity has not been confirmed yet by direct transient absorption spectroscopy. And until this experiment is performed, doubt about assignment of the shortened lifetime to temperature-independent tunneling from room temperature to 77K will remain.

---

[9] B.A. Leland, *Dissertation*, California Institute of Technology, 1986.

[10] (a) P.G. Debrunner and H. Frauenfelder, *Ann. Rev. Phys. Chem.*, **33**, 283 (1982). (b) N. Agmon and J.J. Hopfield, *J. Chem. Phys.*, **78**, 6947 (1983).

The possibility, however, of aggregation of the porphyrin or intermolecular complexation with the quinone moiety seems unlikely. Electronic absorption spectra of $ZnPLQ$ (Figure 4) in 2MTHF at 298K and 77K and ZnP^tBu at 298K (Figure 5) were determined at several concentrations ($10^{-5} - 10^{-3}$M). As the concentration increases, a small bathochromic shift in the Soret band occurs (from 409 nm to 414 nm in ZnP^tBu), bands become slightly broadened (especially the Soret band at 77K), and two minor bands around 440 nm and 500 nm become distinctly more intense in relation to the $S(0,0)$ and $S(0,1)$. Absorbance no longer follows Beer's law at the highest concentrations. The picosecond fluorescence lifetime measurements at low temperature were done at a variety of concentrations $\leq 10^{-5}$M, and the observed non-exponential behavior appeared to be independent of this variable. The shape of the decay curve remained the same at all concentrations examined. The *lack* of lifetime quenching in the bis(bicyclo[2.2.2]octane) linked porphyrin-quinone is also consistent with the view that intermolecular complexation is absent.[9] Another important point is that ZnP^tBu displays clean monoexponential decay behavior at 77K in 2MTHF glass, indicating that the porphyrin itself is not aggregating. Thus, self-quenching or degenerate energy transfer is not an adequate explanation for the low-temperature behavior.

Ligand-metal interactions (and π,π interactions to a lesser extent) are known

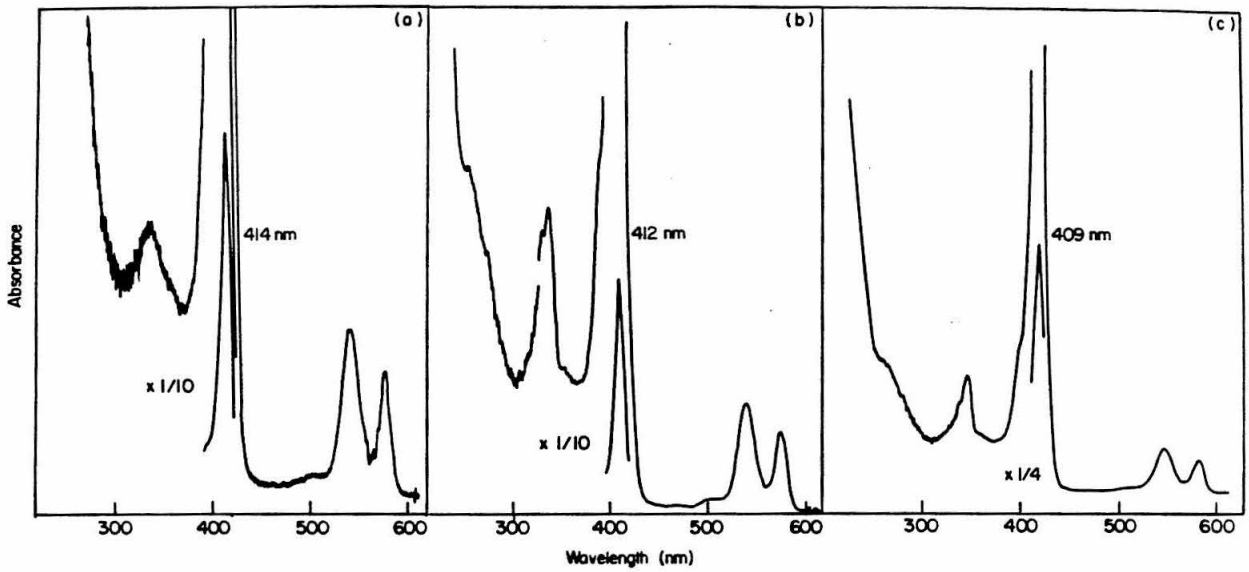

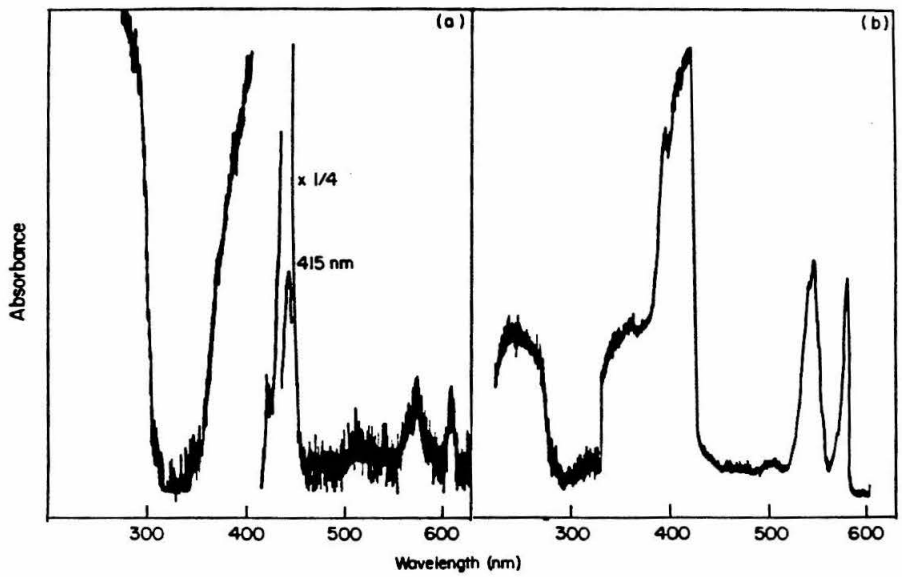

Figure 4(a). Electronic spectrum of $ZnPLQ$ in 2MTHF at 298K at several concentrations. **Figure 4(b).** Electronic spectrum of $ZnPLQ$ in 2MTHF at 77K at several concentrations.

to play a significant role in metalloporphyrin self-aggregation,[11] characterized by fairly low equilibrium constants ($\sim$ 4 M^{-1}).[12] As 2MTHF is a good ligand (electrochemical studies described later in this chapter show a shift of the porphryin oxidation potential (*versus* the ferrocene/ferrocenium reference electrode in 2MTHF compared with non-coordinating solvents such as benzene and even acetonitrile and butyronitrile), due to its electron donor ability, it is not likely to induce aggregation; it might well disrupt it, as is well documented for strongly ligating solvents such as methanol.[11]

Temperature-independent electron transfer has been observed previously in protein-based models of the photosynthetic reaction center. Two principal examples include the modified hemoglobin[13] of Hoffman's group and the Ru modified blue copper protein azurin and cytochrome *c*[14] of Gray and his collaborators. The first system has kinetic activity which resembles that of the cytochrome *c*

---

[11] H. Scheer and J.J. Katz, in K.M. Smith, ed., *Porphyrins and Metalloporphyrins*, Elsevier, Amsterdam, 1975.

[12] D.A. Doughty and C.W. Dwiggins, Jr., *J. Phys. Chem.*, **73**, 423 (1969).

[13] S.E. Peterson-Kennedy, J.L. McGourty, and B.M. Hoffman, *J. Amer. Chem. Soc.*, **106**, 5010 (1984).

[14] (a) N.M. Kostic, R. Margalit, C.-M. Che, and H.B. Gray, *J. Amer. Chem. Soc.*, **105**, 7765 (1983). For evidence of temperature-independence in $Ru(NH_2)_5$-modified cytochrome *c* electron transfer, see (b) J.R. Winkler, D.G. Nocera, K.M. Yocom, E. Bordignon, and H.B. Gray, *J. Amer. Chem. Soc.*, **104**, 5798 (1982) and (c) K.M. Yocom, D.G. Nocera, E. Bordignon, and H.B. Gray, *Chem. Scripta*, **21**, 29 (1983).

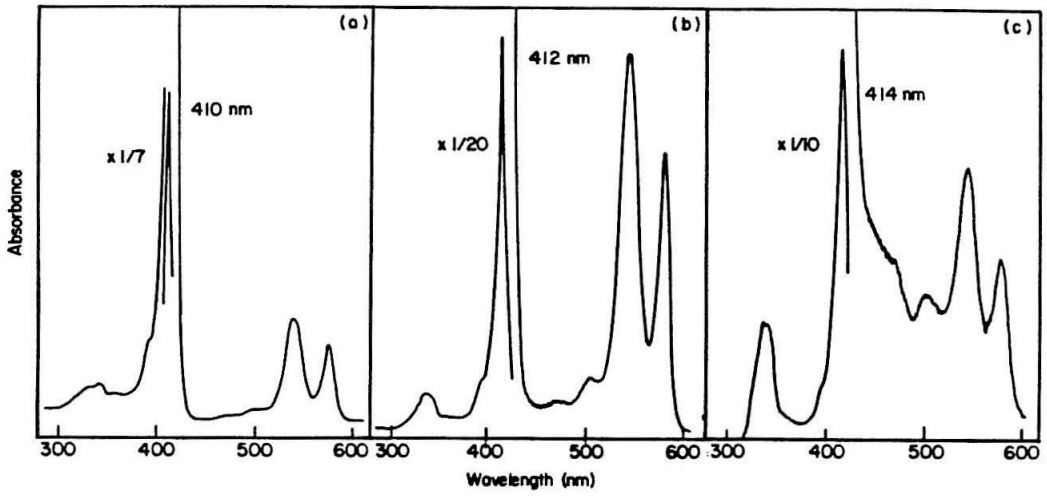

Figure 5. Electronic spectrum of ZnP^tBu in 2MTHF at 298K at several concentrations.

oxidation by the bacteriochlorophyll dimer special pair in having a thermally activated regime and a temperature-independent regime below ~ 100K. The modified azurin exhibits temperature-independent tunneling at all temperatures accessible to the protein (7°-43°C). Pulse radiolysis-initiated reactions are known to occur quite rapidly at 77K in glassy matrices.[15]

These cases lead one to wonder: Why does low-temperature electron trans-

---

[15] J.R. Miller and J.V. Beitz, *J. Chem. Phys.*, **74**, 6746 (1981).

fer among all model systems occur exclusively in *ZnPLQ*, and *not* in the others, in particular the rigid triptycene-linked porphyrin-quinone system?[16] In fact, low-temperature electron transfer activity is expected if tunneling is an important part of the mechanism. A possible interpretation of the differing reactivity is that the *meso*-(quinonetriptycene)phenyl group adopts a conformation highly unfavorable to electron transfer when the molecule is cooled. The fact that at 298K electron transfer occurs with such a high rate constant ($> 10^{11}$ sec^{-1}) suggests that the reaction may indeed be adiabatic, or perhaps intermediate between adiabatic and nonadiabatic. If it is nearly adiabatic, slow solvent, molecular or nuclear motions may dominate the electron transfer reaction, and as a result, appear thermally activated at all temperatures. Only two CC σ bonds separate the edge atoms of the phenyl connecting with the porphyrin and the *p*-benzoquinone of the triptycene-linked porphyrin-quinone. Dreiding models demonstrate that the plane of the *p*-benzoquinone is inclined at near right angles (75-85°) with respect to the porphyrin plane, forming the "edge" of a box, when the *meso*-phenyl group is perpendicular to the porphyrin plane. X-ray diffraction evidence supports this orientation in the crystalline state.[17] The perpendicular conformation may be significant at low temperatures. Another possible explanation is the

---

[16] (a) M.R. Wasielewski, personal communication. (b) M.R. Wasielewski and M.P. Niemczyk, *J. Amer. Chem. Soc.*, **106**, 5043 (1984).

[17] J.L. Hoard, *Science* (*Washington, D.C.*), **174**, 1295 (1971).

lower driving force.

Distance Dependence of Electron Transfer Reactions

Fluorescence lifetime data on *ZnPLQ* are presented in Table III with data on *ZnPLLQ*, the homologous compound prepared by B.A. Leland with two bicyclo[2.2.2]octane moieties in series. Together these compounds allow an estimate of how distance attenuates the electron transfer rate constant. The data collected for four solvents (benzene, 2MTHF, butyronitrile, and acetonitrile) indicate a dramatic reduction in electron transfer rate by a 4 Å increase in distance edge-to-edge between the porphyrin and quinone chromophores, on the order of a factor of 500 to 1500. The lifetimes for *ZnPLQ* and *ZnPLLQ* in benzene are 64 psec and 1.45 nsec, respectively, corresponding to electron transfer rate constants of 1.15×10^{10} sec^{-1} and $\leq 10^{7}$ sec^{-1}. This rate comparison provides an approximation of the decay constant α according to the equation:

$$k = k_0 \exp(-\alpha R). \qquad [4.6]$$

A value of ≥ 1.4 is obtained for α.

Energy Gap Dependence: Electrochemical Studies

Previous studies of electron transfer reactions in model systems have in general lacked the corresponding electrochemical measurements. Knowledge of electron transfer rate constants becomes useful in examining theory only when other properties are known about the systems under consideration. Throughout this

Table III. Fluorescence lifetimes for zinc porphyrins.

Compound	Solvent	χ_R^2 [a]	τ(nsec)	$k_{ET}(\text{sec}^{-1})$
ZnP^{t}Bu	C_6H_6	1.02	1.47	
ZnPLQ	C_6H_6	1.08	0.076,1.51 (71:1)	$1.25\text{x}10^{10}$
ZnPLLQ	C_6H_6	0.93	1.45	$\leq 9\text{x}10^{6}$
ZnP^{t}Bu	MTHF	1.04	1.66	
ZnPLQ	MTHF	1.14	0.090, 1.42 (50:1)	$1.0\text{x}10^{10}$
ZnPLLQ	MTHF	1.02	1.61	$\leq 2\text{x}10^{7}$
ZnP^{t}Bu	nPrCN	1.03	1.59	
ZnPLQ	nPrCN	1.16	0.120, 1.64 (10:1)	$7.7\text{x}10^{9}$
ZnPLLQ	nPrCN	0.99	1.54	$\leq 2\text{x}10^{7}$
ZnP^{t}Bu	CH_3CN	1.03	1.62	
ZnPLQ	CH_3CN	0.98	0.178, 1.60 (20:1)	$5.0\text{x}10^{9}$
ZnPLLQ	CH_3CN	0.99	1.60	$\leq 8\text{x}10^{6}$

[a] P.R. Bevington, *Data Reduction and Error Analysis for the Physical Sciences*, McGraw-Hill, New York, 1969, p. 202.

thesis we have emphasized the importance of knowing the distance between donor and acceptor edges, and even more crucial is the certainty of maintaining this distance as a constant. But without information on reaction thermodynamics, there can be no discussion of the origins of the energetic factors responsible for the observed kinetic behavior. Electrochemistry provides a facile means of determining directly the redox potentials for porphyrin oxidation and quinone reduction.

The overall free energy of reaction $\Delta G^{0\prime}(R)$ in each solvent is computed using the half-wave potentials $E_{1/2}$ for the isolated donor and acceptor redox processes, the singlet excitation energy of the porphyrin, and the electrostatic correction W_P given by Coulomb's Law for point charges separated by distance R. The accuracy of $\Delta G^{0\prime}(R)$ depends on the adequacy of several assumptions. The Coulomb work term as used here approximates the donor and acceptor as point charges when they may indeed better resemble charged disks at the distances being considered. The contribution of the saturated spacer to the effective dielectric constant of the medium has an effect of unknown magnitude on the overall shielding and solvation of the charge-separated species. Calculations of the Coulomb term in more relevant geometries, including attempts to determine the quantitative effect of the linker on the overall dielectric constant, should clarify these issues and perhaps justify the assumptions used in calculation of the exothermicity.

Electrochemical measurements were carried out to obtain the oxidation and

reduction potentials for the porphyrin-quinone molecules. A cyclic voltammogram of *ZnPLQ* in dichloromethane (0.1M tetra-n-butylammonium perchlorate; TBAP) appears in Figure 6, and demonstrates the presence of two oxidative waves attributed to the first and second one-electron oxidations of the metalloporphyrin and one reductive wave assigned to the one-electron reduction of the *p*-benzoquinone moiety. The porphyrin waves are reversible, but the quinone/semiquinone couple is quasi-reversible (*i.e.*, nonnernstian in the heterogeneous electron transfer) on the CV timescale.[18]

The CV in Figure 6 is clearly the superposition of the individual voltammograms for the isolated redox couples. The fact that they are coupled has no effect on their redox behavior, implying that the assumption of little or no direct electronic interaction is valid. Because of this, and because of the limited available quantities of *ZnPLQ*, subsequent studies were performed on the more plentiful isolated chromophores, zinc *meso*-t-butylphenyl porphyrin ZnP^tBu and the methyl *p*-benzoquinone. For the porphyrins modified with a methylbenzoquinone group, a dimethylbenzoquinone group, or a cyanobenzoquinone group, the quinone moieties were modeled by 2,5-dimethyl-*p*-benzoquinone, 2,3,5-trimethyl-*p*-benzoquinone, 2-cyano-5-methyl-*p*-benzoquinone, respectively. The corre-

---

[18] *Cf.* J.H. Wilford, M.D. Archer, J.R. Bolton, T.-F. Ho, J.A. Schmidt, and A.C. Weedon, *J. Phys. Chem.*, **89**, 5395 (1985). Differential pulse voltammograms of the free-base tetraphenylporphyrin substituted by a flexible, trimethylene amide benzoquinone also showed a quasi-reversible wave with ΔE_p(FWHM)$\approx$ 200 mV.

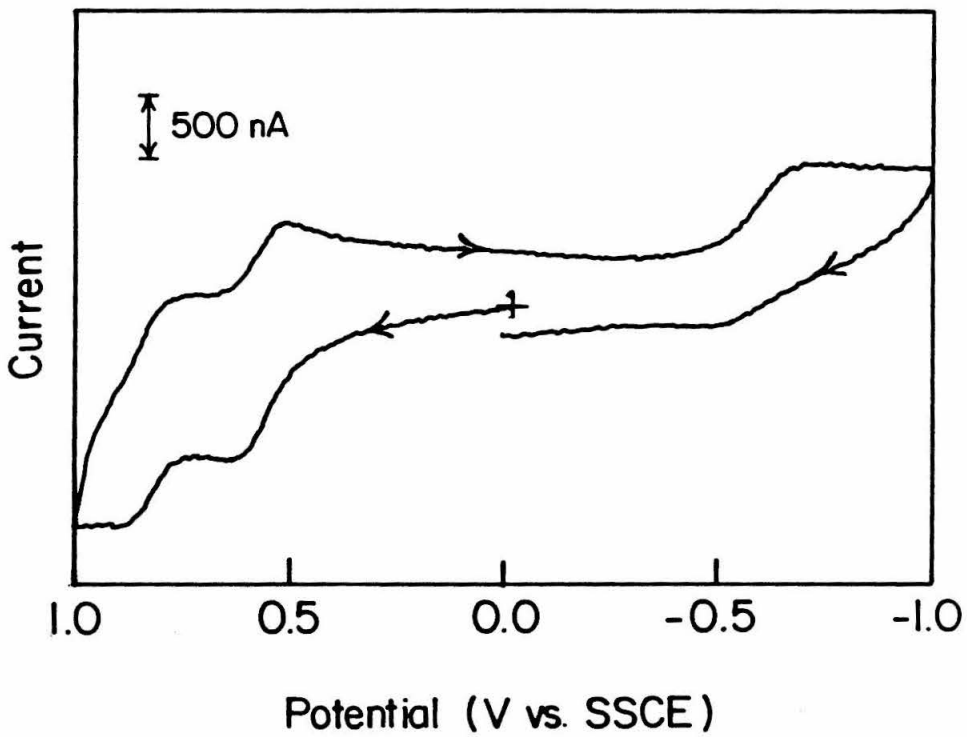

Figure 6. Cyclic voltammogram of *ZnPLQ* in CH_2Cl_2 (0.1M TBAP).

sponding model compounds for the bromo- chloro-, and dichlorobenzoquinones were prepared and analyzed electrochemically by B.A. Leland.[9]

In order to be able to compare redox potentials, electrochemical techniques were kept as constant as the properties of the materials and the methods themselves allowed. Low solubility of the zinc porphyrin in acetonitrile (AN) mandated that a more sensitive measuring method be used in this solvent. So instead of linear sweep voltammetry, differential pulse voltammetry was employed in this solvent at a larger diameter platinum disk electrode (1.6 mm in diameter).

Linear sweep voltammetry at polished platinum disk microelectrodes (25 μ and 127 μ in diameter) was carried out on the model porphyrins and quinones in the solvents: benzene, 2-methyltetrahydrofuran (2MTHF), butyronitrile (BN), and N,N-dimethylformamide. Sample voltammograms for the porphyrin-quinone models and for ferrocene are displayed in Figures 7-8 for 2MTHF and benzene. Redox potentials, indicators of electrochemical reversibility,[19] and precise conditions of supporting electrolyte are presented in Tables IV and V. Use of microelectrode techniques[20] was

---

[19] Electrochemical reversibility of the linear sweep voltammograms is estimated by the Tomeš criterion[19b] $|E_{3/4} - E_{1/4}|$ which denotes a fully reversible couple if equal to 56 mv. (b) A.J. Bard and L.R. Faulkner, *Electrochemical Methods: Fundamentals and Applications*, Wiley, New York, 1980.

[20] (a) R. Lines and V.D. Parker, *Acta Chim. Scand.*, **B31**, 369 (1977). (b) R.M. Wightman, *Anal. Chem.*, **53**, 1125A (1981). (c) R.W. Murray, personal communication.

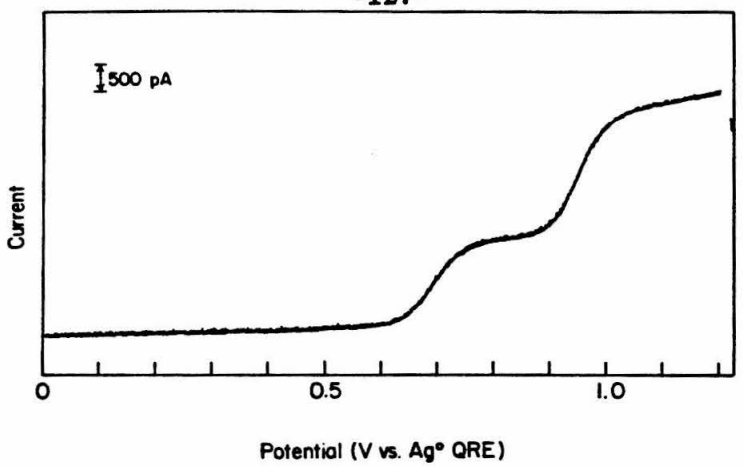

Figure 7(a). LSV of ZnP^tBu in 2MTHF ($\sim 10^{-5}$M, 0.1M THAP).

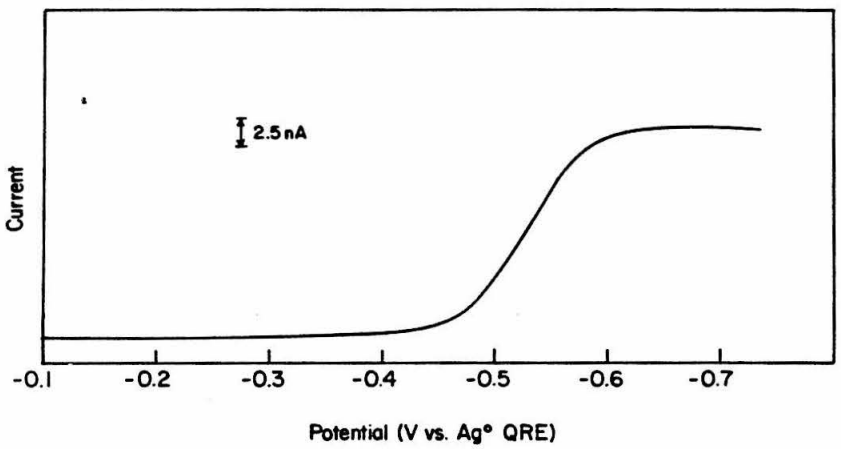

Figure 7(b). LSV of methyl-*p*-benzoquinone in 2MTHF (~0.01M, 0.1M THAP).

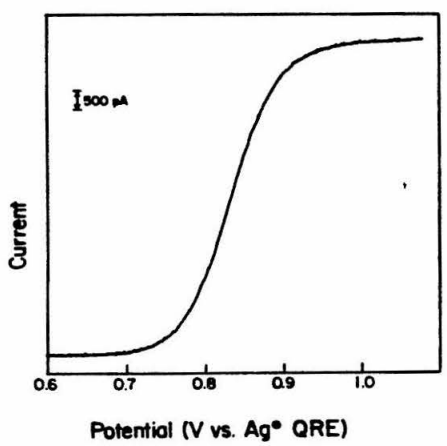

Figure 7(c). LSV of ferrocene in 2MTHF (~0.01M, 0.1M THAP).

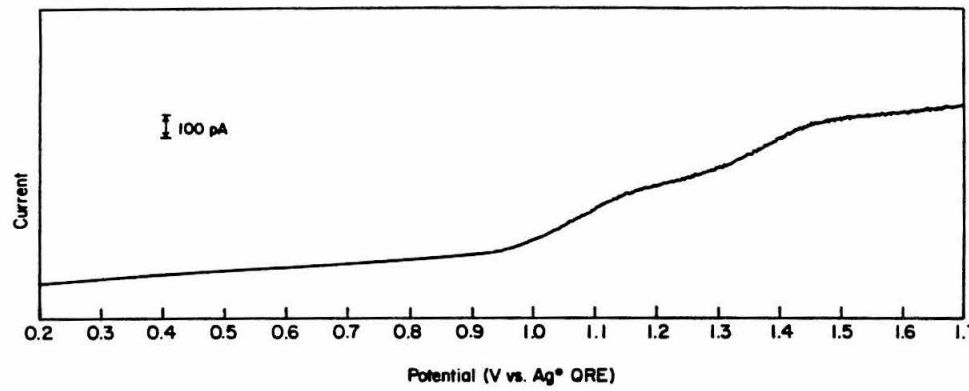

Figure 8(a). LSV of ZnP^tBu in C_6H_6 ($\sim 10^{-5}$M, 0.3M THAP).

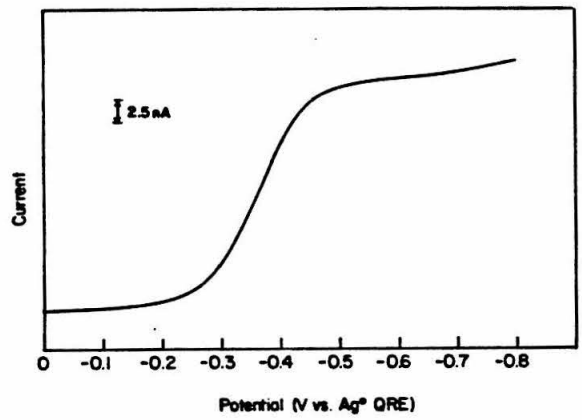

Figure 8(b). LSV of methyl-*p*-benzoquinone in C_6H_6 (~0.01M, 0.1M THAP).

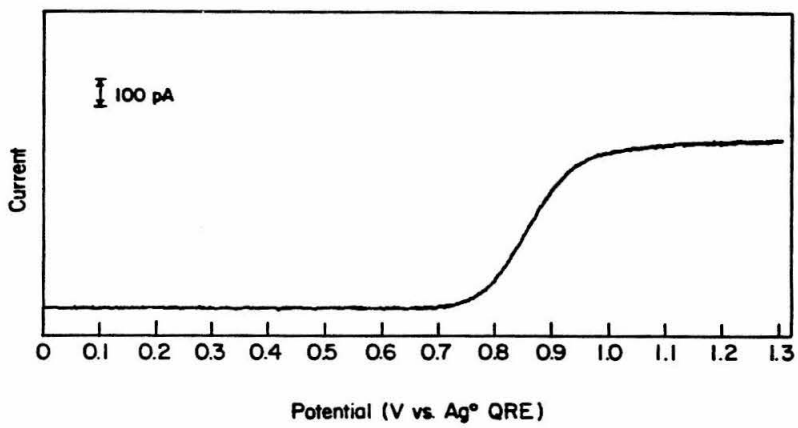

Figure 8(c). LSV of ferrocene in C_6H_6 (~0.01M, 0.1M THAP).

essential for the measurements conducted in highly resistive solvents like benzene and 2MTHF. The reason normal dimension working electrodes cannot be used in these studies is the prohibitive ohmic potential drop, causing a shift in the apparent redox potential to more extreme (non-equilibrium) values. In this situation ionic transference has decreased in comparison to the charging current so that extensive wave broadening occurs, and no signal can be distinguished from background charging.[21] However, for the same solution resistance, there is less current at a small diameter electrode, thus reducing the ohmic drop. The ohmic drop becomes small enough so that thermodynamic values of $E^{0'}$ can be obtained.

The one-electron first reduction potentials (determined *versus* the ferrocene/ferrocenium reference electrode[22]) of methyl-*p*-benzoquinone are given in Table IV, and appear to correlate well[23] with Gutmann's solvent parameter, the acceptor number (AN),[24] which is based on the ^{31}P NMR chemical shift of the

---

[21] See, for example, Ref. 17*b*.

[22] The ferrocene reference electrode is assumed to provide a solvent-independent potential standard: G. Gritzner and J. Kuta, *Pure Appl. Chem.*, **56**, 461 (1984).

[23] (a) J.S. Jaworski, E. Leśniewska, and M.K. Kalinowski, *J. Electroanal. Chem.*, **105**, 329 (1979). (b) J.H. Wilford and M.D. Archer, *J. Electroanal. Chem.*, **190**, 271 (1985).

[24] (a) V. Gutmann, *The Donor-Acceptor Approach to Molecular Interactions*, Plenum Press, New York, 1978. (b) V. Gutmann, *Electrochim. Acta*, **21**, 661 (1976). (c) R.H. Erlich and A. Popov, *J. Amer. Chem. Soc.*, **93**, 5620 (1971).

reference compound triethylphosphine oxide (Et_3PO) in each solvent (Figure 9). The good linear correlation (r =0.984) indicates that the trend in solvation energy for the anion is not disrupted by particular (*e.g.*, steric) properties of any of the solvents.

The half-wave potential for oxidation of the zinc porphyrin *versus* ferrocene in each solvent is shown in Table V, and is plotted graphically (Figure 10) against Gutmann's solvent parameter, the donor number (DN), which corresponds to the enthalpy of formation of the complex of solvent with the reference acceptor antimony pentachloride ($SbCl_5$),[24] measured either by thermochemical methods or by ^{23}Na NMR shifts of $NaClO_4$.[24c] The oxidation potential of ZnP^tBu is not strongly affected by solvent except for 2MTHF and DMF. The simplest interpretation is that the metalloporphyrin undergoes weak ligating interactions at the fifth axial site on zinc by the solvents with high donor numbers. In the aromatic and nitrilic solvents, no specific solvent interaction seems to be occurring, and very much like the solvent-independent ferrocene electrode, the electrochemical properties of the highly delocalized porphyrin are not expected to change appreciably in these solvents.

The question of specific ion-pairing effects in different solvents with supporting electrolyte is somewhat uncertain. In the case of both the porphyrin and the quinones, no major changes in the half-wave potential occurred at a variety of supporting electrolyte concentrations. A study of the effect of positive counterion

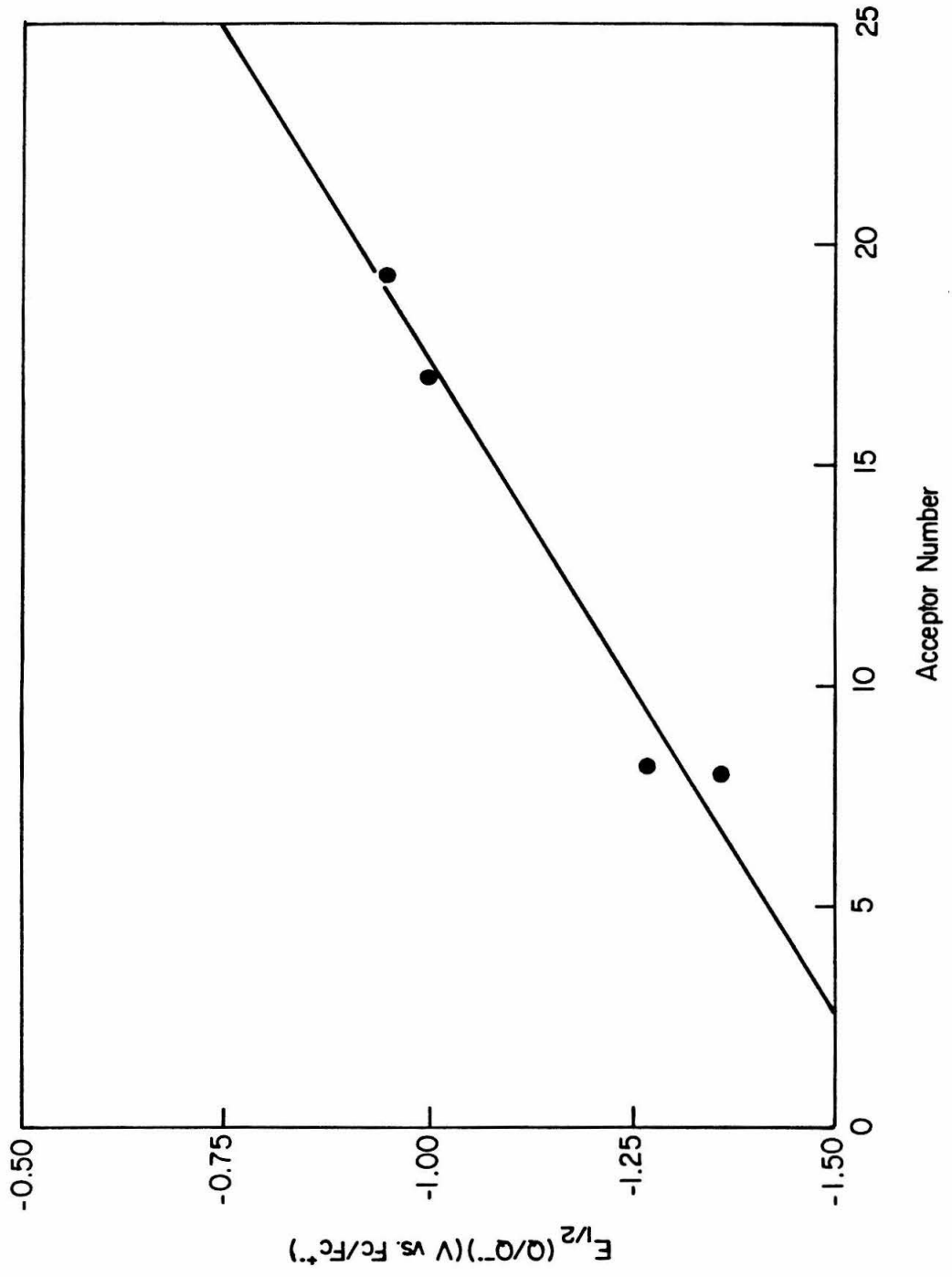

Figure 9. Half-wave potential *vs.* acceptor number for the reduction of methyl-*p*-benzoquinone in various solvents.

Table IV. Half-wave potentials for reduction of methyl-*p*-benzoquinone in various solvents.[a]

Solvent	$E_{1/2}(Q/Q^{-\cdot})$(V)[b]	$\lvert E_{3/4} - E_{1/4}\rvert$ (mV)	Conditions
CH_3CN	−0.95	(~ 200)[c]	0.2M TBAP
nPrCN	−1.00	65	0.1M TBAP
2MTHF	−1.36	59	0.3M THAP
C_6H_6	−1.30	85	0.3M THAP

[a] Determined by linear sweep voltammetry (at a 25 μ dia. Pt microelectrode) except for CH_3CN by differential pulse voltammetry (at a 1.6 mm dia. Pt electrode) due to insolubility in this solvent, using ferrocene/ferrocenium reference electrode.

[b] Half-wave potentials are certain to within ±15mV.

[c] FWHM of peak.

Table V. Half-wave potentials for oxidation of ZnP^tBu in various solvents.[a]

Solvent	$E_{1/2}(P/P^{+\cdot})$(V)[b]	$\lvert E_{3/4} - E_{1/4}\rvert$ (mV)	Conditions
DMF	−0.08	56	0.1M TBAP
CH_3CN	+0.19	(~ 100)[c]	0.2M TBAP
nPrCN	+0.16	56	0.1M TBAP
2MTHF	−0.14	58	0.3M THAP
C_6H_6	+0.18	85	0.1M THAP

[a] Determined by linear sweep voltammetry (at a 25 μ dia. microelectrode) except for CH_3CN by differential pulse voltammetry (at a 1.6 mm dia. electrode) due to insolubility in this solvent, using a ferrocene/ferocenium reference electrode.

[b] Half-wave potentials are certain to within ±15mV.

[c] FWHM of peak.

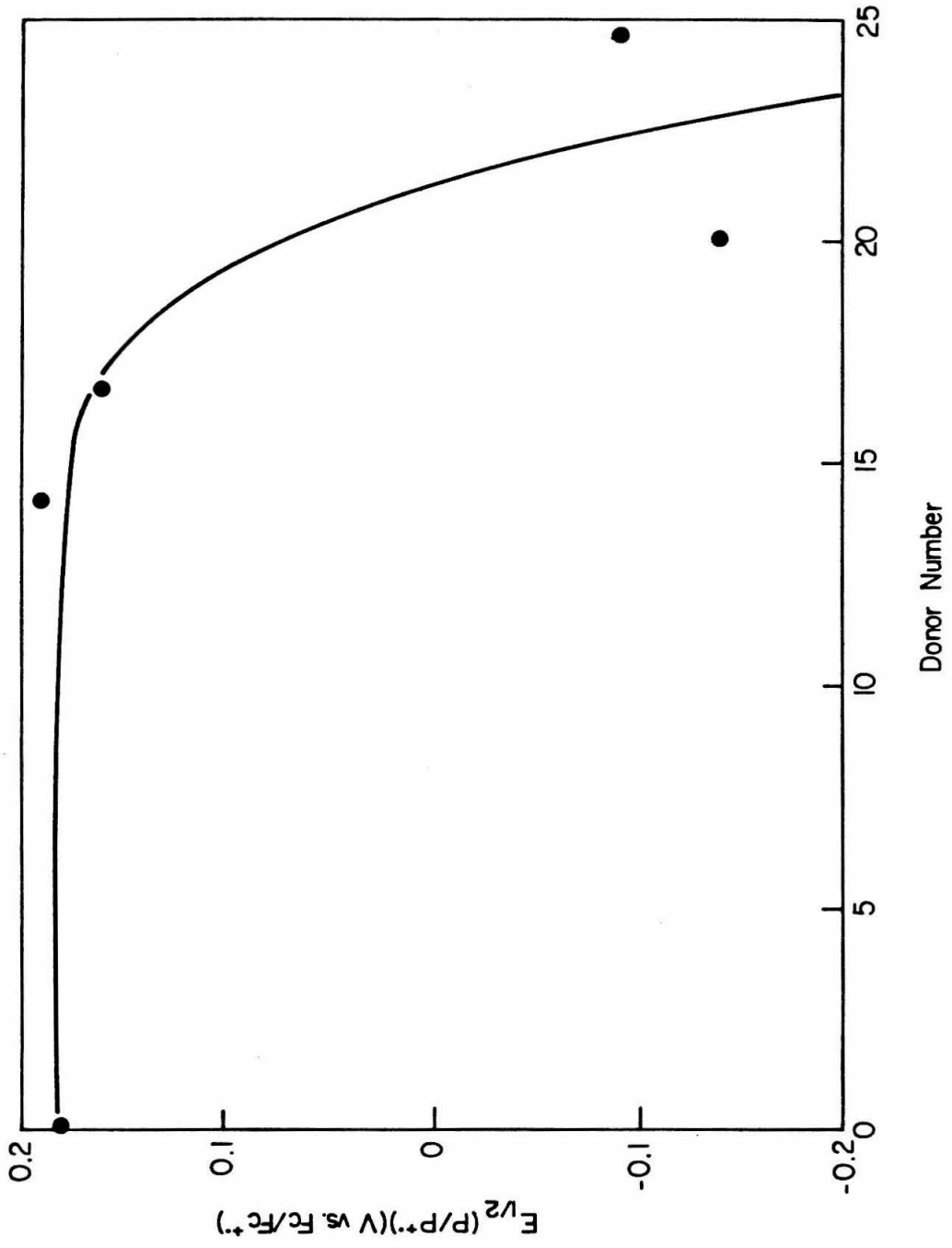

Figure 10. Half-Wave potential *vs.* donor number for the oxidation of ZnP^tBu in various solvents.

of the supporting electrolyte on quinone reduction potential showed the least extent of shifting to positive values when M^{+n} was n-Bu_4N^+; Li^+ gave the largest shift.[25] Tetraalkylammonium salts are used in the present work as supporting electrolytes. Unless the electroactive species are completely ion-paired, this phenomenon is probably not inducing large shifts in the measured redox potentials. A kinetic control experiment in which the supporting electrolyte was added to a benzene solution of *ZnPLQ* and one of *ZnP^{t}Bu* revealed a small increase ($\sim$ 10-15%) in the fluorescence lifetime of the porphyrin-quinone relative to the reference porphyrin, reflecting a slowdown in rate from 1.25×10^{10} to 1.03×10^{10} sec^{-1}, attributable to the effect of increased effective dielectric constant.

The Solvent Effect: Driving Force vs. Reorganization Energy

As mentioned above, in the picosecond fluorescence experiments, it was determined that the electron transfer rate decreases when the solvent polarity is increased. Two properties of the system that can contribute to the dependence of transfer rate on solvent polarity are the driving force of the reaction and the outer-sphere reorganization energy. The overall driving force of the intramolecular electron transfer reaction in a rigid molecule was estimated according to the

---

[25] (a) D.H. Evans, in *The Encyclopedia of Electrochemistry of the Elements, Organic Section*, A. Bard and H. Lund, eds., Marcel Dekker, New York, 1980. (b) T.M. Krygowski and W.R. Fawcett, *J. Amer. Chem. Soc.*, **97**, 2143 (1975).

equation:

$$-\Delta G^{0'}(R) = -E_{1/2}(P/P^{+\cdot}) + E_{1/2}(Q/Q^{-\cdot}) + W^* - W_P, \qquad [4.7]$$

where R=14.8 Å is the center-to-center separation of the porphyrin and quinone, W^*=2.15±0.01 eV is the singlet $S(0,0)$ excitation energy of the porphyrin.

The calculated driving forces for the photoexcited electron transfer at separation R are listed in Table VI as $-\Delta G^{0'}(R)$, and demonstrate the opposing, in fact nearly compensating, effects of ion solvation and dielectric shielding on the electron transfer thermodynamics. The uncorrected energy gaps range over 300 mV in the four solvents studied, the greatest driving force being 1.01 eV in the polar solvent acetonitrile and the lowest driving force being 0.67 eV in the nonpolar solvent benzene. Favorable solvation by the polar media of the ions in the charge-separated state lowers its energy, thereby making the isolated reaction more exothermic in acetonitrile than in benzene. However, in *rigid* donor-acceptor molecules the opposite charges separate to fixed distance, and the energy of the product state is differentially lowered by the electrostatic work term for bringing the oppositely charged moieties from infinite separation to distance R, and may be approximated (with provisos as discussed above) as a simple Coulomb energy W_P. The true magnitude of W_P is difficult to measure or calculate with certainty, but for the sake of discussion, W_P was obtained by application of a simple point

Table VI. Electrochemical Data for Porphryins and Quinones in Several Solvents.[a]

Solvent	$E_{1/2}(Q/Q^{-\cdot})$[b]	$E_{1/2}(P/P^{+\cdot})$[c]	$-W_P^d$	$-\Delta G^{0'}$	$-\Delta G^{0'}(R)$
CH_3CN	−0.95V[e]	+0.19V[e]	0.026eV	1.01ev[f]	1.04eV[f]
n-PrCN	−1.00[g]	+0.16[g]	0.048	0.99	1.04
2MTHF	−1.36[h]	−0.14[h]	0.156	0.93	1.08
C_6H_6	−1.30[h]	+0.18[i]	0.428	0.67	1.10

[a] Half-wave potentials were determined by linear sweep or differential pulse voltammetry, using a ferrocene/ferrocenium reference. All redox couples were reversible or nearly reversible, *i.e.*, $|E_{3/4} - E_{1/4}|$=56 − 85mV (n=1). $\Delta G^{0'} = -E_{1/2}(P/P^{+\cdot}) + E_{1/2}(Q/Q^{-\cdot}) + W^*$, where $W^* = 2.15 \pm 0.01$eV is the singlet excitation energy. $-\Delta G^{0'}(R) = -W_P - \Delta G^{0'}$ is the overall free energy including the electrostatic work term W_P for product formation.[d]

[b] *p*-Methylbenzoquinone.

[c] Zn-5-(*p*-t-butylphenyl-2,3,7,8,12,13,17,18-octamethylporphyrin.

[d] $W_P = \frac{1}{4\pi\epsilon\epsilon_o} e^2/R \approx 14.8/\epsilon R$, where ϵ is the dielectric constant and R(Å)=14.8Åis the center-to-center distance between porphyrin and quinone for $ZnPLQ$.

[e] 0.2M Tetrabutylammonium perchlorate (TBAP); 1.6mm dia. Pt disk working electrode.

[f] Estimated uncertainty is ±0.04V.

[g] 0.1M TBAP; 25μ dia. Pt disk.

[h] 0.3M Tetrahexylammonium perchlorate (THAP); 25μ dia. Pt disk electrode.

[i] 0.1M THAP; 25μ dia. Pt disk electrode.

charge model, according to the equation:

$$W_P = \frac{1}{4\pi\epsilon\epsilon_0}\frac{e^2}{r} \approx 14.38/\epsilon R, \qquad [4.8]$$

where ϵ is the low-frequency dielectric constant of the solvent, ϵ_0 is the dielectric permittivity of vacuum, e is the charge of an electron, and R is the center-to-center distance in Å. As a result, large dielectric solvents shield the charges more efficiently than nonpolar solvents. Conclusions about the effect of solvent reorganization on reaction kinetics must be based on considerations of these opposing factors. The data shown in Table VI suggest that the exothermicity of the electron transfer is only slightly (by less than 60 mV) affected by the solvent polarity, in contrast to several previous studies (see Introduction). The small but consistent trend in the rate data reflects small shifts in the outer-sphere reorganization energy, and in terms of the spectral energy distributions, broadening of the probability distributions by increased polarization in polar solvents produces lower rates.

Energy Gap Dependence: Kinetics

The effect of driving force was addressed directly by the synthesis of seven porphyrin-quinone compounds, each with a different substituent (Chapter 2). This substitution method provided seven points to correlate $\log k_{ET}$ and $-\Delta G^{0'}$. Substituents included cyano-, bromo-, chloro-, and methyl groups in various numbers, thereby giving an energy range of about 0.6 eV. The concept of using only

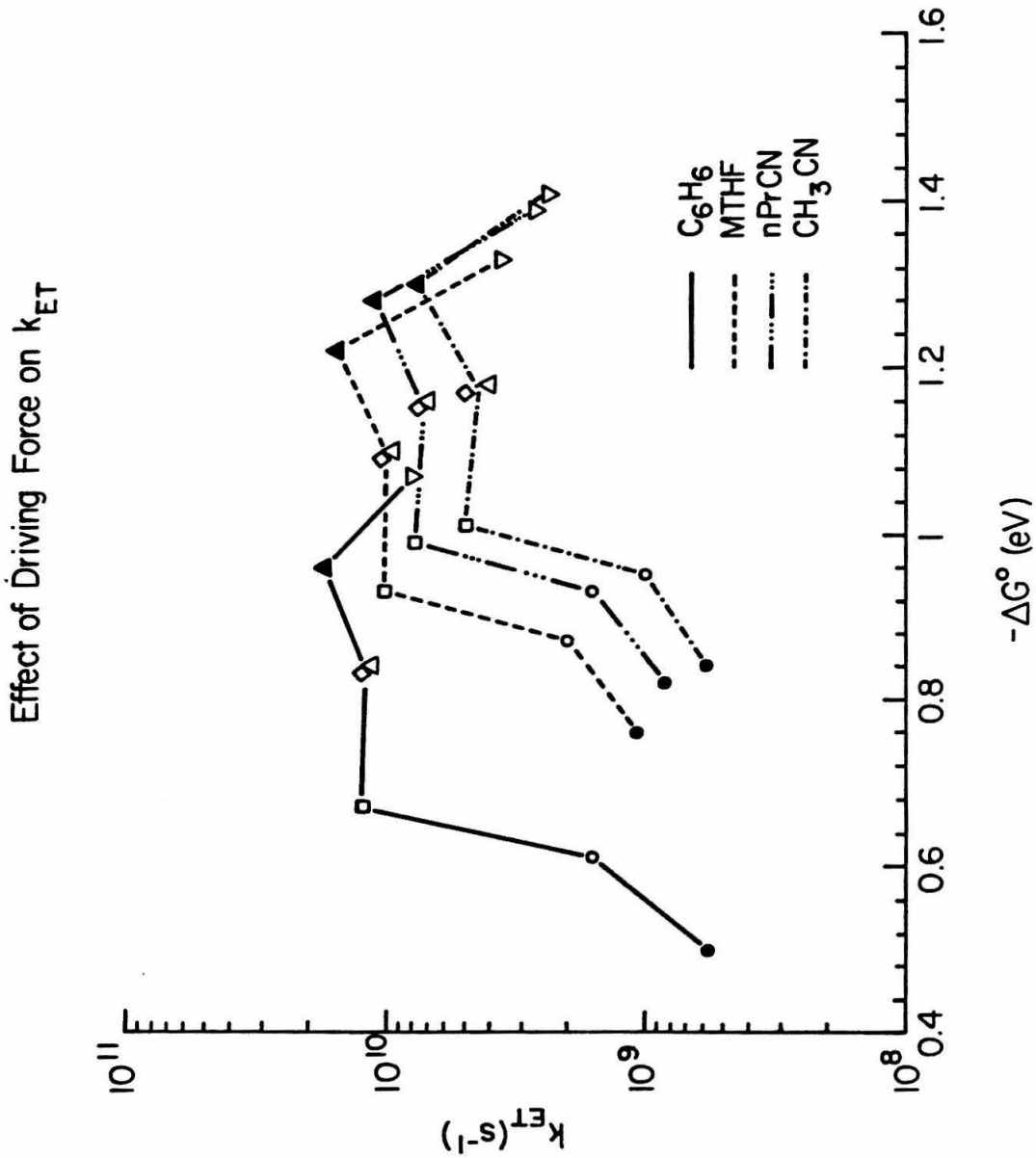

Figure 11. Electron transfer rate constant as a function of driving force.

p-benzoquinone derivatives is expected to provide a homologous reaction series; *i.e.*, the observed rate dependence should reflect variations with the energy gap, and should not be convoluted with effects due to vibrational and solvent reorganization.

The half-wave potentials for the reduction of the model benzoquinones are presented in Table VII. The results of the picosecond fluorescence lifetime measurements are shown in Figure 11 and Table VIII. From the lifetimes, electron transfer rate constants were calculated, using $k_{ET} = 1/\tau - 1/\tau_0$, where τ is the lifetime for $ZnPLQR_1R_2$ and τ_0 is that for ZnP^tBu in the same solvent. What is found is the usual increase in rate with exothermicity in the normal region, and a noticeable flattening of what would be expected according to classical theory in the inverted region ($|\Delta G^{0'}(R)| \geq \lambda$). Only in the most exothermic case where R_1=CN is there a decrease in rate constant; it is $k_{ET} = 2.37 \times 10^9$ sec^{-1} in acetonitrile, whereas $k_{ET} = 5.00 \times 10^9$ sec^{-1} for $R_1 = R_2$ =H, representing a slowdown of a factor of two.

Even though the porphyrin-quinone is structurally homologous, the concern remains as to whether it is in fact *functionally* homologous as well. The danger is that the substitution changes needed to vary $|\Delta G^{0'}(R)|$ may alter the electron density of the quinone enough to change the magnitude of coupling between vibrational and electronic motion. The small dip in electron transfer rate for the cyano compound might be easily attributed to a change in this reorganization en-

ergy. There is hardly any known experimental evidence on quinone/semiquinone self-exchange in a series of substituted quinones. (As the porphyrin is a constant of the system, we need not worry about its reorganization energy in this context.) One EPR study appears to exist,[26] but unfortunately it covers only methyl- and polymethylquinones, and no other substituent. However, this report does reveal that the reorganization energy varies from 0.5 eV for 2,6-dimethylquinone to 0.7 eV for tetramethylquinone in isopropanol/acetone/water. Since the experiment was performed in a polar and hydrogen-bonding solvent mixture, the uncertainty persists as to the origins of the difference in reorganization energy in these two molecules: it is likely due to a combination of both vibrational changes and changes in sterics that make ion or counterion approach more or less favorable or cause a change in solvation. The steric differences may act through the pre-exponential frequency factor, affording different observed self-exchange rates. The ambiguity increases with respect to the assignment of energy contributions if exchange measurements are attempted in nonpolar solvent, where the inner-sphere reorganization energy should dominate. In nonpolar solvent, ion-pairing is a serious issue, and instead of solvent masking the vibrational contribution, there is ion-pairing obscuring the information.

The leveling of the transfer rate as a function of driving force can be understood in terms of the quantum mechanical model of electron transfer. Assuming

---

[26] D. Meisel and R.W. Fessenden, *J. Amer. Chem. Soc.*, **98**, 7505 (1976).

Table VII. Half-wave potentials for reduction of methyl-*p*-benzoquinone substituted by 4-R_1, 5-R_2 groups in acetonitrile.[a]

R_1, R_2	$E_{1/2}(Q/Q^{-\cdot})$(V)[b]	$\lvert E_{3/4} - E_{1/4}\rvert$ (mV)	Conditions
Me,Me	−1.12	62	0.1M TBAP
Me,H	−1.04	75	0.1M TBAP
H,H	−0.95	59	0.1M TBAP
Cl,H	−0.89	56	0.1M TBAP
Br,H	−0.91	56	0.1M TBAP
Cl,Cl	−0.82	56	0.1M TBAP
CN,H	−0.55	55	0.1M TBAP

[a] Determined by linear sweep voltammetry (at a 25 or 127 μ dia. Pt microelectrode) using a ferrocene/ferrocenium reference electrode.

[b] Half-wave potentials are certain to within ±15mV.

there is one fast vibrational mode coupled to the donor and one to the acceptor, Onuchic, Beratan, and Hopfield[7a] have derived the following expression for nonadiabatic electron transfer through a periodic saturated hydrocarbon bridge when there are equal amounts of vibronic coupling with each chromophore:

$$k_{ET} = \frac{2\pi}{\hbar}\left(\frac{\beta_A\beta_D}{\beta}\right)^2 \sum_{j=0}^{M}\left[\epsilon_j^{N+1}\left(\frac{e^{-\gamma}\gamma^j}{j!}\right)^{1/2}\left(\frac{e^{-\gamma}\gamma^{M-j}}{(M-j)!}\right)^{1/2}\right]^2 h(E_D - E_A) \quad [4.9]$$

where

$$\epsilon_j = \frac{\beta}{\Delta_D - \lambda^2/\hbar\Omega - j\hbar\Omega} \quad [4.10]$$

and β is the electronic (Hückel) exchange interaction between repeating linker subunits of length a, β_A and β_D refer to exchange between the terminal bridge orbitals with the acceptor or donor edge atom, respectively; Δ_A is the energy difference between the valence band of the bridge and the acceptor; Δ_D is a similar quantity for the donor; $M = \varepsilon/\hbar\Omega = n + m$ is the total number of vibrational quanta available; ε is the driving force; $\gamma = (E_R/\hbar\Omega) = (\lambda/\hbar\Omega)^2$ is the reorganization energy in terms of units of the vibrational spacing; $\hbar\Omega$ is the spacing between vibrational energy levels; λ is the reorganization energy; ϵ_j is the distance decay constant; N is the number of bridging groups between donor and acceptor. The expression for k_{ET} assumes that electronic motion is nonadiabatic, nuclear motion is treated quantum mechanically, and the solvent is treated classically. Calculations using these equations demonstrate that a plateau in electron trans-

fer rate is possible, depending on the number of repeating units, the energies of the localized states from the valence band of the bridge, the distance between donor and acceptor, and the exact nature of the coupling to the donor and the acceptor (e.g., the number of vibrational modes or solvent modes).[7a]

Observation of inverted reactivity behavior can be obscured by quantum effects such as coupling to many modes or by the enhancement of transfer rate by overlap with more than one acceptor state. Another possibility is the involvement of the nearly degenerate porphyrin electronic ground states of both symmetries a_{1u} and a_{2u}, thus giving a broadening effect to the $\ln k_{ET}$ *vs.* $|\Delta G^{0'}(R)|$ dependence.

Recently, the biochemical analogue of the quinone-substitution experiment has been examined.[27] In this work, preparations of the bacterial photosynthetic reaction center were depleted of Q_A and substituted with a series of quinones of different redox potential. Rate measurements of the electron transfer from pre-reduced semiquinone to the hole on the special pair dimer $(BChl)_2$ showed classical behavior in the normal region and rate independence on $|\Delta G^{0'}(R)|$ in the expected inverted region, a result similar to the present findings.

---

[27] M.R. Gunner, N. Woodbury, W.W. Parson, and P.L Dutton, "Electron Transfer in Reaction Centers with Various Quinones Functioning as Q_A," Abstracts, Conference on Protein Structure: Molecular and Electronic Reactivity, Philadelphia, Pennsylvania, 15-17 April 1985.

Table VIII. Fluorescence Lifetimes and Electron Transfer Rates as a Function of Energy Gap.

Compound	Solvent	$-\Delta G^{0'}$ [a] (eV)	χ_R^2 [b]	τ (nsec)	k_{ET} (sec^{-1})	log k_{ET}
Me,Me	C_6H_6	0.50	0.913	0.801,1.722(9:1)	5.68×10^8	8.75
Me,H	C_6H_6	0.61	1.080	0.443,1.161(20:1)	1.58×10^9	9.20
H,H	C_6H_6	0.67	1.081	0.076,1.490(71:1)	1.25×10^{10}	10.10
Br,H[c]	C_6H_6	0.83	0.902	0.075,1.362(50:1)	1.27×10^{10}	10.10
Cl,H[c]	C_6H_6	0.84	1.103	0.082,1.549(200:1)	1.15×10^{10}	10.06
Cl,Cl[c]	C_6H_6	0.96	1.063	0.055,1.894(167:1)	1.75×10^{10}	10.24
CN,H	C_6H_6	1.07	0.990	0.114,1.520(1:2)	8.09×10^9	9.91
Me,Me	MTHF	0.76	0.935	0.594,1.488(7:1)	1.08×10^9	9.03
Me,H	MTHF	0.87	0.997	0.384,1.591(16:1)	2.00×10^9	9.30
H,H	MTHF	0.93	1.017	0.092,1.537(11:1)	1.03×10^{10}	10.01
Br,H	MTHF	1.09	0.942	0.090,1.611(20:1)	1.05×10^{10}	10.02
Cl,H	MTHF	1.10	1.118	0.099,1.661(77:1)	9.50×10^9	9.98
Cl,Cl	MTHF	1.22	1.156	0.062,1.629(42:1)	1.55×10^{10}	10.19
CN,H	MTHF	1.33	1.056	0.236,1.717(2:3)	3.63×10^9	9.56
Me,Me	nPrCN	0.82	1.014	0.679,1.798(4:1)	8.44×10^8	8.93
Me,H	nPrCN	0.93	1.004	0.448,1.295(7:1)	1.60×10^9	9.20
H,H	nPrCN	0.99	1.005	0.118,1.467(20:1)	7.85×10^9	9.89
Br,H	nPrCN	1.15	0.953	0.121,1.512(8:1)	7.64×10^9	9.88
Cl,H	nPrCN	1.16	0.959	0.132,1.576(25:1)	6.95×10^9	9.84
Cl,Cl	nPrCN	1.28	0.965	0.085,1.445(23:1)	1.11×10^{10}	10.05
CN,H	nPrCN	1.39	1.007	0.302,1.811(1:1)	2.68×10^9	9.43
Me,Me	CH_3CN	0.84	1.004	0.829,1.569(2:1)	5.89×10^8	8.77
Me,H	CH_3CN	0.95	0.920	0.617,1.430(6:1)	1.01×10^9	9.00
H,H	CH_3CN	1.01	0.976	0.178,1.601(20:1)	5.00×10^9	9.70
Br,H	CH_3CN	1.17	0.973	0.178,1.513(5:1)	5.00×10^9	9.70
Cl,H	CH_3CN	1.18	1.111	0.215,1.491(2:1)	4.03×10^9	9.61
Cl,Cl	CH_3CN	1.30	1.026	0.121,1.283(24:1)	7.65×10^9	9.88
CN,H	CH_3CN	1.41	1.030	0.335,1.660(1:1)	2.37×10^9	9.37

[a] Electrochemical redox values were obtained for H,H in all solvents and for all compounds in acetonitrile; other values were estimated by assuming the same changes in redox value found for H,H among different solvents for the other compounds.

[b] P.R. Bevington, *Data Reduction and Error Analysis for the Physical Sciences*, McGraw-Hill, New York, 1969, p. 202.

[c] These compounds were prepared by B.A. Leland.

Future synthetic systems may exhibit unobscured inverted reactivity, if some structural changes are made. For example, current theory of Beratan and Hopfield predicts a more sharply defined slowdown of rate with distance, if the localized states of the donor and acceptor can be pushed away from the valence states of the linker. The possibility that the wavefunction may exhibit different distance dependences as a function of the reaction driving force may be responsible as well. Evidence exists for this phenomenon in long-distance electron transfer in proteins.[28] Finally, it may be easier to observe classical inverted behavior if chromophores with smaller vibronic coupling are utilized. In this way the onset of the inverted region should occur at less extreme driving force.

---

[28] (a) B.S. Brunschwig, P.J. DeLaive, A.M. English, M. Goldberg, H.B. Gray, S.L. Mayo, and N. Sutin, *Inorg. Chem.*, **24**, 3743 (1985). (b) S.L. Mayo, W.R. Ellis, R.J. Crutchley, and H.B. Gray, *Science* (*Washington, D.C.*), submitted (1986).

Chapter 5

Conclusions

Conclusions

This thesis has described a series of synthetic and physical investigations attempting to elucidate the roles of solvent polarization, vibrational reorganization, tunneling, temperature, geometry, and driving force in the electron transfer processes occurring in biological systems. In light of previous flexibly coupled donor-acceptor systems, the clear advantage of well-defined distance and geometry is evident in the ability to interpret the results of the physical studies carried out.

• Solvent modulates the electron transfer rate only slightly in the limit of non-adiabatic electronic factors, lending support to the view that dielectric relaxation occurs too fast to be rate-limiting. Because of the lack of an initial polarization, solvent reorganization occurs "independently" after the electron transfer in molecules reacting from neutral initial states. Thus, static solvent properties and not solvent dynamics are important for the forward electron transfers in $ZnPLQ$ at room temperature.

• Nearly temperature-independent electron transfer in all the porphyrin-quinones examined (R=Me, H, Cl, Cl_2) suggests that nuclear tunneling must be accompanying the electron tunneling presumed to provide the mechanism for transferring an electron through the bicyclo[2.2.2]octane over 11 Å. This is the first non-protein model system evidenced to undergo low-temperature charge-separation

reactions. Nonexponentiality in the fluorescence decays of $ZnPLQ$ in 2MTHF or BN glass confirms the assumption of nonadiabaticity.

• The first known structurally homologous reaction series was examined for the occurrence of the inverted effect of electron transfer theory, and the results obtained show insensitivity of the rate to the driving force in the so-called inverted region ($|\Delta G^{0'}(R)|$ >1 eV) over a range of $\sim$ 0.35 eV, possibly indicating a role for vibronic coupling to both donor and acceptor during the electron transfer.

The precise structural definition offered by the synthetic method can continue to contribute in a major way to the experimental investigation of electron transfer processes.

Chapter 6

Experimental Procedures

Experimental Procedures

Melting points were measured, using a Thomas-Hoover Capillary Melting Point Apparatus and are reported uncorrected. Electronic spectra were recorded on either a Beckman 25 or a Cary 219 UV-Visible Spectrophotometer. Infrared spectra were obtained, using a Perkin-Elmer Model 257 or a Shimadzu IR-435 Infrared Spectrophotometer. Proton nuclear magnetic resonance (NMR) spectra were measured using a Varian Associates EM-390 NMR Spectrometer, a Varian Associates XL-200 NMR Spectrometer, a Japan Electro-Optical Laboratories (JEOL) FX-90Q NMR Spectrometer, a JEOL GX-400 NMR spectrometer, or a Bruker WM-500 NMR spectrometer, operating at 90MHz, 200MHz, 89.56MHz, 399.65MHz, and 500.13MHz, respectively. Carbon NMR spectra were obtained using broadband proton decoupling techniques on the FX-90Q, the XL-200, or the GX-400, operating at 22.4MHz, 50.31MHz, and 100.40MHz, respectively. Chemical shifts (δ) are reported in parts per million (ppm) relative to an internal standard (tetramethylsilane, TMS) or a solvent residual peak: $CHCl_3$, 7.24 ppm (for ^1H NMR) and 77.0 ppm (for ^{13}C NMR); CH_2Cl_2, 5.3 ppm (^1H NMR) and 53.8 ppm (^{13}C NMR). Low- and high-resolution mass spectra were determined by Mr. Larry Henling at the Caltech Analytical Facility, using a DuPont Mass Spectrometer or by the Midwest Center for Mass Spectrometry (NSF Regional Instrumentation Facility), University of Nebraska, Lincoln, Nebraska, by applying either electron impact (EI) or fast-atom bombardment (FAB) techniques,

depending on the volatility of the particular compound. Elemental analyses were performed by Spang Microanalytical Laboratory, Eagle Harbor, Michigan. Thin layer chromatography (TLC) was carried out on silica gel 60 F-254 (E. Merck; 250μ thick) precoated analytical plates. For preparative layer chromatography (PLC) precoated 2mm 60 F-254 plates were used. Flash column chromatography[1] was performed using a 41mm I.D. glass column and silica gel 60 (230-400 mesh ASTM; E.M. Reagents).

Analytical gas chromatography was carried out using a Hewlett-Packard 5700A gas chromatograph outfitted with a Hewlett-Packard 18704A inlet splitter, an SE-54 fused silica capillary column (15m x 0.32mm I.D.), and a flame ionization detector. Quantitative analysis of chromatograms made use of a Hewlett-Packard 3390A electronic integrator. Hydrogen was the carrier gas, and nitrogen was the make-up gas.

Reagents and Solvents. 2,5-Dimethoxy toluene was purchased from Pfaltz & Bauer and used as received. Triethylorthoformate, 1,4-dimethoxybenzene, ethyl crotonate, α,α-dichloromethyl methyl ether, *p*-tosylmethylisocyanide, methylmagnesium bromide, methyl acrylate, 2-nitropropane, and n-butyllithium were obtained from Aldrich Chemical Co. and used without further purification. Boron triiodide and methylmagnesium iodide are from Alfa Ventron. *p*-Tolyl ace-

---

[1] W.C. Still, M. Kahn, and A. Mitra, *J. Org. Chem.*, **43**, 2923 (1978).

tonitrile and *trans, trans*-1,4-diacetoxy-1,3-butadiene were used as received from Fluka Chemical Co. 2,3-Dimethylhydroquinone was a gift from Fairfield Chemical Co. Hydrobromic acid (32% in acetic acid) was either used directly from a newly opened bottle (J.T. Baker Chemical Co.) or prepared fresh before use. Hydrogen bromide, hydrogen chloride, and boron trifluoride gases were obtained from Matheson Gas Products, Inc. Sulfuryl chloride (Aldrich) was distilled under argon prior to use. Silver(I) oxide (Mallinckrodt) and lead(IV) oxide (Baker) were used as supplied. *p*-t-Butylbenzaldehyde was a gift from Research Organic Chemical Co.

Tetrahydrofuran (Matheson, Coleman, & Bell) was distilled under argon from sodium/benzophenone ketyl. Butyronitrile (Aldrich) was distilled from sodium carbonate and potassium permanganate and then re-distilled from phosphorous pentoxide. Spectro-grade benzene, acetonitrile, and *N,N*-dimethyl formamide (Burdick & Jackson) were distilled from calcium hydride under argon. 2-Methyltetrahydrofuran (Aldrich) was distilled from calcium hydride and then from sodium/benzophenone ketyl under argon. Dioxane (Eastman) was used from new bottles. Carbon tetrachloride (Baker, reagent grade), methanol (Baker, Photrex grade), dichloromethane (MCB or Burdick & Jackson), trichloroethylene (MCB), absolute ethanol (U.S. Industrial Chemicals, dehydrated U.S.P. grade), and dimethyl sulfoxide (Sigma Chemical Co.) were used without further treatment.

Precautions for Handling Porphyrins. The porphyrins and porphyrin-quinone derivatives described below are sensitive to light and oxygen.[2] Photodegradation by singlet oxygen[3] and porphyrin-photosensitized reduction of the quinone moiety in the presence of trace water[4] are two possible modes of decomposition. The octaalkylporphyrin chromophore also has been found to undergo rapid decay in chlorinated solvents on exposure to light.[5] All porphyrinic compounds were stored in the crystalline state, with complete exclusion of light, and preferably in an inert atmosphere. Even with these precautions, all porphyrin-quinones were routinely repurified by flash chromatography before all physical measurements. In the frequent event that the porphyrin-hydroquinone was the major impurity, treatment with the appropriate oxidant, followed by column chromatography, produced pure porphyrin-quinone. Due to their substantial insolubility in both highly polar and non-polar solvents, the porphyrins could be substantially purified by trituration (for example, with n-hexane or absolute methanol). Thin-layer and column chromatography were carried out in very dim

---

[2] (a) K.M. Smith, ed., *Porphyrins and Metalloporphyrins*, Elsevier, New York, 1975. (b) J.W. Buchler in D. Dolphin, ed., *The Porphyrins*, IA, Chapter 10 (1978).

[3] T. Matsuura, N. Yoshimura, A. Nishinaga, and I. Saito, *Tetrahetron Letters* (21), 1669 (1969).

[4] T. Matsuura, A. Nishinaga, N. Yoshimura, T. Arai, K. Omura, H. Maatsushima, and S. Kato, and I. Saito, *Tetrahedron Letters* (21), 1673 (1969).

[5] Z. Gasyna, W.R. Browett, and M.J. Stillman, *Inorg. Chim. Acta*, **92**, 37 (1984).

light to minimize decomposition.

Preparation of Bicyclo[2.2.2]octylbenzaldehydes **16**, **17**, *and* **18**

Dimethyl 4-cyano-4-phenylheptan-1,7-dioate (5). This compound was prepared by analogy to the procedure of Bruson and Riener[6] used for the cyanoethylation of ketones. A 2000 mL, two-neck round bottom flask fitted with a reflux condenser and a pressure-equalizing addition funnel was charged with benzyl cyanide (206 mL, 1.7mol), methyl acrylate (315 mL, 3.5mol), and dry dioxane (400 mL). To the stirred solution was added dropwise a solution containing benzyltrimethylammonium hydroxide (40% in methanol, 10 g) diluted with 20 mL dioxane. The mixture was heated at reflux for two hours. On cooling, the mixture was poured onto an equal volume of 5% hydrochloric acid, and extracted with 3×150 mL ether. The combined organic layers were washed with sodium chloride, dried over sodium sulfate, filtered, and concentrated to afford a clear oil, which crystallized and weighed 470 g (yield, 90%). mp 46-47°. IR ($CHCl_3$, NaCl): ν_{max} 2990, 2940, 2210 (C≡N), 1730 (C=O), 1490, 1450, 1435, 1370, 1295, 1270, 1220, 1170, 1015, 890, 690 cm^{-1}. ^1H NMR (200MHz, $CDCl_3$, TMS): δ 7.45-7.36 (m, 5H, C_6H_5), 3.58 (s, 6H, 2×OCH_3), 2.49-2.11 (m, 8H, 4×CH_2) ppm.

4-Cyano-4-phenyl-2-carbomethoxycyclohexanone (6). The method

---

[6] H.A. Bruson and T.W. Riener, *J. Amer. Chem. Soc.*, **64**, 2850 (1942).

of Trie, Touda, and Vyro[7] was followed to synthesize the keto ester. A suspension of sodium hydride (60% in oil, 75 g) in toluene (1L) and methanol (5 mL) was vigorously stirred using a mechanical stirrer under an atmosphere of argon, and a solution of *dimethylester* **5** (360 g, 1.2mol) in toluene (200 mL) was gradually added over one hour. The mixture was heated at reflux for 4 hours. On cooling excess sodium hydride was destroyed with glacial acetic acid. Aqueous extractive work-up gave 230 g (yield, 73%) of *ketoester* **6** as a crystalline solid. mp 93-94°[lit.[8] 95-96°]. IR ($CHCl_3$, NaCl): ν_{max} 2990, 2930, 2850, 2210 (C≡N), 1660 (C=O), 1615 (C=O), 1490, 1445, 1420, 1385, 1365, 1290, 1235, 1090, 1070, 1060, 995, 810, 690 cm^{-1}. ^1H NMR (200MHz, CD_2Cl_2, TMS): δ 7.53-7.35 (m, 5H, 2′,3′,4′,5′,6′-C*H*), 3.78 (s, 3H, 2-CO_2CH_3), 3.06-2.20 (m, 7H, 3,5,6-CH_2, 2-C*H*) ppm. ^{13}C NMR (50MHz, $CDCl_3$): δ 206.4 (1-*C*), 170.6 (2-CO_2CH_3), 139.8 (1′-*C*), 129.1, 128.6, 125.6 (2′,3′,4′,5′,6′-*C*H, 122.0 (4-*C*≡N), 51.7 (2-CO_2CH_3), 41.1 (6-CH_2), 34.9 (1-*C*H), 31.4 (CH_2), 29.7 (4-*C*), 27.1 (CH_2) ppm.

4-Cyano-4-phenylcyclohexanone (7). This material was synthesized using the general method of Krapcho and Long.[9] In a 1000 mL round bottom flask connected to a reflux condenser was dissolved the *cyanoketoester* **6** (200 g,

---

[7] H. Trie, F. Touda, and S. Vyro, *J. Chem. Soc.* 1446 (1959).

[8] E.C. Horning, M.G. Horning, M.S. Fish, and M.W. Rutenberg, *J. Amer. Chem. Soc.*, **74**, 773 (1952).

[9] A.P. Krapcho and A.J. Long, *Tetrahedron Letters*, 957 (1973).

0.78mol) in dimethyl sulfoxide (450 mL) and water (45 mL). Sodium chloride (50 g, 0.86mol) was added, and the stirred mixture was heated at reflux till evolution of carbon dioxide ceased (approximately two to three hours). The cooled mixture was poured onto ice water and extracted with 4×150 mL benzene. The organic layers were washed with water (150 mL) and saturated sodium chloride, dried over sodium sulfate, filtered, and concentrated *in vacuo* to afford white crystals of *cyano ketone* **7**, weighing 135 g (yield, 87%). mp 115-117°[lit.[8,10] 114.5-115°, 115-117°]. IR ($CHCl_3$, NaCl): ν_{max} 2998, 2940, 2900, 2850, 2210 (C≡N), 1715 (C=O), 1490, 1445, 1420, 1330, 1220, 1175, 1115, 955, 690 cm^{-1}. ^1H NMR (200MHz, $CDCl_3$, TMS): δ 7.55-7.37 (m, 5H, 2′,3′,4′,5′,6′-C*H*), 2.91 (dt, 2H, 2×C*H*CO J=14Hz), 2.62-2.21 (m, 6H, 2×CH_2, C*H*CO) ppm. ^{13}C NMR (50MHz, $CDCl_3$): δ 207.3 (*C*=O), 138.5 (1′-*C*), 129.3 (2×*C*H), 128.6 (4′-*C*), 125.4 (2×*C*H), 121.3 (*C*N), 43.1 (4-*C*), 38.6 (2×*C*H_2), 36.95 (2×*C*H_2) ppm.

8-Cyano-8-phenyl-1,4-dioxaspiro[4.5]decane (8). This compound was made by the procedure of Swenton, Blankenship, and Sanitra.[10] The *cyanoketone* **7** (90 g, 0.45mol) was dissolved in toluene (60 mL) in a 1000 mL round bottom flask fitted with a Dean-Stark azeotropic distillation head and a Liebig condenser. Ethylene glycol (260 mL) and *p*-toluenesulfonic acid (4 g) were added, and the mixture was distilled azeotropically till no more water was collected. On cool-

---

[10] J.S. Swenton, R.M. Blankenship, and R. Sanitra, *J. Amer. Chem. Soc.*, **97**, 4941 (1975).

ing, the mixture was neutralized with 10% sodium carbonate and washed with water and saturated sodium chloride. The organic layer was dried over sodium sulfate, filtered, and evaporated *in vacuo*. Crystals were obtained weighing 90 g (yield, 82%). mp 114-118°[lit.[8,10] 124-5°, 111-114°]. IR ($CHCl_3$, NaCl): ν_{max} 2910, 2970, 2210 (C≡N), 1440, 1365, 1100, 962, 938, 920, 865 cm^{-1}. ^1H NMR (200MHz, $CDCl_3$, TMS): δ 7.55-7.30 (m, 5H, 2′,3′,4′,5′,6′-C*H*), 3.99 (m, 4H, 2×CH_2O), 2.2-1.8 (m, 8H, 4×CH_2) ppm. ^{13}C NMR (50MHz, $CDCl_3$): δ 140.1 (1′-*C*), 128.9 (2×*C*H), 127.9 (4′-*C*H), 125.6 (2×*C*H), 122.6 (*C*N), 64.6 (O*C*H_2), 64.4 (O*C*H_2), 43.4 (4-*C*), 34.9 (2×*C*H_2), 32.4 (2×*C*H_2) ppm.

4-Acetyl-4-phenylcyclohexanone (9). The method of Swenton, Blankenship, and Sanitra[10] was followed to derive this material. The *cyanoketal* **8** (44 g, 0.2mol) was dissolved in dry benzene (400 mL). To the stirred solution was added methylmagnesium bromide (3.2M, 188 mL, 0.6mol) under an atmosphere of argon. The mixture was heated at reflux for 24 hours. On cooling, hydrochloric acid (80 mL concentrated acid diluted with 200 mL distilled water) was cautiously added. The two-phase mixture was stirred vigorously and heated at reflux for five hours. Layers were separated, and the aqueous phase was washed with 3×80 mL diethyl ether. The combined organic layers were washed with 2×100 mL saturated sodium bicarbonate and 100 mL water. Drying over sodium sulfate, concentration *in vacuo*, and vacuum distillation gave a clear viscous oil weighing 17 g (yield, *ca.* 50%). bp 146-148°/0.38mm [lit.[10] 124-128°/0.2mm]. IR

($CHCl_3$, NaCl): ν_{max} 3470, 3380, 2900, 2840, 1718 (C=O), 1700 (C=O), 1595, 1350, 1330, 1090, 970, 580 cm^{-1}. ^1H NMR (90MHz, $CDCl_3$, TMS): δ 7.35 (s, 5H, 2′,3′,4′,5′,6′-C*H*), 2.7-2.0 (m, 8H, 2,3,5,6-CH_2), 1.95 (s, 3H, 4-COCH_3) ppm.

1-Ethoxy-4-phenylbicylco[2.2.2]octan-3-one (10). This material was produced using the general procedure of Morita and Kobayashi.[11] A solution of *acetyl cyclohexanone* **9** (22.18 g, 0.10mol) and triethylorthoformate (36 mL, 0.33mol) in absolute ethanol (200 mL) was cooled to 0-5° under an atmosphere of argon. Hydrogen chloride gas was bubbled into the cold solution. After 15mins, the reaction mixture was heated at reflux for 40mins. Solvents were evaporated. Addition of ether and washing with water and 10% sodium carbonate, followed by drying over sodium sulfate, gave 22 g of crude *ketoether* 4a (yield, >95%). An analytical sample was obtained by recrystallization from absolute ethanol. mp 88-90°[lit.[12] 88°]. ^1H NMR (90MHz, $CDCl_3$, TMS): δ 7.25 (m, 5H, 2′,3′,4′,5′,6′-C*H*), 3.45 (q, 2H, OCH_2CH$_3$, J=7Hz), 2.55 (s, 2H, CH_2CO), 2.2-1.8 (*AA′BB′ m, 8H, 5,6,7,8-*CH_2), 1.2 (t, 3H, OCH$_2$CH_3, J=7Hz) ppm.

1-Ethoxy-4-phenylbicyclo[2.2.2]octane (11). This substance was produced by slight modification of the reaction conditions of Suzuki and Morita.[13]

---

[11] K.-I. Morita and T. Kobayashi, *J. Org. Chem.*, **31**, 229 (1966).

[12] J. Colonge and R. Vuillemet, *Bull. Soc. Chim. France*, 2235 (1961).

[13] Z. Suzuki and K. Morita, *J. Org. Chem.*, **32**, 31 (1967).

The *ketoether* **10** (22 g, 96 mmol) and solid potassium hydroxide (22 g, 0.39mol) were suspended in diethylene glycol (250 mL) and hydrazine hydrate (14 mL, 0.29mol). The mixture was heated for four hours at 200° (pot temperature). After cooling, colorless crystals were collected by filtration, washed with water, and dried, giving 11 g (yield, 56%). mp 59-61°. IR (CH_2Cl_2, NaCl): ν_{max} 2850, 1597, 1490, 1350, 1330, 1090, 1040, 1030 cm^{-1}. ^1H NMR (90MHz, $CDCl_3$, TMS): δ 7.2 (m, 5H, 2′,3′,4′,5′,6′-C*H*), 3.4 (q, 2H, OCH_2CH_3, J=7Hz), 1.8 (*AA′BB′ q, 12H*, J=4.5Hz), 1.1 (t, 3H, OCH_2CH_3, J=7Hz) ppm. ^{13}C NMR (100.4MHz, $CDCl_3$): δ 148.48 (1′-*C*), 127.77, 125.07 (2′,3′,5′,6′-*C*H), 125.35 (4′-*C*H), 73.59 (1-*C*OCH_2CH_3), 56.46 (OCH_2CH_3), 34.43 (4-*C*), 33.39, 30.52 (2,3,5,6,7,8-*C*H_2), 16.54 (OCH_2CH_3) ppm.

4′-Bromo-4-phenylbicyclo[2.2.2]octan-1-ol (12). *Method A.* A solution of *1-ethoxy-4-phenylbicyclo[2.2.2]octane* **11** (3 g, 13 mmol), benzoyl peroxide (6.9 g, 26 mmol), and lithium bromide (2.5 g, 26 mmol) in acetonitrile (30 mL) was treated with bromine (3 mL, 60 mmol). The mixture was stirred at room temperature. Aliquots (10 μL) were periodically withdrawn and quenched with 3N potassium hydroxide (aq) and extracted with dichloromethane. The progress of the reaction was followed by injection of 1 μL of the organic layer into an SE-54 fused glass capillary gas chromatography column (oven temperature, 200°). When starting material (retention time, t_r=1.1 min) disappeared and no more product (t_r=2.2 min) formed, the reaction mixture was poured onto ice/1%

sodium borohydride. Extraction with dichloromethane, washing with 10% potassium hydroxide, drying over sodium sulfate, and concentration gave essentially pure *bromo alcohol* **12**, weighing 3.2 g (yield, 90%).

Method B. Bromine (1.5 mL) was added to a stirred solution of *1-ethoxy-4-phenylbicyclo[2.2.2]octane* **11** (1.0 g, 4.3 mmol) and lithium benzoate (1.34 g) in acetonitrile (10 mL). The resulting solution was heated to reflux. The reaction was monitored as in Method A. Extraction with dichloromethane, washing with 10% potassium hydroxide, drying over sodium sulfate, and concentration gave essentially pure *bromo alcohol* **12**, 1.07 g (yield, 88%). mp 120-2°. IR (CH_2Cl_2, NaCl): ν_{max} 3630, 3570, 3460br, 2900, 2850, 1605, 1490, 1350, 1085, 1005, 880 cm^{-1}. ^1H NMR (400MHz, $CDCl_3$, TMS): δ 7.41, 7.39 ($\frac{1}{2}AA'BB'$ q, 2H, 3′,5′-C*H*, J=8.6Hz), 7.18, 7.16 ($\frac{1}{2}AA'BB'$ q, 2H, 2′,6′-C*H*, J=8.6Hz), 1.97-1.93 (m, 6H, 3×CH_2), 1.79-1.75 (m, 6H, 3×CH_2) ppm. ^{13}C NMR (100.4MHz, $CDCl_3$): 147.26 (1′-*C*), 130.87, 127.07 (2′,3′,5′,6′-*C*H), 119.36 (4′-*C*), 69.64 (1′-*C*), 35.51 (4′-*C*), 34.45, 33.65 (2,3,5,6-CH_2) ppm. Mass spectrum (EI, 70eV): *m/z* (relative intensity, %) 282 ($M^+[^{81}Br]$, 21.5), 280 ($M^+[^{79}Br]$, 22.4), 264 (8), 262 (8.6), 236 (10), 223 (10), 210 (85), 212 (79), 129 (100), 115 (37). Exact mass for $C_{14}H_{17}{}^{79}BrO$: calcd 280.0463, obsd 280.0451; $C_{14}H_{17}{}^{81}BrO$: calcd 282.0442, obsd 282.0451. *Anal.* Calcd for $C_{14}H_{17}BrO\cdot\frac{1}{2}\ H_2O$: 57.94%C, 6.25%H. Found: 57.54%C, 5.77%H.

4″-Bromo-2′,5′-dimethoxy-1,4-diphenylbicyclo[2.2.2]octane (13). A

three-neck, 250 ml round bottom flask fitted with condenser, gas inlet adapter, and argon bubbler was charged with *4'-bromo-4-phenylbicyclooctyl alcohol* **12** (1.0 g, 3.6 mmol), 1,4-dimethoxybenzene (2.5 g, 18 mmol), *p*-toluenesulfonic acid (10 mg), and trichloroethylene (70 mL). The solution was cooled to 0-5°C, and boron trifluoride gas was admitted for 15 mins. The mixture was heated at reflux for 40 hours under argon atmosphere. On cooling, saturated sodium bicarbonate was added. The water layer was extracted with 3x30 mL dichloromethane, and the combined organic layer was washed with saturated sodium chloride, dried over sodium sulfate, and concentrated. The residue was heated in a Kugelrohr oven at 125°/10μ Hg. After no more excess dimethoxybenzene sublimed into the trap, the crude product was purified by flash column chromatography (32-64μ SiO_2; toluene; R_f=0.60) to afford colorless crystals, weighing 750 mg (yield, 55%). mp 175-8°. UV-Vis (CH_2Cl_2): λ_{max} 358 (ϵ 45), 286 (2100), 238 (2920) nm. IR (CH_2Cl_2, NaCl): ν_{max} 2900, 2880, 2820, 1605, 1585, 1490, 1460sh, 1410sh, 1205, 1175, 1075, 1045, 1025, 1000, 815 cm^{-1}. ^1H NMR (400MHz, $CDCl_3$): δ 7.42, 7.40 ($\frac{1}{2}AA'BB'$ q, 2H, 2',6'-C*H*, J=8.6Hz), 7.24, 7.22 ($\frac{1}{2}AA'BB'$ q, 2H, 3',5'-C*H*, J=8Hz), 6.81 (dd, 2H, 3',4'-C*H*, J=3.1, 9.3Hz), 6.70 (dd, 1H, 6'-C*H*, J=3.2, 8.8Hz), 3.80 (s, 3H, OCH_3), 3.76 (s, 3H, OCH_3), 2.06 (m, 6H, 3×CH_2), 1.89 (m, 6H, 3×CH_3) ppm. ^{13}C NMR (100.4MHz; $CDCl_3$): δ 153.09, 152.70 (2',5'-*C*OCH$_3$), 149.03, 138.03 (1',1''-*C*), 130.76, 127.19 (2'',3'',5'',6''-*C*H), 119.05 (4''-*C*Br), 114.34, 112.22, 109.87 (3',4',6'-*C*H), 55.75 (2',5'-O*C*H$_3$), 35.50, 34.63

(1,4-*C*), 32.83. 30.20 (2,3-CH_2) ppm. Mass spectrum (EI, 70eV): *m/z* (relative intensity, %) 402 ($M^+[^{81}Br]$, 71), 400 ($M^+[^{79}Br]$, 72), 332 (11), 248 (17), 190 (100), 175 (21), 159 (31), 81 (24), 69 (55). Exact mass for $C_{22}H_{25}{}^{79}BrO_2$: calcd 400.1038, obsd 400.1043; $C_{22}H_{25}{}^{81}BrO_2$: calcd 402.1018, obsd 402.1025. *Anal.* Calcd for $C_{22}H_{25}BrO_2$: 65.84%C, 6.28%H. Found: 65.61%C, 6.13%H.

4″-Formyl-2′,5′-dimethoxy-1,4-diphenylbicyclo [2.2.2]octane (16). A flame-dried two-neck, 25 mL round bottom flask fitted with argon inlet and rubber septum was charged with *bromophenyldimethoxybenzene* **13** (310 mg, 0.77 mmol) and dissolved with distilled tetrahydrofuran (10 mL). Under an argon atmosphere the solution was cooled to -78°and treated with n-butyl lithium (2.5M, 0.62 mL, 1.6 mmol). The solution was stirred at - 78° for one hour and treated with freshly distilled *N,N*-dimethylformamide (0.25 mL, 3.2 mmol). Stirring continued at -78° for one hour. The mixture was warmed to room temperature over one to two hours, poured into water, and extracted with 3×25 mL diethyl ether. The combined organic extract was washed with 2×20 mL saturated aqueous sodium chloride and water, dried over magnesium sulfate, filtered, and concentrated *in vacuo*. The residue was purified by flash column chromatography (ether/hexane, 1:1; R_f=0.42), affording 205 mg of colorless needles (yield, 76%). mp 152-154°. UV-Vis (CH_3CN): λ_{max} 324 (ϵ 160), 264sh (3400) nm. IR (CH_2Cl_2, NaCl): ν_{max} 2900, 2850, 2820, 2720, 1695 (C=O), 1602, 1580, 1570, 1490, 1200, 1170, 1120, 1045, 1020, 1003, 850, 820 cm^{-1}. ^1H NMR (400MHz,

$CDCl_3$, TMS): δ 9.98 (s, 1H, C*H*O), 7.83, 7.81 ($\frac{1}{2}AA'BB'$ q, 2H, 2″,6″-C*H*, J=8.1Hz), 7.55, 7.53 ($\frac{1}{2}AA'BB'$ q, 2H, 3″,5″-C*H*, J=8.1Hz), 6.82 (m, 2H, 3″,4″-C*H*), 6.71 (m, 1H, 6″-C*H*), 3.81 (s, 3H, OCH_3), 3.78 (s, 3H, OCH_3), 2.10 (m, 6H, 3×CH_2), 1.97 (m, 6H, 3×CH_2) ppm. ^{13}C NMR (100.4MHz, $CDCl_3$): δ 191.11 (4″-*C*HO), 157.39, 153.10 (2′,5′-*C*OCH$_3$), 152.68 (1″-*C*), 137.85 (1′-*C*), 133.85 (4″-*C*), 129.35, 126.01 (2″,3″,5″,6″-*C*H), 114.35, 112.23, 109.91 (3′,4′,6′-*C*H), 55.75 (2′,5′-O*C*H$_3$), 35.59 (1,4-*C*), 32.73, 30.13 (2,3-*C*H$_2$) ppm. MS (EI, 70eV): *m/z* (%) 351 (M^++1, 25), 350 (M^+, 100), 190 (67), 175 (18), 159 (27), 91 (14), 69 (11). Exact mass for $C_{23}H_{26}O_3$: calcd 350.1882, obsd 350.1886. *Anal.* Calcd for $C_{23}H_{26}O_3$: 78.82%C, 7.48%H. Found: 78.66%C, 7.46%H.

4″-Bromo-2′, 5′-dimethoxy-4′-methyl-1, 4-diphenylbicyclo[2.2.2]-octane (14). A solution of *bromo alcohol* **12** (1.0 g, 3.56 mmol), 2,5-dimethoxytoluene (2.7 g, 17.8 mmol), and *p*-toluenesulfonic acid (15 mg) in trichloroethylene (75 mL) was treated with boron trifluoride gas at 0-5° for 15 mins. The cooling bath was replaced with a heating mantle, and the mixture was boiled for 30 hours under argon. On cooling, 10% sodium bicarbonate was added. The water layer was extracted with 2×50 mL dichloromethane. The combined organic layer was washed with brine and water, dried over sodium sulfate, filtered, and concentrated *in vacuo*. The dark oil was heated in a Kugelrohr oven at 120°/0.1mm Hg for 2 hours. The residue was purified by flash column chromatography (ether/hexane, 1:1; R_f=0.66), giving 600 mg of colorless crystals (yield,

41%). mp 154-7°. IR (CH_2Cl_2, NaCl): ν_{max} 2895, 2850, 1495, 1485, 1460, 1385, 1370, 1190, 1170, 1070, 1040, 1000, 960, 855, 835, 815 cm^{-1}. ^1H NMR (500MHz, $CDCl_3$, TMS): δ 7.31, 7.40 ($\frac{1}{2}AA'BB'$ q, 2H, 3′,5′-C*H*, J=8.5Hz), 7.24, 7.22 ($\frac{1}{2}AA'BB'$ q, 2H, 2′,6′-C*H*, J=8.5Hz), 6.74 (s, 1H, 3″-C*H*), 6.70 (s, 1H, 5″-C*H*, 3.79 (s, 6H, 2×OCH_3), 2.20 (s, 3H, 4″-CH_3), 2.08 (m, 6H, 3×CH_2), 1.89 (m, 6H, 3×CH_2) ppm. ^{13}C NMR (100.4MHz, $CDCl_3$): δ 152.14, 151.03 (2′,5′-*C*OCH$_3$), 149.04, 134.58 (1′,1″-*C*), 130.75, 127.19 (2″,3″,5″,6″-*C*H), 124.49 (4′-*C*CH$_3$), 119.04 (4″-*C*Br), 114.94, 110.40 (3′,6′-*C*H), 56.37, 55.89 (2′,5′-O*C*H$_3$), 35.33, 34.61 (1,4-*C*), 32.87, 31.27 (2,3-*C*H$_2$), 16.09 (4′-*C*H$_3$) ppm. Mass spectrum (EI, 70eV): *m/z* (relative intensity, %) 416 (M^+[^{81}Br], 46), 414 (M^+[^{79}Br], 48), 367 (22), 343 (20), 341 (13), 312 (16), 244 (18), 237 (18), 204 (26), 181 (29), 149 (50). Exact mass for $C_{23}H_{27}{}^{79}BrO_2$: calcd 414.1194, obsd 414.1171; $C_{23}H_{27}{}^{81}BrO_2$, calcd 416.1174, obsd 416.1174. *Anal.* Calcd for $C_{23}H_{27}BrO_2$: 66.51%C, 6.55%H. Found: 66.85%C, 6.80%H.

4″-Formyl-2′, 5′-dimethoxy-4′-methyl-1, 4-diphenylbicyclo [2.2.2]-octane (17). A flame-dried 25 mL round bottom flask was charged with *methyl aryl bromide* **14** (40 mg, 96 μmol) under a flow of argon. The bromide was dissolved with dry tetrahydrofuran (40 mL), cooled to -78° (Dry Ice/acetone), and treated with excess n-butyllithium (1.6M in hexane; 180 μmol). After stirring at -78° for 1 hour, freshly distilled *N,N*-dimethylformamide (30 μL) was injected. The mixture was gradually warmed to room temperature (2 hours),

quenched with water, and extracted with 4×15 mL diethyl ether. The combined organic layer was washed with saturated sodium chloride, dried over sodium sulfate, and concentrated. The residue was subjected to flash chromatography (CH_2Cl_2; R_f=0.39) to afford pure *methyl aryl aldehyde* **17** (30 mg; yield, 85%). mp 151-153°. IR ($CHCl_3$, NaCl): ν_{max} 2910, 2850, 2730, 1695 (C=O), 1605, 1570, 1490, 1460, 1390, 1370, 1310, 1000, 535 cm^{-1}. ^1H NMR (400MHz, $CDCl_3$, TMS): δ 9.98 (s, 1H, C*H*O), 7.83, 7.81 ($\frac{1}{2}AA'BB'$ q, 2H, 3″,5″-C*H*, J=7.8Hz), 7.55, 7.53 ($\frac{1}{2}AA'BB'$ q, 2H, 2″,6″-C*H*, J=8.1Hz), 6.75 (s, 1H, 3′-C*H*), 3.81 (s, 6H, 2×OCH_3), 2.20 (s, 3H, 4′-CH_3), 2.14-2.10 (m, 6H, 3×CH_2), 1.98-1.94 (m, 6H, 3×CH_2) ppm. ^{13}C NMR (100.4MHz, $CDCl_3$): δ 191.43 (*C*HO), 157.43, 152.20 (*C*OCH$_3$), 151.14 (1″-*C*), 134.46 (4″-*C*), 129.37, 126.04 (2″,3″, 5″,6″-*C*H), 127.79, 124.65 (1′,4′-*C*), 115.03, 110.50 (3′,6′-*C*H), 56.45, 55.92 (O*C*CH$_3$), 32.99, 32.92 (1,4-*C*), 32.82, 30.37 (6×*C*H$_2$) ppm. Mass spectrum (EI, 70eV): *m/z* (relative intensity, %)365 (M^++1, 26), 364 (M^+, 98), 341 (9), 260 (15), 241 (27), 204 (100), 189 (26), 173 (23), 91 (22). Exact mass for $C_{24}H_{28}O_3$: calcd 364.2038, obsd 364.2020.

4″-Bromo-2′,5′-dimethoxy-3′,4′-dimethyl-1, 4-diphenylbicyclo[2.2.-2]octane (15). A 100 mL, 3-neck round bottom flask was fitted with a condenser, topped by an argon intake, an adapter connected to a boron trifluoride tank, and a gas bubbler. *Bromophenylbicyclooctyl alcohol* **12** (1.4 g, 5 mmol), 1,4-dimethoxy-2,3-dimethylbenzene (3.23 g, 9 mmol), and *p*-toluenesulfonic acid

(15 mg) were dissolved with trichloroethylene (50 mL). Boron trifluoride gas was admitted into the stirred reaction mixture over 15 mins. With the gas inlet closed the mixture was heated at reflux for 36 hours. Ten percent sodium carbonate was cautiously added to the cooled reaction mixture, which was then washed with saturated sodium chloride, dried over sodium sulfate, and evaporated. The residue was heated in a Kugelrohr oven (150°/0.1mm Hg), and then subjected to preparative layer chromatography (2mm SiO_2; ether/hexane, 1:1; R_f= 0.69) gave pure *diarylbicyclooctane* (300 mg, 14%). mp 127-30°. IR ($CHCl_3$, NaCl): ν_{max} 2910, 2850, 1480, 1455, 1390, 1300, 1120, 1090, 1005, 950 cm^{-1}. ^1H NMR (400MHz, $CDCl_3$, TMS): δ 7.43, 7.40 ($\frac{1}{2}AA'BB'$ q, 2H, 2″,6″-C*H*, J=8.8Hz), 7.25, 7.23 ($\frac{1}{2}AA'BB'$ q, 2H, 3″,5″-C*H*, J=8.8Hz), 6.65 (s, 1H, 6′-C*H*), 3.80 (s, 3H, OCH_3), 3.69 (s, 3H, OCH_3), 2.21 (s, 3H, 4′-CH_3), 2.12 (s, 3H, 3′-CH_3), 2.11 (m, 6H, 3×CH_2), 1.92 (m, 6H, 3×CH_2) ppm. ^{13}C NMR (100.4MHz, $CDCl_3$): δ 152.75, 152.04 (2′,5′-*C*OCH$_3$), 148.91 (1″-*C*), 137.97 (1′-*C*), 131.13 (3′-*C*CH$_3$), 130.80, 127.18 (2″,3″,5″,6″-*C*H), 124.57 (4′-*C*CH$_3$), 119.11 (4″-*C*CHO), 107.38 (6′-*C*H), 61.19 , 56.08 (2′,5′-O*C*H$_3$), 35.84, 34.63 (1,4-*C*), 32.99, 31.51 (2,3,5,6,7,8-*C*H$_2$), 14.18, 12.21 (3′,4′-*C*H$_3$) ppm. Mass spectrum (EI, 70eV): *m/z* (relative intensity, %) 430 (M^+[^{81}Br], 99.7), 428 (M^+[^{79}Br], 100), 241 (10), 218 (98), 203 (63), 188 (20), 165 (30), 115 (22), 91 (15). Exact mass for $C_{24}H_{29}{}^{79}BrO_2$: calcd 428.1351, obsd 428.1347; $C_{24}H_{29}{}^{81}BrO_2$: calcd 430.1331, obsd 430.1338.

4″-Formyl-2′,5′-dimethoxy-3′,4′-dimethyl-1,4-diphenylbicyclo[2.2.-

2]octane (18). A 25 mL round bottom flask charged with *bromobenzene* **15** (130 mg, 0.3 mmol) was flushed with argon for 30mins. The solid was dissolved with distilled tetrahydrofuran (4 mL) and cooled to -78° (dry ice/acetone). While stirring under an argon atmosphere, n-butyl lithium (1.5M in hexanes, 1.4 mL, 2 mmol) was added gradually over five minutes. The reaction mixture was kept at -78° for one hour before treatment with freshly distilled *N,N*-dimethylformamide (250 μL, 3 mmol), and slowly warmed to room temperature over one hour. Water was added, and the mixture was extracted with 4×10 mL diethyl ether. The combined organic layers were washed with water and saturated aqueous sodium chloride, and then dried over sodium sulfate. Filtration, evaporation of solvent, and flash chromatography (ether/n-hexane, 1:1; R_f=0.42) gave essentially pure *dimethyldimethoxyarylaldehyde* **18** weighing *ca.* 30 mg (yield, 26%). IR ($CHCl_3$, NaCl): ν_{max} 2890, 2840, 2720, 1695 (C=O), 1600, 1565, 1450, 1300, 1120, 1090, 995 cm^{-1}. ^1H NMR (400MHz, $CDCl_3$, TMS): δ 9.98 (s, 1H, 4″-C*H*O), 7.84, 7.82 ($\frac{1}{2}AA'BB'$ q, 2H, 3″,5″-C*H*, J=8.2Hz), 7.56, 7.54 ($\frac{1}{2}AA'BB'$ q, 2H, 2″,6″-C*H*, J=8.6Hz), 6.66 (s, 1H, 6′-C*H*), 3.81 (s, 3H, OCH_3), 3.70 (s, 3H, OCH_3), 2.22 (s, 3H, 3′/4′-CH_3), 2.12 (s, 3H, 3′/4 ′-CH_3), 2.2-2.1 (m, 6H, 3×CH_2), 2.0-1.9 (m, 6H, 3×CH_2) ppm. ^{13}C NMR (100MHz, $CDCl_3$): δ 191.43 (4″-*C*HO), 157.24 (1″-*C*), 152.73, 152.00 (2′,5′-*C*OCH$_3$), 137.77 (1′-*C*), 133.85 (4″-*C*CHO), 131.14 (3′-*C*CH$_3$), 129.37, 125.99 (2″,3″,5″,6″-*C*H), 124.63 (4′-*C*CH$_3$), 107.31 (6′-*C*H), 61.18, 56.07 (2′,5′-O*C*H$_3$), 35.83, 35.56 (1,4-*C*), 32.84, 31.40 (2,3,5,6,7,8-*C*H$_2$),

14.18, 12.21 (3′,4′-CH_3) ppm. Mass spectrum (EI, 70eV): *m/z* (relative intensity, %) 379 ($M^+ + 1$, 25.6), 378 (M^+, 100), 363 (4.6), 336 (4), 218 ($C_{14}H_{18}O_2^+$, 29), 204 (12), 203 ($C_{13}H_{15}O_2^+$, 25), 189 (13), 165 (14), 91 (11). Exact mass for $C_{25}H_{30}O_3$: calcd 378.2195, obsd 378.2192.

2,3-Dimethyl-1,4-dimethoxybenzene (40). The synthesis of the hydroquinone dimethyl ether was based on an analogous preparation by Smith and Opie.[14] A 250 mL round bottom flask surmounted by a condenser was charged with 2,3-dimethylhydroquinone (5.30 g, 38.4 mmol), potassium hydroxide (35 g), methanol (75 mL), and water (25 mL). Dimethyl sulfate (30 mL) was added over 20 mins, and the mixture was heated at reflux for five hours. On cooling, the mixture was poured into water and ether, and the organic layer was washed with saturated sodium chloride, dried over sodium sulfate, filtered, concentrated, and purified by flash column chromatography (ether/n-hexane, 1:1; R_f=0.60). The evaporated solid was recrystallized from ether/n-hexane to give 2.9 g of colorless prisms. mp 70-71°[lit.[15] 78°]. IR ($CHCl_3$, NaCl): ν_{max} 2890, 2820, 1595, 1450, 1380, 1090, 1000, 590 cm^{-1}. ^1H NMR (90MHz, $CDCl_3$, TMS): δ 6.55 (s, 2H, 5,6-C*H*), 3.7 (s, 6H, 1,4-OCH_3), 2.1 (s, 6H, 2,3-CH_3) ppm.

Preparation of 1,19-ac-Biladiene Dihyrobromide **30**

---

[14] L.I. Smith and J.W. Opie, *J. Amer. Chem. Soc.*, **63**, 427 (1941).

[15] L.I. Smith and R.B. Carlin, *J. Amer. Chem. Soc.*, **64**, 524 (1942).

3-(Ethoxycarbonyl)-4-methylpyrrole (19). This material was prepared by the method of Cheng, Bowman, and LeGoff.[16] In a 1000 mL, one-neck round bottom flask fitted with addition funnel, sodium hydride (60% in oil, 8.0 g, mmol) was suspended in anhydrous ethyl ether (100 mL). The vigorously stirred suspension was treated dropwise with a solution of *p*-toluenesulfonylmethylisocyanide (19.5 g, 100 mmol) in diethyl ether (200 mL) and dry dimethyl sulfoxide (100 mL). The dark solution was stirred for 30 mins more, and then the excess sodium hyrdride was destroyed by the cautious addition of water (100 mL). The aqueous layer was extracted with 8×50 mL ether. The organic extracts were passed through a 2in×0.5in I.D. column of neutral alumina, eluting with dichloromethane (1000 mL). The evaporated residue (13 g) crystallized on standing and was found pure enough to be used directly in the subsequent reaction (crude yield, 82%). IR ($CHCl_3$, NaCl): ν_{max} 3495, 3340 (NH), 3000, 2940, 2880, 1690 (C=O), 1570, 1525, 1445, 1400, 1385, 1330, 1250, 1150, 1080, 900 cm^{-1}. ^1H NMR (90MHz, $CDCl_3$, TMS): δ 9.7 (*br* s, 1H, N*H*), 7.4 (m, 1H, 5-C*H*), 6.6 (*br* s, 1H, 2-C*H*), 4.3 (q, 2H, OCH_2CH_3, $J\approx$9Hz), 2.25 (s, 3H, 4-CH_3), 1.3 (t, 3H, OCH_2CH_3, $J\approx$9Hz) ppm.

3,4-Dimethylpyrrole (20). The procedure of Cheng, Bowman, and LeGoff[16] was followed. To a solution of sodium bis(2-methoxyethoxy)aluminum

---

[16] D.O. Cheng, T.L. Bowman, and E. LeGoff, *J. Heterocyclic Chem.*, **13**, 1145 (1976).

hydride (70% in toluene, 236 mL, 0.82 mol), stirred under an argon atmosphere, a solution of *3-ethoxycarbonyl-4-methylpyrrole* **19** (50 g, 0.33 mol) in benzene (250 mL) was added dropwise. The mixture was stirred at 25°C for 24h, and then slowly poured into ice water. Extraction with 4×50 mL ether, drying, filtration, and distillation at reduced pressure gave 6.1 g clear oil (yield, *ca.* 20-35%), bp 69-70°/26mm Hg [lit.[16] bp 69-70°/10mm Hg], which crystallized on standing to give colorless plates. mp 29.5-31° [lit.[17,18] mp 32-33°, 33°]. IR ($CHCl_3$, NaCl): ν_{max} 3460 (NH), 2850, 2720, 1575, 1090, 970 cm^{-1}. ^1H NMR (90MHz, $CDCl_3$, TMS): δ 7.5 (*br* s, 1H, N*H*), 6.38 (d, 2H, 2,5-C*H*, *J*=2.4Hz), 2.0 (s, 6H, 2×CH_3) ppm.

2-Formyl-3,4-dimethylpyrrole (21). A solution of *dimethylpyrrole* **20** (6.8 g, 71.5 mmol) in *N,N*-dimethylformamide (35 mL) was cooled to 0-5°. Over three minutes, benzoyl chloride (8.3 mL, 71.5 mmol) was added. Cooling was continued while swirling the solution. Ether (50 mL) was added, and the precipitate was filtered. The solid dissolved in minimum water. Sodium carbonate (10 g) was added resulting in a thick precipitate. After standing several hours, the crystals were collected, washed with water, and dried affording 7.55 g of *aldehyde* (yield, 86%). mp 129-130°[lit.[17,19] 129-130°, 133°]. IR ($CHCl_3$, NaCl): ν_{max}

---

[17] G.M. Badger, R.L.N. Harris, and R.A. Jones, *Aust. J. Chem.*, **17**, 1022 (1964).

[18] H. Fischer and J. Hierners, *Liebigs Ann. Chem.*, **492**, 21 (1931).

[19] H. Fischer and H. Höfelmann, *Liebigs Ann. Chem.*, **533**, 216 (1938).

3425 (NH), 1635 (C=O), 1350, 890 cm^{-1}.^{1}H NMR (400MHz, $CDCl_3$, TMS): δ 9.58 (s, 1H, C*H*O), 6.86 (*br* s, 1H, 5-C*H*), 2.27 (s, 3H, 3/4-CH_3), 2.02 (s, 3H, 3/4-CH_3) ppm. ^{13}C NMR (100.4MHz, $CDCl_3$, TMS): δ 176.82 (2-*C*HO), 130.94 (3/4-*C*), 129.42 (2-*C*), 124.53 (5-*C*H), 120.80 (3/4-*C*), 9.75 (*C*H_3), 8.87 (*C*H_3) ppm.

[2′-(Ethoxycarbonyl)-2′-cyanovinyl]-3,4-dimethylpyrrole (22).[20] A solution of *dimethylpyrrole aldehyde* **21** (9g, 73 mmol), ethyl cyanoacetate (11 mL, 100 mmol), and diethylamine (2 mL) in absolute ethanol (15 mL) was heated for 20 minutes in a 250 mL round bottom flask. Benzene (75 mL) was added, and a condenser and a Dean-Stark trap were attached. The mixture was azeotropically distilled until no more water appeared in the trap. Cooling resulted in a crystalline yellow product (yield, *ca.* 60%). An analytical sample was obtained by recrystallization from absolute ethanol giving yellow needles. mp 159-160°[lit.[21] 194-195°(*ex* methanol)]. IR ($CHCl_3$, NaCl): ν_{max} 3420 (NH), 2900, 2850, 2200 (C≡N), 1710 (C=O), 1585, 1545, 1365, 1095, 1005, 875 cm^{-1}. ^{1}H NMR (90MHz, $CDCl_3$, TMS): 9.8 (*br* s, 1H, N*H*), 8.05 (s, 1H, 1′-C*H*), 7.0 (d, 1H, 5-C*H*, J=3Hz), 4.3 (q, 2H, OCH_2CH$_3$, J=7.5Hz), 2.2 (s, 3H, 3/4-CH_3), 2.05 (s, 3H, 3/4-CH_3), 1.3 (t, 3H, OCH$_2$CH_3, J=7.5Hz) ppm. ^{13}C NMR (50MHz, $CDCl_3$): δ 164.2 (*C*=O), 139.4 (C=*C*H), 134.4 (3-*C*), 127.6 (5-*C*H), 124.8 (4-*C*), 121.9 (2-*C*), 119.6(*C*≡N), 88.4 (*C*=CH), 61.8 (O*C*H$_2$CH$_3$), 14.3 (OCH$_2$*C*H$_3$), 9.8 (3/4-*C*H$_3$),

---

[20] J.B. Paine III, R.B. Woodward, and D. Dolphin, *J. Org. Chem.*, **41**, 2826 (1976).

9.4 (3/4-CH_3) ppm.

3-Methylpentane-2,4-dione (23).[21] A 1000 mL round bottom flask fitted with a reflux condenser was loaded with 2,4-pentanedione (205 mL, 2mol), iodomethane (149 mL, 2.4mol), potassium carbonate (262 g, 1.9mol), and distilled acetone (380 mL). The stirred mixture was heated at reflux for six hours under an atmosphere of dry nitrogen. On cooling, petroleum ether (bp 35-60°)/acetone (1:1, 200 mL) was added to complete precipitation of potassium iodide. The mixture was filtered, concentrated *in vacuo,* and was distilled to give 179 g (yield, 78%) of colorless oil, bp 165-170°/760mm Hg. IR ($CHCl_3$, NaCl): ν_{max} 3430, 2920, 1700 (C=O), 1600, 1355, 1140, 960, 890 cm^{-1}. ^1H NMR (90MHz, CCl_4, TMS): δ (enol + keto) 5.4 (s, 1H, O*H*), 3.55 (q, 1H, C*H*CH_3, J=10Hz), 2.1 (s, 3H, CH_3), 2.05 (s, 3H, CH_3), 1.95 (s, 6H, COCH_3), 1.80 (s, 3H, CH_3), 1.25 (d, 3H, CHCH_3, J=10Hz) ppm.

t-Butyl-3,4,5-trimethylpyrrole-2-carboxylate (24). This compound was prepared in accord with the procedure of Paine, Woodward, and Dolphin.[20] In an ice bath t-butyl acetate (158 g, 1 mol) was dissolved in glacial acetic acid (250 mL). To the stirred solution was added sodium nitirite (69.0 g, 1 mol) dissolved in water (85 mL) at such a rate that the temperature remained below 40°C. In a separate round-bottom flask fitted with a condenser, mechanical

---

[21] A.W. Johnson, E. Markham, and R. Price, *Org. Syn. Coll. Vol.*, **V**, 785 (1973).

stirrer, and thermometer, was dissolved *3-methyl-2,4-pentanedione* **23** (114 g, 1 mol) in glacial acetic acid (250 mL). Alternating, the oximine and zinc powder (200 g, 3.08 mol) were added. The temperature was maintained between 85° and 95°. The stirred mixture was heated at reflux for one hour, then poured into ice water. The crystalline mass was filtered through a Büchner funnel and recrystallized by dissolving the filter cake in dichloromethane, separating the water layer, refiltering the organic layer, and evaporating while adding methanol. This procedure produces white crystals (weighing 77.5 g), which together with a second crop gives a total of 87.5 g (yield, 42%). mp 137-138°[lit.[20,22] 138.5° , 137-138°]. IR ($CHCl_3$, NaCl): ν_{max} 3425 (NH), 2900, 2850, 1665 (C=O), 1365, 1325, 1105 cm^{-1}. ^1H NMR (90MHz, CCl_4, TMS): δ 9.6 (*br* s, 1H, N*H*), 2.15 (s, 3H, CH_3), 2.1 (s, 3H, CH_3), 1.8 (s, 3H, CH_3), 1.5 (s, 9H, C(CH_3)$_3$)$_3$ ppm. ^{13}C NMR (100.4MHz, $CDCl_3$): δ 161.11 (*C*=O), 128.64, 126.17, 117.70 (3,4,5-*C*), 116.54 (2-*C*$CO_2{}^t$Bu), 79.85 (O*C*(CH$_3$)$_3$), 28.78 (OC(*C*H$_3$)$_3$), 11.63, 11.00, 9.01 (3,4,5-*C*H$_3$) ppm.

2-Formyl-3,4,5-trimethylpyrrole (25). This compound was synthesized according to the procedure of Paine, Woodward, and Dolphin.[20] In a 500 mL Erlenmeyer flask was dissolved *2-t-butoxycarbonyl-3,4,5-trimethylpyrrole* (20.8 g, 0.1mol) with *N,N*-dimethylformamide (50 mL) and heated to boiling. Benzoyl

---

[22] E. Bullock, A.W. Johnson, E. Markham, and K.B. Shaw, *J. Chem. Soc.* 1438 (1958).

chloride (21.5 mL, 0.185mol) in DMF (50 mL) was added over two minutes. Heating was continued for ten minutes, with darkening and gas evolution. The mixture was cooled over two hours. Solids were collected by filtration and rinsed with DMF and diethyl ether. The crude salts were dissolved in water, filtered through diatomaceous earth, heated and treated with concentrated ammonium hydroxide till no more precipitate formed. The granular orange solid was filtered and dried to afford 8 g of *pyrrole aldehyde* **25** (yield, 58%). ^{1}H NMR (90MHz, CCl_4, TMS): δ 9.35 (s, 1H, C*H*O), 2.2 (s, 3H, CH_3), 2.15 (s, 3H, CH_3), 1.85 (s, 3H, CH_3) ppm.

2-(2′-Cyano-2′-ethoxycarbonylvinyl)-3,4,5-trimethylpyrrole (26). A procedure based on one of Paine, Woodward, and Dolphin[20] was followed. A solution of *2-formyl-3,4,5-trimethylpyrrole* **25** (7 g, 0.051 mol) and ethyl cyanoacetate (11 mL, 0.103 mol) in methanol (50 mL) was treated with diethylamine (1mL) and taken to dryness on the steam bath. Benzene (50 mL) and more diethylamine (1 mL) were added, and a Dean-Stark trap was attached. The mixture was heated at reflux until no additional water distilled. Solvents were evaporated. The oily solid product was dissolved in dichloromethane, filtered, and the solvent was displaced with methanol, yielding 8.26 g (yield, 70%) of a yellow powder. IR ($CHCl_3$, NaCl): ν_{max} 3405 (NH), 2195 (C≡N), 1700 (C=O), 1590, 1090, 1020sh cm^{-1}. ^{1}H NMR (400MHz, $CDCl_3$, TMS): δ 9.48 (*br* s, 1H, N*H*), 7.91 (s, 1H, C=C*H*), 4.31 (q, 2H, OCH_2CH$_3$, J=7.3Hz), 2.30 (s, 3H, CH_3), 2.16

(s, 3H, CH_3), 1.95 (s, 3H, CH_3), 1.36 (t, 3H, OCH_2CH_3, J=7.4Hz) ppm. ^{13}C NMR (100.4MHz, $CDCl_3$, TMS): δ 164.29 (C=O), 138.48 (5-C), 137.57 (C=CH), 135.53 (3-C), 123.04 (4-C), 120.20 (2-C), 119.49 ($C\equiv$N), 85.29 (C=C(CN)), 61.53 (OCH_2CH_3), 14.66 (OCH_2CH_3), 12.61 (CH_3), 10.05 (CH_3), 9.05 (CH_3) ppm.

5-Chloromethyl-2-(2′-cyano-2′-ethoxycarbonylvinyl)-3,4-dimethylpyrrole (27).[20] The *3,4,5-trimethylpyrrole* **26** (6.0 g, 25.8 mmol) in dichloromethane (6 mL) was added dropwise over three minutes at room temperature. The dichloromethane was boiled away while adding diethyl ether. The yellow product crystallizes from the reaction mixture, and is collected by filtration providing 5.13 g (yield, 75%). An analytical sample was obtained by recrystallization from dichloromethane/diethyl ether (1:1), affording light yellow sheaves. mp 166-168°. IR ($CHCl_3$, NaCl): ν_{max} 3405 (NH), 2910vw, 2850vw, 2200 (C≡N), 1705 (C=O), 1590, 1550, 1365, 1090 cm^{-1}. ^1H NMR (90MHz, $CDCl_3$, TMS): δ 8.0 (s, 1H, CH=C), 4.6 (s, 2H, CH_2Cl), 4.3 (q, 2H, OCH_2CH_3, J=7Hz), 2.2 (s, 3H, CH_3), 2.0 (s, 3H, CH_3), 1.3 (t, 3H, OCH_2CH_3, J=7Hz) ppm.

5,5′-Bis(2′-cyano-2′-ethoxycarbonylvinyl)-3,3′,4,4′-tetramethyl-2,2′-dipyrrylmethane (28). *Method A.* A modified procedure for the reported bis-(methoxycarbonyl) compound was followed.[20] A solution of stannic chloride (1.35 mL, 11.5 mmol) in dichloromethane (10 mL) was added to a solution of *2-(2′-cyano-2′-ethoxycarbonylvinyl)-3,4-dimethylpyrrole* **22** (2.04 g, 9.3 mmol) and *5-chloromethyl-2-(2′-cyano-2′-ethoxycarbonylvinyl)-3,4-dimethylpyrrole* **27** (2.52 g,

9.4 mmol) in dichloromethane (50 mL). The resulting green solution was kept at room temperature for two hours. Concentrated hydrochloric acid (1 mL) and then water (60 mL) were added. Layers were separated. The organic layer was washed with water (2×30 mL), dried over potassium carbonate, filtered, and concentrated. The crude brown powder (2.81 g; yield, >70%) was purified by trituration with methanol, and then crystallization from dichloromethane/ethanol.

Method B. To a solution of *2-(2′-cyano-2′-ethoxycarbonylvinyl)-3,4-dimethylpyrrole* **22** (2.18 g, 10 mmol) and 1,1-dimethoxymethane (1 mL, 11.3 mmol) in dichloromethane (25 mL) was added a solution of stannic chloride (1.1 mL, 9.4 mmol) in dichloromethane (5 mL). After being stirred at 25°for 90 minutes, concentrated hydrochloric acid and water were added. Similar work-up as in Method A gave 0.82 g of yellow crystals (yield, 37%). IR (KBr): ν_{max} 3400 (NH), 2900, 2190 (C≡N), 1705 (C=O), 1590, 1540, 1215, 1085, 1010, 755, 525 cm^{-1}. ^1H NMR (90MHz, $CDCl_3$, TMS): δ 9.5 (*br* s, 2H, 2×N*H*), 7.9 (s, 2H, C*H*=C), 4.2 (q, 4H, 2×OCH_2CH$_3$, J=7Hz), 3.95 (s, 2H, CH_2py$_2$), 2.15 (s, 6H, 2×CH_3), 2.0 (s, 6H, 2×CH_3), 1.3 (t, 6H, 2×OCH$_2$CH_3, J=7Hz) ppm. ^{13}C NMR (22.4MHz, $CDCl_3$): δ 164.1 (C=O), 138.4 (2,2′-*C*), 135.8 (*C*H=C), 135.1 (4,4′-*C*), 123.8 (5,5′-*C*), 119.7 (*C*≡N; 3,3′-*C*), 87.8 (CH=*C*), 61.6 (O*C*H$_2$CH$_3$), 24.4 (*C*H$_2$py$_2$), 14.2 (OCH$_2$*C*H$_3$), 9.7 (*C*H$_3$), 8.8 (*C*H$_3$) ppm.

5,5′-Diformyl-3,3′,4,4′-tetramethyl-2,2′-dipyrrylmethane (29). The procedure of Paine, Woodward, and Dolphin[20] was used to prepare the di-

aldehyde. The *divinyl dipyrrylmethane* **28** (1.08 g, 2.4 mmol) was dissolved in methanol (100 mL) and treated with a solution of potassium hydroxide (10.1 g), in water (20 mL). The mixture was heated on a steam bath to boil off methanol. The aqueous residue was heated for 3-4 hours at 100°C. The precipitated solid was periodically filtered, washed with copious water, and dired *in vacuo* to afford 0.48 g of light tan powder. mp 287-289°[lit.[20] 295-298°]. IR (KBr): ν_{max} 3205 (NH), 2900w, 2830w, 1610 (C=O), 1485, 1435, 1385, 1330, 1315, 1240, 850, 770, 730, 690 cm^{-1}. ^1H NMR (200MHz, DMSO-d_6, TMS): δ 9.46 (*br* s, 2H, N*H*), 3.83 (s, 2H, CH_2), 2.17 (s, 6H, 2×CH_3), 1.90 (s, 6H, 2×CH_3) ppm. ^{13}C NMR (22.4MHz, DMSO-d_6): δ 176.3 (*C*HO), 134.5, 130.5, 127.9, 116.8, 22.4 (CH_2py_2), 8.83 (CH_3), 8.37 (CH_3) ppm.

1,19-Dideoxy-2,3,7,8,12,13,17,18-octamethyl-*ac*-biladiene dihydrobromide (30). This material was prepared by analogy to the method of Johnson and Kay.[23] An Erlenmeyer flask covered with aluminum foil was charged with *3,4-dimethylpyrrole* (110 mg, 1.16 mmol), *5,5'-diformyl-3,3',4,4'-tetramethyldipyrrylmethane* (144 mg, 0.56 mmol), and methanol (8 mL). Upon the addition of 48% hydrobromic acid (1 mL), the mixture was swirled and heated over a steam bath for one minute. The flask was covered with foil and set aside to stand at room temperature for 3 hours. The precipitated red-brown solid was filtered and washed with methanol containing hydrobromic acid and finally anhydrous ether.

---

[23] A.W. Johnson and I.T. Kay, *J. Chem. Soc.* 1620 (1965).

The resulting powder was dried and stored at -20°C till used. mp >300°. UV-Vis ($CHCl_3$): λ_{max} 370 (ϵ 12,700), 458 (21,500), 521 (175,000) nm. ^1H NMR (500MHz, $CDCl_3$, TMS): δ 7.64 (s, 2H, 1,19-C*H*), 7.23 (s, 2H, 10,20-C*H*), 5.24 (s, 2H, 15-CH_2), 2.31 (s, 6H, 2×CH_3), 2.26 (s, 6H, 2×CH_3), 2.09 (s, 6H, 2×CH_3), 1.95 (s, 6H, 2×CH_3) ppm. Mass spectrum (EI, 70eV): *m/z* (relative intensity, %)412 (M^+− 2HBr, 3.1), 410 (M^+− 2HBr − 2H, 8), 332 (8.3), 257 (4.6), 240 (2.2), 207 (3.1), 181 (4.5). Exact mass for $C_{27}H_{30}N_4$ (M^+− 2HBr − 2H): calcd 410.2470, obsd 410.2487. *Anal.* Calcd for $C_{27}H_{34}N_4Br_2$: 56.46%C, 5.97%H, 9.76%N. Found: 56.19%C, 6.03%H, 9.64%N.

5-{4′-[4″-(2‴,5‴-Dimethoxyphenyl)bicyclo[2.2.2] octyl]phenyl}-2,-3,7,8,12,13,17,18-octamethylporphyrin (31). The general procedure of Harris, Johnson, and Gaete-Holmes[24] was followed to prepare the *meso*-substituted porphyrins. *Aryl aldehyde* **16** (50 mg, 0.14 mmol) and *ac-biladiene dihydrobromide* (88 mg, 0.15 mmol) were suspended in methanol (5 mL), and treated with three drops of 32% hydrobromic acid (in acetic acid) in the dark. The suspension was heated at reflux in an aerobic atmosphere with the complete exclusion of light for 24 hours. On cooling, sodium bicarbonate (200 mg) was added, and the mixture was filtered, washed with methanol and water, and air-dried. The crude *porphyrin* was purified by flash column chromatography

---

[24] D. Harris, A.W. Johnson, and R. Gaete-Holmes, *Bioorganic Chemistry*, **9**, 63 (1980).

(dichloromethane/acetonitrile, 9:1, R_f=0.65), affording 50 mg of reddish-purple crystals (yield, 48%). UV-Vis (CH_2Cl_2/MeOH, 1:1): λ_{max} 290 (ϵ 9900), 401 (120,000) 501 (9600), 534 (4400), 569 (4300), 621 (1500) nm. ^{1}H NMR (500MHz, $CDCl_3$, TMS): δ 10.11 (s, 2H, 10,20-C*H*), 9.89 (s, 1H, 15-C*H*), 7.90, 7.88 ($\frac{1}{2}AA'BB'$ q, 2H, 2′,6′-C*H*, J=7.8Hz), 7.68, 7.67 ($\frac{1}{2}AA'BB'$ q, 2H, 3′,5′-C*H*, J=7.9Hz), 6.94 (d, 1H, 6‴-C*H*, J=3Hz), 6.86 (d, 1H, 3‴-C*H*, J=8.8Hz), 6.74 (dd, 1H, 4‴-C*H*, J=2.8, 8.8Hz), 3.88 (s, 3H, OCH_3), 3.82 (s, 3H, OCH_3), 3.59 (s, 6H, 13,17-CH_3), 3.56 (s, 6H, 12,18-CH_3), 3.50 (s, 6H, 2,8-CH_3), 2.41 (s, 6H, 3,7-CH_3), 2.25 (s, 12H, 6×CH_2), -3.19, -3.30 (2*br* s, 2H, 2×N*H*) ppm. Mass spectrum (EI, 70eV): *m/z* (relative intensity, %)743 (M^+ + 1, 11), 742 (M^+, 26), 729 (8), 703 (12), 701 (13), 678 (12), 667 (3.6), 641 (26), 640 (55), 616 (31), 529 (13), 262 (100), 217 (30), 183 (72). Exact mass for $C_{50}H_{54}N_4O_2$: calcd 742.4247, obsd 742.4254.

5-{4′-[4″-(2‴,5‴-Dimethoxy-4‴-methylphenyl)bicyclo[2.2.2]oct-yl]phenyl}-2,3,7,8,12,13,17,18-octamethyl porphyrin (32). A suspension of *methylarylaldehyde* **17** (65 mg, 0.18 mmol) and freshly prepared *ac-biladiene dihydrobromide* (102 mg, 0.18 mmol) in methanol (6 mL) was treated with four drops of 32% hydrobromic acid in acetic acid and heated at reflux for 24 hours under air with light excluded. After cooling, solid sodium bicarbonate (200 mg) was added, and the mixture was filtered, washed with methanol and water and dried in air. The crude product was purified by flash chromatography

(dichloromethane/acetonitrile, 9:1; R_f=0.75), providing 70 mg of purple crystals (yield, 51%). UV-Vis (CH_2Cl_2/2% CH_3CN): λ_{max} 293, 406, 502, 534, 571, 623 nm. ^{1}H NMR (400MHz, $CDCl_3$): δ 10.10 (s, 2H, 10,20-C*H*), 9.89 (s, 1H, 15-C*H*), 7.92, 7.90 ($\frac{1}{2}AA'BB'$ q, 2H, 2′,6′-C*H*, J=7.2Hz), 7.70, 7.68 ($\frac{1}{2}AA'BB'$ q, 2H, 3′,5′-C*H*, J=7.2Hz), 6.86 (s, 1H, 3‴-C*H*), 6.76 (s, 1H, 5‴-C*H*), 3.87 (s, 3H, OCH_3), 3.86 (s, 3H, OCH_3), 3.59 (s, 6H, 13,17-CH_3), 3.56 (s, 6H, 12,18-CH_3), 3.50 (s, 6H, 2,8-CH_3), 2.41 (s, 6H, 3,7-CH_3), 2.25 (s, 12H, 6×CH_2), 2.23 (s, 3H, 4‴-CH_3), -3.22 (*br* s, 1H, N*H*), -3.30 (*br* s, 1H, N*H*) ppm.

5-{4′-[4″-(2‴,5‴-Dimethoxy-3‴,4‴-dimethylphenylbicyclo[2.2.2]-octyl]phenyl}-2,3,7,8,12,13,17,18-octamethylporphyrin (33). *Dimethylaryl aldehyde* **18** (20 mg, 0.05 mmol) and *ac-biladiene dihydrobromide* **30** (80 mg, 0.14 mmol) were suspended in methanol (10 mL) in a 25 mL round bottom flask wrapped in aluminum foil and fitted with a condenser. The mixture was treated with glacial acetic acid saturated with hydrogen bromide (4 drops) and heated at reflux for 24 hours open to the atmosphere in complete darkness. Work-up as in previous examples and flash chromatography (dichloromethane/acetonitrile, 9:1; TLC, R_f=0.63) gave *ca.* 10 mg of *porphyrin dimethyl ether* **33** (yield, 26%). UV-Vis (CH_2Cl_2): λ_{max} 284 (ϵ 8200 estd), 404 (170,000 estd), 502 (13,000 estd), 534 (6000 estd), 570 (6000 estd), 623 (1900 estd) nm. ^{1}H NMR (400MHz, $CDCl_3$): δ 10.11 (s, 2H, 10,20-C*H*), 9.89 (s, 1H, 15-C*H*), 7.92, 7.90 ($\frac{1}{2}AA'BB'$ q, 2H, 2′,6′/3′,5′-C*H*, J=7.7Hz), 7.70, 7.68 ($\frac{1}{2}AA'BB'$ q, 2H, 2′,6′/3′,5′-C*H*, J=8.1Hz),

6.77 (s, 1H, 6‴-C*H*), 3.86 (s, 3H, OCH_3), 3.77 (s, 3H, OCH_3), 3.59 (s, 6H, 13,17-CH_3), 3.56 (s, 6H, 12,18-CH_3), 3.50 (s, 6H, 2,8-CH_3), 2.41 (s, 6H, 3,7-CH_3), 2.26 (s, 12H, 2″,3″,5″,6″,7″,8″-CH_2), 2.24sh (s, 3H, 3‴/4‴-CH_3), 2.16 (s, 3H, 3‴/4‴-CH_3), -3.24 (*br* s, 2H, 2NH) ppm. Mass spectrum (Fast Atom Bombardment, positive ion, *m*-nitrobenzyl alcohol matrix): *m/z* (relative intensity, %) 772 ($M^+ + 2$, 55), 771 ($M^+ + 1$, 100), 770 (M^+, 25), 741 (13), 727 (10), 460 (50), 371 (70). Exact Mass for $C_{52}H_{59}N_4O_2$ ($M^+ + 1$): calcd 771.4638, obsd 771.4623.

5-{4′-[4″-(2‴,5‴-Dimethoxy-4‴-cyanophenyl)-bicyclo[2.2.2] octyl]phenyl}-2,3,7,8,12,13,17,18-octa methylporphyrin (34). In a 25 mL round bottom flask fitted with a condenser were suspended *cyano benzaldehyde* **52** (46 mg, 0.12 mmol) and freshly prepared *ac-biladiene dihydrobromide* **30** (77 mg, 0.13 mmol) in methanol (10 mL). The mixture was treated with five drops of 32% hydrobromic acid in acetic acid and was heated at reflux for 24 hours in an air atmosphere with compete exclusion of light. After cooling to room temperature, solid sodium bicarbonate (180 mg) was added. The mixture was filtered, and the filter cake was repeatedly washed with methanol and with water and then dried in air. The crude *porphyrin* was purified by flash chromatography (dichloromethane/acetonitrile, 9:1; R_f=0.75). UV-Vis (CH_2Cl_2): 328, 404, 503, 536, 574, 625 nm. ^{1}H NMR (400MHz, $CDCl_3$, TMS): δ 10.13 (s, 2H, 10,20-C*H*), 9.92 (s, 1H, 15-C*H*), 7.95, 7.93 ($\frac{1}{2}AA'BB'$ q, 2H, 2′,6′-C*H*, J=8.3Hz), 7.71, 7.69

($\frac{1}{2}AA'BB'$ q, 2H, 3',5'-C*H*, J=8.3Hz), 7.05 (s, 1H, 3'''-C*H*), 6.98 (s, 1H, 6'''-C*H*), 3.97 (s, 3H, OCH_3), 3.90 (s, 3H, OCH_3), 3.61 (s, 6H, 13,17-CH_3), 3.58 (s, 6H, 12,18-CH_3), 3.52 (s, 6H, 3,16-CH_3), 2.43 (s, 6H, 2,17-CH_3), 2.26 (s, 12H, 6×CH_2), -3.18 (*br* s, 1H, N*H*), -3.29 (*br* s, 1H, N*H*) ppm. Mass spectrum (Fast Atom Bombardment, positive ion; dithioerythritol/dithiothreitol): *m/z* (%) 768 (M^+, 54), 666 (8), 563 (28), 512 (33), 411 (21), 152 (52), 135 (100). Exact mass for $C_{51}H_{54}N_5O_2$: calcd 768.4277, obsd 768.4260.

[5-{4'-[4''-(2''', 5'''-Dimethoxy-4'''-cyanophenyl)-bicyclo[2.2.2]octyl]phenyl}-2,3,7,8,12,13,17,18-octamethylporphyrinato]zinc(II) (34a). The free-base *porphyrin* **34** was metallated with zinc(II)acetate dihydrate in methanol-chloroform (1:10), and purified by flash chromatography and trituration of the crystalline solid obtained with n-hexane and methanol, and finally dried *in vacuo*. UV-Vis (CH_2Cl_2): λ_{max} 323, 402, 500sh, 532, 570 nm. ^{1}H NMR (500MHz, CD_2Cl_2): δ 10.11 (s, 2H, 10,20-C*H*), 9.94 (s, 1H, 15-C*H*), 7.97, 7.95 ($\frac{1}{2}AA'BB'$ q, 2H, 2',6'-C*H*, J=8Hz), 7.76, 7.74 ($\frac{1}{2}AA'BB'$ q, 2H, 3',5'-C*H*, J=8Hz), 7.08 (s, 1H, 3'''-C*H*), 7.02 (s, 1H, 6'''- C*H*), 3.98 (s, 3H, OCH_3), 3.90 (s, 3H, OCH_3), 3.60 (s, 6H, 13,17-CH_3), 3.58 (s, 6H, 12,18-CH_3), 3.53 (s, 6H, 2,8-CH_3), 2.45 (s, 6H, 3,7-CH_3), 2.29 (s, 12H, 6×CH_2) ppm.

5-{4'-[4''-(4'''-Cyano-2''', 5'''-dihydroxyphenyl)-bicyclo[2.2.2]octyl]-phenyl}-2,3,7,8,12,13,17,18-octamethylporphyrin (38). A solution of free-base *porphyrin cyanodimethoxybenzene* **34** (*ca.* 5 mg, 7 μmol) in dichloromethane

(1 mL) was treated with boron triiodide (250 mg, 100 eq) in dichloromethane (3 mL) at 0° in an atmosphere of argon and kept in the freezer (-20°) overnight. Excess boron triiodide was destroyed by addition of aqueous ammonia. The organic layer was washed with water, dried over sodium sulfate, filtered, evaporated, and purified by column chromatography. TLC (dichloromethane/acetonitrile, 9:1): R_f=0.25. UV-Vis (CH_2Cl_2): λ_{max} 275sh, 404, 503, 536, 570, 624 nm. ^{1}H NMR (400MHz, DMSO-d_6, referenced to 2.49 ppm): δ 10.42 (s, 2H, 10,20-C*H*), 9.66 (s, 1H, 15-C*H*), 7.92, 7.90 ($\frac{1}{2}AA'BB'$ q, 2H, 2′,6′-C*H*, $J\approx$8Hz), 7.78, 7.76 ($\frac{1}{2}AA'BB'$ q, 2H, 3′,5′-C*H*, $J\approx$8Hz), 6.55 (*br s*, 3‴/6‴-C*H*), 6.50 (s, 1H, 3‴/6‴-C*H*), 3.61 (s, 6H, 13,17-CH_3), 3.59 (s, 6H, 12,18-CH_3), 3.51 (s, 6H, 2,8-CH_3), 2.40 (s, 6H, 3,7-CH_3), 2.20 (m, 6H, 3×CH_2), 2.07 (m, 6H, 3×CH_2) ppm.

5-{4′-[4″-(2‴, 5‴-Benzoquinone)bicyclo[2.2.2]octyl]phenyl}-2,3,7,-8,12,13,17,18-octamethyl porphyrin (35). The *porphyrin hydroquinone diether* **31** (50 mg, 67 μmol) was dissolved in dichloromethane (20 mL) in a dry 50 mL round bottom flask covered with aluminum foil. After thorough purging with argon, a solution of boron triiodide (0.81M, 3.2 g weighed in an inert atmosphere box, dissolved in 10 mL dichloromethane, 2 mL, 1.7 mmol) was added over one minute at 0°. The reaction mixture was gradually warmed to room temperature over 30 mins and quenched with excess water and dilute ammonia. After shaking in a separatory funnel, the organic layer was dried over sodium sulfate, filtered, and used directly in the subsequent oxidation. This solution of *porphyrin hy-*

droquinone was treated with excess lead dioxide (530 mg). After ten minutes at room temperature, the mixture was filtered, concentrated, and purified by flash chromatography (dichloromethane/acetonitrile, 9:1; R_f=0.41), providing 10 mg of purple crystals (yield, 21% for the two-step sequence). UV-Vis (CH_2Cl_2): λ_{max} 248 (ϵ 23,600), 401 (183,000), 500 (13,000), 533 (5800), 569 (5720), 623 (1900) nm. IR (KBr): ν_{max} 1655 (C=O) cm^{-1}. ^1H NMR (500MHz, CD_2Cl_2, TMS): δ 10.11 (s, 2H, 10,20-C*H*), 9.90 (s, 1H, 15-C*H*), 7.93, 7.92 ($\frac{1}{2}AA'BB'$ q, 2H, 2′,6′-C*H*, J=7.1), 7.66, 7.65 ($\frac{1}{2}AA'BB'$ q, 2H, 3′,5′-C*H*, J=7.7), 6.73 (s, 2H, 3‴,4‴-C*H*), 6.65 (s, 1H, 6‴-C*H*), 3.60 (s, 6H, 13,17-CH_3), 3.57 (s, 6H, 12,18-CH_3), 3.50 (s, 6H, 3,16-CH_3), 2.40 (s, 6H, 2,17-CH_3), 2.24 (m, 6H, 3×CH_2), 2.11 (m, 6H, 3×CH_2), -3.20 (*br* s, 2H, 2×N*H*) ppm. Mass spectrum (Fast Atom Bombardment, *o*-nitrophenyloctyl ether, positive ion): *m/z* (relative intensity, %) 715 (M^+ + 2H + 1, 7), 714 (M^+ + 2H, 9), 713 (M^+ + 1, 18), 712 (M^+, 16), 711 (7), 503 (33), 502 (30), 501 (33), 486 (33), 252 (75), 140 (100), 123 (92). Exact mass (FAB, formic acid/glycerol) for $C_{48}H_{51}N_4O_2$ (M^+ + 2H + 1): calcd 715.4011, obsd 715.3974.

5-{4′-[4″-(4‴-Methyl-2‴,5‴-benzoquinone)bicyclo[2.2.2]octyl]phenyl}-2,3,7,8,12,13,17,18-octamethylporphyrin (36). *Porphyrin hydroquinone diether* **32** (70 mg, 92 μmol) was dissolved in dichloromethane (5 mL), and under an argon atmosphere was treated with a freshly prepared solution of boron triiodide (0.81M in dichloromethane; 4.6 mL, 3.7 mmol) over one minute

at 0°. After twenty minutes the reaction mixture was gradually warmed to room temperature, and water and ammonia were added. The organic layer was separated. The presence of *porphyrin hydroquinone* was supported by thin layer chromatography (dichloromethane/acetonitrile, 9:1; R_f=0.28; fluoresces red under longwavelength ultraviolet light), and the product was submitted directly in the subsequent oxidation step. The *porphyrin hydroquinone* solution was allowed to react with lead dioxide (290 mg, 1.2 mmol) in the presence of anhydrous sodium sulfate (10 g) at 25°. Filtration and concentration *in vacuo* gave essentially pure *porphyrin quinone*, which was then purified further by flash chromatography (dichloromethane/acetonitrile, 20:1; R_f=0.50). ^{1}H NMR (400MHz, $CDCl_3$, TMS): δ 10.17 (s, 2H, 10,20-C*H*), 9.95 (s, 1H, 15-C*H*), 8.01, 7.99 ($\frac{1}{2}AA'BB'$ q, 2H, 2′,6′-C*H*, J=7.0Hz), 7.74, 7.72 ($\frac{1}{2}AA'BB'$ q, 2H, 3′,5′-C*H*, J=6.3Hz), 6.67 (s, 1H, 3″-C*H*), 6.62 (s, 1H, 6″-C*H*), 3.64 (s, 6H, 13,17-CH_3), 3.60 (s, 6H, 12,18-CH_3), 3.54 (s, 6H, 2,8-CH_3), 2.44 (s, 6H, 3,7-CH_3), 2.27 (m, 6H, 3×CH_2), 2.17 (m, 6H, 3×CH_2), 2.09 (s, 3H, 4″-CH_3), -1.20 (*br* s, 1H, N*H*), -2.20 (*br* s, 1H, N*H*) ppm.

5-{4′-[4″-(3‴,4‴-Dimethyl-2‴,5‴-benzoquinone)bicyclo[2.2.2]octyl]phenyl}-2,3,7,8,12,13,17,18-octamethylporphyrin (37). In a two-neck round bottom flask fitted with an argon inlet adapter and a septum, *porphyrin dimethylhydroquinone dimethyl ether* **33** (*ca.* 2 mg, 2 μmol) was dissolved in dichloromethane (4 mL). The solution was treated with boron triiodide (80 mg,

0.2 mmol) at 0°in the absence of light in an inert atmosphere. After stirring for 1.5 hours, aqueous ammonia was added, the mixture was stirred vigorously, and layers were separated. The organic layer was dried over sodium sulfate, filtered, and subjected to flash chromatography (TLC: dichloromethane/acetonitrile (20:1), R_f=0.51), affording a dark red film of the *dimethylbenzoquinone porphyrin.* UV-Vis ($CHCl_3$): λ_{max} 262 (ϵ 18,000 estd), 402 (143,000 estd), 500 (12,000 estd), 533 (5200 estd), 568 (5000 estd), 621 (1700 estd) nm. ^{1}H NMR Mass spectrum (Fast Atom Bombardment, NBA matrix, postive ion): *m/z* (relative intensity, %) 743 ($M^+ + 3$, 5), 742 ($M^+ + 2$, 8), 741 ($M^+ + 1$, 11), 613 (7), 593 (6), 575 (6), 460 (60), 371 (100). Exact mass for $C_{50}H_{53}N_4O_2$ ($M^+ + 1$): calcd 741.4168, obsd 741.4157.

[5-{4′-[4″-(4‴-Cyano-2‴, 5‴-dihydroxyphenyl)bicyclo[2.2.2]octyl]-phenyl}-2,3,7,8,12,13,17,18-octamethyl porphyrinato]zinc(II) (39) The free-base *porphyrin cyanohydroquinone* **38** (*ca.* 1 mg) was metallated in chloroform (10 mL) in the usual manner using zinc(II) acetate dihydrate (25 mg) in methanol (1 mL). After aqueous work-up, the *metalloporphyrin* was purified by flash chromatography. TLC (dichloromethane): R_f=0.11; (dichloromethane/acetonitrile, 20:1): R_f=0.15. UV-Vis (CH_2Cl_2): λ_{max} 347, 404, 532, 569 nm. ^{1}H NMR (400MHz, $CDCl_3$): δ 10.12 (s, 2H, 10,20-C*H*), 10.01 (s, 1H, 15-C*H*), 7.95, 7.93 ($\frac{1}{2}AA'BB'$ q, 2H, 2′,6′-C*H*, $J\approx$8Hz), 7.67, 7.65 ($\frac{1}{2}AA'BB'$ q, 2H, 3′,5′-C*H*, $J\approx$8Hz), 6.67 (s, 1H, 3‴-C*H*), 6.45 (s, 1H, 6‴-C*H*), 3.60 (s, 12h, 12,13,17,18-

CH_3), 3.50 (s, 6H, 2,8-CH_3), 2.40 (s, 6H, 3,7-CH_3), 2.25 (m, 6H, 3×CH_2), 2.10 (m, 6H, 3×CH_2) ppm.

[5-{4′-[4″-(2‴, 5‴-Benzoquinone)bicyclo[2.2.2]octyl]phenyl}-2,3,7,-8,12,13,17,18-octamethylporphyrinato]zinc(II) (1). The free-base *benzoquinone porphyrin* **35** (*ca.* 0.5 mg) was dissolved in chloroform (10 mL) and treated with a saturated solution of zinc(II) acetate dihydrate (25 mg) in methanol. The mixture was heated at reflux till the 623 nm electronic absorption band disappeared. Water was added, and the organic layer was separated, washed once with saturated sodium chloride, and dried over sodium sulfate. The filtrate was immediately submitted to the subsequent oxidation by adding unactivated lead dioxide (50 mg), stirring for five minutes, filtration, concentration *in vacuo*, and purification by flash chromatography. TLC (dichloromethane): R_f=0.50. UV-Vis (CH_2Cl_2): λ_{max} 246 (ϵ 27,000), 340 (15,000), 404 (375,000), 533 (16,000), 569 (16,000) nm. ^{1}H NMR (400MHz, CD_2Cl_2): δ 10.19 (s, 2H, 10,20-C*H*), 10.09 (s, 1H, 15-C*H*), 7.96, 7.94 ($\frac{1}{2}AA'BB'$ q, 2H, 2′,6′-C*H*, J=8.2Hz), 7.73, 7.71 ($\frac{1}{2}AA'BB'$ q, 2H, 3′,5′-C*H*, J=7.9Hz), 6.73 (s, 1H, 6‴-C*H*), 6.724, 6.719 (d, 1H, 4‴-C*H*, J=2.1Hz), 6.657, 6.652 (d, 1H, 3‴-C*H*, J=2.1Hz), 3.64 (s, 12H, 12,13,17,18-CH_3), 3.54 (s, 6H, 2,8-CH_3), 2.44 (s, 6H, 3,7-CH_3), 2.25 m, 6H, 3×CH_2), 2.14 (m, 6H, 3×CH_2) ppm. Mass spectrum (Fast Atom Bombardment, positive ion, CH_2Cl_2/*o*-nitrophenyloctylether matrix): *m/z* (relative intensity, %) 776 (M^+ + 2, 81), 775 (M^+ + 1, 30), 774 (M^+, 49), 735 (M^+ –

COCH, 78), 718 (45), 690 (62), 486 (85), 252 (84), 121 (100). Exact mass for $C_{48}H_{46}N_4O_2Zn$: calcd 774.2912, obsd 774.2944.

[5-{4′-[4″-(4‴-Methyl-2‴,5‴-benzoquinone)bicyclo[2.2.2]octyl]-phenyl}-2,3,7,8,12,13,17,18-octamethyl porphyrinato]zinc(II) (2). The free-base *porphyrin-benzoquinone* **36** (*ca.* 1 mg) was dissolved in chloroform (15 mL) and treated with saturated zinc(II) acetate dihydrate (2 mL) in methanol at reflux till no UV-visible absorption at 625nm remained. The mixture was cooled, extracted with water, dried over sodium sulfate, filtered, and concentrated *in vacuo*. The crystalline residue was dissolved in dichloromethane (10 mL) and applied to a flash chromatography column, eluting with n-hexane/dichloromethane (7:4, $R_f = 0.44$). UV-Vis (C_6H_6): λ_{max} 332, 405, 534, 570 nm; (CH_2Cl_2/CH_3OH, 95:5): λ_{max} 256sh (ϵ 30,000 estd), 344 (27,000 estd), 406 (350,000 estd), 537 (23,000 estd), 572 (18,000 estd)nm. ^{1}H NMR (400MHz, $CDCl_3$): δ 10.11 (s, 2H, 10,20-C*H*), 10.00 (s, 1H, 15-C*H*), 7.95, 7.93 ($\frac{1}{2}AA'BB'$ q, 2H, 2′,6′-C*H*, J=8Hz), 7.67, 7.65 ($\frac{1}{2}AA'BB'$ q, 2H, 3′,5′-C*H*, J=8Hz), 6.98 (s, 1H, 6‴-C*H*), 6.63 (*br* s, 1H, 3‴-C*H*), 3.60 (s, 12H, 7,8,12,13-CH_3), 3.51 (s, 6H, 2,8-CH_3), 2.40 (s, 6H, 3,7-CH_3), 2.22 (m, 6H, 3×CH_2), 2.12 (m, 6H, 3×CH_2), 2.04 (s, 3H, 4‴-CH_3) ppm. Mass spectrum (Fast Atom Bombardment, positive ion, dithiothreitol/dithioerythritol): *m/z* (relative intensity, %) 882 (60), 881 (M^+ − Zn + DTE/DTT, 73), 761 (15), 729 (30), 613 (20), 152 (1). Exact mass for $C_{53}H_{60}N_4O_4S_2$ (M^+ − Zn + DTE/DTT + 1): calcd 881.4056, obsd 881.4089.

[5-{4′-[4″-(3‴,4‴-Dimethyl-2‴,5‴-benzoquinone)bicyclo[2.2.2]octyl]phenyl}-2,3,7,8,12,13,17,18-octamethylporphyrinato]zinc(II) (3). The free-base *porphyrin dimethylbenzoquinone* **37** (*ca.* 4 mg, 5 μmol) was dissolved in chloroform (10 mL) and treated with zinc(II) diacetate dihydrate (90 mg, 0.4 mmol) dissolved in methanol (1 mL). The resulting solution was heated in the dark till the 623 nm electronic absorption band disappeared (~ 1 hour). The mixture was washed with saturated sodium chloride, dried over sodium sulfate, filtered, evaporated, and purified by flash chromatography. TLC (dichloromethane): R_f=0.61. UV-Vis (2MTHF): ν_{max} 256, 344, 412, 542, 576 nm. ^{1}H NMR (400MHz, $CDCl_3$): δ 10.10 (s, 2H, 10,20-C*H*), 9.97 (s, 1H, 15-C*H*), 7.95, 7.93 ($\frac{1}{2}AA'BB'$ q, 2H, 2′,6′-C*H*, J=7.9Hz), 7.68, 7.66 ($\frac{1}{2}AA'BB'$ q, 2H, 3′,5′-C*H*, J=7.9Hz), 6.60 (s, 1H, 6‴-C*H*), 3.59 (s, 12H, 12,13,17,18-CH_3), 3.50 (s, 6H, 2,8-CH_3), 2.41 (s, 6H, 3,7-CH_3), 2.22 (m, 6H, 3×CH_2), 2.11 (m, 6H, 3×CH_2), 2.06 (s, 3H, CH_3), 2.03 (s, 3H, CH_3) ppm. Mass spectrum (Fast Atom Bombardment, *o*-nitrophenyloctyl ether, positive ion): *m/z* (relative intensity, %) 802 (M^+ , 8), 737 ($M^+ - Zn$, 10), 735 ($M^+ - Zn - 2$, 13), 719 (5), 690 (8), 598 (5), 460 (60), 371 (100). Exact mass for $C_{50}H_{50}N_4O_2Zn$ (M^+): calcd 802.3240, obsd 802.3225.

[5-{4′-[4″-(4‴-Cyano-2‴,5‴-benzoquinone)bicyclo[2.2.2]octyl]phenyl}-2,3,7,8,12,13,17,18-octamethylporphyrinato]zinc(II) (4). A solution of the *cyanohydroquinone porphyrin* **39** (*ca.* 0.1 mg) in dichloromethane

(1 mL) benzene (1 mL) was treated with excess silver(I) oxide in the presence of sodium sulfate (50 mg) at room temperature in the absence of light. The reaction mixture was stirred for five to ten minutes and then filtered. The filter paper was washed extensively with dichloromethane and benzene. The filtrate was concentrated *in vacuo*. The product could not be purified without decomposition, and could not be rigorously characterized. ^{1}H NMR (400MHz, $CDCl_3$): δ 10.29 (s, 2H, 10,20-C*H*), 10.13 (s, 1H, 15-C*H*), 7.83, 7.69 ($\frac{1}{2}AA'BB'$ q, 2H, 2′,6′/3′,5′-C*H*), 7.52, 7.25 ($\frac{1}{2}AA'BB'$ q, 2H, 2′,6′/3′/5′-C*H*), 3‴-C*H*obscured by $CDCl_3$ residual), 6.67 (s, 1H, 3‴-C*H*), 3.49 (s, 12H, 12,13,17,18-CH_3), 3.27 (s, 6H, 2,8-CH_3), 2.24 (m, 6H, 3×CH_2), 2.18 (s, 6H, 3,7-CH_3), 2.07 (m, 6H, 3×CH_2), ppm.

Preparation of Cyanobenzaldehyde **52**

Dimethyl 4-cyano-4-(4′-methyl)phenylheptan-1,7-dioate (41). This material was made by a procedure analogous to that of Bruson and Riener.[6] In a two-liter, three-neck round bottom flask fitted with a condenser and addition funnel were dissolved *p*-tolylacetonitrile (100 mL, 0.78mol) and methyl acrylate (136 mL, 1.51mol) in dry dioxane (300 mL). To the stirred mixture, a solution of trimethylbenzylammonium (40% in methanol, 5 g) in dioxane (50 mL) was added dropwise over 30 minutes. The solution was heated at reflux for two hours. On cooling one volume of ether was added, and the mixture was washed with dilute hydrochloric acid, water, and 10% (w/v) sodium carbonate. Drying over magnesium sulfate and concentration *in vacuo* gave a clear yellow oil weighing

200 g (crude yield, 85%). An analytical sample was obtained by vacuum distillation. bp 183-4°/0.01mm Hg. IR (neat, NaCl): ν_{max} 2950, 2215 (CN), 1738 (C=O), 1515, 1440, 1370, 1295, 1195, 1170, 1097, 1020, 815 cm^{-1}. ^1H NMR (400MHz, $CDCl_3$, TMS): δ 7.28, 7.26 ($\frac{1}{2}AA'BB'$ q, 2H, 2′,6′/3′,5′-C*H*), 7.22, 7.17 ($\frac{1}{2}AA'BB'$ q, 2H, 2′,6′/3′,5′-C*H*), 3.61 (s, 6H, 1,7-CO_2CH_3), 2.51-2.09 (m, 8H, 2,3,5,6-CH_2), 2.35 (s, 3H, 4′-CH_3) ppm. ^{13}C NMR (100.4MHz, $CDCl_3$): δ 171.82 (1,7-*C*=O), 137.81, 132.68 (1′,4′-*C*), 129.53, 125.42 (2′,3′,5′,6′-*C*H), 120.78 (4-*C*N), 51.71 (1,7-CO_2CH_3), 46.60 (4-*C*), 35.83, 30.19 (2,3,5,6-CH_2), 21.04 (4′-CH_3) ppm. Mass spectrum (EI, 70eV): *m/z* (relative intensity, %)304 (M^+ + 1, 0.3), 303 (M^+, 2.4), 244 (M^+ − $CH_3OC{\equiv}O$, 1.6), 240 (6), 216 (M^+ − C_2H_4 − $CH_3OC{\equiv}O$, 11), 184 (7.8), 156 (M^+ − C_2H_4 − $2CH_3OC{\equiv}O$ − H, 100), 143 (14), 116 (8), 91 ($C_7H_7^+$, 12.6). Exact mass for $C_{17}H_{21}NO_4$: calcd 303.1471; obsd 303.1468. *Anal.* Calcd for $C_{17}H_{21}NO_4$: 67.31%C, 6.98%H, 4.62%N. Found: 67.17%C, 7,23%H, 4.66%N.

4-Cyano-2-methoxycarbonyl-4-(4′-methyl)phenylcyclohexanone (42). A three-neck, three-liter round bottom flask fitted with a condenser connected to a bubbler, mechanical stirrer, and pressure-equalizing addition funnel was charged with sodium hydride (60% in oil; 6 g, 0.15 mol), dry toluene (150 mL), and methanol (3 mL) under argon. A solution of *tolyl diester* **41** (33 g, 0.11mol) in toluene (40 mL) was added slowly to the stirred sodium hydride suspension while heating at reflux. Slow evolution of dihydrogen occurs. (*Warn-*

ing! In the absence of methanol, uncontrolled exothermic reaction results.) After heating for four hours at reflux, excess hydride was neutralized with acetic acid. Water was added, and the organic layer was washed with water, saturated sodium bicarbonate, and saturated sodium chloride, and then dried over sodium sulfate. Filtration and concentration *in vacuo* gave a light yellow oil which crystallized from methanol to afford white crystals weighing 24.5 g (yield, 82%). An analytical sample was recrystallized from ether/n-hexane, 1:1. TLC (ether/n-hexane, 1:1): R_f=0.38. mp 94-96°. IR ($CHCl_3$, NaCl): ν_{max} 2910, 2850, 2215 (C≡N), 1655 (C=O), 1615 (C=O), 1438, 1420sh, 1350, 1285, 1178, 1090, 1055, 958 cm^{-1}. ^1H NMR (400MHz, $CDCl_3$, TMS): δ 7.39, 7.36 ($\frac{1}{2}AA'BB'$ q, 2H, 2′,6′/3′,5′-C*H*, J=8.3Hz), 7.22, 7.20 ($\frac{1}{2}AA'BB'$ q, 2H, 2′,6′/3′,5′-C*H*, J=8.1Hz), 3.76 (s, 3H, OCH_3), 3.00, 2.96 (d, 1H, 3-CH_{ax}, J=16.4Hz), 2.85-2.75 (m, 1H, 5-CH_{ax}), 2.67, 2.63 (d, 1H, 3-CH_{eq}, J=16.1Hz), 2.49, 2.44 (ddd, 1H, 5-CH_{eq}, J=2, 5, 18.8Hz), 2.35 (s, 3H, 4′-CH_3), 2.25-2.13 (m, 2H, 6-CH_2) ppm. ^{13}C NMR (100.4MHz, $CDCl_3$): δ 171.29, 170.08 (1-*C*=O, 2-*C*O_2CH_3), 137.74, 135.92 (1′,4′-*C*), 129.34, 125.10 (2′,3′,5′,6′-*C*H), 121.78 (4-*C*N), 94.83 (2-*C*H), 51.67 (2-CO_2*C*H_3), 40.83 (4-*C*), 34.85, 31.66, 27.21 (3,5,6-*C*H_2), 21.07 (4′-*C*H_3) ppm. Mass spectrum (EI, 70eV): *m/z* (relative intensity, %)272 (M^+ + 1, 44), 271 (M^+ , 30), 240 (M^+ − OCH_3, 5), 185 (M^+ − C_2H_4 − $CH_3OC{\equiv}O$, 5), 143 (M^+ − $C_6H_8O_3$, 64), 128 ($C_6H_8O_3^+$, 100), 96 (27). Exact mass for $C_{16}H_{17}NO_3$: calcd 271.1208; obsd 271.1208. *Anal.* Calcd for $C_{16}H_{17}NO_3$: 70.83%C, 6.32%H, 5.16%N. Found:

70.92%C, 6.22%H, 5.12%N.

4′-Cyano-4-(4′-methyl)phenylcyclohexanone (43). In a 500 mL round bottom flask fitted with a reflux condenser, *cyanoketoester* **42** (80 g, mol) was dissolved in dimethyl sulfoxide (150 mL) and water (20 mL). Sodium chloride (20 g; mol) was added and the mixture was heated at reflux for three hours. On cooling, the mixture was poured onto ice water in a one-liter separatory funnel, and was extracted with ethyl acetate. The organic layer was washed with 10% sodium carbonate, water, and saturated sodium chloride, and then dried over sodium sulfate, filtered, and concentrated *in vacuo*. A crystalline solid was obtained, weighing 50 g (yield, 80%). An analytical sample was recrystallized from acetone and triturated with absolute methanol. TLC (ether/n-hexane, 1:1): R_f=0.18. mp 79-80°. IR ($CHCl_3$, NaCl): ν_{max} 2900, 2840, 2210 (C≡N), 1715 (C=O), 1440, 1330, 1110, 980, 955 cm^{-1}. ^1H NMR (400MHz, $CDCl_3$, TMS): δ 7.41, 7.38 ($\frac{1}{2}AA'BB'$ q, 2H, 2′,6′/3′,5′-C*H*, J=8.3Hz), 7.23, 7.21 ($\frac{1}{2}AA'BB'$ q, 2H, 2′,6′/3′,5′-C*H*, J=8.1Hz), 2.86, 2.85 (ddd, 2H, 3-CH_{ax}, J=6, 14Hz), 2.53, 2.43 (dq, 2H, 2-CH_{eq}, J=2, 15Hz), 2.43-2.35 (s, 3H, 4′-CH_3), 2.26, 2.24 (dt, 2H, 2-CH_{ax}, J=4, 14Hz) ppm. ^{13}C NMR (100.4MHz, $CDCl_3$): δ 206.72 (1-*C*=O), 138.18, 135.31 (1′,4′-*C*), 129.61, 125.06 (2′,3′,5′,6′-*C*H), 121.19 (4-*C*≡N), 42.88 (4-*C*), 38.78, 37.21 (2,3,5,6-CH_2), 21.22 (4′-CH_3) ppm. Mass spectrum (EI, 70eV): *m/z* (relative intensity, %)214 (M^+ + 1, 2.2), 213 (M^+ , 24), 185 ($M^+ - C_2H_4$, 3), 156 ($M^+ - C_2H_4 - CO - H$, 12), 143 ($M^+ - C_4H_6O$, 100),

129 (5), 115 (18), 91 ($C_7H_7^+$, 20). Exact mass for $C_{14}H_{15}NO$: calcd 213.1154; obsd 213.1145. *Anal.* Calcd for $C_{14}H_{15}NO$: 78.84%C, 7.09%H, 6.57%N. Found: 78.91%C, 7.03%H, 6.58%N.

8-Cyano-8-(4′-methyl)phenyl-1,4-dioxaspiro[4.5]decane (44). The *cyanoketone* **43** (40 g, 0.188mol) was dissolved in toluene (250 mL) in a 1000 mL round bottom flask surmounted by a Dean-Stark distillation trap and reflux condenser. Ethylene glycol (110 mL) and *p*-toluenesulfonic acid (50 mg) were added, and the mixture was distilled with azeotropic take-off till no more water was collected. On cooling, the mixture was neutralized with saturated sodium bicarbonate and then washed with water and saturated sodium chloride. The organic layer was dried over sodium sulfate, filtered, and evaporated. Colorless crystals were obtained, weighing 34 g (yield, 70%). mp 107-108°. IR ($CHCl_3$, NaCl): ν_{max} 2940, 2880, 2215 (CN), 1510, 1445, 1435sh, 1365, 1335, 1285, 1280, 1140, 1100, 1030, 960, 940, 810 cm^{-1}. ^1H NMR (400MHz, $CDCl_3$, TMS): δ 7.41, 7.39 ($\frac{1}{2}AA'BB'$ q, 2H, 2′,6′/3′,5′-C*H*, J=8.1Hz), 7.21, 7.19 ($\frac{1}{2}AA'BB'$ q, 2H, 2′,6′/3′,5′-C*H*, J=7.9Hz), 4.01, 4.00, 3.98, 3.96 (AB q, 4H, 2,3-CH_2, J=5Hz), 2.35 (s, 3H, 4′-CH_3), 2.17-1.85 (m, 8H, 6,7,9,10-CH_2) ppm. ^{13}C NMR (100.4MHz, $CDCl_3$): δ 137.48, 136.93 (1′,4′-*C*), 129.29, 125.24 (2′,3′,5′,6′-*C*H), 121.99 (8-*C*N), 106.97 (5-*C*), 64.62, 64.41 (2,3-*C*H_2), 43.20 (8-*C*), 35.22, 32.68 (6,7,9,10-*C*H_2, 21.20 (4′-*C*H_3) ppm. Mass spectrum (EI, 70eV): m/z (relative intensity, %)257 (M^+, 0.25), 230 ($M^+ - C_2H_4 + 1$, 2.3), 229 ($M^+ - C_2H_4$, 14), 156

(2), 143 ($C_{10}H_9N^+$, 5.7), 128 (2.4), 115 (5.6), 99 ($C_5H_7O_2^+$, 47), 86 ($C_4H_6O_2^+$, 100). Exact mass for $C_{16}H_{19}NO_2$: calcd 257.1416, obsd 257.1415. *Anal.* Calcd for $C_{16}H_{19}NO_2$: 74.68%C, 7.44%H, 5.44%N. Found: 74.75%C, 7.42%H, 5.40%N.

4-Acetyl-4-(4′-methyl)phenylcyclohexanone (45). The *cyano ketal* **44** (14.65 g, 57 mmol) was dissolved in dry benzene (200 mL) in a three-neck round bottom flask fitted with a reflux condenser, a graduated pressure-equalizing addition funnel, and an argon inlet. Methylmagnesium bromide solution (3.1M in ether, 73 mL, 228 mmol) was transferred under argon pressure *via* stainless steel canula to the addition funnel and then to the stirred benzene solution. The mixture was heated at reflux for 48 hours under argon. After cooling, hydrochloric acid (50 mL concentrated acid diluted with 300 mL water) was cautiously added. The two-phase mixture was heated at reflux for five hours. When cooled, the aqueous phase was extracted with 4×75 mL benzene, and the combined organic layer was washed with 10% sodium carbonate, water, and saturated sodium chloride. Drying over sodium sulfate, and solvent removal *in vacuo* gave 14 g of a viscous yellow oil which crystallized on standing (yield, >90%). mp 99-101°. IR ($CHCl_3$, NaCl): ν_{max} 2910, 2850sh, 1720 (C=0), 1460, 1410sh, 1355, 1338sh, 1310, 1155, 1115, 1095, 1040, 1015, 975, 940, 920sh, 890, 865, 600, 580, 565, 535 cm^{-1}. ^1H NMR (500MHz, $CDCl_3$, TMS): δ 7.25, 7.23 ($\frac{1}{2}AA'BB'$ q, 2H, 2′,6′/3′,5′-C*H*, J=8.3Hz), 7.21, 7.20 ($\frac{1}{2}AA'BB'$ q, 2H, 2′,6′/3′,5′-C*H*, J=8.3Hz), 2.57 (m, 2H, 3,5-C*H*), 2.45 (m, 2H, 3,5-C*H*), 2.39 (m, 2H, 2,6-C*H*), 2.35 (s, 3H, 4′-

CH_3), 2.31 (m, 2H, 2,6-C*H*), 1.99 (s, 3H, $COCH_3$) ppm. ^{13}C NMR (100.4MHz, $CDCl_3$): δ 209.58, 208.21 (1-*C*O, 4(1‴)-*C*O), 137.09, 136.52 (1′,4′-*C*), 129.64, 125.88 (2′,3′,5′,6′-*C*H), 55.06 (4-*C*), 38.28, 32.83 (2,3,5,6-CH_2), 25.34, 21.16 (4′-CH_3, 4(2‴)-CH_3CO) ppm. Mass spectrum (EI, 70eV): *m/z* (relative intensity, %)231 ($M^+ + 1$, 5), 230 (M^+, 17), 187 ($M^+ -$ CH_3CO, 100), 143 (26), 119 (22), 105 (42). Exact mass for $C_{15}H_{18}O_2$: calcd 230.1307, obsd 230.1305. *Anal.* Calcd for $C_{15}H_{18}O_2$: 78.23%C, 7.88%H. Found: 78.28%C, 7.93%H.

1-Methoxy-4-(4′-methyl)phenylbicyclo[2.2.2]octan-3-one (46). A solution of *tolyl diketone* **45** (13 g, 56 mmol) in methanol (100 mL) was treated with trimethylorthoformate (18.5 mL, 169 mmol). The solution was cooled to 0-5°, and dry hydrogen chloride gas was bubbled into it for 15 mins during which time the color turns a dark reddish brown. The ice bath was removed and replaced with a heating mantle. The mixture was heated at reflux for 35 mins. Solvents were evaporated, and water was added. The mixture was extracted with 8×50 ml diethyl ether. The combined organic layer was washed with saturated sodium bicarbonate and sodium chloride and then dried over sodium sulfate, and concentrated to afford 18 g of yellow crystals, which were recrystallized from dichloromethane/methanol (yield, 90%). mp 106-108°. IR ($CHCl_3$, NaCl): ν_{max} 2920, 2850, 2800, 1715 (C=O), 1500, 1450, 1420sh, 1332, 1310, 1125, 1095, 1010, 555 cm^{-1}. ^1H NMR (500MHz, $CDCl_3$, TMS): δ 7.16, 7.15 ($\frac{1}{2}AA'BB'$ q, 2H, 2′,6′/3′,5′-C*H*, J=8.0Hz), 7.08, 7.06 ($\frac{1}{2}AA'BB'$ q, 2H, 2′,6′/3′,5′-C*H*, J=8.2Hz),

3.29 (s, 3H, OCH_3), 2.59 (s, 2H, CH_2CO), 2.33 (s, 3H, 4′-CH_3), 2.24 (m, 2H, 6,8-C*H*), 2.09 (m, 2H, 6,8-C*H*), 1.99 (m, 2H, 5,7-C*H*), 1.91 (m, 2m, 5,7-C*H*) ppm. ^{13}C NMR (100.4MHz, $CDCl_3$): δ 210.32 (3-*C*=O), 136.67, 136.18 (1′,4′-*C*), 128.53, 126.90 (2′,3′,5′,6′-*C*H), 74.11 (4-*C*C=O), 49.85 (2-CH_2C=O), 49.56 (1-*C*O), 48.20 (1-OCH_3), 29.53, 29.25 (5,6,7,8-CH_2), 21.25 (4′-CH_3) ppm. Mass spectrum (EI, 70eV): *m/z* (relative intensity, %)245 ($M^+ + 1$, 6.5), 244 (M^+, 38), 200 (35), 187 (43), 170 (100), 144 (63), 129 (40), 118 (56), 105 (29). Exact mass for $C_{16}H_{20}O_2$: calcd 244.1463, obsd 244.1460. *Anal.* Calcd for $C_{16}H_{20}O_2 \cdot \frac{1}{3}H_2O$: 76.77%C, 8.19%H. Found: 77.17%C, 8.07%H.

1-Methoxy-4-(4′-methyl)phenylbicyclo[2.2.2]octane (47). To a suspension of *ketoether* **46** (3.52 g, 14.4 mmol) in diethylene glycol (75 mL) were added hydrazine hydrate (2.1 mL, 43.3 mmol) and potassium hydroxide (2.8 g, 49 mmol). The mixture was heated at 200-220° for five hours. Cooling, dilution with one volume of water, extraction with 3×20 mL diethyl ether, and removal of solvents *in vacuo* gave white crystalline *bicyclooctyl ether* weighing 2.1 g (yield, 63%). mp 60-62°. UV-Vis (CH_2Cl_2): λ_{max} 308 (ϵ 32), 273 (334), 266 (400), 262sh (334) nm. IR ($CHCl_3$, NaCl): ν_{max} 2900, 2850, 1450, 1410sh, 1355, 1095, 1025sh cm^{-1}. ^{1}H NMR (500MHz, $CDCl_3$, TMS): δ 7.20, 7.18 ($\frac{1}{2}AA'BB'$ q, 2H, 2′,6′/3′,5′-C*H*, *J*=8Hz), 7.10, 7.09 ($\frac{1}{2}AA'BB'$ q, 2H, 2′,6′/3′,5′-C*H*, *J*=8Hz), 3.21 (s, 3H, OCH_3), 2.30 (s, 3H, 4′-CH_3), 1.94 (m, 6H, 3×CH_2), 1.76 (m, 6H, 3×CH_2) ppm. ^{13}C NMR (100.4MHz, $CDCl_3$): δ 145.40 (1′-*C*), 134.79 (4′-*C*),

128.50, 124.97 (2′,3′,5′,6′-*C*H), 73.83 (1-*C*OCH$_3$), 49.19 (1-O*C*H$_3$), 34.03 (4-*C*), 33.38, 29.93 (2,3,5,6,7,8-*C*H$_2$), 21.07 (4′-*C*H$_3$) ppm. Mass spectrum (EI, 70eV): *m/z* (relative intensity, %)231 ($M^+ + 1$, 6), 230 (M^+, 33), 198 (4.3), 170 (2.3), 146 ($M^+ - OCH_3 - C_2H_4 - C_2H_2 + H$, 100), 131 (10), 118 (6), 105 (6), 91 (3.5). Exact mass for $C_{16}H_{22}O$: calcd 230.1671, obsd 230.1669. *Anal.* Calcd for $C_{16}H_{22}O$: 83.43%C, 9.63%H. Found: 83.46%C, 9.57%H.

2′,5′-Dimethoxy-4″-methyl-1,4-diphenylbicyclo[2.2.2]octane (48). In a 100 mL, 3-neck round-bottom flask, fitted with a condenser, inlets for argon and boron trifluoride gas, and a mineral oil bubbler, a solution of the *bicyclooctyl methyl ether* **47** (1.5 g, 6.5 mmol) in trichloroethylene (60 mL) was treated with *p*-toluenesulfonic acid (25 mg) and boron trifluoride gas for 30 minutes at 0-10°. The mixture was heated for 20 hours at reflux. Water and aqueous sodium carbonate (10%) were added. The aqueous layer was washed with 2×15 mL dichloromethane. The combined organic layer was washed with saturated aqueous sodium chloride, dried over sodium sulfate, filtered, and concentrated. The residue was Kugelrohred at 100°/0.01mm Hg for 2 hours and then flash chromatographed (toluene/dichloromethane, 9:1, R_f=0.66) to give pure *diarylbicyclooctane* weighing 1.35 g (yield, 62%). An analytical sample was obtained by recrystallization from ethanol/dichloromethane (4:1) giving colorless needles. mp 164-5°. UV-Vis (CH_2Cl_2): λ_{max} 285 (ϵ 2680), 237 (3660) nm. IR ($CHCl_3$, NaCl): ν_{max} 2890, 2850, 2835, 1600, 1580, 1475, 1455, 1415sh, 1275, 1160sh, 1115, 1000,

535 cm^{-1}. ^1H NMR (500MHz, $CDCl_3$, TMS): δ 7.28, 7.26 ($\frac{1}{2}AA'BB'$ q, 2H, 2′,6′/3′,5′-C*H*, J=8.2Hz), 7.13, 7.11 ($\frac{1}{2}AA'BB'$ q, 2H, 2′,6′/3′,5′-C*H*, J=8.0Hz), 6.83 (m, 1H, 6′-C*H*, J=3.0Hz), 6.82, 6.80 (d, 1H, 3′-C*H*, J=8.8Hz), 6.71, 6.70, 6.69, 6.68 (dd, 1H, 4′-C*H*, J=8.8Hz, 3.0Hz), 3.81 (s, 3H, OCH_3), 3.77 (s, 3H, OCH_3), 2.32 (s, 3H, 4″-CH_3), 2.08 ($AA'BB'$ m, 6H, 3×CH_2, J=4.4Hz, 7.3Hz), 1.93 ($AA'BB'$ m, 6H, 3×CH_2, J=4.5Hz, 8.3Hz) ppm. ^{13}C NMR (100.4MHz, $CDCl_3$): δ 153.53, 153.10 (2′,5′-*C*OCH_3), 147.38 (1′-*C*), 138.66, 134.87 (1″,4″-*C*), 128.73, 125.42 (2″,3″,5″,6″-*C*H), 114.50, 112.60 110.17 (3′,4′,6′-C*H*), 55.98, 55.92 (2′,5′-O*C*H_3), 35.86, 34.63 (1,4-*C*), 33.31, 30.71 (2,3-*C*H_2) ppm. Mass spectrum (EI, 70eV): *m/z* (relative intensity, %)337 (M^+ + 1, 31), 336 (M^+, 100), 192 (40), 190 ($M^+ - 2C_2H_4 - C_7H_7$, 70), 159 (30), 105 (17), 91 (13). Exact mass for $C_{23}H_{28}O_2$: calcd 336.2089, obsd 336.2087. *Anal.* Calcd for $C_{23}H_{28}O_2$: 82.10%C, 8.38%H. Found: 82.30%C, 8.62%H.

2′,5′-Dimethoxy-4′-formyl-4″-methyl-1,4-diphenylbicyclo[2.2.2]octane (49). The general method of Rieche, Gross, and Höft[20] was applied in the preparation of the formyl compound. Stannic chloride (3.5 mL, 2 eq) was added to a solution of *dimethoxyphenylbicyclooctane* **48** (5.0 g, 14.8 mmol) in dichloromethane (35 mL) at 0° under an argon atmosphere. α,α-Dichloromethyl methyl ether (1.34 mL, 1 eq) was added dropwise at 0°. The stirred mixture was warmed to 25° over 30 minutes and then heated to 35° for 20 minutes. The cooled

[20] A. Rieche, H. Gross, and E. Höft, *Org. Syn.*, **47**, 1 (1967).

mixture was poured onto ice water, and extracted with dichloromethane. The organic layer was concentrated and flash-chromatographed (dichloromethane, R_f=0.43), providing 4.4 g of pure *dimethoxyphenylaldehyde* (yield, 82%). Colorless prisms resulted from recrystallization from ether/n-hexane (1:1). mp 185-187°. UV-Vis ($CHCl_3$): λ_{max} 354 (ϵ 8070), 268 (17,700) nm. IR ($CHCl_3$, NaCl): 2900, 2850, 2750, 1670, 1605, 1570, 1480, 1458, 1390, 1358sh, 1310, 1260, 1165, 1120, 975, 865, 605, 530 cm^{-1}. ^1H NMR (500MHz, $CDCl_3$, TMS): δ 10.40 (s, 1H, C*H*O), 7.29 (s, 1H, 3′-C*H*), 7.27, 7.25 ($\frac{1}{2}AA'BB'$ q, 2H, 2″,6″/3″,5″-C*H*), 7.14,7.12 ($\frac{1}{2}AA'BB'$ q, 2H, 2″,6″/3″,5″-C*H*), 6.90 (s, 1H, 6′-C*H*), 3.90 (s, 3H, OCH_3), 3.84 (s, 3H, OCH_3), 2.32 (s, 3H, 4″-CH_3), 2.10 (m, 6H, 3×CH_2), 1.94 (m, 6H, 3×CH_2) ppm. ^{13}C NMR (400MHz, $CDCl_3$): δ 188.66 (4′-*C*HO), 156.09, 152.65 (2′,5′-*C*OCH$_3$), 146.58, 146.40 (1′,1″-*C*), 134.75 (4″-*C*CH$_3$), 128.56, 125.11 (2″,3″,5″,6″-*C*H), 122.47 (4′-*C*CHO), 111.48, 109.14 (3′,6′-*C*H), 56.25, 55.66 (2′,5′-O*C*H$_3$), 36.71, 34.27 (1,4-*C*), 32.73, 30.11 (2,3,5,6,7,8-*C*H$_2$), 21.13 (4″-*C*H$_3$) ppm. Mass spectrum (EI, 70eV): *m/z* (relative intensity, %)365 (M^+ + 1, 4.6), 364 (M^+ , 17.6), 337 (24), 336 (M^+ − CO, 100), 298 (6), 192 (21), 190 (40), 159 (8.5). Exact mass for $C_{24}H_{28}O_3$: calcd 364.2038, obsd 364.2048. *Anal.* Calcd for $C_{24}H_{28}O_3$: 79.09%C, 7.74%H. Found: 79.07%C, 7.64%H.

4′-Cyano-2′,5′-dimethoxy-4″-methyl-1,4- diphenylbicyclo[2.2.2]octane (50). In a 50 mL round-bottom flask a solution of *benzaldehyde* **49** (3.0 g, 8 mmol), hydroxylamine hydrochloride (860 mg, 12 mmol), and sodium formate

(653 mg, 9.6 mmol), in formic acid (95-100%; 25 mL) was heated at reflux for six hours. On cooling, the solution was poured onto ice-water, brought to neutral *p*H, and extracted with 3×40 mL diethyl ether. The combined organic layer was washed with saturated aqueous sodium chloride and water, dried over sodium sulfate, and solvents were evaporated *in vacuo*. Chromatography gave 2.8 g (yield, 95%) of the *cyano benzene*. TLC (dichloromethane): R_f=0.62. mp 203-206°. IR ($CHCl_3$, NaCl): ν_{max} 2900, 2850, 2210 (C≡N), 1490, 1455, 1385, 1105 cm^{-1}. ^1H NMR (400MHz, $CDCl_3$, TMS): δ 7.19, 7.17 ($\frac{1}{2}AA'BB'$ q, 2H, 2″,6″/3″,5″-C*H*, J=8.3Hz), 7.06, 7.04 ($\frac{1}{2}AA'BB'$ q, 2H, 2″,6″/3″,5″-C*H*, J=8.3Hz), 6.89 (s, 1H, 3′-C*H*), 6.79 (s, 1H, 5′-C*H*), 3.81 (s, 3H, OCH_3), 3.73 (s, 3H, OCH_3), 2.24 (s, 3H, 4″-CH_3), 2.00 (m, 6H, 3×CH_2), 1,86 (m, 6H, 3×CH_2) ppm. ^{13}C NMR (100.4MHz, CD_2Cl_2): δ 155.57, 152.63 (2′,5′-*C*OCH$_3$), 146.88, 145.05 (1″,4″-*C*), 135.02 (1′-*C*), 128.77, 125.35 (2″,3″,5″,6″-*C*H), 116.71 (4′-*C*N), 115.43, 111.54 (3′,6′-*C*H), 98.63 (4′-*C*CN), 56.78, 56.12 (2′,5′-O*C*H$_3$), 36.99, 34.54 (1,4-*C*), 33.03, 30.36 (2,3,5,6,7,8-*C*H$_2$) ppm. Mass spectrum (EI, 70eV): *m/z* (relative intensity, %)362 (M^+ + 1, 27), 361 (M^+ , 95), 217 (100), 189 (6), 144 (11), 105 (10). Exact mass for $C_{24}H_{27}NO_2$: calcd 361.2042, obsd 361.2057. *Anal.* Calcd for $C_{24}H_{27}NO_2 \cdot \frac{1}{2}H_2O$: 77.80%C, 7.56%H, 3.78%N. Found: 78.14%C, 7.82%H, 3.31%N.

4′-Cyano-2′,5′-dimethoxy-4″-(bromo)methyl-1,4-diphenylbicyclo-[2.2.2]octane (51). In a 25 mL round-bottom flask surmounted by a Liebig

condenser, *cyanotoluene* **50** (390 mg, 1.08 mmol) was dissolved in carbon tetrachloride (15 mL). The solution was treated with *N*-bromosuccinimide (207 mg, 1.2 mmol) and benzoyl peroxide (*ca.* 50 mg) and warmed to reflux for five hours. The progress of the reaction was monitored by withdrawing 1 mL aliquots and examining their ^{1}H NMR spectra. The reaction mixture was cooled, filtered, and concentrated to afford crude *cyanobenzylbromide* **51**, used directly in the next reaction. ^{1}H NMR (400MHz, $CDCl_3$, TMS): δ 7.36, 7.34 ($AA'BB'$ d, 4H, 2″,3″,5″,6″-C*H*, J= Hz), 6.98 (s, 1H, 3′/6′-C*H*), 6.86 (s, 1H, 3′/6′-C*H*), 4.50 (s, 2H, $C_6H_4CH_2Br$), 3.90 (s, 3H, 2′/5′-OCH_3), 3.82 (s, 3H, 2′/5′-OCH_3), 2.07 (m, 6H, 3×CH_2), 1.94 (m, 6H, 3×CH_2) ppm. Mass spectrum (EI, 70eV): *m/z* (relative intensity, %)441 (M^+ [^{81}Br], 30), 439 (M^+ [^{79}Br], 26), 386 (35), 361 (48), 360 (M^+ − Br, 100), 248 (14), 217 ($C_{13}H_{15}NO_2^+$, 78), 215 ($C_{13}H_{13}NO_2^+$, 51). Exact mass for $C_{24}H_{26}{}^{81}BrNO_2$: calcd 441.1127, obsd 441.1135; $C_{24}H_{26}{}^{79}BrNO_2$: calcd 439.1147, obsd 439.1160.

4′-Cyano-2′,5′-dimethoxy-4″-formyl-1,4-diphenylbicyclo[2.2.2]octane (52).[25] The *cyanobenzylbromide* **51** (*ca.* 1 mmol) was dissolved in dimethylsulfoxide in a 50 mL round-bottom flask. Sodium bicarbonate (190 mg) was added, and the stirred suspension was heated at reflux under argon for four hours. After cooling the mixture was poured onto ice water and extracted with 3×40 mL ethyl acetate. The combined organic layer was washed with saturated

---

[25] *Cf.* H.R. Nace and J.J. Monagle, *J. Org. Chem.*, **24**, 1792 (1959).

sodium chloride and then dried over sodium sulfate and evaporated to give 80 mg crude *cyano benzaldehyde*. An analytical sample was obtained by crystallization from ethanol/dichloromethane (5:1) giving colorless needles. mp 205-207°(dec). UV-Vis (CH_2Cl_2): λ_{max} 325sh (ϵ 4600), 318 (4650), 247 (9900) nm. IR ($CHCl_3$, NaCl): ν_{max} 2900, 2850, 2730, 2210 (C≡N), 1700 (C=O), 1690 (C=O), 1605, 1570, 1490, 1455, 1380, 1315, 1005, 965, 900, 535 cm^{-1}. ^1H NMR (500MHz, $CDCl_3$, TMS): δ 9.99 (s, 1H, C*H*O), 7.84, 7.83 ($\frac{1}{2}AA'BB'$ q, 2H, 3″,5″-C*H*), 7.54, 7.53 ($\frac{1}{2}AA'BB'$ q, 2H, 2″,6″-C*H*), 6.99 (s, 1H, 3′-C*H*), 6.86 (s, 1H, 5′-C*H*), 3.91 (s, 3H, OCH_3), 3.83 (s, 3H, OCH_3), 2.10 (m, 6H, 3×CH_2), 1.98 (m, 6H, 3×CH_2) ppm. ^{13}C NMR (100.4MHz, $CDCl_3$): δ 191.39 (4″-*C*HO), 156.70 (1″-*C*), 155.31, 152.15 (2′,5′-*C*OCH$_3$), 144.07 (1′-*C*), 133.97 (4″-*C*CHO), 129.42, 125.96 (2′,5′-*C*OCH$_3$), 116.45 (4′-*C*N), 115.11, 111.15 (3′,6′-*C*H), 98.71 (4′-*C*CN), 56.52, 55.87 (2′,5′-O*C*H$_3$), 36.60, 35.47 (1,4-*C*), 32.44, 29.85 (2,3,5,6,7,8-*C*H$_2$) ppm. Mass spectrum (EI, 70eV): *m/z* (relative intensity, %)376 (M^+ + 1, 26), 375 (M^+, 100), 217 (15), 215 (53), 200 (12), 184 (9), 151 (3.5), 115 (2.8), 91 (3.6). Exact mass for $C_{24}H_{25}NO_3$: calcd 375.1834, obsd 375.1835.

Preparation of meso-p-t-Butylphenylporphyrins **53** *and* **54**.

5-(4′-t-Butylphenyl)-2,3,7,8,12,13,17,18-octamethylporphyrin (53). A suspension of ac-*biladiene dihydrobromide* **30** (300 mg, 0.5 mmol) and 4-t-butylbenzaldehyde (0.6 mL, 3.7 mmol) in methanol (30 mL) was treated with 32% hydrobromic acid in glacial acetic acid (4 drops). The mixture was heated

at reflux in darkness under an air atmosphere for 24 hours. On cooling, solid sodium bicarbonate (300 mg) was added. Filtration and washing with methanol and water gave crude *porphyrin,* which was purified by flash chromatography (acetonitrile/dichloromethane, 9:1; TLC: R_f=0.69). mp >300°. UV-Vis (CH_2Cl_2): λ_{max} 279 (ϵ 6700), 402 (187,000), 500 (14,000), 534 (6100), 570 (6000), 623 (2100) nm. ^{1}H NMR (500MHz, $CDCl_3$, TMS): δ 10.13 (s, 2H, 10,20-C*H*), 9.92 (s, 1H, 15-C*H*), 7.94, 7.93 ($\frac{1}{2}AA'BB'$ q, 2H, 2′,6′-C*H*, J=8.1Hz), 7.74, 7.73 ($\frac{1}{2}AA'BB'$ q, 2H, 3′,5′-C*H*, J=8.2Hz), 3.62 (s,6H, 13,17-CH_3), 3.59 (s,6H, 12,18-CH_3), 3.52 (s, 6H, 2,8-CH_3), 2.44 (s, 6H, 3,7-CH_3), 1.61 (s, 9H, 4′-[C(CH_3)$_3$]) ppm. Mass spectrum (EI, 70eV): *m/z* (relative intensity, %)555 (M^+ + 1, 41), 554 (M^+ , 100), 422 (2.4), 262 (20), 183 (12). Exact mass for $C_{38}H_{42}N_4$: calcd 554.3409, obsd 554.3394. *Anal.* Calcd for $C_{38}H_{42}N_4$: 82.27%C, 7.63%H, 10.11%N. Found: 82.56%C, 7.71%H, 9.99%N.*

[5-(4′-t-Butylphenyl)-2,3,7,8,12,13,17,18-octamethylporphyrinato]-zinc(II) (54). The free-base *porphyrin* was metallated in chloroform with excess zinc(II) acetate dihydrate in methanol. Aqueous extraction followed by drying, filtration, and flash chromatography gave pure *metalloporphyrin.* mp >300°. UV-Vis (CH_2Cl_2): λ_{max} 247 (ϵ 7500), 408 (388,000), 500sh (2200), 533 (16,500), 570 (16,000) nm. ^{1}H NMR (500MHz, $CDCl_3$, TMS): δ 9.97 (s, 2H, 10,20-C*H*), 9.70 (s, 1H, 15-C*H*), 7.95, 7.94 ($\frac{1}{2}AA'BB'$ q, 2H, 2′,6′-C*H*, J=7.5Hz), 7.74, 7.72

---

* Microanalysis performed by Galbraith Laboratories, Inc., Knoxville, Tennessee.

($\frac{1}{2}AA'BB'$ q, 2H, 3′,5′-C*H*, J=7.8Hz), 3.51 (s, 6H, 13,17-CH_3), 3.49 (s, 6H, 12,18-CH_3), 3.47 (s, 6H, 2,8-CH_3), 2.43 (s, 6H, 3,7-CH_3), 1.62 (s, 9H, 4′-[C(CH_3)$_3$]) ppm. Mass spectrum (EI, 70eV): *m/z* (relative intensity, %)620 (M^+ + 4, 41), 617 (M^+ + 2, 63), 617 (M^+ + 1, 50), 616 (M^+ , 100), 615 (M^+ − 1, 19), 554 (M^+ − Zn + 2H, 38), 262 (19), 183 (14). Exact mass for $C_{38}H_{40}N_4Zn$: calcd 616.2544, obsd 616.2536. *Anal.* Calcd for $C_{38}H_{40}N_4Zn{\cdot}H_2O$: 71.75%C, 6.65%H, 8.81%N. Found: 71.65%C, 6.48%H, 8.78%N.

Preparation of (meso-Benzoquinone)octamethylporphyrin **56**

5-(2′,5′-Dimethoxyphenyl)-2,3,7,8,12,13,17,18-octamethylporphyrin (55). A suspension of *ac-biladiene dihydrobromide* (100 mg, 0.17 mmol) and 2,5-dimethoxybenzaldehyde (Aldrich; 0.32 g, 1.9 mmol) in methanol (25 mL) was heated at reflux open to the air and with protection from direct light. After about 24 hours the mixture was cooled to room temperature and solid sodium bicarbonate (*ca.* 2 g) was added. The filtered solid was washed with copious water and methanol. Drying gave 98 mg crude red-violet powder. Flash chromatography (chloroform) afforded 45 mg of pure *porphyrin* (yield, 46%). TLC (dichloromethane/acetonitrile, 9:1): R_f=0.73. UV-Vis (CH_2Cl_2): ν_{max} 402 (ϵ 181,000), 499 (15,700), 532 (7460), 569 (6870), 622 (2790) nm. ^{1}H NMR (400MHz, CD_2Cl_2): δ 10.17 (s, 2H, 10,20-C*H*), 9.98 (s, 1H, 15-C*H*), 7.37, 7.36, 7.35, 7.34 (dd, 1H, 4′-C*H*, J=2.7, 9Hz), 7.30, 7.296, 7.27 (1:2:1, dd, 2H, 3′,6′-C*H*, J=3.1, 9.4Hz), 3.85 (s, 3H, OCH_3), 3.69 (s, 3H, OCH_3), 3.63 (s, 6H, 13,17-

CH_3), 3.60 (s, 6H, 12,18-CH_3), 3.56 (s, 6H, 2,8-CH_3), 2.60 (s, 6H, 3,7-CH_3), -3.56 (*br* s, 2H, 2×N*H*) ppm. Mass spectrum (EI, 70eV): *m/z* (relative intensity, %)559 (M^+ +1, 41), 558 (M^+ , 100), 529 (22), 248 (21), 241 (22). Exact mass for $C_{36}H_{38}N_4O_2$: calcd 558.2995, obsd 558.2978.

5-(2′,5′-Benzoquinone)-2,3,7,8,12,13,17,18-octamethylporphyrin (56). The *porphyrin diether* **55** (14.1 mg, 25 μmol) was dissolved in dichloromethane (10 mL) and treated with boron tribromide (1M in dichloromethane, 1.5 mL) at 25°C. After being stirred for three hours, water and triethylamine were added. The aqueous layer was extracted with 3×20 mL dichloromethane and the combined organic layer was washed with 20 mL water. Purification by flash chromatography (dichloromethane/acetone, 95:5) gave the *porphyrin hydroquinone.* A suspension of the *hydroquinone* (*ca.* 3 mg, 5.6 μmol) in methanol (10 mL) was allowed to react with 2,3-dichloro-5,6-dicyanoquinone (10 mg, 44 μmol) in the dark at reflux. After 30 minutes the mixture was cooled to room temperature. Solvent was evaporated, and the residue was dissolved with dichloromethane and applied to a silica gel column. TLC (dichloromethane/acetone, 95:5): 0.8. UV-Vis (CH_2Cl_2): ν_{max} 401, 499, 531, 569, 623 nm. ^{1}H NMR (400MHz, CD_2Cl_2): δ 10.12 (s, 2H, 10,20-C*H*), 9.83 (s, 1H, 15-C*H*), 7.44, 7.41 (d, 1H, 3′-C*H*, J_{ortho}=10.1Hz), 7.38, 7.37, 7.356, 7.349 (dd, 1H, 4′-C*H*, J_{ortho}=10.1Hz, J_{meta}=2.3Hz), 7.342, 7.336 (d, 1H, 6′-C*H*, J_{meta}=2.3Hz), 3.59 (s, 6H, 13,17-CH_3), 3.58 (s, 6H, 12,18-CH_3), 3.52 (s, 6H, 2,8-CH_3), 3.16 (s, 6H, 3,7-

CH_3) ppm. Mass spectrum (Fast Atom Bombardment, positive ion, dithithreitol/dithioerythritol): *m/z* 685 (M^+ + DTT/DTE + 2H + 1, 25), 684 (M^+ + DTT/DTE + 2, 55), 683 (M^+ + DTT/DTE + 1, 100), 529 (M^+ , 20).

Electrochemical Measurements

Solvents and Chemicals. The quality of electrochemical measurements in non-aqueous solvents depends critically on the level of water present in the sample and on the condition of the surface of the working electrode. Solvents were purified as follows. 2-Methyltetrahydrofuran was distilled from calcium hydride and then from sodium/benzophenone ketyl. Spectrograde acetonitrile (Burdick & Jackson) and benzene (Aldrich) were distilled from calcium hydride under argon. Butyronitrile (Aldrich) was distilled either from calcium hydride, or first from potassium permanganate/sodium carbonate and then from phosphorus pentoxide. Supporting electrolytes used included tetra-n-butylammonium perchlorate (Alfa) for butyronitrile and acetonitrile and tetra-n-hexylammonium perchlorate (Alfa or G. Frederick Smith Chemical Co.) for 2MTHF and benzene, and were dried *in vacuo* at 75° for 24 hours prior to use in voltammetry. Porphyrins were purified by flash chromatography before electrochemical measurements. Methyl-*p*-benzoquinone (Aldrich) was purified by chromatography. 2,5-Dimethyl-*p*-benzoquinone was prepared from 2,5-dimethylphenol (Aldrich) by the procedure of Teuber[26] using Fremy's salt. Trimethyl-*p*-benzoquinone was made by oxidation of trimethylhydroquinone (Aldrich) using unactivated manganese(IV) dioxide.[27] Chloro-*p*-benzoquinone, bromo-*p*-benzoquinone, and

---

[26] H.-J. Teuber, *Ber.*, **86**, 1036 (1953).

[27] *Cf.* J.M. Bruce, S. Fitzjohn, and R.T. Pardasani, *J. Chem. Res.* (*Synop.*), 252

2,3-dichloro-*p*-benzoquinone were prepared by B.A. Leland.[28] 2-Cyano-5-methyl-*p*-benzoquinone was synthesized by formylation of 2,5-dimethoxytoluene[29], oximine formation with hydroxylamine hydrochloride and sodium formate in formic acid,[30] ether cleavage with boron triiodide in dichloromethane,[31] and oxidation with nitrogen tetroxide in carbon tetrachloride.[32]

Sample Preparation. Concentrations of the porphyrins and quinones were in the range of 10^{-3}-10^{-5}M. The supporting electrolyte was present at 0.1-0.3M. Appropriate amounts of the supporting electrolyte were weighed into round bottom flasks and stoppered in an inert atmosphere box to minimize the absorption of water by the hygroscopic salts. After dissolving them in the respective solvents the solutions were transferred to the microcell and purged of air by bubbling high-purity argon for 15 minutes before electrochemical measurements. It was found that optimal voltammetric response (reproduceability and electrochemical reversibility) resulted from the use of extensively polished working electrodes. Redox potentials are referred to the ferrocene/ferrocenium (Fc/Fc^+) couple meas-

---

(1981).

[28] B.A. Leland, *Dissertation*, California Institute of Technology, 1986.

[29] *Cf.* Ref. 20.

[30] *Cf.* T. van Es, *J. Chem. Soc.* 1564 (1965).

[31] *Cf.* Ref. 24.

[32] *Cf.* A.G. Brook, *J. Chem. Soc.* 5040 (1952).

ured independently in each solvent studied. The one-electron redox potentials for reference redox couple are given in Table I *versus* the silver quasi-reference electrode.

Equipment and Cells. Electrochemical measurements (using linear sweep, differential, and normal pulse voltammetry) were carried out using an EG&G Princeton Applied Research (PAR) 174A Polarographic Analyzer or a PAR 175 Universal Programmer interfaced with a PAR 173 Potentiostat. Voltammograms were recorded on a Houston Instruments 2000 X-Y Plotter. Additional differential pulse voltammetry measurements were performed on the Bioanalytical Systems (BAS) Electrochemical Analyzer (BAS 100) using electronic resistance compensation. The electrochemical sample was contained in a 15 mL capacity cylindrical voltammetry cell (BAS, VC-2), which has a teflon cap with three holes, one for an argon purge tube and the remaining two for the working and reference electrodes. A platinum wire counter electrode was used in lieu of the one provided in the cap. The reference electrode was either an aqueous silver/silver chloride (BAS, RE-1) electrode or a saturated sodium calomel electrode or a silver wire quasi-reference electrode, consisting of a coil around the working electrode. The latter was either a 25 μ diameter platinum disk microelectrode (details of construction given below), a 127 μ platinum disk microelectrode, or a commerical 1.6 mm diameter platinum disk electrode (BAS, PTE). The smallest microelectrodes were necessary for the most resistive solvents (*i.e.*, benzene and 2MTHF).

Construction of Microelectrodes. The method of Lines and Parker[33] was modified as follows for the preparation of the platinum microelectrodes (Figure 1). About 2 cm of 25 μ diameter platinum wire (Alfa) was sealed into the end of a heat-constricted 50 μL borosilicate capillary pipette using a cool flame. After cooling, excess wire extruding from the sealed end was abraded off by rough polishing on 600 grit carborundum paper. The surface was further polished using, in succession, 1 μ, 0.3 μ, and 0.05 μ alumina (Fisher) wetted with water on microcloth polishing pads for the purpose (Buchler or BAS). Efficient polishing was essential to free the platinum disk surface of defects, adsorbent insulating oxides, etc., and to obtain an electrochemical area as close as possible to the geometrical flat surface area. The interior cavity of the capillary tube was filled with one drop of mercury. A copper wire extending into the mercury pool and about one inch extending from the upper end was inserted. The upper end was sealed either with a cool flame or with silicone rubber.

Steady-State Fluorescence Emission Spectroscopy

Chemicals and Solvents. The porphyrins were purified by chromatography prior to the spectral measurements. Acetonitrile (Burdick & Jackson) and benzene (Burdick & Jackson) were distilled from calcium hydride. *N,N*-Dimethylformamide was distilled under reduced pressure from calcium hydride.

---

[33] R. Lines and V.D. Parker, *Acta Chim. Scand.*, **B31**, 369 (1977).

Table I. Half-Wave Potentials of Ferrocene/Ferrocenium in Various Solvents *versus* the Silver Quasi-reference Electrode.

Solvent	$E^{a}_{1/2}$(mV)	$\mid E_{3/4} - E_{1/4} \mid$ (mV)	Conditions
CH_3CN	+630	56	0.1M TBAP[b]
n-PrCN	+618	56	0.1M TBAP
2MTHF	+833	65	0.1M THAP[c]
C_6H_6	+890	86	0.3M THAP

[a] Half-wave potential for the first oxidation determined by linear sweep voltammetry at 25 μ or 127 μ diameter Pt disk microelectrodes at slow sweep rates (v= 5 – 10 mV/sec), 25°C.

[b] Tetra-n-butylammonium perchlorate.

[c] Tetra-n-hexylammonium perchlorate.

Dichloromethane was spectro-grade (Aldrich) and was used without further purification. Butyronitrile (Aldrich) was allowed to stand over potassium carbonate for 24 hours and then distilled from phosphorus pentoxide.

Sample Preparation. Paired solutions of the *meso-p*-t-butylphenylporphyrins and the porphyrin-quinones were matched in concentration by dissolving each to give roughly a concentration of $10^{-5} - 10^{-6}$M and then adding more solvent to the less concentrated solution of the pair until optical densities at the Soret band ($\sim$ 400 nm) were the same ($\pm$ 10%). Measurements were made under aerobic conditions using 1 cm square quartz fluorescence cells with teflon caps. The integrity

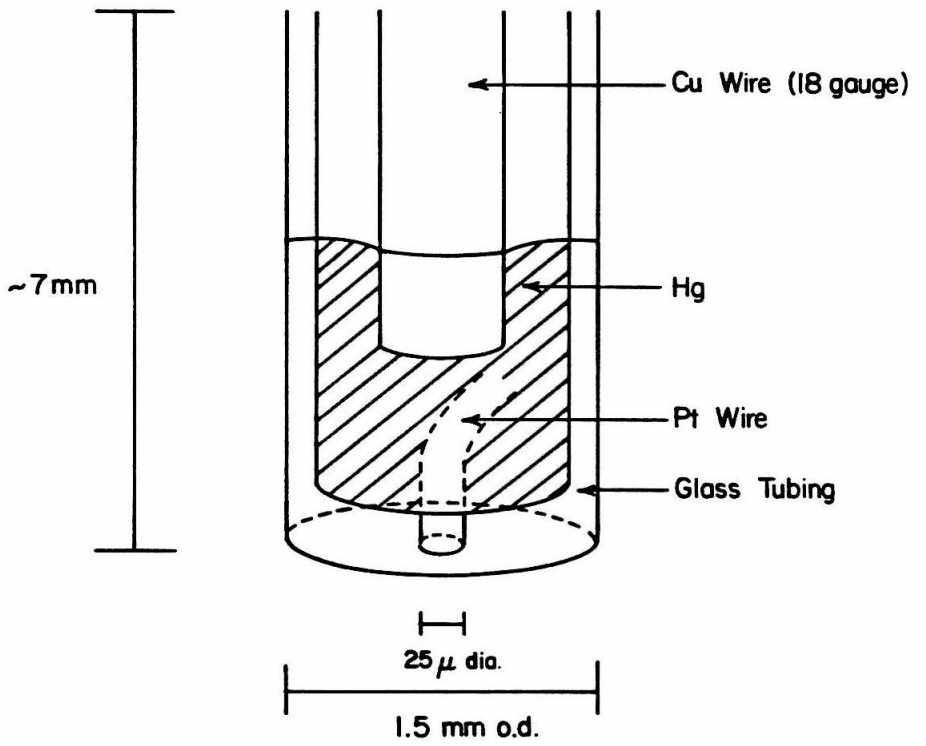

Figure 1. Microelectrode Construction.

of the compound studied was checked following each fluorescence measurement by examination of the electronic absorption spectrum.

Equipment. The fluorescence emission spectra were recorded on a custom-built instrument constructed by Steven F. Rice, of H. B. Gray's Group. The light source was a 200W Hg/Xe lamp. The required wavelength of light was selected by a Spex Minimate monochromator. After passing through fixed slits, the light was modulated by a beam chopper, further selected by an interference or band-pass filter (Oriel 5644), and focussed onto the sample. Emitted light collected at right angles was filtered, collimated, focussed onto the slits (2-3mm wide) of a Spex monochromator with a motorized wavelength scan drive, and detected using a Hamamatsu R955 photomultiplier tube. The detector signal was amplified by a Princeton Applied Research PAR 181 preamplifier and a PAR 186A lock-in amplifier in phase with the beam chopper. The spectrum was recorded on a Hewlett-Packard strip-chart recorder. The free-base porphyrin emission spectra were scanned from 600 to 720 nm and the zinc porphyrin spectra from 550 to 700 nm.

Picosecond Fluorescence Spectroscopy: Time-Correlated Single Photon Counting.

Time-resolved picosecond fluorescence spectra were determined using time-correlated single photon counting techniques.[34]

Equipment. Most analyses were conducted by P.M. Felker on a system (Scheme I) designed by him primarily for studies of fluorescence in molecular beams with A.H. Zewail.[35,36] A train of 15 psec FWHM light pulses ($\sim$ 30 mW full output power) generated by a mode-locked, argon-ion laser synchronously pumped a rhodamine 6G cavity dumped dye laser, which produced tuneable probe pulses at a repetition rate of 4MHz tuned to 570 nm. Each probe pulse was divided into two pulses. One pulse excites the sample. Emitted light was filtered to remove scattering contributions, collimated, and detected at right angles by a photomultiplier tube (PMT, Hamamatsu R1564U). The electrical pulse is then fed to a constant fraction discriminator (Ortec 473A or Tennelec 455) to select uniform pulses to start the clock (time-to-amplitude converter, TAC; Ortec 457). The other pulse leads to a fast photodiode (Hewlett-Packard 5082-4203), which, after shaping by a discriminator, stopped the timing clock (TAC). Only

---

[34] For example, see C.C. Lo, B. Leskover, P.R. Harteg, and K. Sauer, *Rev. Sci. Instrum.*, **47**, 1113 (1976).

[35] P.M. Felker, *Dissertation*, California Institute of Technology, 1985.

[36] W.R. Lambert, P.M. Felker, A.H. Zewail, *J. Chem. Phys.*, **81**, 2217 (1984).

matched start-stop pairs are collected. The clock records the time of triggering for each photon "event." The number of events per time channel were accumulated and stored in the multichannel analyzer (Tracor-Northern TN-1706). To avoid multiple simultaneous photon detection events, a low photon counting rate was employed (about 1% of the laser repetition rate). The temporal distribution of photon detection events as a function of channel gives the observed fluorescence decay data, which at the end of the accumulation were stored and analyzed statistically, using either a Digital Equipment Corp. PDP-11/23 minicomputer or a Compaq Computer Corp. Compaq Plus Personal Computer, configured with 640K RAM and a 10 Megabyte hard disk-drive.

The resolution of the system is limited by "jitter" in the photomultiplier tube to about 80 psec FWHM; the laser pulse is not limiting in this respect. A response function $R(t)$ was obtained before or after each data accumulation using a scattering sample (*e.g.*, a colloidal suspension of milk in water). The true decay $I(t)$ could then be deconvoluted from the distorted observed decay data $F(t)$ according to the equation:[37]

$$F(t) = \int_0^t R(t')I(t-t')dt'. \qquad [6.1]$$

The decay data were fit to single, double, or occasionally triple exponential func-

---

[37] C. Lewis, W.R. Ware, L.J. Doemeny, and T.L. Nemzek, *Rev. Sci. Instrum.*, **44**, 107 (1973).

tions using a nonlinear, least-squares fitting algorithm,[38] as adapted by B.A. Leland. By this method the sum of squares of the weighted residuals

$$\chi^2 = \sum_i \frac{(N(t_i) - F(t_i))^2}{W(t_i)} \qquad [6.2]$$

is minimized by adjusting parameters used to calculate the decay function $F(t_i)$ with $N(t_i)$ being the measured number of counts in channel i. $W(t_i)$ is the weighting for each data point and is equal to $N(t_i)$ in the limit of Poisson statistics' being valid.[38] The minimized value of χ^2 is taken as the goodness-of-fit statistic, with 1.15 or lower corresponding to acceptable fits to the observed decay data.

Solvents. Benzene and acetonitrile were HPLC grade and distilled from calcium hydride. Butyronitrile was distilled from potassium permanganate/sodium carbonate and then from phosphorus pentoxide. 2-Methyltetrahydrofuran was distilled from sodium/benzophenone ketyl. *N,N*-Dimethyl formamide (Aldrich, spectrograde) and pyridine was distilled from calcium hydride. *o*-Xylene (Burdick & Jackson) and *o*-dioxane were distilled from sodium/benzophenone ketyl.

Sample Preparation. All porphyrins were purified by flash-column chromatography prior to each set of spectral measurements. A dilute solution ($10^{-5} - 10^{-6}$M) of the porphyrin was prepared in the appropriate solvent, and freed of particulate matter by filtration through 0.15 μ Millipore (type FH) fil-

---

[38] P.R. Bevington, *Data Reduction and Error Analysis for the Physical Sciences*, McGraw-Hill, New York, 1969.

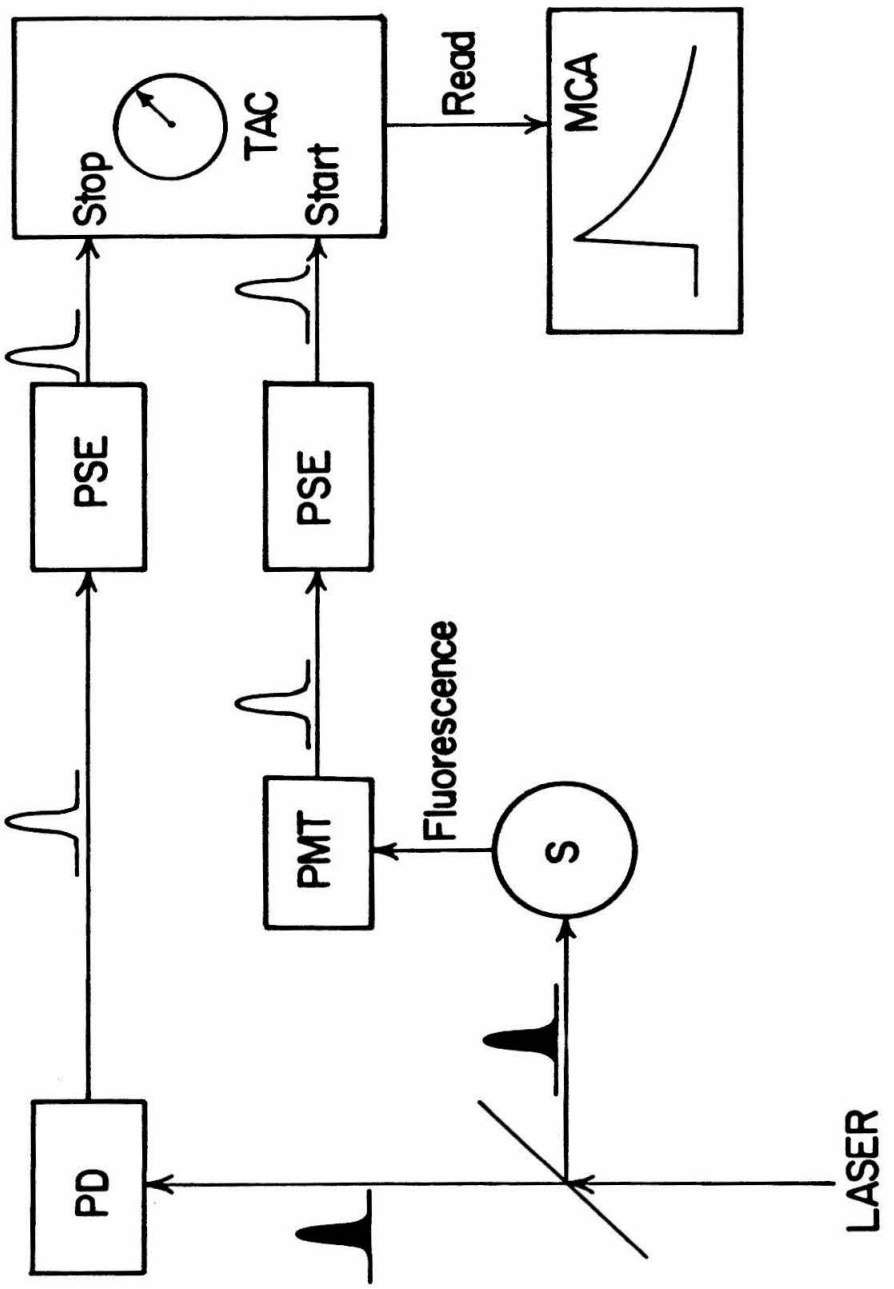

Scheme I. Single-Photon Counting Apparatus Schematic.

ters. The filtrate was transferred to a specially constructed optical cell possessing a Pyrex storage bulb, a standard taper 24/40 female ground-glass joint for connection to a high-vacuum line, a Teflon stopcock, and a 1 cm square fused quartz fluorescence cell (NSG Cells, type 163). The sample was de-aerated by subjecting the solution to at least four freeze-pump-thaw cycles using an oil diffusion pump ($< 10^{-5}$mm). Low-temperature samples were prepared by similar procedures except that the cell used was a cylindrical quartz tube (Wilmad Glass Co., #701-PQ) fused to a standard taper 14/35 ground glass male joint. Response functions at low temperatures were acquired, using frozen polycrystalline solvent in the same equipment configuration as the sample to be analyzed. Stable temperatures of 77($\pm$2)K and 1($\pm$2)°C were obtained by immersion of the sample tube in a silvered, evacuated finger dewar with a quartz optical path using either liquid nitrogen cryogen or water ice, respectively.

Electron Spin Resonance Techniques

ESR Spectra were recorded on a Varian E-Line ESR Spectrometer, observing at X-band, following standard techniques. High-intensity light sources included a 200 mW Hg-Xe arc lamp with 350 nm or 450 nm cut-off filters, or a 1 mW He-Ne CW laser. Lossy solvents were studied at room temperature using flat thin cells. Low temperature samples were examined in silvered finger dewars maintained at 77K with liquid nitrogen.